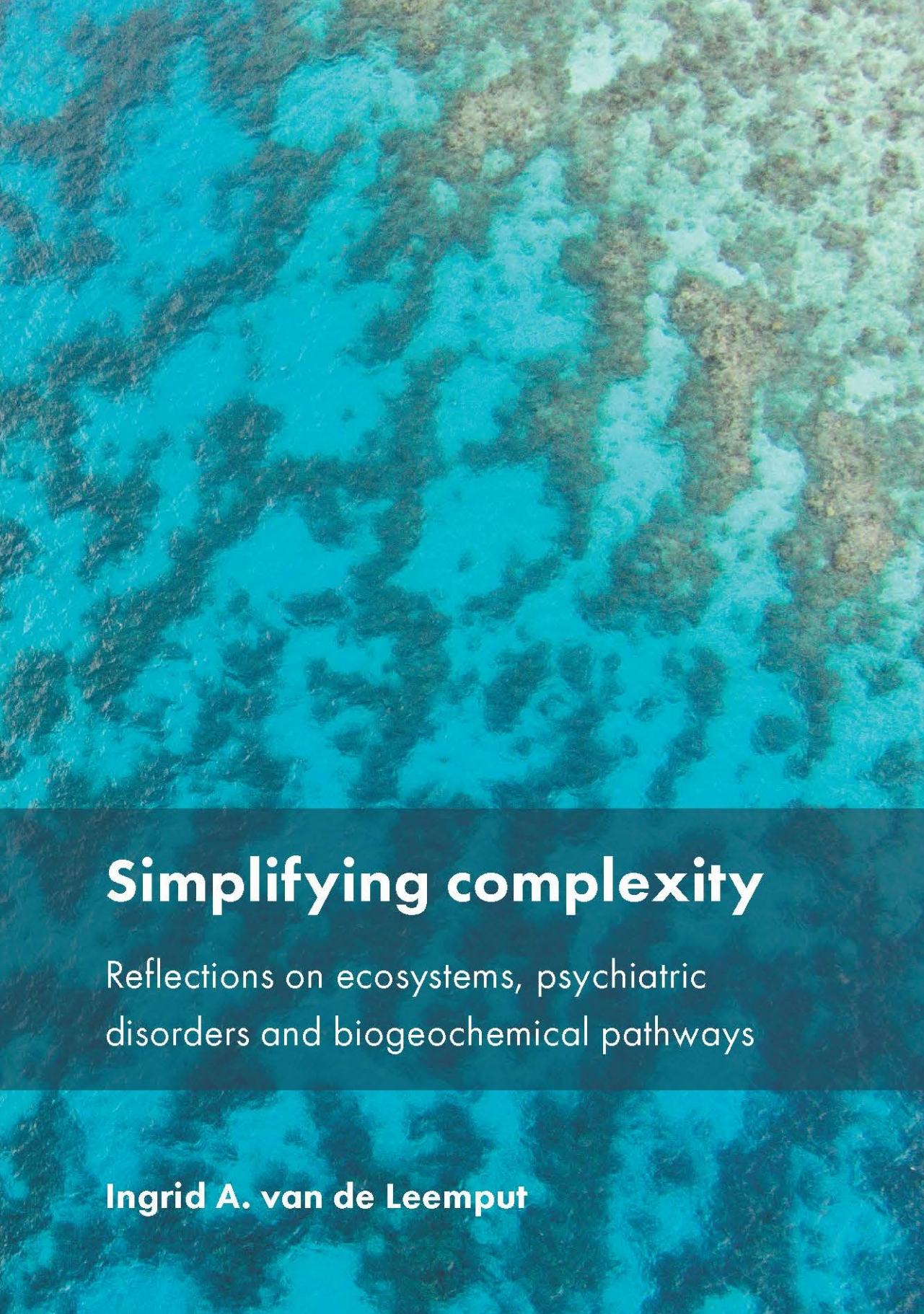

Simplifying complexity

Reflections on ecosystems, psychiatric disorders and biogeochemical pathways

Ingrid A. van de Leemput

Simplifying complexity

Reflections on ecosystems, psychiatric disorders and biogeochemical pathways

Ingrid A. van de Leemput

Thesis committee

Promotor
Prof. Dr M. Scheffer
Professor, Department of Aquatic Ecology and Water Quality Management
Wageningen University, The Netherlands

Co-promotor
Dr E.H. van Nes
Associate Professor, Department of Aquatic Ecology and Water Quality Management
Wageningen University, The Netherlands

Other members
Prof. Dr R. de Boer, Utrecht University
Prof. Dr J.A.P. Heesterbeek, Utrecht University
Prof. Dr C.K. Hemelrijk, University of Groningen
Prof. Dr J.L. van Leeuwen, Wageningen University

This research was conducted under the auspices of the Graduate School for Socio-Economic and Natural Sciences of the Environment (SENSE)

Simplifying complexity

Reflections on ecosystems, psychiatric disorders
and biogeochemical pathways

Ingrid A. van de Leemput

Thesis
submitted in fulfillment of the requirements for the degree of doctor
at Wageningen University
by the authority of the Rector Magnificus
Prof. Dr A.P.J. Mol,
in the presence of the
Thesis Committee appointed by the Academic Board
to be defended in public
on Friday 3 June 2016
at 11 a.m. in the Aula.

Ingrid A. van de Leemput
Simplifying complexity. Reflections on ecosystems, psychiatric disorders and biogeochemical pathways
214 pages

PhD thesis, Wageningen University, Wageningen, NL (2016)
With references, with summary in English

ISBN: 978-94-6257-793-0

Contents

Chapter 1

General introduction

Ingrid A. van de Leemput

Complex systems

The whole is more than the sum of its parts – Aristotle

Biogeochemical cycles, ecosystems, the climate, the financial market, the human being (physical and mental), and social networks (physical and online) are all examples of complex systems. Understanding the properties and dynamics of complex systems motivates many scientific questions. While *complexity* and *complex systems* are currently scientific buzzwords, a single concise definition of a *complex system* does not exist, and is dependent on the scientific discipline in which the concept is used. Following the Oxford English Dictionary, the word *complex* has different meanings. The first is "*consisting of many different and connected parts*". This is not very distinctive as every system on earth essentially consists of many different and connected parts (e.g. atoms, molecules, individuals, etc.). The second meaning of complex is more relevant: "*not easy to analyze or understand; complicated or intricate*". The parts of a system will generally interact with each other, and with the environment. These interactions can make systemic behavior difficult to understand or predict. In this thesis, a *complex system* is considered to be a system composed of a number of interconnected parts, where the systemic behavior leads to the emergence of properties that would not be expected from behavior or properties of the parts of the system (Gell-Mann 1988).

Full characterization of the parts, interactions and resulting dynamics of complex systems is a scientific challenge of all times. Many systems are subject to slow changes in the environment, for example due to increasing demand for resources, climate change, and stronger interdependence of economies and markets. Mechanistic insight of systemic dynamics may help to predict a systems' response to environmental change. In this thesis, I discuss the use of dynamical systems theory as a tool to understand particular observed dynamics. I address three different complex systems: the microbial nitrogen cycle, the coral reef ecosystem, and the psychological condition of human beings. Each of these systems is of great importance to humanity, and extensively studied. Yet, our understanding of what drives their overall dynamics has somehow remained surprisingly fragmentary.

The analysis of complex system dynamics

There is no silver-bullet approach to analyze a complex system. In general, a combined approach of field observations, experiments, and mathematical modeling is required to gain insight into the processes and interactions that are underlying observed dynamics of any complex natural system. The complementarity of empirical

and theoretical approaches is highlighted in most standard books on methods in ecology (see for example Henderson 2003). Each approach has its advantages and limitations. Field measurements allow a researcher to observe completely natural behavior, but conditions cannot be controlled, so cause and effect of processes are difficult to distinguish. Lab experiments are more controlled, and can provide insight into specific processes, or sub-systems, however only a part of the system is studied. Mathematical models can simulate system dynamics in order to provide insights in particular observed dynamics, and may be used to predict future dynamics. However, mathematical models cannot prove causality, as they are always a simplification. Several types of mathematical models can be distinguished, ranging from fully parameterized complex models, to simple strategic models (see for example for coral reefs Weijerman *et al.* 2015). Fully mechanistic models map out the most relevant parts of the system, and use estimates of parameters and interactions based on experiments or field measurements. Such models are generally specifically parameterized to predict future trajectories of one particular case or location. However, due to the high complexity of systems, accurate mechanistic modeling can be difficult (Oreskes *et al.* 1994). Moreover, fully mechanistic models are difficult to analyze, especially if non-linear interactions are involved. In this thesis, I use dynamical strategic models (i.e. abstract, simple models; Scheffer and Beets 1994), to illustrate how certain, often unexpected, behavior and pattern formation can arise from relatively simple interactions. A strategic model is generally used to generate hypotheses on the underlying processes. It may also provide an alternative, fresh view on the systemic dynamics.

Strategic models to explore complexity

In dynamical systems theory, systems are viewed from a very abstract perspective describing qualitative behavior. Strategic models generally consist of just one or a few mathematical equations, and are usually deterministic (i.e. without stochasticity). Still the emergent behavior of dynamical systems is often complex due to non-linear interactions (i.e. cause and effect are not proportional). Researchers tend to look especially for particular emergent phenomena, such as cycles, chaos, critical transitions (Strogatz 1994), and in the spatial realm Turing patterns, and moving fronts (Murray 2003). Because of the simplicity of such models, one can fully analyze changes in stability and dynamics as a result of altering conditions. Obviously the link between such simple mathematical structures and real complex systems is difficult to make, and may easily lead to an overestimation of the applicability of clear and beautiful mathematical insights. The drawback of this is illustrated by the fierce discussion on Catastrophe Theory in the 70s.

The use of dynamical systems to model non-linear change in nature gained popularity with the development of Chaos theory, formalized in 1963 by Edward Lorenz (Lorenz 1963), and Catastrophe theory, formalized in 1972 by René Thom (Thom 1972). Both mathematical theories became well known for their proclaimed universality and potential to apply to natural and social systems. While the broad applicability of Chaos Theory was controversial, the scientific enthusiasm regarding Catastrophe Theory experienced a particularly severe storm of critique leading to a demise of its popularity. Catastrophe Theory considers the phenomenon that small changes in parameters of a nonlinear system can cause stable equilibria to appear or disappear, leading to sudden changes in the behavior of the system. One of the models introduced by Thom was the cusp-catastrophe model (see also Glossary), which is appealing to non-mathematicians, because it can explain abrupt behavior of a system quite intuitively, without understanding the underlying mathematics. After the introduction of Thom's ideas, the scientific community went through a period of great interest and enthusiasm, in which many examples of systems corresponding with the theory were published (for a selection of papers see Zeeman and Sussmann 1979). Obviously, the media picked this up as well, and phrases such as "*the most important development since calculus*" (Newsweek) were not uncommon. In response, the usefulness of the theory, and the evidence for the example systems were strongly criticized (Zahler and Sussmann 1977; Sussmann and Zahler 1978). Consequently, the theory was devaluated into a purely mathematical exercise, and set aside as an intellectual bubble of little consequence (Horgan 1997). Decades later, the fierce extremes were reviewed and explained by the overenthusiasm of the so-called catastrophists, often missing a mechanistic explanation, and misstatements based on misunder-standing of the mathematical concepts from both catastrophists and criticizers (Rosser 2007). The main weakness of the pioneering work was that the theory was imposed on observed dynamics, without much mechanistic understanding. So the applicability of Catastrophe Theory was initially overstated. As a result, the entire theory was disputed. In the hindsight this may have been an overreaction, and "*the baby was thrown out with the bathwater*" (Oliva and Capdevielle 1980; Rosser 2007).

Over the past decades we understand better what we can learn from abstract mathematical phenomena, such as the cusp-catastrophe model, in relation to real complex systems. Interestingly, the term *Catastrophe Theory* did not return in most scientific disciplines. New popular terms regarding the theory of abrupt transitions include *critical transitions*, *tipping points*, *regime shifts*, and sometimes *catastrophic shifts*. More in general, strategic models are starting to generate testable hypotheses and suggest practical ways of managing and predicting the behavior of complex systems. Yet, building bridges between the abstract mathematical world of non-

linear dynamical systems, and real-world complex systems remains one of the main challenges. In this thesis I take up this challenge in an effort to carve corridors of clarity into the complexity of a set of quite different systems.

The microbial nitrogen cycle

In **chapter 2** I propose to view the microbial nitrogen cycle as a dynamical system. Because of the immense experimental effort required, no study so far has addressed all nitrogen pathways simultaneously. However, in order to reconstruct the evolution of the current microbial pathways, and to predict consequences of environmental change, a full understanding of key processes and interactions of biogeochemical cycles such as the nitrogen cycle is required. I address the question which of the multitude of potential biogeochemical pathways are feasible in an ecological context, and should therefore be expected to exist in nature. Chapter 2 introduces a model based on hypothetical nitrogen pathways that compete for nitrogen compounds. The uptake rates and competitive strength of the pathways are simply based on the stoichiometry and energy yield of the performed redox reactions. Because of competition, the model attains a dynamic equilibrium in which a subset of pathways outcompetes the others. While the model is obviously a strong simplification of reality, it can explain most of the observed architecture of the microbial nitrogen cycle. Indeed with a recent discovery (Daims *et al.* 2015; van Kessel *et al.* 2015), 10 out of the 11 pathways this model predicts are now found in nature.

The coral reef ecosystem

A classical example of a highly diverse and complex ecosystem is a coral reef. Coral reefs provide habitat to many different benthic and mobile species, and provide a variety of ecosystem services, such as fisheries, tourism, and coastal protection (Moberg and Folke 1999). Currently, climate change and increasing human activity put high pressure on coral reefs around the world (Hughes *et al.* 2003). Not surprisingly, there is an urgent need to understand the dynamics and get an estimate of the resilience of these complex ecosystems. In **chapter 3**, I show that the shape of coral patches has become extremely structured and organized in some places. Although this is not easily recognized when snorkelling or diving, aerial and satellite pictures reveal regular spatial patterns of coral at certain locations. I propose that these spots of seemingly organized patches can reveal new information on what facilitates or limits coral growth. I present the coral reef ecosystem as

a spatially explicit dynamical system. We relate these regularly spaced coral reef patches observed on the Great Barrier Reef and New Caledonia to self-organized patterns as described by the mathematician Alan Turing in 1952 (Turing 1952). Without knowing the actual mechanism underlying the patterns, based on the observation of regular patterns we outline a specific set of hypotheses on lagoonal coral reef growth, and on reef resilience.

These two studies illustrate that using non-linear dynamical system theory to analyze the dynamics of real-world complex systems can help to generate hypotheses on key processes and interactions in the system. However, scientific progress can also often simply benefit from bridging existing insights. Certainly, when it comes to dynamical systems theory, many of the slightly counter-intuitive predictions are poorly known among more empirically oriented scientists. **Chapter 4** illustrates how showing theoretically well understood phenomena in a specific context may help to resolve debates. I compile a list of interactions in the coral reef ecosystem that result in positive feedbacks. Many feedbacks have not been recognized as such, and may individually be too weak to contribute to the generation of alternative stable states. I then use a simple mathematical model to illustrate how multiple positive feedbacks can, even if they are weak, collectively lead to alternative stable states, and therefore to abrupt transitions. This illustrates that the existence of alternative stable states and critical transitions depends largely on the interplay of feedbacks and conditions. Thus, a system that often responds smoothly to changing conditions, may, under other circumstances show an abrupt shift to an alternative stable state. This should come as no surprise to theoreticians that are familiar with models in dynamical systems theory. However, it sheds a new light on the polarized discussion in the literature about alternative stable states of reefs.

Anticipating critical transitions

The second half of my thesis is devoted to a relatively young scientific field that builds a bridge between the abstract world of bifurcation theory, and the potential application of indicating changes in the resilience of a system. It has been proposed that loss of resilience in ecological systems can be detected without prior knowledge on the processes and interactions of a specific system (i.e. early warning signals) (Scheffer *et al.* 2015b). Most of these proposed early warning signals are based on the phenomenon of critical slowing down (see also Glossary), which is based on generic properties of zero-eigenvalue bifurcations (van Nes and Scheffer 2007).

In **chapter 5**, I review the recent insights on such generic indicators of proximity to critical transitions, and highlight aspects of the architecture of complex systems that

play a role in the occurrence of critical transitions. A range of statistical measures as indicators of critical slowing down or changes in the stability landscape, limitations of the suggested approaches, and new applications are continuously being discovered. It is exciting that theoreticians from different scientific directions are now adopting these new developments. However, we should take care not to overstate the applications, and fall into the same trap that led to the dismissal of the Catastrophe Theory.

In **chapter 6** I analyze the differences between well-mixed systems and spatially extended systems with local alternative stable states. While alternative stable states and critical transitions have been well studied in isolated, well-mixed systems, systems are often much more complex in reality. For example, most landscapes are spatially extended, in the sense that local interactions play an important role. I show that local perturbations can spread through space as a moving front, and link the mathematical theory of moving fronts to phenomena in spatially extended ecosystems with local alternative stable states. I show that essential properties of such spatial dynamics can be understood from the existence of the so-called Maxwell point, a point in parameter space at which the global stability of the system shifts.

In **chapter 7** I propose that one could monitor recovery of strong local disturbances in spatially extended ecosystems in order to get an indication of the proximity to a systemic transition. The most direct indicator of critical slowing down is the recovery rate after a small disturbance (van Nes and Scheffer 2007). However, the models on which these predictions are based, assume a well-mixed system, so they don't take into account the complexity of spatially extended systems or networks. In this chapter we illustrate and discuss the differences of the recovery trajectory between strong local disturbances and weak global disturbances.

The human state of mind

The third complex system addressed in this thesis is the mental state of human beings. Depression is one of the main mental health hazards of our time (Bijl *et al.* 1998). Psychologists however have little insight in how depressions develop. While until recently depression was seen as a traditional disease in the sense that it has one common cause, a complex systems view has recently been proposed (Cramer *et al.* 2010; Borsboom *et al.* 2013; Schmittmann *et al.* 2013). The idea is that the interactions between personal entities, such as emotions and behaviors, can result in complex behavior, such as depression. While the first attempts to map out the architecture and connections of such personal networks have been made using observed correlations between depression symptoms (Bringmann *et al.* 2013)

a systemic analysis remains challenging. In **chapter 8**, I propose to view the mood of a person as a dynamical system, with interacting emotions as network entities. We analyze the self-reported mood of a group of depressed and of healthy patients, showing that the proposed measures are indicative of the proximity to a transition.

In **chapter 9**, I reflect and prospect on the applicability and limitations of models inspired by dynamical systems theory as a tool to study complex systems.

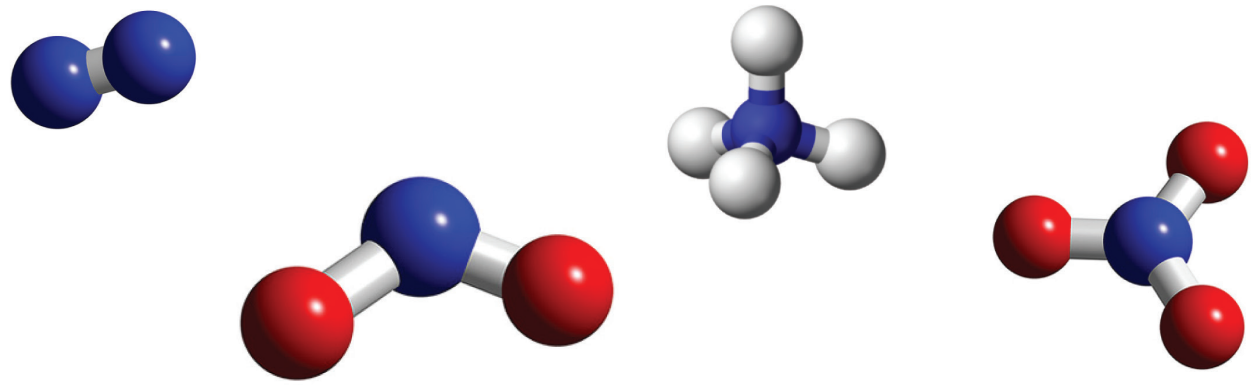

Chapter 2

Predicting microbial nitrogen pathways from basic principles

Ingrid A. van de Leemput,
Annelies J. Veraart,
Vasilis Dakos,
Jeroen J.M. de Klein,
Marc Strous,
and Marten Scheffer

Published in *Environmental Microbiology:*

van de Leemput IA, Veraart AJ, Dakos V, de Klein JJM, Strous M, Scheffer M. 2011. Predicting microbial nitrogen pathways from basic principles. *Environ Microbiol* **13**: 1477–87.

Abstract

Nitrogen compounds are transformed by a complicated network of competing geochemical processes or microbial pathways, each performed by a different ecological guild of microorganisms. Complete experimental unraveling of this network requires a prohibitive experimental effort. Here we present a simple model that predicts relative rates of hypothetical nitrogen pathways, based only on the stoichiometry and energy yield of the performed redox reaction, assuming competition for resources between alternative pathways. Simulating competing pathways in hypothetical freshwater and marine sediment situations, we surprisingly found that much of the variation observed in nature can simply be predicted from these basic principles. Investigating discrepancies between observations and predictions led to two important biochemical factors that may create barriers for the viability of pathways: enzymatic costs for long pathways and high ammonium activation energy. We hypothesize that some discrepancies can be explained by non-equilibrium dynamics. The model predicted a pathway that has not been discovered in nature yet: the dismutation of nitrite to the level of nitrate and dinitrogen gas.

Introduction

In nature, several competing microbial pathways are responsible for the transformation of nitrogen compounds. Each pathway is performed by a different guild of microorganisms under different environmental conditions. This network of microbial nitrogen pathways is known as the microbial nitrogen cycle, and includes pathways such as nitrification, denitrification, dissimilatory nitrate reduction to ammonium (DNRA, also called nitrate ammonification), anaerobic ammonium oxidation (anammox), nitrate reduction to nitrite, and nitrogen fixation (Fig. 2.1). The biogeochemical nitrogen cycle is affected intensely by human activity (Rockström *et al.* 2009), and a good understanding of the outcome of competition between nitrogen pathways as a function of the environmental conditions is essential if we wish to project the consequences of the human induced changes.

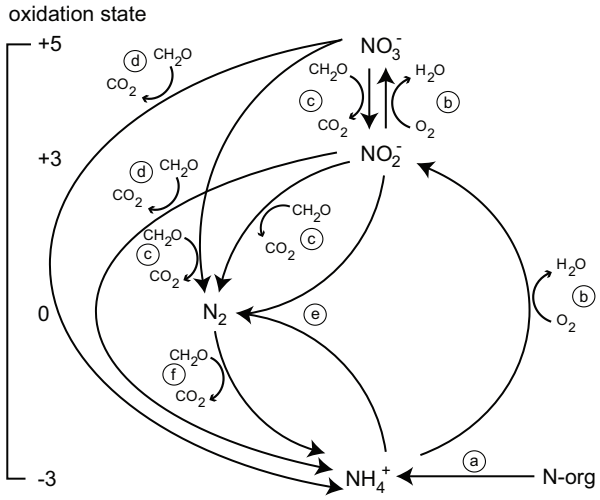

Figure 2.1. The microbial nitrogen cycle, involving known pathways between nitrogen compounds, oxygen and organic material: **a)** mineralization, **b)** nitrification in two steps: ammonium-oxidation and nitrite-oxidation, **c)** denitrification from nitrite and nitrate, **d)** dissimilatory nitrite and nitrate reduction to ammonium (DNRA), **e)** anaerobic ammonium oxidation (anammox) and **f)** nitrogen fixation.

Previous studies have modeled the competitive strength of nitrogen pathways using a semi-empirical approach: activity rates of competing pathways were measured in experiments or in the field and used as input for models, to estimate nitrogen conversion rates under different environmental conditions (e.g. Spérandio and Queinnec 2004; Liu *et al.* 2005; Canavan *et al.* 2007). However, because of the immense experimental effort required, no study so far has addressed all nitrogen pathways simultaneously. Besides, it could well be that our current inventory of nitrogen transforming pathways is still incomplete; for example, only very recently a pathway was discovered that dismutates nitric oxide into oxygen and nitrogen (Ettwig *et al.* 2010).

Here, we circumvent these problems by taking a completely different approach that may complement the semi-empirical results obtained so-far. We assume no

prior knowledge on the microbial nitrogen cycle as we know it. Instead, following Broda's proposition that microbes may realize all energetically profitable pathways (Broda 1977), we use the chemical properties of the nitrogen compounds in a simple energy-based model to predict the relative success of catabolic, thermodynamically feasible, pathways as a function of the environmental conditions. This may sound strange from an ecological perspective, as in nature organisms compete, not reactions. However, a functional approach that puts reactions rather than species or populations central is increasingly used in microbial ecology. For instance, locally collected samples of enzymes (metaproteomics) or genetic material (metagenomics) can give a clue to the reactions occurring on a site.

We define differential equations for the dynamics of the substrates nitrate, nitrite, nitric oxide, nitrous oxide, ammonium, dinitrogen gas, organic material and oxygen. For simplicity the only non-nitrogen substrates considered are oxygen (as an alternative electron acceptor) and organic compounds (as an alternative electron donor). Furthermore, we define a differential equation for each thermodynamically feasible redox reaction, in other words a 'theoretical pathway'. The equations describe the growth of the 'volume' of that pathway as a function of its substrate affinity, determined by the stoichiometry of the reaction, and its energy yield. To make it less abstract one may think of the volume of a pathway as the biomass of a guild of microbes performing that particular pathway even though we do not model mass balances explicitly. Pathway volume is in this sense directly related to pathway activity. The mathematical formulation of our model is given in the Experimental Procedures section.

Note that it is not our ambition to produce a model for accurate quantitative prediction of nitrogen dynamics in nature. Rather we seek to explore what is a minimum set of assumptions needed to explain which pathways are found in practice. More specifically we ask how much of the observed reactions can be simply explained from resource competition, stoichiometry and energy yield. The model is based on three main assumptions.

Firstly, we assume that the rates of all transformations are controlled by the delivery of fresh substrates (by mass transport), rather than by microbial processing capacity (enzyme turnover). This is a reasonable assumption because most nitrogen conversion takes place in the chemocline where the delivery of fresh substrates is limiting (Jensen *et al.* 2009; Halm *et al.* 2009).

Secondly, we assume that the volume yield for each microbial guild depends linearly on the energy yield (the Gibbs free energy change) of the associated pathway. This linear relationship was previously shown to approximate reality (Liu *et al.* 2007). Some pathways are obviously less efficient than others in this sense (Tijhuis *et al.* 1993).

Thirdly, we assume for all microbial guilds that the substrate affinity is proportional to the stoichiometric factor, that is, the relative consumption of that substrate in that pathway. In reality, substrate affinity is mainly determined by the flux of substrate towards the single cells and is therefore proportional to the stoichiometric factor as well as the cell size (Schulz and Jørgensen 2001). However, assuming cell size to be roughly equal for each microbial guild, we neglect this source of variation.

In addition to these three assumptions, we impose a thermodynamic restriction on pathways consuming ammonium, because of its high activation energy (Strous *et al.* 1999; Dosta *et al.* 2008). Both anammox and nitrification need additional electrons for the ammonium reaction, which are transferred from reactions later in the pathway (Fig. 2.2). Anammox bacteria use a NO radical to activate ammonium to the level of hydrazine (N_2H_4) (Fig. 2.2a) (Strous *et al.*, 2006), while nitrifying bacteria oxidize ammonium directly with activated oxygen yielding hydroxylamine (NH_2OH) (Fig. 2.2b). It is therefore assumed that ammonium can only be activated directly by a reactive species (Hooper *et al.* 2004). In our model, a theoretical pathway is considered thermodynamically feasible when each ammonium molecule can react at a one-to-one ratio with a reactive chemical species (e.g. NO or O_2) as the primary substrate or intermediate.

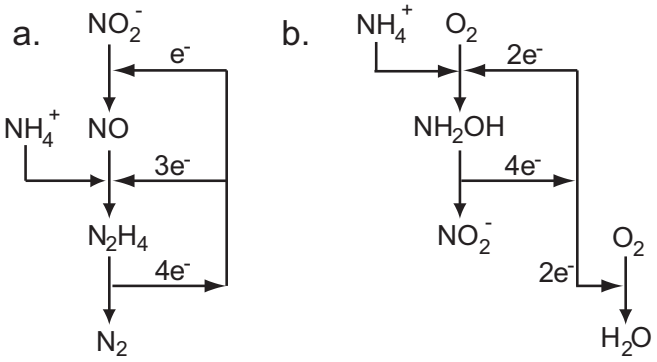

Figure 2.2. Microbial ammonium oxidation pathways of **a)** anammox (Strous *et al.* 2006) and **b)** nitrification (Ferguson *et al.* 2007). Anammox bacteria make use of the nitric oxide radical to activate ammonium directly to the level of hydrazine while nitrifying bacteria use activated oxygen to react with ammonium directly to hydroxylamine. It is hypothesized that ammonium has to react with a reactive species at a one-to-one ratio, to overcome its high activation energy. This could explain why electrons are transported from other oxidation reactions in the pathways to the ammonium oxidation step.

These assumptions led to a model that allows us to simulate the competition of thermodynamically feasible pathways simultaneously. The only inputs to this model are the continuous inflow of nitrogen compounds, oxygen and organic material into the system. For simplicity, organic material is assumed to be completely labile. We did not consider the inflow of nitrous oxide or nitric oxide, as the concentrations of these compounds are typically too low to contribute significantly to mass balances

of nitrogen. Thus, nitric oxide and nitrous oxide in the model are only available if produced.

A dynamic equilibrium arises when pathway growth equalizes decay and continuous inflow and outflow equalize both consumption and production. The model outputs are the volume of each theoretical pathway and the final concentration of each nutrient, after stabilization of the system.

Results

Even if a pathway could take place in isolation (i.e. the pathway is 'feasible'), this does not mean that it is 'viable' in the sense that it would yield a positive volume in a situation where it is competing with other pathways. In order to screen the overall viability of the theoretical pathways, the model was run for 10,000 random sets of substrate inflow rates. From all 45 thermodynamically feasible pathways, 11 were found to be viable in this analysis (Table 2.1). Most pathways known to occur in nature are covered by this theoretically predicted list (Table 2.1: Eqns. 1-9). This suggests that the thermodynamic principles implemented may indeed explain much of the patterns observed in reality. The model predicted two pathways that have not been discovered in nature: complete nitrification from ammonium to nitrate by a single organism, which we call 'total nitrification' (Table 2.1: Eqn. 10), and simultaneous oxidation and reduction of nitrite, producing nitrate and dinitrogen gas, which we call 'nitrite dismutation' (Table 2.1: Eqn. 11).

Table 2.1. The 11 predicted viable nitrogen pathways out of the 45 thermodynamically feasible pathways. We considered a pathway viable with an equilibrium activity higher than 0.001 in at least one of the 10.000 simulations of the model with random inflow levels of nitrate, nitrite, ammonium, dinitrogen gas, oxygen and organic material.

	Pathway	Reaction
1	Anammox	$NO_2^- + NH_4^+ \rightarrow N_2 + 2\ H_2O$
2	Denitrification NO_2^-	$4\ NO_2^- + 3\ CH_2O + 4\ H^+ \rightarrow 2\ N_2 + 3\ CO_2 + 5\ H_2O$
3	Denitrification NO_3^-	$4\ NO_3^- + 5\ CH_2O + 4\ H^+ \rightarrow 2\ N_2 + 5\ CO_2 + 7\ H_2O$
4	DNRA NO_2^-	$2\ NO_2^- + 3\ CH_2O + 4\ H^+ \rightarrow 2\ NH_4^+ + 3\ CO_2 + H_2O$
5	DNRA NO_3^-	$NO_3^- + 2\ CH_2O + 2\ H^+ \rightarrow NH_4^+ + 2\ CO_2 + H_2O$
6	Heterotrophic N_2 fix.	$2\ N_2 + 3\ CH_2O + 4\ H^+ + 3\ H_2O \rightarrow 4\ NH_4^+ + 3\ CO_2$
7	Nitrification (NH_4^+-ox.)	$2\ NH_4^+ + 3\ O_2 \rightarrow 2\ NO_2^- + 4\ H^+ + 2\ H_2O$
8	Nitrification (NO_2^--ox.)	$2\ NO_2^- + O_2 \rightarrow 2\ NO_3^-$
9	Respiration	$CH_2O + O_2 \rightarrow CO_2 + H_2O$
10	'Total nitrification'	$NH_4^+ + 2\ O_2 \rightarrow NO_3^- + 2\ H^+ + H_2O$
11	'Nitrite dismutation'	$5\ NO_2^- + 2\ H^+ \rightarrow 3\ NO_3^- + N_2 + H_2O$

In order to compare the model predictions with patterns in natural systems, we defined a number of hypothetical environments in terms of their relative inflow of ammonium, organic material, nitrate and nitrite. To have a concrete situation in mind we think of these environments as freshwater and marine sediments. We chose the conditions in such a way that each viable theoretical pathway in the model can be discussed. Then, we simply assume a sediment to have a linear gradient of oxygen inflow. For pristine freshwater and marine sediments (i.e. without any anthropogenic inflow), we assumed a constant inflow of organic material. The only nitrogen source was ammonium, assumed to be produced by mineralization (Fig. 2.3a and 2.4a). For freshwater sediments the inflow of organic material was assumed to be five times higher than ammonium, while in marine sediments it was assumed to be five times lower, due to the activity of for example sulphate reducers (Fig. 2.4a). We considered both nitrate and nitrite inflow for eutrophic freshwater sediments (Fig. 2.3b, c and d), and only nitrate inflow for the eutrophic (e.g. coastal) marine sediment (Fig. 2.4b).

Along the oxygen inflow gradient in each hypothetical sediment, the model produced stable estimates of: the relative volume of each pathway (Fig. 2.3 and 2.4: Pathway volume), the relative concentration of each substrate and product (Fig. 2.3 and 2.4: Nutrient concentration), and the percentage of substrate uptake relative to the inflow per pathway (Fig. 2.3 and 2.4: Consumption of nutrient inflow (CH_2O, O_2, NH_4^+, NO_2^- and NO_3^-).

In a pristine freshwater sediment, the model predicted dominance of aerobic respiration, total nitrification and denitrification (Fig. 2.3a: Pathway volume). At high oxygen inflow, the equilibrium oxygen concentration was high, while at low oxygen inflow, anoxic conditions were established (Fig. 2.3a: Nutrient concentration). This was mainly due to the activity of the aerobic respiration pathway (Fig. 2.3a: O_2). At high oxygen inflow, organic material (Fig. 2.3a: CH_2O) and ammonium (Fig. 2.3a: NH_4^+) were consumed by aerobic respiration and nitrification pathways, while both substrates accumulated under low oxygen levels (Fig. 2.3a: Nutrient concentration). At intermediate oxygen inflow levels, where the equilibrium oxygen concentration was low (Fig. 2.3a: Nutrient concentration), nitrification was predicted to be coupled to denitrification (Fig. 2.3a: Pathway volume). At the oxic-anoxic boundary, some partial nitrification to the level of nitrite coupled to anammox activity was predicted (Fig. 2.3a: O_2 and NH_4^+).

Freshwater sediments with an inflow of nitrate (Fig. 2.3b and c) were predicted to be dominated by nitrification and aerobic respiration at high oxygen levels, and by denitrification and DNRA at low oxygen levels. At relatively low nitrate inflow levels, DNRA outcompeted denitrification at low oxygen inflow levels (Fig.

2.3b), while at high nitrate inflow levels, DNRA was outcompeted by denitrification along the whole oxygen inflow gradient (Fig. 2.3c). The amount of nitrate inflow influenced the location of the oxic-anoxic boundary. This can be understood from the competition for substrates. At high nitrate and low oxygen inflow, denitrification wins the competition from respiration and completely consumes the available organic material. The available oxygen is then consumed by nitrification. However, ammonium is more limited than organic material, so the available oxygen is not completely consumed by the nitrification pathway. Therefore, the depth at which positive oxygen levels may be found (the thickness of the oxic layer) increased with nitrate inflow levels.

A freshwater sediment with a high inflow level of nitrite (Fig. 2.3d) and high inflow levels of oxygen, was predicted to be dominated both by nitrification from nitrite to nitrate and by total nitrification. In the layers with lower oxygen inflow levels, the unknown 'nitrite dismutation' pathway consumed the available nitrite. At the lowest levels, anammox was predicted to coexist with this pathway.

A pristine marine sediment (Fig. 2.4a) was predicted to be dominated by total nitrification coupled to denitrification at high oxygen inflow levels, shifting to ammonium-to-nitrite nitrification coupled to anammox with decreasing oxygen inflow. Due to high ammonium levels, oxygen was the limiting substrate over the whole inflow gradient, so anoxic conditions were created even at high oxygen inflow levels.

A marine sediment with an inflow of nitrate (Fig. 2.4b) showed similar pathway activity rates as a pristine marine sediment, only denitrification rates were higher at low oxygen levels. Even higher nitrate inflow levels in the simulated marine sediments showed the same pathway activity rates, because nitrate was not a limiting substrate (results not shown).

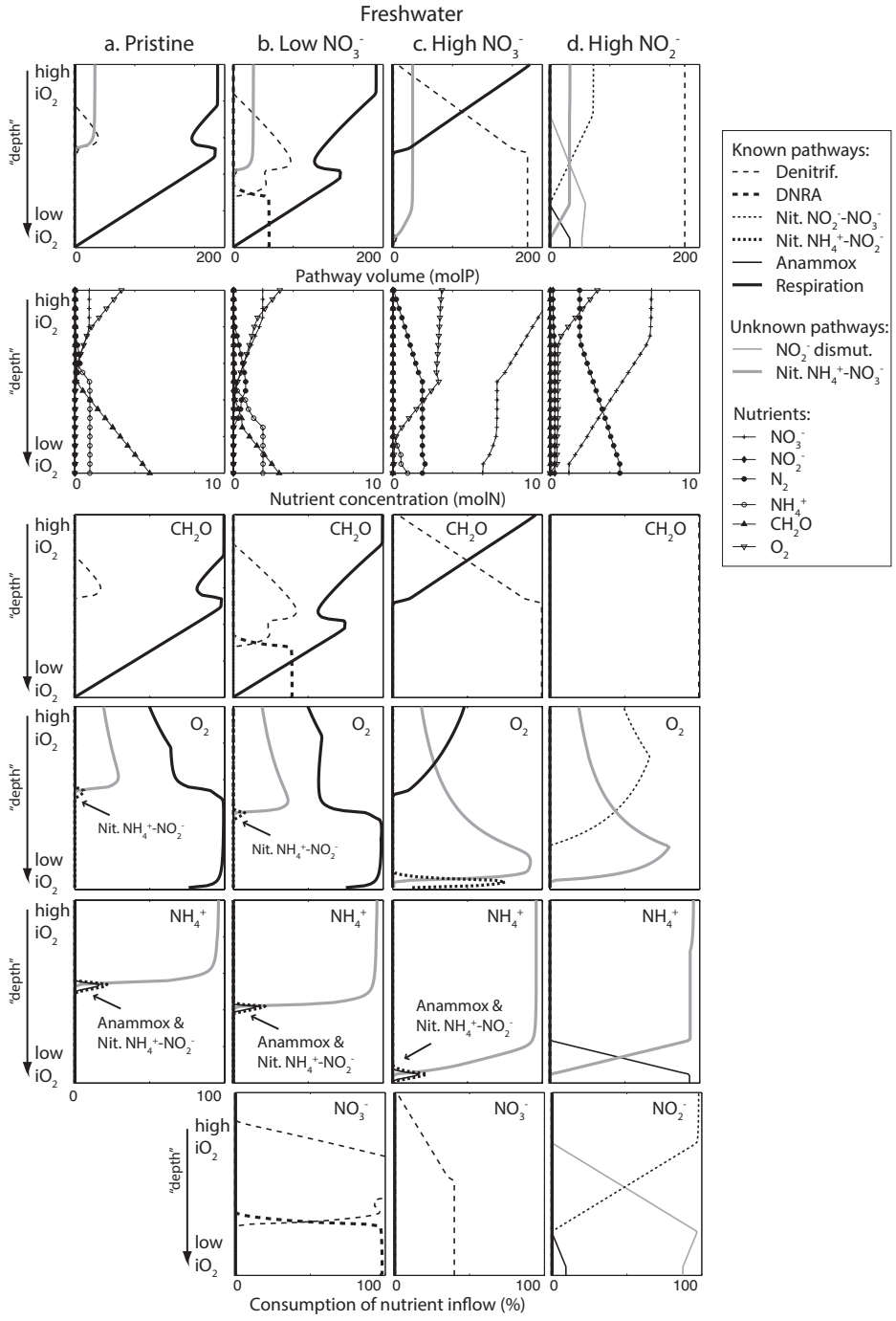

Figure 2.3. Competition simulations of the model representing four hypothetical freshwater sediments. Steady state conditions, for each simulation, of pathway volume (activity), nutrient concentration, and percentage of nutrient inflow consumed per pathway for different combinations of nutrient inflow levels along a gradient of oxygen inflow. **a)** Pristine sediment ($iNO_3^- = 0$, $iNO_2^- = 0$, $iNH_4^+ = 1$, $iCH_2O = 5$), **b)** Eutrophic (iNO_3^- low) sediment ($iNO_3^- = 1$, $iNO_2^- = 0$, $iNH_4^+ = 1$, $iCH_2O = 5$), **c)** Eutrophic (iNO_3^- high) sediment ($iNO_3^- = 10$, $iNO_2^- = 0$, $iNH_4^+ = 1$, $iCH_2O = 5$), **d)** Eutrophic (iNO_2^- high) sediment ($iNO_3^- = 0$, $iNO_2^- = 10$, $iNH_4^+ = 1$, $iCH_2O = 5$).

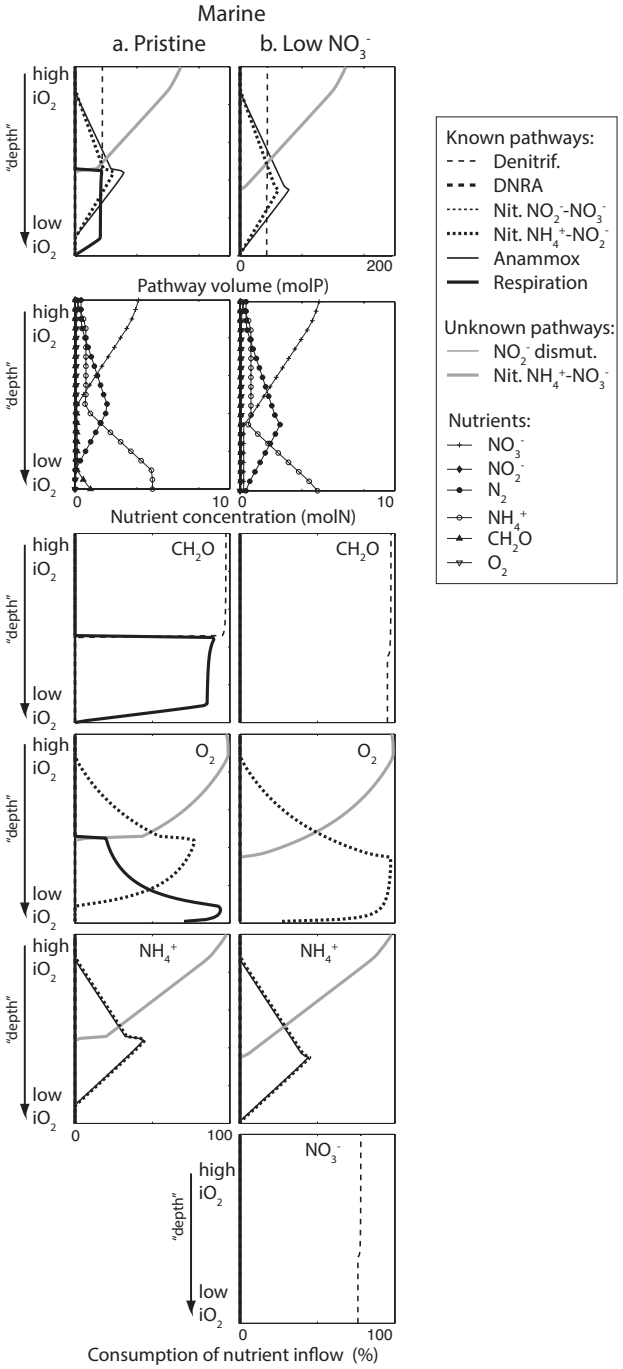

Figure 2.4. Competition simulations of the model representing two hypothetical marine sediments (as in Figure 2.3). **a)** Pristine sediment ($iNO_3^- = 0$, $iNO_2^- = 0$, $iNH_4^+ = 5$, $iCH_2O = 1$), **b)** Eutrophic (iNO_3^- low) sediment ($iNO_3^- = 1$, $iNO_2^- = 0$, $iNH_4^+ = 5$, $iCH_2O = 1$).

Because truncated denitrification to the level of nitrite, nitric oxide or nitrous oxide, were not predicted to be viable pathways (Table 2.1), we followed the non-equilibrium dynamics of the truncated denitrification pathways. We simulated a pulse of nitrate influx in an anoxic, organic environment and followed the pathway activity in time (Fig. 2.5). As long as both substrates were not limited, denitrification to the level of nitrite, nitric oxide and nitrous oxide were predicted. However, when pathways started to compete (at $t \approx 2.4$), the activity rate of denitrification to the level of dinitrogen gas continued increasing, while the activity of other pathway decreased.

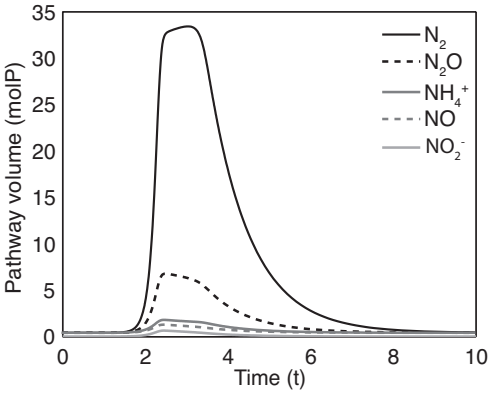

Figure 2.5. Activity of nitrate reduction pathways to the level of N_2, N_2O, NO, NH_4^+ and NO_2^- in time after a pulse of nitrate ($iNO_3^- = 10$) at $t = 1$ ($iNO_2^- = 0$, $iNH_4^+ = 0$, $iO_2 = 0$, $iCH_2O = 10$).

To test if our results are sensitive to the implemented limitation on ammonium activation, we explored the outcome of the model without this restriction. Two additional strong ammonium-consuming pathways were predicted: direct ammonium oxidation with oxygen to the level of dinitrogen gas (as a single redox reaction) and anammox using nitrate (Fig. A2.1 and A2.2). None of these pathways have been found in nature, suggesting that, indeed, ammonium oxidation requires a one-to-one reactive species.

Discussion

The model predicted the viability of almost all nitrogen pathways known to exist in nature (Table 2.1). Interestingly, this suggests that the combination of basic thermodynamic principles (stoichiometry, energy yield), and competition for substrates can already explain why most pathways are found in practice. In other words, these principles may largely determine the competitive strength of a pathway.

Strikingly, our basic principles model also predicted the viability of two unknown pathways, namely ‘nitrite dismutation’ and ‘total nitrification’ (Table 2.1). One

possibility is that these pathways do exist in nature but are not discovered. A likely alternative explanation for their absence in observations is that other biochemical restrictions may impact the viability of these pathways. Some observed pathways were not predicted by the model, but observed in nature, such as the truncated denitrification pathways. Here, we first compare the activity of known pathways for model simulations and for measurements in natural systems, then we discuss the possible existence of the two unknown pathways predicted by the model.

In the hypothetical sediments oxygen inflow was modeled as a gradient. This gradient can be thought of as sediment depth, with high oxygen inflow close to the sediment water interface. However, it is important to realize that oxygen inflow layers were modeled separately, so we did not consider diffusion of substrates through the modeled layers or porosity of the sediment. The model predictions show many similarities, but also show some deviations from what is found in nature (Fig. 2.3). These deviations may give us a hint about additional biochemical limitations or factors influencing the activity of a certain pathway. Here, we discuss for each predicted viable pathway how the model results relate to observations in nature.

DNRA is only predicted by the model in eutrophic organic sediments, when nitrate inflow is not too high (Fig. 2.3b). In nature, DNRA is indeed encountered at high $C:NO_3^-$ ratios, which is explained by the fact that DNRA, despite having a lower energy yield, consumes less nitrate per C than denitrification (Table 2.1) (Tiedje 1988; Kelso *et al.* 1997). Also, DNRA is only predicted at strictly anoxic conditions, whereas denitrification is predicted at both low and high equilibrium oxygen concentrations (Fig. 2.3b,c and 2.4b). In natural environments, DNRA is indeed measured under anoxic conditions and in deeper sediment layers than denitrification (Buresh and Patrick 1981; Jørgensen 1989; Kelso *et al.* 1997). Most denitrification activity is reported in anoxic or suboxic conditions (Seitzinger *et al.* 2006). The model suggests that denitrification could thrive in oxic conditions, when nitrate co-occurs with oxygen (Fig. 2.3c), as recently found by Gao *et al.* (2010). The lack of predicted DNRA activity in marine sediments, could be due to the fact that we did not consider sulfur compounds, while in natural systems, DNRA activity can be coupled to sulfur cycling (Brunet and Garcia-Gil 1996; An and Gardner 2002).

Anammox is mainly predicted to occur coupled to partial nitrification, due to the necessity of nitrite. In the modeled freshwater sediments, both pathways are only found at the oxic-anoxic boundary at very low rates (Fig. 2.3a, b, and c), while in the marine sediments, they are predicted over a larger range of depth under anoxic conditions. This follows from the competition for oxygen between nitrification and respiration: when ammonium levels are high compared to organic material levels (i.e. marine sediment), partial nitrification can flourish along a large range of depth by consuming the incoming oxygen and ammonium, creating anoxia, and supplying

anammox with nitrite (Fig. 2.4a and b). Anammox coupled to partial nitrification is indeed a process used in ammonium-rich wastewater treatment under oxygen limitation (Sliekers *et al.* 2002; Jetten *et al.* 2003). Not much evidence has been found for anammox in natural freshwater systems. Schubert *et al.* (2006), however, showed anammox activity at the oxic-anoxic boundary of the water column of a large lake. In marine environments, anammox is indeed found at high rates (Dalsgaard *et al.* 2005; Brandes *et al.* 2007) under strictly anoxic conditions (Kuypers *et al.* 2003; Dalsgaard *et al.* 2005; Schmid *et al.* 2007). While anammox is expected to have a high global contribution to dinitrogen production (Strous and Jetten 2004), under laboratory conditions, anammox has a very low growth rate (Strous *et al.* 1999). This cannot be explained by the model. This suggests that the low growth rate may be due to other factors than thermodynamic feasibility or resource competition.

The model predicts that partial nitrification may win the competition over total nitrification in marine sediments when oxygen is more limited than ammonium (Fig. 2.4a and b), because partial nitrification consumes less oxygen per unit of N. Experiments indeed show that partial nitrification is supported by high ammonium inflow and relatively low oxygen conditions (Ciudad *et al.* 2005). At high ammonium and oxygen inflow levels, total nitrification is predicted to feed denitrification with nitrate (Fig. 2.4a and b). Nitrification-denitrification coupling is indeed a common process found in oxic sediments and close to macrophytes (Risgaard-Petersen *et al.* 1994; Eriksson and Weisner 1999). However, as discussed before, total nitrification is in nature performed in two steps by two different pathways.

One of the unknown pathways predicted by our model, the 'nitrite dismutation' pathway, has already been suggested as a potential microbial pathway by Strohm *et al.* (2007), based on its energy yield. Generally, nitrite input in nature is much lower than nitrate input, therefore the chance to encounter this pathway is expected to be low. However, our model suggests that 'nitrite dismutation' could be directly coupled to denitrification, through nitrate (in the presence of organic material). Therefore, we suggest that it might have been overlooked in natural environments. If this pathway has evolved, we speculate that, based on our model results, 'nitrite dismutation' could be found in deeper, anoxic, layers of freshwater systems with high inflow of nitrite.

From the viability tests and the above comparison of predicted conditions with observed conditions, we can deduce that resource competition proves to be a crucial model ingredient to understand why pathways are active in certain conditions. In our model pathways and substrates are interacting dynamically, so each pathway can both limit substrate availability (i.e. anoxia), and create conditions in which other pathways can flourish (i.e. coupled nitrification-denitrification). As a result, the ecological fitness of each pathway is determined by its efficiency of consuming substrates.

There is, however, a conspicuous deviation between the model predictions and the patterns observed in nature. Our model predicted the highest fitness for the longest pathways, whereas this is not always the case in nature. For instance, complete denitrification in the model always outcompeted the truncated denitrification found in nature. In addition, the second unknown pathway predicted by our model, total nitrification, existed side by side in the simulations with ammonium oxidation to nitrite, while nitrification from nitrite was not predicted at all. What might explain such differences between our theoretical prediction and reality?

Interestingly, after a pulse of nitrate, activity of denitrification pathways to the level of nitrous oxide, nitric oxide and nitrite is temporarily high (Fig. 2.5). This result nicely shows that during an ecological feast, when resources are abundant, the selective forces are weak, as there is hardly any competition. Experiments indeed show higher denitrification activity to the level of nitrous oxide with high nitrate concentrations (Firestone *et al.* 1980). In our former analyses, we considered only equilibrium conditions (arising when at least one of the substrates becomes limited). Thus, the pulse simulation illustrates that the lack of dynamic conditions (feast and famine) may explain why these analyses do not predict truncated denitrification pathways.

Still, such non-equilibrium dynamics do not appear to explain the fact that total nitrification is not observed in nature. Costa *et al.* (2006) suggested that the more steps are included in a pathway, the more enzymes and (possibly toxic) intermediates are involved, which makes long pathways less beneficial than short pathways. We explored whether this could explain the lack of total nitrification in nature, by adapting individual maintenance costs relative to an estimated number of steps in a pathway (Appendix A2). Indeed, we found a parameter range of pathway length costs where total nitrification was always outcompeted by the two partial nitrification pathways and where nitrate to nitrite reduction was additionally predicted at high nitrate inflow levels. However, for that parameter range, anammox showed relatively high activity, also in oxic conditions, while denitrification and DNRA were relatively weak competitors (Fig. A2.3 and A2.4). This suggests that costs may indeed be an important factor influencing the fitness of long pathways, and thus the existence of pathways like total nitrification. However, assuming a linear relation between the number of enzymes and costs is probably too simplistic. Obviously, differences in regulatory mechanisms, protein sizes, and the level of toxicity of intermediates may also play a role.

Apart from the two exceptions described, our analysis suggests that the current inventory of nitrogen cycle pathways may be complete. However, many of the other pathways of Table A2.1 that were predicted to have low fitness today may still have been important in the past, before the evolution of the currently observed pathways. For example, it has been suggested that the oxidation and reduction of toxic nitrogen cycle intermediates such as nitric oxide was a prerequisite for the evolution of the current nitrogen cycle processes (Klotz and Stein 2008; Klotz *et al.* 2008). In our model systems such toxic compounds never accumulated, only occurred as intermediates or were consumed by other processes. Therefore, there was no need to consider toxicity or inhibition in our model.

Obviously, many relevant aspects were excluded or highly simplified in our model. For instance, we do not account for the inflow of alternative electron donors or acceptors, such as S-, and Fe- compounds (Brunet and Garcia-Gil 1996; Weber *et al.* 2001, 2006), or the effect of temperature on pathway activity (Tijhuis *et al.* 1993). Also, we did not consider environmental variation in inflow of substrates, such as the availability and quality of organic material which could affect the activity of the nitrogen pathways (Burford and Bremner 1975). Inclusions of such aspects in future models may allow a more complete prediction of theoretical pathways. However, our minimal model analysis suggests that much of the seemingly complex repertoire of nitrogen pathways in nature may be understood from a few simple basic principles.

Conclusions

The realism of the results we obtained suggests that our minimal model may capture much of the essence of what drives microbial nitrogen processes in the real world. Our findings imply that the fitness of a catabolic nitrogen pathway may be determined largely by stoichiometry and energy yield of the performed redox reaction, and that the activity of each pathway at certain environmental conditions can simply be explained from competition for limited resources.

The few discrepancies between predictions and observations hint at the importance of non-equilibrium dynamics and of biochemical barriers that may exclude certain nitrogen pathways, such as a high ammonium activation energy and costs relative to pathway length. An interesting remaining discrepancy is the prediction of the dismutation of nitrite, to the level of nitrate and dinitrogen gas. We suggest that this could well be a viable, yet undiscovered, pathway that might well play a role in systems with high nitrite and low oxygen levels.

Experimental procedures

Theoretical pathways

We created a list of theoretical pathways (Table A2.1) in several steps. First, we determined all possible half reactions involving organic material (CH_2O), oxygen (O_2) and the nitrogen compounds nitrate (NO_3^-), nitrite (NO_2^-), nitric oxide (NO), nitrous oxide (N_2O), dinitrogen gas (N_2) and ammonium (NH_4^+). Then, we combined the electron accepting and electron donating half reactions resulting in a complete list of possible redox reactions. We then removed redox reactions with overlapping intermediates in both half reactions, because if a reductant of a half reaction is the oxidant in the complementary half reaction and vice versa, the reaction cannot proceed. Finally, we calculated the Gibbs free energy change per electron transfer for each reaction, by subtracting the total standard formation energy of substrates from the total standard formation energy of products, for standard conditions: 1 atm pressure, 1 M concentration, pH $=7$ (as in Madigan *et al.* (2003)). For organic material, we used the standard formation energy of glucose. Reactions with a negative Gibbs free energy change, and thus energy yield, were included in the final pathway list. This resulted in 62 thermodynamically possible pathways (Table A2.1).

The list of theoretical pathways was modified to include the ammonium activation restriction. Pathways in which NH_4^+ is not oxidized by O_2 as the primary substrate, or NO as an intermediate or primary substrate, were removed from the list. NO was considered an intermediate or primary substrate when the oxidation state of the substrate was lower or the oxidation state of the product was higher or equal than that of NO ($+2$). Pathways that could be activated by O_2 or NO, were removed from the list when the [oxidizer: NH_4^+] ratio was smaller than 1. The final model consisted of 45 pathways (Table A2.1).

Model description

Our model is an ordinary differential equation (ODE) model with 53 differential equations, namely 45 competing theoretical pathways and 8 nutrients (NO_3^-, NO_2^-, NO, N_2O, N_2, NH_4^+, O_2 and CH_2O). The model equations and parameters are given in Table 2.2.

In this study, we are interested in relative rather than absolute differences between pathway volume and between nutrient concentrations, therefore the units of these variables are undefined, and called ‘molP’ and ‘molS’. For the same reason, most general parameters applying to all pathways were simply set to one. The individual

pathway parameters are the nutrient concentrations involved in the transfer of one electron (s), and the energy yield for the transfer of one electron (ΔG). Both parameters were derived from the theoretical pathways list (Table A2.1).

Table 2.2. Model equations and parameters of the model.

Nutrient concentration (in molS):

$$\frac{dN_k}{dt} = i_k - \sum_{j=1} s_{k,j} M_j P_j + \sum_{j=1} p_{k,j} M_j P_j - eN_k \qquad k=1,...8\ j=1,...45 \qquad (1)$$

Electron transfer rate (in molP-1t-1) for pathway j using nutrients N_1 and N_2:

$$M_j = r\left(\frac{N_1}{N_1 + s_{1,j}}\right)\left(\frac{N_2}{N_2 + s_{2,j}}\right) \qquad j=1,...45 \qquad (2)$$

Pathway volume (in molP):

$$\frac{dP_j}{dt} = b\Delta G_j M_j P_j - dP_j \qquad j=1,...45 \qquad (3)$$

Parameters	Description	Value	Units
ΔG_j	Gibbs free energy yield for the transfer of one electron, for pathway j	Table A2.1	kJ
$s_{k,j}$ and $p_{k,j}$	Stoichiometric factor for nutrient k, for pathway j	Table A2.1	molS
i_k	Inflow of nutrient k	0-10	molS t^{-1}
e	Outflow rate	1	t^{-1}
r	Maximum electron transfer rate	1	molP^{-1}t^{-1}
b	Energy-to-volume-conversion rate	-0.1	molP kJ^{-1}
d	Maintenance costs	1	t^{-1}

Nutrients (N) are assumed to flow through the system with a constant inflow (i) and a concentration dependent outflow rate (e), while being consumed and produced by the theoretical pathways, like a chemostat (Table 2.2: Eqn. 1). Nutrient consumption and production of each pathway are calculated by multiplying the nutrient concentration involved in the transfer of one electron (s and p), the electron transfer rate per molP (M) and the pathway volume (P).

The electron transfer rate per molP (M) for each pathway is assumed to be limited by mass transfer. We captured this in the model by implementing double Monod kinetics, with the nutrient concentration of the substrates involved in the transfer of one electron (s) as the half saturation factor (Table 2.2: Eqn. 2). In this way, the maximum electron transfer rate (r) is reached at lower nutrient concentrations when nutrient consumption per electron is low.

The growth of each pathway per molP is calculated by multiplying the energy yield for the transfer of one electron (ΔG), the electron transfer rate per molP (M), and the pathway volume (P). Maintenance costs (d) are considered constant per molP (Table 2.2: Eqn. 3). Because energy yield is negative, ΔG is converted to volume by an energy-to-volume-conversion factor (b), in this way the maximal growth rate ranges from approximately 1 to 17 molP/t.

An equilibrium is established when nutrient concentrations and pathway activity do not change in time. The final nutrient concentration is the residual of inflow, consumption and production. Total consumption stabilizes when each pathway has depleted one of its nutrients. Thus the final pathway volume in the model is determined by the relative differences in nutrient inflow rates. Therefore, pathway volume, or activity, is a relative measure as well, so it can only be judged qualitatively, not quantitatively. We studied different combinations of substrate inflow levels, for both random and competition simulations. All simulations were carried out in Grind for Matlab (http://www.sparcs-center.org/grind).

Appendix A2

Model without ammonium activation restriction

To investigate the effect of the ammonium activation restriction, we repeated the simulations as in Figure 2.3 and 2.4 in the main text, including pathways in which ammonium can not be activated one-to-one with a reactive species (Table A2.1: starred pathway numbers). Two unknown pathways showed strong activity (Fig A2.1 and A2.2): ammonium oxidation to the level of dinitrogen gas (Table A2.1: Eqn. 61) and anammox using nitrate (Table A2.1: Eqn. 14).

Maintenance costs relative to pathway length

A theoretical explanation considering enzymatic and intermediate costs has been proposed by Costa *et al.* (2006). The more steps are included in a pathway, the more enzymes and intermediates are involved. This implies that a long pathway is associated with relatively high costs, since enzyme synthesis requires ATP, carbon and other substrates while intermediates can have toxic effects (Pfeiffer and Bonhoeffer 2004; Costa *et al.* 2006).

To implement this constraint in our model, we made a general estimation for the number of enzymes involved in a theoretical pathway. We assumed that every step involving the making and breaking of N-O, N-N, C-O and O-O bonds needs to be catalyzed by one enzyme. For example for denitrification from NO_3^- to N_2 three oxygen atoms have to be removed and one nitrogen atom has to be added, therefore the estimated number of enzymes for this half reaction is four. This estimation is correct for the majority of the known pathways, for example the denitrification pathway includes four enzymes catalyzing the following steps: $NO_3^- \rightarrow NO_2^- \rightarrow NO \rightarrow N_2O \rightarrow N_2$ (van Spanning *et al.* 2007). We included the costs-for-pathway-length as a constant decay rate in the pathway biomass equation:

$$\frac{dP_j}{dt} = b\Delta G_j M_j P_j - dP_j - cLP_j$$

where L is the estimated pathway length, and c the costs-for-pathway-length.

We performed several simulations with different costs factors. At c=0.4, 'total nitrification' could not win the competition in any of the simulations with random inflow levels (Fig. A2.3 and A2.4). For this parameter setting, two other known 'short pathways' appeared: nitrate reduction to nitrite (active at high nitrate levels), and denitrification from the level of nitrite to dinitrogen (active at high nitrite levels under anoxic conditions). Anammox showed relatively high activity, also at oxic conditions, while denitrification and DNRA were weak competitors.

Table A2.1. Theoretical pathways involving the nitrogen compounds nitrate (NO_3^-), nitrite (NO_2^-), nitric oxide (NO), nitrous oxide (N_2O), nitrogen gas (N_2), ammonium (NH_4^+), organic material (CH_2O) and oxygen (O_2). The reaction coefficients and the energy yield are calculated per electron transfer. The pathways indicated with a star were not included in the model, due to the ammonium activation restriction.

Nr	Reactants		Products	ΔG
1	$1/2\ NO_3^- + NO + 1/2\ H_2O$	→	$1\ 1/2\ NO_2^+ + H^+$	-7.8645
2 *	$1/2\ NO_3^- + 1/6\ NH_4^+$	→	$2/3\ NO_2^- + 1/3\ H^+ + 1/6\ H_2O$	-8.7375
3 *	$1/2\ NO_3^- + 1/5\ NH_4^+$	→	$1/2\ NO_2^- + 1/5\ NO + 1/5\ H^+ + 3/10\ H_2O$	-8.9121
4 *	$1/2\ NO_3^- + 1/4\ NH_4^+$	→	$1/2\ NO_2^- + 1/8\ N_2O + 1/4\ H^+ + 3/8\ H_2O$	-29.027
5 *	$1/2\ NO_3^- + 1/3\ NH_4^+$	→	$1/2\ NO_2^- + 1/6\ N_2 + 1/3\ H^+ + 1/2\ H_2O$	-8.421
6	$1/2\ NO_3^- + 1/4\ CH_2O$	→	$1/2\ NO_2^- + 1/4\ CO_2 + 1/4\ H_2O$	-82.65
7 *	$1/3\ NO_3^- + 1/5\ NH_4^+ + 2/15\ H^+$	→	$8/15\ NO + 7/15\ H_2O$	-6.2906
8 *	$1/3\ NO_3^- + 1/4\ NH_4^+ + 1/12\ H^+$	→	$1/3\ NO + 1/8\ N_2O + 13/24\ H_2O$	-26.405
9 *	$1/3\ NO_3^- + 1/3\ NH_4^+$	→	$1/3\ NO + 1/6\ N_2 + 2/3\ H_2O$	-65.8
10	$1/3\ NO_3^- + 1/4\ C\ H_2O + 1/3\ H^+$	→	$1/3\ NO + 1/4\ CO_2 + 5/12\ H_2O$	-80.028
11*	$1/4\ NO_3^- + 1/4\ NH_4^+$	→	$1/4\ N_2O + 1/2\ H_2O$	-44.947
12*	$1/4\ NO_3^- + 1/3\ NH_4^+$	→	$1/8\ N_2O + 1/6\ N_2 + 1/12\ H^+ + 5/8\ H_2O$	-84.342
13	$1/4\ NO_3^- + 1/4\ CH_2O + 1/4\ H^+$	→	$1/8\ N_2O + 1/4\ CO_2 + 3/8\ H_2O$	-98.57
14*	$1/5\ NO_3^- + 1/3\ NH_4^+$	→	$4/15\ N_2 + 2/15\ H^+ + 3/5\ H_2O$	-98.989
15	$1/5\ NO_3^- + 1/4\ CH_2O + 1/5\ H^+$	→	$1/10\ N_2 + 1/4\ CO_2 + 7/20\ H_2O$	-113.22
16	$1/8\ NO_3^- + 1/4\ CH_2O + 1/4\ H^+$	→	$1/8\ NH_4^+ + 1/4\ CO_2 + 1/8\ H_2O$	-76.097
17	$NO_2- + 1/2\ H^+$	→	$1/2\ NO_3^- + 1/4\ N_2O + 1/4\ H_2O$	-31.841
18	$5/6\ NO_2^- + 1/3\ H^+$	→	$1/2\ NO_3^- + 1/6\ N_2 + 1/6\ H_2O$	-50.946
19	$1/2\ NO_2^- + NO$	→	$1/2\ NO_3^- + 1/2\ N_2O$	-71.547
20	$1/2\ NO_2^- + 1/2\ NO$	→	$1/2\ NO_3^- + 1/4\ N_2$	-80.352
21	$1/2\ NO_2^- + 1/2\ N_2O$	→	$1/2\ NO_3^- + 1/2\ N_2$	-89.157
22	$1/2\ NO_2^- + 1/4\ O_2$	→	$1/2\ NO_3^-$	-37.067
23*	$NO_2^- + 1/5\ NH_4^+ + 4/5\ H^+$	→	$6/5\ NO + 4/5\ H_2O$	-1.0476
24*	$NO_2^- + 1/4\ NH_4^+ + 3/4\ H^+$	→	$NO + 1/8\ N_2O + 7/8\ H_2O$	-21.162
25*	$NO_2^- + 1/3\ NH_4^+ + 2/3\ H^+$	→	$NO + 1/6\ N_2 + H_2O$	-60.557
26	$NO_2^- + 1/4\ CH_2O + H^+$	→	$NO + 1/4\ CO_2 + 3/4\ H_2O$	-74.785
27	$1/2\ NO_2^- + 1/4\ NH^{4+} + 1/4\ H^+$	→	$3/8\ N_2O + 5/8\ H_2O$	-60.868
28	$1/2\ NO_2^- + 1/3\ NH_4^+ + 1/6\ H^+$	→	$1/4\ N_2O + 1/6\ N_2 + 3/4\ H_2O$	-100.26
29	$1/2\ NO_2^- + 1/4\ CH_2O + 1/2\ H^+$	→	$1/4\ N_2O + 1/4\ CO_2 + 1/2\ H_2O$	-114.49
30	$1/3\ NO_2^- + 1/3\ NH_4^+$	→	$1/3\ N_2 + 2/3\ H_2O$	-119.37
31	$1/3\ NO_2^- + 1/4\ CH_2O + 1/3\ H^+$	→	$1/6\ N_2 + 1/4\ CO_2 + 5/12\ H_2O$	-133.6
32	$1/6\ NO_2^- + 1/4\ CH_2O + 1/3\ H^+$	→	$1/6\ NH_4^+ + 1/4\ CO_2 + 1/12\ H_2O$	-73.912
33	$4/3\ NO + 1/6\ H_2O$	→	$1/3\ NO_3^- + 1/2\ N_2O + 1/3\ H^+$	-74.168
34	$5/6\ NO + 1/6\ H_2O$	→	$1/3\ NO_3^- + 1/4\ N_2 + 1/3\ H^+$	-82.974

35	$1/3\ NO + 1/2\ N_2O + 1/6\ H_2O$	→	$1/3\ NO_3^- + 1/2\ N_2 + 1/3\ H^+$	-91.779
36	$1/3\ NO + 1/4\ O_2 + 1/6\ H_2O$	→	$1/3\ NO_3^- + 1/3\ H^+$	-39.689
37	$2\ NO + 1/2\ H_2O$	→	$NO_2^- + 1/2\ N_2O + H^+$	-79.411
38	$3/2\ NO + 1/2\ H_2O$	→	$NO_2^- + 1/4\ N_2 + H^+$	-88.216
39	$NO + 1/2\ N_2O + 1/2\ H_2O$	→	$NO_2^- + 1/2\ N_2 + H^+$	-97.022
40	$NO + 1/4\ O_2 + 1/2\ H_2O$	→	$NO_2^- + H^+$	-44.931
41	$NO + 1/4\ NH_4^+$	→	$5/8\ N_2O + 1/4\ H^+ + 3/8\ H_2O$	-100.57
42	$NO + 1/3\ NH_4^+$	→	$1/2\ N_2O + 1/6\ N_2 + 1/3\ H^+ + 1/2\ H_2O$	-139.97
43	$NO + 1/4\ CH_2O$	→	$1/2\ N_2O + 1/4\ CO_2 + 1/4\ H_2O$	-154.2
44	$1/2\ NO + 1/3\ NH_4^+$	→	$5/12\ N_2 + 1/3\ H^+ + 1/2\ H_2O$	-148.77
45	$1/2\ NO + 1/4\ CH_2O$	→	$1/4\ N_2 + 1/4\ CO_2 + 1/4\ H_2O$	-163
46	$1/5\ NO + 1/4\ CH_2O + 1/5\ H^+ + 1/20\ H_2O$	→	$1/5\ NH_4^+ + 1/4\ CO_2$	-73.738
47	$5/8\ N_2O + 1/8\ H_2O$	→	$1/4\ NO_3^- + 1/2\ N_2 + 1/4\ H^+$	-73.236
48	$1/8\ N_2O + 1/4\ O_2 + 1/8\ H_2O$	→	$1/4\ NO_3^- + 1/4\ H^+$	-21.146
49	$3/4\ N_2O + 1/4\ H_2O$	→	$1/2\ NO_2^- + 1/2\ N_2 + 1/2\ H^+$	-57.316
50	$1/4\ N_2O + 1/4\ O_2 + 1/4\ H_2O$	→	$1/2\ NO_2^- + 1/2\ H^+$	-5.2258
51	N_2O	→	$NO + 1/2\ N_2$	-17.61
52*	$1/2\ N_2O + 1/3\ NH_4^+$	→	$2/3\ N_2 + 1/3\ H^+ + 1/2\ H_2O$	-157.58
53	$1/2\ N_2O + ¼\ CH_2O$	→	$1/2\ N_2 + 1/4\ CO_2 + 1/4\ H_2O$	-171.81
54	$1/8\ N_2O + 1/4\ CH_2O + 1/4\ H^+ + 1/8\ H_2O$	→	$1/4\ NH_4^+ + 1/4\ CO_2$	-53.623
55	$1/10\ N_2 + 1/4\ O_2 + 1/10\ H_2O$	→	$1/5\ NO_3^- + 1/5\ H+$	-6.4991
56	$1/6\ N_2 + 1/4\ CH_2O + 1/3\ H^+ + 1/4\ H_2O$	→	$1/3\ NH_4^+ + 1/4\ CO_2$	-14.228
57	$1/8\ NH_4^+ + 1/4\ O_2$	→	$1/8\ NO_3^- + 1/4\ H^+ + 1/8\ H_2O$	-43.62
58	$1/6\ NH_4^+ + 1/4\ O_2$	→	$1/6\ NO_2^- + 1/3\ H^+ + 1/6\ H_2O$	-45.804
59*	$1/5\ NH_4^+ + 1/4\ O_2$	→	$1/5\ NO + 1/5\ H^+ + 3/10\ H_2O$	-45.979
60*	$1/4\ NH_4^+ + 1/4\ O_2$	→	$1/8\ N_2O + 1/4\ H^+ + 3/8\ H_2O$	-66.094
61*	$1/3\ NH_4^+ + 1/4\ O_2$	→	$1/6\ N_2 + 1/3\ H^+ + 1/2\ H_2O$	-105.49
62	$1/4\ CH_2O + 1/4\ O_2$	→	$1/4\ CO_2 + 1/4\ H_2O$	-119.72

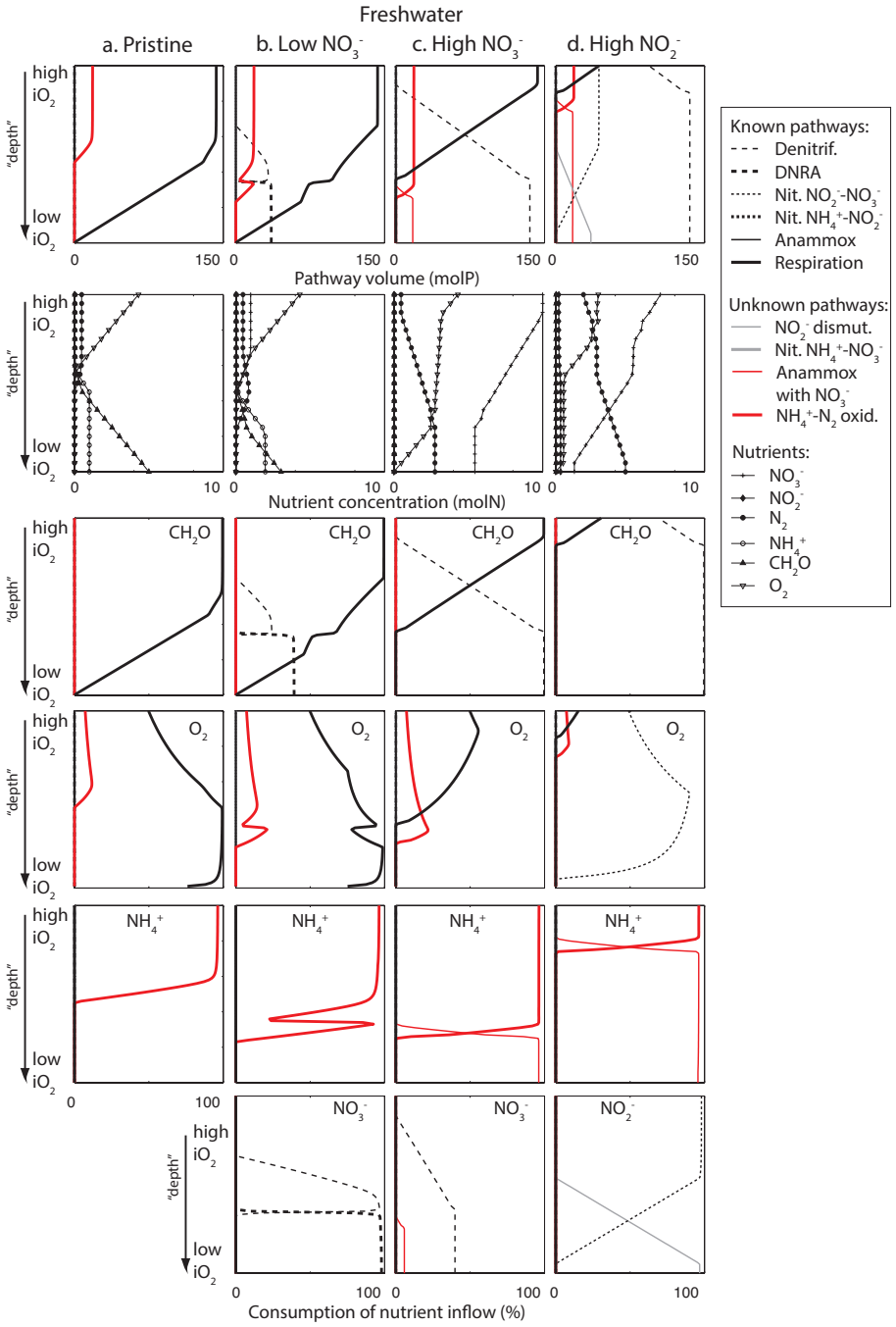

Figure A2.1. Competition simulations of the model without ammonium activation restriction representing four hypothetical freshwater sediments. Steady state conditions, for each simulation, of pathway volume (activity), nutrient concentration, and percentage of nutrient inflow consumed per pathway for different combinations of nutrient inflow levels along a gradient of oxygen inflow. **a)** Pristine sediment ($iNO_3^- = 0$, $iNO_2^- = 0$, $iNH_4^+ = 1$, $iCH_2O = 5$), **b)** Eutrophic (iNO_3^- low) sediment ($iNO_3^- = 1$, $iNO_2^- = 0$, $iNH_4^+ = 1$, $iCH_2O = 5$), **c)** Eutrophic (iNO_3^- high) sediment ($iNO_3^- = 10$, $iNO_2^- = 0$, $iNH_4^+ = 1$, $iCH_2O = 5$), **d)** Eutrophic (iNO_2^- high) sediment ($iNO_3^- = 0$, $iNO_2^- = 10$, $iNH_4^+ = 1$, $iCH_2O = 5$).

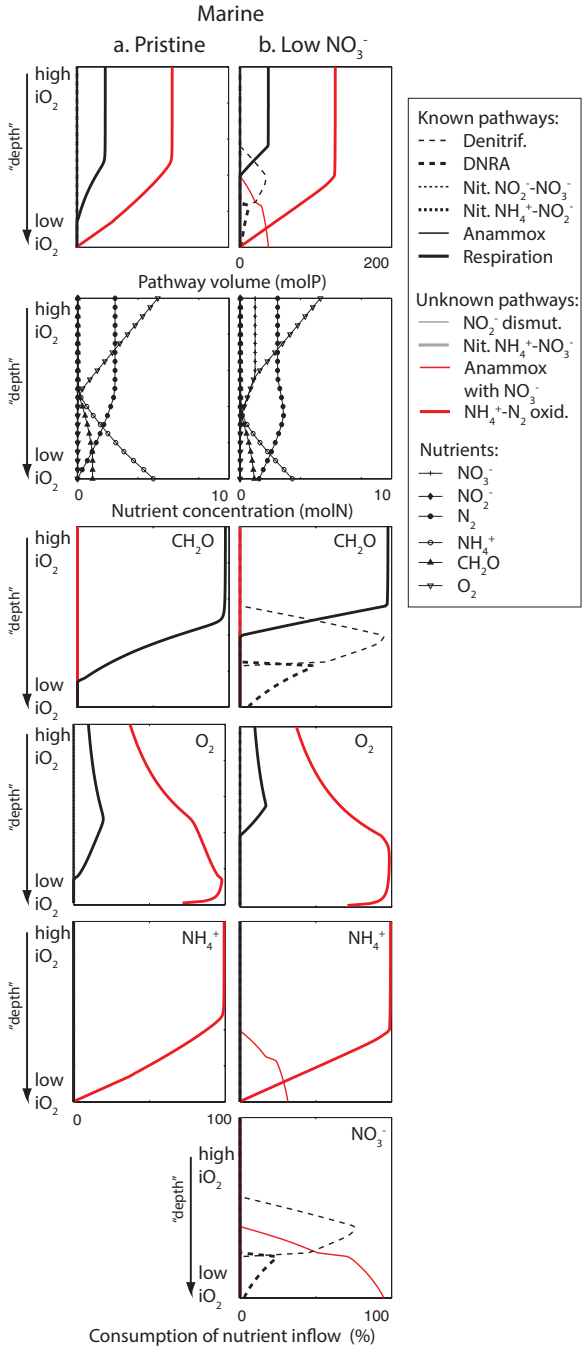

Figure A2.2. Competition simulations of the model without ammonium activation restriction representing two hypothetical marine sediments (as in Figure A2.1). **a)** Pristine sediment ($iNO_3^- = 0$, $iNO_2^- = 0$, $iNH_4^+ = 5$, $iCH_2O = 1$), **b)** Eutrophic (iNO_3^- low) sediment ($iNO_3^- = 1$, $iNO_2^- = 0$, $iNH_4^+ = 5$, $iCH_2O = 1$).

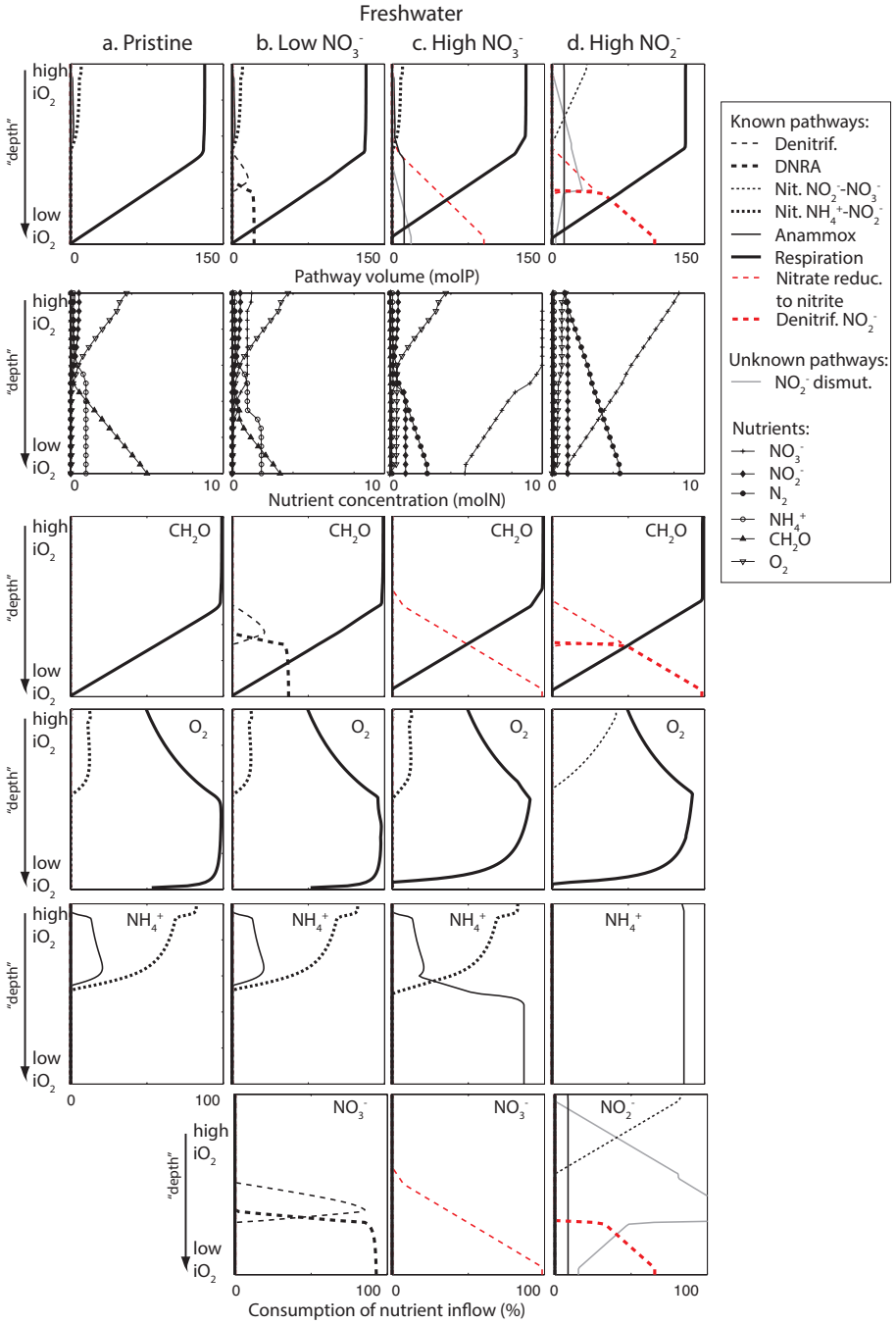

Figure A2.3. Competition simulations of the model including the costs-for-pathway-length assumption, representing four hypothetical freshwater sediments. Steady state conditions, for each simulation, of pathway volume (activity), nutrient concentration, and percentage of nutrient inflow consumed per pathway for different combinations of nutrient inflow levels along a gradient of oxygen inflow. **a)** Pristine sediment ($iNO_3^- = 0$, $iNO_2^- = 0$, $iNH_4^+ = 1$, $iCH_2O = 5$), **b)** Eutrophic (iNO_3^- low) sediment ($iNO_3^- = 1$, $iNO_2^- = 0$, $iNH_4^+ = 1$, $iCH_2O = 5$), **c)** Eutrophic (iNO_3^- high) sediment ($iNO_3^- = 10$, $iNO_2^- = 0$, $iNH_4^+ = 1$, $iCH_2O = 5$), **d)** Eutrophic (iNO_2^- high) sediment ($iNO_3^- = 0$, $iNO_2^- = 10$, $iNH_4^+ = 1$, $iCH_2O = 5$).

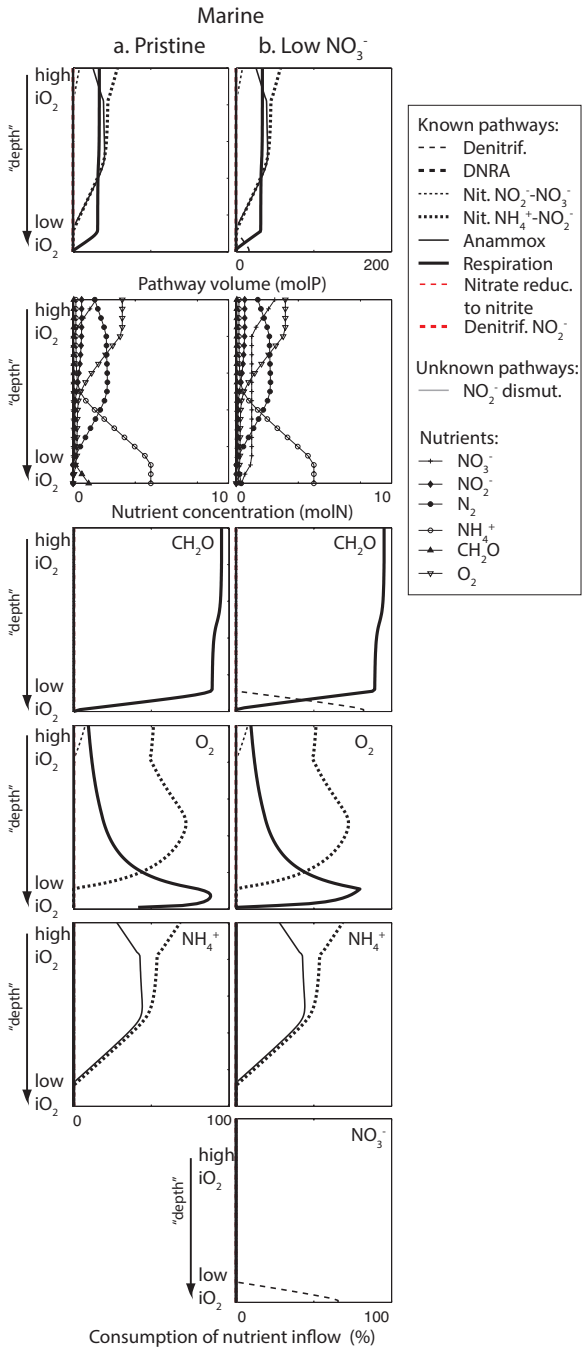

Figure A2.4. Competition simulations of the model including the costs-for-pathway-length assumption, representing two hypothetical marine sediments (as in Figure A2.3). **a)** Pristine sediment ($iNO_3^- = 0$, $iNO_2^- = 0$, $iNH_4^+ = 5$, $iCH_2O = 1$), **b)** Eutrophic (iNO_3^- low) sediment ($iNO_3^- = 1$, $iNO_2^- = 0$, $iNH_4^+ = 5$, $iCH_2O = 1$).

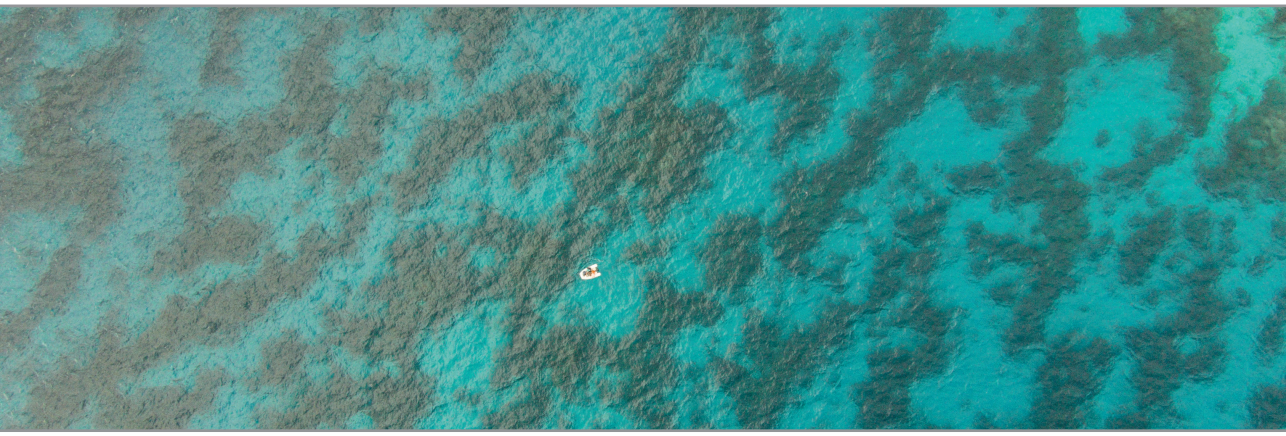

Chapter 3

Turing patterns linked to growth and resilience of coral reefs

Ingrid A. van de Leemput,
Egbert H. van Nes,
Johan van de Koppel,
Terry P. Hughes,
Sjoerd Doggen,
Babak M. S. Arani,
and Marten Scheffer

Abstract

Regular patterns in nature ranging from leopard skins to vegetation bands are driven by a fundamental class of self-organizing mechanisms discovered by the mathematician Alan Turing. Here we show the widespread occurrence of previously unrecognized Turing patterns on coral reefs in Australia and New Caledonia. Since the fundamental conditions for the formation of Turing patterns are well understood, our finding points to a specific set of testable mechanisms that govern reef growth at these scales. Moreover, the characteristic spectrum of dots, labyrinths, gaps and bands that we reveal reflects a gradient in stress, and thus indicates differences in resilience. Our finding points at novel ways to use remotely sensed information for assessment of coral reef resilience.

In a classical paper in 1952, Alan Turing demonstrated how spontaneous spatial pattern formation can be explained by the principle of diffusion-driven instability (Turing 1952). Addressing the fundamental question of how an initially perfectly symmetric group of identical cells could start to differentiate into an embryo, Turing showed that under particular conditions a homogeneous distribution of matter can become unstable. A slight perturbation is then enough to trigger a spontaneous redistribution that produces a regular spatial pattern. Such 'Turing instability' has recently been shown to drive the embryonic development of feathers (Harris *et al.* 2005) and limbs (Raspopovic *et al.* 2014). The same fundamental principle can explain a particular set of patterns that are found across remarkably different systems in nature, for example on animal skins (Murray 2003) (Fig. 3.1a-b) (e.g. tiger, leopard, zebra, many fish species), and in different ecosystems, such as arid vegetation (Rietkerk *et al.* 2002) (Fig. 3.1c), peatlands (Rietkerk and van de Koppel 2008; Eppinga *et al.* 2009) (Fig. 3.1d), and intertidal flats (Weerman *et al.* 2010).

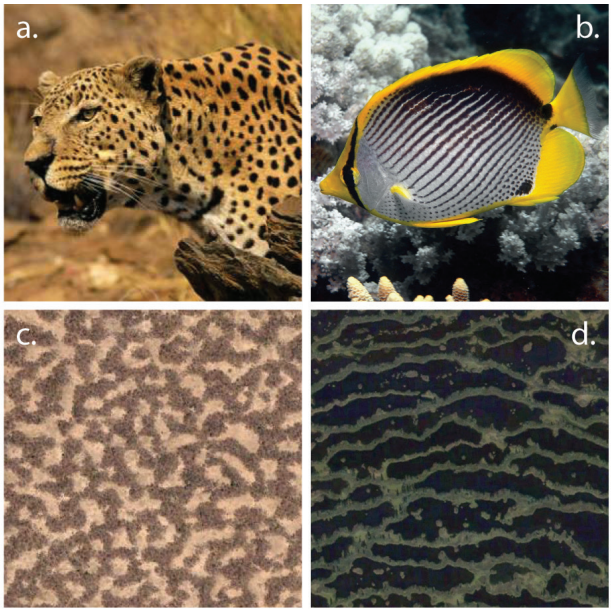

Figure 3.1. Examples of observed Turing patterns in nature: **a)** leopard skin, **b)** fish skin (butterfly fish), **c)** desert vegetation (Niger, Google Earth [12°38'19"N 3°13'04"E]), and **d)** peatland (Finland, Google Earth [62°48'51"N 30°48'13"E]).

Turing patterns can be distinguished from other regular patterns by the characteristic repertoire of sub-types, including spots, labyrinth, gaps, and parallel bands (Rietkerk *et al.* 2002). The entire repertoire is often encountered together, because all sub-types can arise from a single mechanism driven by Turing instability, with local conditions determining the actual pattern (Klausmeier 1999; von Hardenberg *et al.* 2001; Rietkerk *et al.* 2004). In ecosystems, Turing patterns are often linked to spatial fluxes of resources and growth inhibitors,

resulting in productive patches and non-productive regions between patches (Meinhardt 1982). Moreover, a consistent change of spatial patterning can be indicative of a loss of ecological resilience (Meron *et al.* 2004; Rietkerk *et al.* 2004).

Here we report the widespread occurrence of previously unnoticed Turing patterns in coral reefs (Figs. 3.2 and 3.3). Analyzing Google Earth satellite images, we found small-scale (10s of meters) regular patterns across the Great Barrier Reef and in New Caledonia (Fig. 3.2, see also Appendix A3). The patterns are located in the lagoonal habitat in the lee of the individual platform and ribbon reefs (Fig. 3.2) at depths ranging from 8 to 20 meters, and comprise corals patches surrounded by soft sediments (see underwater images in Appendix A3). The patterns can be distinguished on aerial photographs (Fig. 3.2), and on the latest high-resolution satellite images (see Appendix A3). Currently, images of only a small number of reefs are available in high definition, so it is likely that the patterns are much more common and widespread than indicated in Figure 3.2.

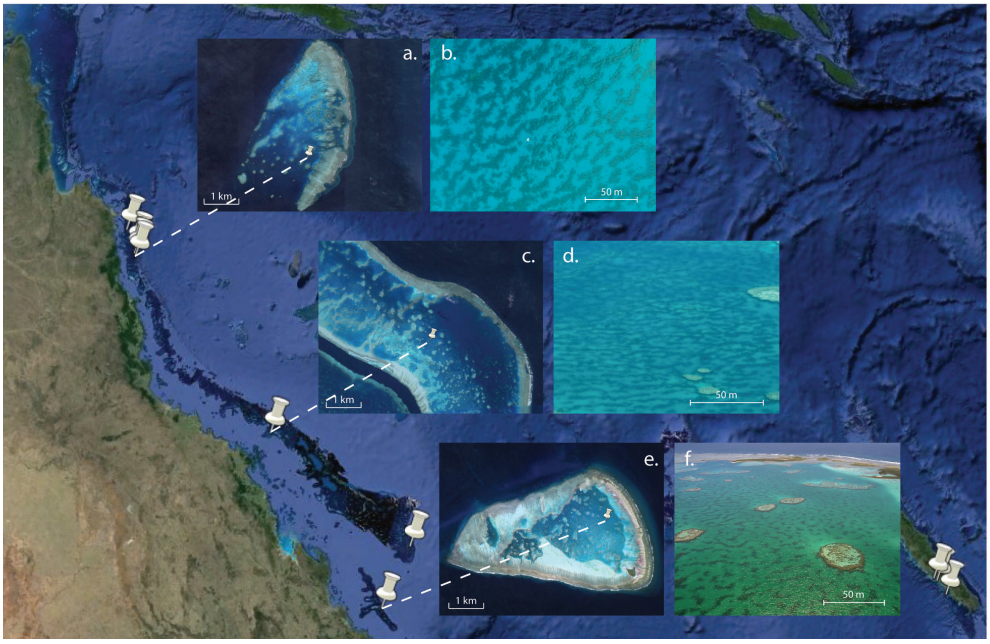

Figure 3.2. Observed Turing patterns on the Great Barrier Reef and New Caledonia. White pins indicate locations at which patterns were observed. **a)** Agincourt Reef (Google Earth [15°57'25"S 145°49'20"E]), **b)** patterns on Agincourt Reef (photo by Sjoerd Doggen), **c)** Hardy Reef (Google Earth [19°45'59"S 149°14'58"E]), **d)** patterns on Hardy Reef (photo by GBRMPA), **e)** One Tree Island Reef (Google Earth [23°29'40"S 152°5'2"E]), **f)** patterns on One Tree Island Reef (photo by GBRMPA). Scales were estimated using satellite images. The scales in panels d and f are specific to the location of the bar.

Several lines of evidence indicate that the detected patterns are indeed generated by a mechanism involving Turing instability. First of all, a spectral wave analysis of aerial images (as in Renshaw and Ford (1983)) reveals that the patterns are significantly regular (see Fig. A3.1). Such regularity excludes the possibility that the observed patterns simply arise from aggregation through growth and settlement of corals on randomly distributed hard substrate, such as coral rubble or shells. Simple physical forces can create regular patterns as in ripples and dunes. On coral reefs, one may think for example of rows of storm-generated fragments on reef flats (Scoffin 1993), or the linear spur and groove systems that are aligned with the flow of onshore waves, commonly observed on shallow exposed fore-reefs around the world (Roberts *et al.* 1992). However, such phenomena cannot explain the presence of the characteristic full repertoire of Turing patterns we have documented in sheltered lagoons. Indeed, the entire set of sub-types (i.e. spots, labyrinths, gaps and bands) that is predicted from models of Turing instability (Fig. 3.3e-h) (see Methods) occurs in the field (Fig. 3.3a-d) often even within the sheltered lagoon of a single reef (e.g. see Appendix A3). Further support for the role of Turing instability comes from the observation that banded patterns (e.g. Fig. 3.3d) are found perpendicular to the water flows in and out of lagoons through shallow passes (e.g. see satellite images in Appendix A3). This is consistent with the prediction that banded Turing patterns tend to arise perpendicular to the direction of advective transport, in this case, water movement (Fig. 3.3h).

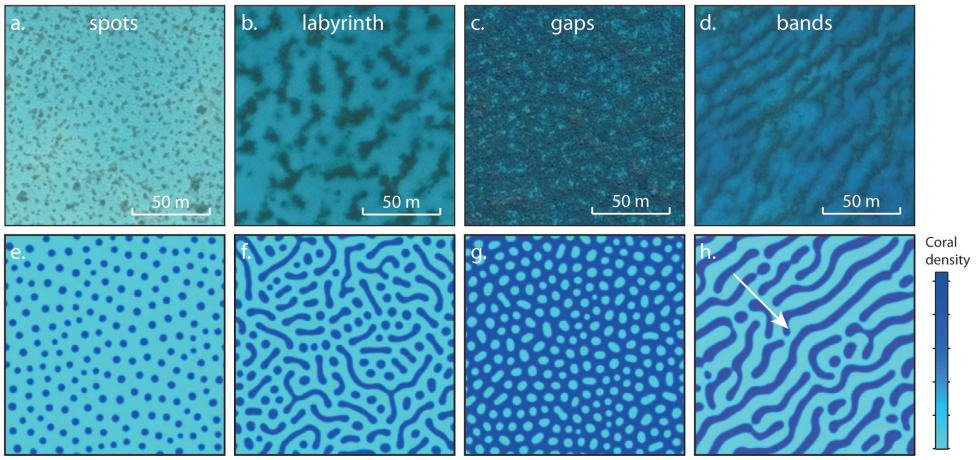

Figure 3.3. The entire repertoire of Turing sub-types as observed on satellite images **(a-d)**, and as predicted by a model of Turing instability **(e-h)**. **a)** spots in New Caledonia [21°48'27.49"S 165°42'8.62"E], **b)** labyrinth on One Tree Island Reef, Australia [23°29'40.15"S 152° 5'2.66"E], **c)** gaps in New Caledonia [22° 5'46.65"S 166° 1'22.79"E], **d)** bands on Hardy Reef, Australia [19°44'39.87"S 149°12'41.79"E]. The model results (panels e-h) are produced by a resource accumulation model (with i reflecting the inflow level of the resource). **e)** spots ($i = 0.04$), **f)** labyrinth ($i = 0.1$), **g)** gaps ($i = 0.2$), **h)** bands ($i = 0.13$, $U_x = 1$, $U_y = 1$, with U_x and U_y reflecting the x- and y-direction of a directional flow of the modeled resource, indicated by the white arrow). Note that similar patterns can be generated by other models (e.g. see Fig. A3.2).

While the detection of these previously unrecognized patterns is interesting per se, the phenomenon also points to a set of mechanisms that determine reef formation and functioning because the generic conditions for Turing patterns to emerge are quite specific. In general terms, such patterns are produced from the combination of a small scale positive feedback with a long-range negative feedback (Meinhardt 1982; Rietkerk and van de Koppel 2008). More specifically, when it comes to ecosystems, Turing patterns arise if an organism has a reinforcing effect on its own local growth (the local positive feedback), but a negative effect on growth at a greater distance (the long-range negative feedback) (Fig. 3.4a) (Meinhardt 1982; Rietkerk and van de Koppel 2008). This combination can arise through the influence of the organism on the spatial distribution of resources or growth inhibitors (Fig. 3.4b-c) (Meinhardt 1982). An example of resource redistribution occurs in arid ecosystems where surface-water infiltration to the soil is higher in patches of vegetation, facilitating local vegetation growth. A direct consequence is that growth is inhibited outside the patches where water runs off before it can infiltrate the soil and so moisture is depleted (Rietkerk *et al.* 2002; van de Koppel and Rietkerk 2004). This example illustrates how organisms may promote accumulation of resources in patches, thus depleting the resource level between the patches ('resource accumulation' mechanism, Fig. 3.4b). The complementary class of mechanisms occurs when organisms repel growth inhibitors. This reduces stress arising from the growth inhibitor within the patches, while raising stress levels between patches (i.e. 'stress divergence' mechanism, Fig. 3.4c) (e.g. see van de Koppel and Crain (2006)). Obviously, combinations of mechanisms on different spatial scales are possible too (Gierer and Meinhardt 1972).

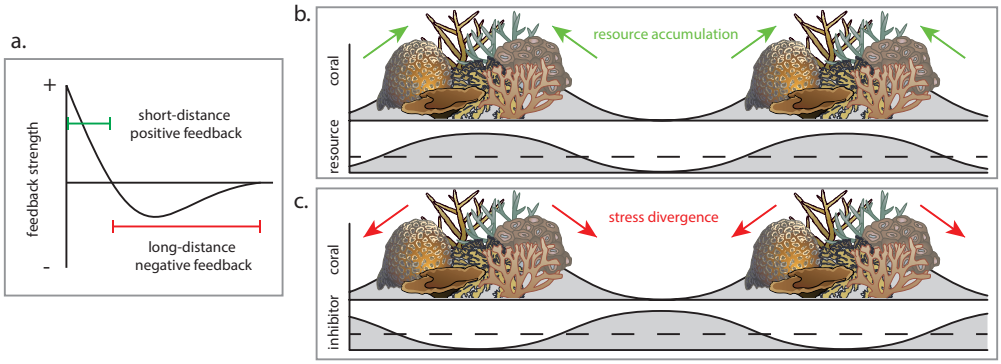

Figure 3.4. General conditions for Turing patterns in ecosystems. **a)** Turing patterns can arise if an organism has a positive effect on its own growth at a short distance, and a negative effect at a longer distance. Two generic classes of mechanisms can generate this situation: **b)** resource accumulation, i.e. a patch of organisms attracts a net flux of resources causing resource depletion at a distance, or **c)** stress divergence, i.e. a patch of organisms deflects a growth inhibitor leading to stress accumulation at a distance.

Quite independently of the precise formulation, different kinds of mathematical models based on either of the two generic classes of mechanisms tend to produce Turing patterns (See Methods for a specific example of a 'resource accumulation' model, and Appendix A3 for a 'stress divergence' model). These fundamental classes thus allow us to narrow down the search image for mechanisms regulating the formation of the coral reef patterns we recorded. The first class of mechanisms would imply that corals attract and accumulate a resource, such that this resource becomes too scarce between patches to allow coral growth or settlement. Corals are known to actively enhance mass transfer rates, increasing the efficiency of their uptake of dissolved nutrients (Shapiro *et al.* 2014). Also, microbes (Wild *et al.* 2004) and sponges (de Goeij *et al.* 2013) recycle dissolved organic matter released by corals and algae, making it available again to corals as particulate organic matter. Such tight, local recycling could potentially generate Turing patterns, provided that the recycling leads to a decrease in dissolved organic matter between patches, preventing successful patch development.

The second general class of mechanisms (stress divergence) could arise from corals repelling a growth inhibitor, resulting in stress alleviation on coral patches, with the side effect of stress accumulation between patches (Fig. 3.4c). Potential candidates for such inhibitors include coral waste products (e.g. dissolved oxygen (Mass *et al.* 2010; Osinga *et al.* 2011)), allelochemicals (e.g. from soft corals and sponges) (Puglisi *et al.* 2014), and sediment particles. Sediment particles can stress corals, for example, light levels are reduced due to smothering and elevated turbidity. Also, coral larvae are unable to settle on sediment-covered areas (Rogers 1990). Corals can redistribute sediment away from live tissue both passively and actively (Stafford-Smith 1993). Passive mechanisms involve colony morphology and its effect on water turbulence, whereas active rejection of sediment particles happens through ciliary activity, mucus secretion, and tissue expansion (Stafford-Smith 1993). In addition, parrotfish graze and scrape coral patches, consuming algae and generating sediment which they defecate off the edge of reefs, exporting an increased sediment load to the surroundings (Bellwood 1995). The resulting reduction in algal-coral competition by grazing, and the export of sediment from coral patches, may thus generate the specific combination of local positive feedback and longer-range negative feedback that can generate Turing patterns. While the Turing patterns provide a search image for mechanisms that govern lagoonal coral growth (resource accumulation or stress divergence), further research will be needed to determine the actual key processes.

Importantly, the Turing patterns we revealed may also put us on the track of gradients of environmental stress and of resilience of these reefs. The sequence of gaps, labyrinths and spots reflects an increasing scarcity of resources or increasing levels of growth inhibitors (Fig. 3.3e-h). The local variety of Turing patterns may therefore reflect a gradient in local resilience against environmental change, with a sparse spotted pattern corresponding to areas with the lowest resilience where corals may be most easily lost (Rietkerk *et al.* 2004). Moreover, slowly degrading conditions will be reflected in changing pattern types. Therefore, systematic changes in Turing patterns on the kinds of reefs we studied might serve as early indicators of changes in reef resilience at a larger scale.

The Turing patterns we discovered offer an entirely new approach to exploring and understanding the resilience of corals. Not only do they pave a novel way to map and monitor resilience, Turing patterns also provide a fresh search image for the mechanisms governing coral growth. In view of the global coral reef crisis there is an urgent need for such tools that help understand and assess resilience.

Methods

We used the resource-accumulation model below to generate Figure 3.3e-h.

$$\frac{\partial C}{\partial t} = \frac{gaR}{1+ahR}C - cC^2 - mC + D_C\nabla^2 C$$

$$\frac{\partial R}{\partial t} = i - eR - \frac{aR}{1+ahR}C + D_R\nabla^2(R-bC) - U_x\frac{\partial(R-bC)}{\partial x} - U_y\frac{\partial(R-bC)}{\partial y}$$

The term $\frac{gaR}{1+ahR}C$ represents growth of an organism (e.g. coral) with maximal growth rate g. Resource uptake follows a Holling Type II functional response, with attack rate a and handling time h. The terms cC^2 and mC account for mortality, due for example to competition, decay, and predation. Dynamics of the limiting resource are represented by a source (i) and a loss (eR) term. The spatial spread of the organism is modeled by the diffusion term $D_C\nabla^2 C$. Resource mixing or diffusion is assumed to be lowered by the presence of the organism, and is modeled by the diffusion term $D_R\nabla^2(R-bC)$. A directional flow of the resource (e.g. through water) is represented by the advection terms $U_x\frac{\partial(R-bC)}{\partial x}$ and $U_y\frac{\partial(R-bC)}{\partial y}$. This model can lead to the entire repertoire of Turing patterns including bands (Fig. 3.3e-h). Default parameters: landscape size = 50x50, $g=1.1$, $a=1.6$, $h=1$, $c=1.0$, $m=0.2$, $D_C=0.01$, $e=0.05$, $D_R=1$, $b=3$, $U_x=0$, $U_y=0$. Simulations were performed using Grind for Matlab.

Appendix A3

Spectral wave analysis to test for regularity

We performed a two-dimensional spectral wave analysis on several aerial pictures from the most northern Agincourt Reef, Australia, that were taken with a drone (see for method description Renshaw and Ford 1983; Couteron and Lejeune 2001; van de Koppel *et al.* 2005a). First, we cropped selected images to a square image, downsized them to 128x128 pixels, and selected the green values from the RGB-data of the image (giving the highest contrast). Then, we performed the spectral analyses as depicted in Figure A3.1. The periodogram represents the portion of image variance σ^2 that can be accounted for by a cosine wave repeating itself r times (i.e. wavenumber) along the direction θ (i.e. wave angle). The centre of the periodogram corresponds to $r = 0$. To investigate periodicity, we obtained a radial spectrum by binning the periodogram values for each successive wavenumber. The radial spectra were re-scaled by dividing by σ^2. The high peaks with very low wavenumber ($r = 1$–3) reflect a gradient created by the reflection of the sun. The other peaks are generated by the actual coral patches. These peaks show clear periodicity both for spots and labyrinth, however the signal is stronger for the labyrinth.

A stress-divergence model

Here, we show that a relatively simple stress-divergence model can also generate Turing patterns:

$$\frac{\partial C}{\partial t} = rC\left(1 - \frac{C}{K}\right) - mC\frac{S^2}{S^2 + h^2} + D_C\nabla^2 C$$

$$\frac{\partial S}{\partial t} = i - eS + D_S\nabla^2(SC) - U_x\frac{\partial(SC)}{\partial x} - U_y\frac{\partial(SC)}{\partial y}$$

The term $rC\left(1 - \frac{C}{K}\right)$ represents logistic growth of an organism (e.g. coral) with r representing the maximal growth rate, and K the carrying capacity of C. An extra mortality by a stressor (e.g. sediment) is modeled following a sigmoidal response, with m the maximal mortality rate, and h the stress level at which the mortality rate is $\frac{1}{2}m$. The stressor equation contains an inflow term i, and an outflow term eS. Movement of the stressor is modeled by the diffusion term $D_S\nabla^2(SC)$, and depends on the local density of C and S, in the sense that the stressor moves faster when the density of the organism is high. A directional flow (e.g. water flow) affecting the direction in which the stressor is affected by the organism is represented by the advection terms $U_x\frac{\partial(SC)}{\partial x}$ and $U_y\frac{\partial(SC)}{\partial y}$. Default parameters: landscape size = 50x50,

$r = 0.8$, $K = 1$, $m = 1$, $h = 0.5$, $D_C = 0.02$, $e = 0.1$, $D_S = 2$, $U_x = 0$, $U_y = 0$. This model can lead to the entire repertoire of Turing patterns, including bands (Fig. A3.2).

Aerial, underwater, and satellite images

https://www.dropbox.com/sh/u6lzlraxpjeac8n/AAAMF7RKmLFutiRURD7BR981a?dl=0

This database contains (1) underwater pictures and movies taken at the most northern Agincourt Reef in Australia, (2) aerial pictures taken at the most northern Agincourt Reef (with a drone), and (3) a Google Earth file pointing to Turing patterns on the Great Barrier Reef and New Caledonia.

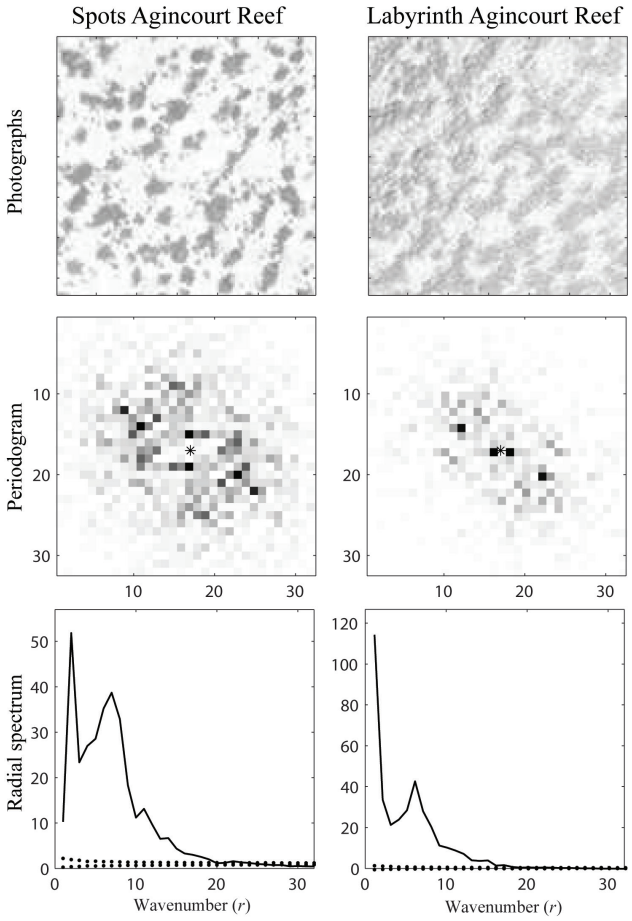

Figure A3.1. Spectral wave analysis of two aerial photographs of Agincourt Reef. The **upper panels** represent black-and-white photographs of two types of coral patterns (i.e. spots and labyrinth) observed on Agincourt Reef. The **middle panels** represent the periodograms of the pictures, with the center indicated by a star. The **lower panels** represent the radial spectra of the periodograms and indicate the dominant wave number (number of waves in the photographs) of the pattern.

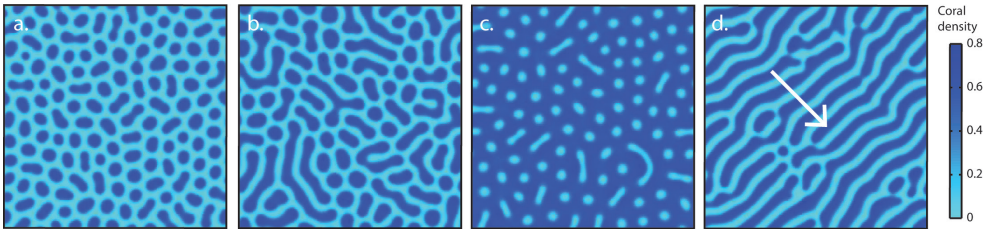

Figure A3.2. Stable Turing patterns simulated by an example model based on the stress-divergence mechanism described in Appendix A3. **a)** spots ($i = 0.12$), **b)** labyrinth ($i = 0.09$), **c)** gaps ($i = 0.05$), **d)** bands ($i = 0.1$, $U_x = 1$, $U_y = 1$). The white arrow indicates the flow direction of the stressor.

Chapter 4

Multiple feedbacks and the prevalence of alternative stable states in coral reefs

Ingrid A. van de Leemput,
Terry P. Hughes,
Egbert H. van Nes,
and Marten Scheffer

Published in *Coral Reefs:*

van de Leemput IA, Hughes TP, van Nes EH, and Scheffer M. 2016. Multiple feedbacks and the prevalence of alternate stable states in coral reefs. Coral Reefs (early-online), doi:10.1007/s00338-016-1439-7

Abstract

The prevalence of alternative stable states on coral reefs has been disputed, although there is universal agreement that many reefs have experienced substantial losses of coral cover. Alternative stable states require a strong positive feedback that causes self-reinforcing runaway change when a threshold is passed. Here we use a simple model of the dynamics of corals, macroalgae and herbivores to illustrate that even weak positive feedbacks, that individually cannot lead to alternative stable states, can nonetheless do so if they act in concert and reinforce each other. Since the strength of feedbacks varies over time and space, our results imply that we should not reject or accept the general hypothesis that alternative stable states occur in coral reefs. Instead, it is plausible that shifts between alternative stable states can occur sporadically, or on some reefs but not others depending on local conditions. Therefore, we should aim at a better mechanistic understanding of when and why alternative stable states may occur. Our modeling results point to an urgent need to recognize, quantify, and understand feedbacks, and to reorient management interventions to focus more on the mechanisms that cause abrupt transitions between alternative states.

Introduction

Many ecosystems exhibit marked regime shifts from one set of species to another, such as the transitions between clear and turbid lakes (Scheffer 1998), forest and grassland (Hirota *et al.* 2011; Staver *et al.* 2011b), kelp beds and sea urchin barrens (Steneck *et al.* 2003; Watson and Estes 2011), or between tropical corals and assemblages of macroalgae and other weedy species (e.g. Done 1992; Hughes 1994; Mumby *et al.* 2007; Hughes *et al.* 2010). Positive and negative feedbacks play a critical role in shaping the stability of these ecosystems and in determining the responses they display to increases or decreases in anthropogenic drivers, such as pollution, over-harvesting or climate change.

Positive feedback as a cause of alternative stable states

A feedback is defined as a closed loop process where the results affect the inputs, influencing future results (DeAngelis *et al.* 1986). In complex ecosystems, feedbacks result from circular chains of interactions (e.g. A affects B, and B affects A) between ecosystem components (e.g. species, abiotic conditions, humans). A feedback is negative when the results dampen an initial rate of change, causing the initial change to slow down (DeAngelis *et al.* 1986) (e.g. increase in A $\rightarrow$ increase in B $\rightarrow$ decrease in A). Positive feedbacks, on the other hand, amplify an initial small change, potentially propelling the system away from its previous state (DeAngelis *et al.* 1986) (e.g. increase in A $\rightarrow$ increase in B $\rightarrow$ further increase in A).

Deterministic models (i.e. excluding natural variability) can be used to study crucial system dynamics, and states at which the system is in equilibrium. A stable equilibrium is established by a negative feedback that causes the system to return to the original equilibrium after a disturbance. Negative feedbacks are therefore often called stabilizing feedbacks (Schröder *et al.* 2005). Negative feedbacks are ubiquitous in ecosystems, because in the absence of negative feedbacks populations would grow infinitely. In contrast, an unstable equilibrium is established by a positive feedback that causes acceleration away from that equilibrium after a small disturbance (i.e. a snowball effect). In a system with alternative stable states, an unstable equilibrium separates two stable equilibria. For this reason, a strong positive feedback is a necessary (but not sufficient) condition for alternative stable states (Thomas 1981). Positive feedbacks are therefore often called destabilizing feedbacks (Schröder *et al.* 2005).

Due to positive feedbacks, systems can respond in unexpected ways to changing conditions or small disturbances (Fig. 4.1a). The equilibrium response of an ecosystem to a gradually increasing driver is often smooth, meaning that there is

only one stable state for each level of driver (Fig. 4.1b). If a positive feedback is strong enough to generate alternative states, the response to a driver becomes hysteretic (Fig. 4.1c). In Figure 4.1c there are two particular threshold values for the driver, also called 'tipping points', where a stable equilibrium collides with an unstable equilibrium and disappears. If the driver brings the system close to such a tipping point the unstable equilibrium approaches the stable equilibrium, implying that even a small perturbation may push the system across this unstable boundary invoking a critical transition to the alternative stable state. Reversing the change in the driver is not enough to induce a shift back to the original state, as the system tends to remain trapped in the new alternative state, a phenomenon known as hysteresis. Hysteresis thus increases with the strength of the positive feedback. The stronger the positive feedback, the larger the range of driver levels for which alternative stable states exist (Fig. 4.1a).

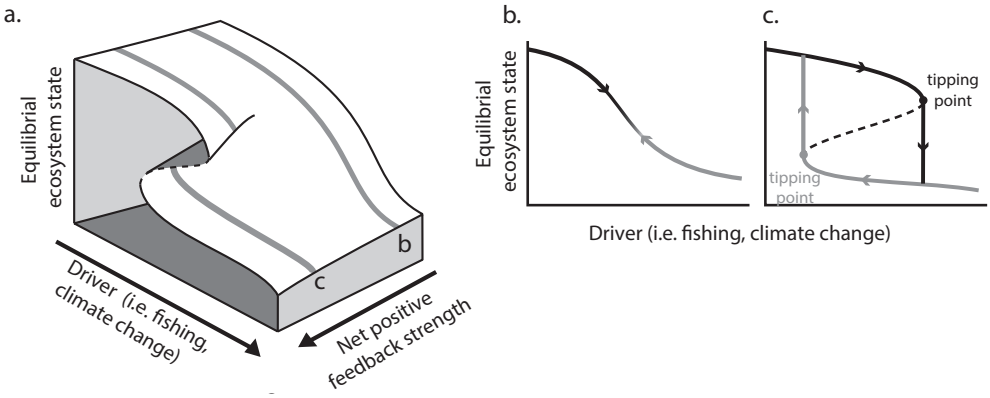

Figure 4.1. The cusp-catastrophe plot. **a)** A positive feedback can lead to a qualitatively different equilibrium response of an ecosystem to an external driver (e.g. fishing pressure and/or climate change), depending on the strength of the feedback. **b)** A weak positive feedback may lead to a smooth response, and a single equilibrium, along the entire range of driver, from low to high. **c)** A strong positive feedback may cause the response curve to fold inwards, such that two alternative stable states exist over the same intermediate range of drivers. The response of the system as a result of an increasing driver (in black) shows a tipping point at which the system will abruptly shift to another regime. If the driver is lowered again, the response will follow a different trajectory (in grey), because the system remains trapped in the alternative regime until the driver reaches a level at which the system is tipped back to its original state.

In reality, multiple positive and negative feedbacks act together and may counteract each other. This complex interplay of feedbacks, in combination with many random effects, will shape the actual response of an ecosystem to slowly changing conditions.

Feedback mechanisms in coral reef ecosystems

Although the role of positive feedbacks for coral reef dynamics has previously been analysed (Mumby and Steneck 2008; Mumby 2009; Nyström *et al.* 2012), the fundamental consequences of the interplay between multiple feedbacks have hardly been addressed. To formulate a model that explores this interplay we first searched the literature to identify positive feedbacks that have been described for coral reef ecosystems (Table 4.1, see Appendix A4 for list of references). We found that over 20 positive feedback mechanisms have been documented, although they have very seldom been quantified, and in most cases their potential role in promoting critical transitions or alternative states has not been recognized. The feedbacks can be classified into five general categories, based on the dominant process involved: predation, competition, density-dependent demography, facilitative interactions between species and/or between species and their environment, and social-ecological interactions (Table 4.1). These categories overlap and are not mutually exclusive.

Table 4.1. Positive feedbacks on coral reefs suggested in the literature (see Appendix A4 for list of references).

Scheme	#	Feedback mechanism	Refs
Predator-prey interactions: predation pressure per capita prey decreases with prey density			1
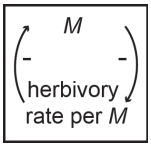	1	Higher algal cover can lead to a saturated herbivore population (e.g. sea urchins, fish), and thus to a lower herbivory rate per algae. This may occur if the herbivore population does not change with algal cover: • If: population growth of herbivores is recruitment limited rather than food limited • If: preferred alternative food sources (e.g. turf algae) are available	3,4 5,6 7
	2	Higher algal cover can lead to more mature algae, which can lead to decreased food handling and digestion time of herbivores (e.g. decreased palatability of mature algae, increased dominance of algae that are mechanically or chemically defended).	8–10
	3	Higher algal cover can lead to dense stands, which may be avoided by adult herbivorous fish, leading to a decreased herbivory rate per algae.	11
	4	Higher algal cover can create nursery habitat for micropredators, leading to increased post settlement mortality of herbivorous echinoids (opposite has also been shown[2]).	12
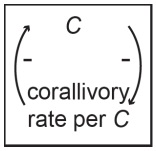	5	Higher coral cover can lead to a saturated corallivore population (e.g. *Drupella spp.*, *Acanthaster planci*, some parrotfish) and thus to a lower corallivory rate per coral. This may occur if the corallivore population does not change with coral cover: • If: preferred alternative food sources are available (i.e. many corallivorous fish are facultative instead of obligate corallivores)	13–17 18

Competition: interspecific competition (e.g. between corals and algae) exceeds intraspecific competition (e.g. among corals, or among algae)		23,24
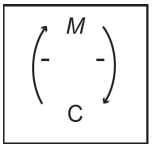	6	Higher algal cover can lead to stronger inhibition of settlement of coral larvae. 25,26
	7	Higher algal cover can lead to stronger physical interference (e.g. overgrowing, overtopping, or abrasion) of juvenile or adult corals. 26–33
	8	Higher algal cover can lead to stronger chemical effects of algae on corals (e.g. allelopathy, enhanced microbial activity, disease transmission). 34–37
	9	Higher coral cover can lead to stronger physical interference (extrusion of mesenterial filaments) of algae, damaging algal segments. 38
Density dependent demographic processes: net growth rate increases with population size (Allee effect)		39
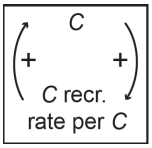	10	In a self-seeded population, loss or gain of adult brood stock can affect local recruitment disproportionately. Net recruitment per capita adult coral may decrease at low coral cover (Allee effect), if fertilization success decreases with distance between coral colonies, due to dilution of gametes. 40–44
	11	Higher coral cover can lead to increased settlement rates, because coral larvae move towards reef sounds. 45
	12	Higher coral cover can lead to increased herbivory, which can increase the presence of crustose coraline algae that facilitate settlement and post-settlement survival of coral larvae. 46–48
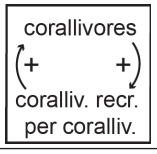	13	Lower corallivore (*Acanthaster*) population density can lead to reduced larval survival rates. A pulse of nutrient input, or predator removal, may lead to temporary increased recruitment rates, resulting in a long-lasting starfish outbreak. 49
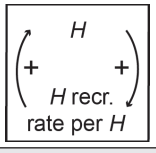	14	Lower herbivore population density (observed for *Diadema* and fish) can lead to reduced fertilization success. 50,51
Facilitative interactions between two species, or between a species and its environment		
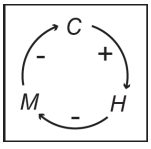	15	Higher coral cover can have a positive effect on herbivore abundance, by providing shelter and food to herbivores, thereby lowering the competition pressure between macroalgae and coral. 52–63
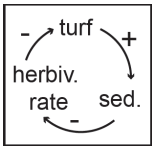	16	Turf algae can trap sediment, which can decrease herbivory on turf algae. Algal turfs and sediment also reduce coral recruitment, which can, on the long term, also decrease herbivory on turf algae. 64,65

Social-ecological feedbacks: facilitative interactions between social and ecological system		
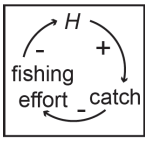	17 A decreased herbivorous fish population can lead to a decrease in catches. Fishers need to reach a certain yield/income, and lack alternatives for their income. Therefore, they may increase fishing effort, by fishing more often, or using other methods.	19,20
	18 A decreased herbivorous fish population can lead to a decrease in catch. To reach the yield needed, governments may subsidize fishers when incomes fall.	21,22
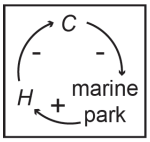	19 Higher coral cover can influence the placement of new marine parks. The protection of herbivores can positively affect coral cover.	66

Arguably, the best-known positive feedback arises from the interaction between corals and herbivores (Table 4.1). Corals provide habitat and shelter to herbivores (Friedlander and Parrish 1998; Graham *et al.* 2006; Lee 2006), and in turn, herbivores have a positive effect on corals by grazing on algae that compete with them for space (e.g. Lirman 2001). This is a positive feedback loop where coral cover decline could lead to further decline through the following chain of events: coral cover decline → herbivore stocks decline → macroalgae increase → coral cover decline through increased competition with macroalgae (Fig. 4.2). The intensity of this feedback is likely to vary in response to variation in the morphological structure of different coral assemblages, the size and species composition of herbivores, and their reliance on corals.

An additional positive feedback arises from the interaction between herbivores and macroalgae (Table 4.1, Fig. 4.2). As herbivorous fishes become depleted by overfishing, grazing pressure per unit of macroalgae is reduced, and too few herbivores may become swamped by too much macroalgae (Mumby *et al.* 2007; Scheffer *et al.* 2008). Grazing pressure can become further reduced if algae become less palatable as they mature and grow (McClanahan *et al.* 2002). For example, on many overfished reefs in the Caribbean, regional-scale blooms of macroalgae occurred following mass mortality due to disease of grazing sea urchins, because overfished stocks of herbivorous fishes were unable to consume enough algae (Hughes 1994). Similarly, a bloom of seaweed following a pulse of nutrients may also arise in part from a lower grazing pressure per unit of macroalgae (Scheffer *et al.* 2008). This feedback between herbivores and macroalgae could potentially lead to the replacement of corals by faster growing seaweed (Hughes 1994; Mumby *et al.* 2007; Scheffer *et al.* 2008). However, on reefs with intact herbivore populations, this herbivore-macroalgae feedback may be very weak. For example, exposed reef crests on the Great Barrier Reef routinely lose most of their coral cover during recurrent cyclones, but return afterwards to high coral cover rather than flipping to a macroalgal state (Connell 1997). Consequently, local

variation in fishing pressure on herbivores, in their species composition, and in palatability of macroalgae, are all likely to influence the strength of this feedback.

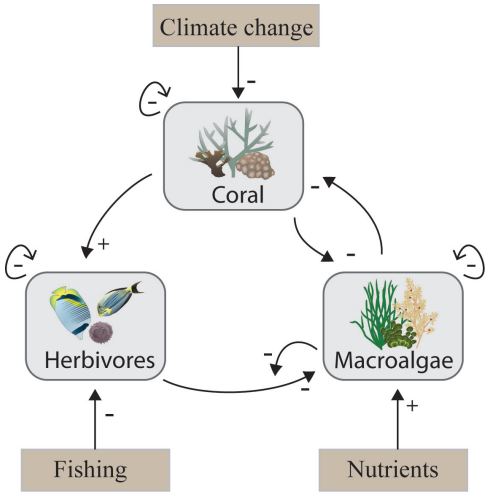

Figure 4.2. An overview of the modelled feedbacks and drivers of change in coral reefs. The qualitative effect of each feedback route in the diagram can be determined by multiplying the signs on the arrows of the route taken. Two negative effects thus combine to cause a positive feedback. For instance, herbivores reduce the biomass of macroalgae, but abundant macroalgae can reduce the impact of herbivores if they swamp grazing pressure and become less palatable. Such a double negative effect can result in a positive feedback. A three-phase positive feedback occurs between corals, herbivores, and macroalgae (+, -, -). Negative feedbacks act to balance runaway change. For instance, maximum densities of all populations are ultimately limited by competition represented by small negative feedback loops that depict self-limitation. For a more extensive overview of documented positive feedbacks on coral reefs, see Table 4.1.

Positive feedbacks on coral reefs can also arise from human behavior (Table 4.1). For example, the intensity of fishing often increases in response to declining catch rates, which can drive stocks further downward. This positive feedback can occur, for instance, if government subsidies are linked to dwindling catches, if fishers switch to a more efficient type of gear when catches decline, or if they target seasonal spawning aggregations in depleted fisheries (Mackinson *et al.* 1997). As with feedbacks that are strictly biological, the strength of social feedbacks varies greatly from place to place and over time.

Importantly, empirical evidence for the existence of any specific positive feedback mechanism does not prove that alternative stable states occur, because the feedback may be too weak or intermittent. Also, empirical information on spatial and temporal variation in almost all of these feedbacks (Table 4.1) is either non-existent or very sparse. This makes it challenging to understand the response of any particular coral reef to accumulating stress. Our aim here is to improve the general understanding of the interplay of feedbacks in coral reefs in relation to the occurrence of alternative stable states, with an ultimate goal of preventing unexpected transitions to undesired states.

In this paper, we develop a simple model of a coral reef ecosystem to illustrate how multiple positive feedbacks can interplay, and to explore how differences in local environmental conditions, and thus in feedback strength, can affect the stability of coral reefs, leading in some circumstances to the emergence of alternative stable states. Previous work on alternative stable states on coral reefs includes more elaborate models examining hysteresis (e.g. Mumby *et al.* 2007; Blackwood *et al.* 2010), and the effect of multiple stressors (e.g. Blackwood *et al.* 2011; Fung *et al.* 2011). Here, we focus explicitly on a scenario in which multiple weak positive feedbacks interact. Because the strength of negative and positive feedbacks is contingent on synergies between them, and on the vagaries of local conditions, we conclude that a complex ecosystem such as a coral reef will likely exhibit a wide variety of responses to external drivers, that may or may not include alternative stable states.

Model

To explore how multiple interacting feedbacks could affect the dynamics of coral reefs, we developed a model that explicitly incorporates three positive feedback mechanisms. We set the strength of each of these feedbacks in such a way that individually they are too weak to generate alternative stable states. Subsequently, we combined the three weak feedbacks to study their collective effects. Parameter analyses to determine the stable and unstable states for each parameter value were performed in Matlab, using MatCont and Grind for Matlab.

Cover by corals (C) and macroalgae (M) are represented in our models as the proportion of space occupied, while herbivore abundance (H) is defined as a proportion of the carrying capacity of herbivores. Corals and macroalgae are assumed to compete for unoccupied space (S), with cover by corals, macroalgae and unoccupied space summing to 1 (Eqn. 1). More complex models could add further benthic categories, or subdivide corals and macroalgae into functional groupings, but for our purposes we focus on the simplest case of shifts in dominance of corals and macroalgae.

$$S = 1 - C - M \tag{1}$$

$$\frac{dC}{dt} = \left(i_C + b_C C\right) S - d_C C \tag{2}$$

$$\frac{dM}{dt} = \left(i_M + b_M M\right) S - gHM \tag{3}$$

$$\frac{dH}{dt} = rH\left(1 - H\right) - fH \tag{4}$$

In this model, two mechanisms cause the expansion of coral and macroalgae, which are both proportional to the unoccupied space in the system. External import of propagules of coral and macroalgae has a constant rate (resp. i_C and i_M) independently of the local cover of adults. This reflects demographically open populations with dispersal of juvenile stages. Additionally, local expansion of existing adults of both functional groups is proportional to the existing cover (with rates b_C and b_M). Mortality of corals is represented by a constant decay rate (d_C) (Eqn. 2), and mortality of macroalgae by a constant grazing rate per herbivore (g) (Eqn. 3). Herbivores (e.g. fish and sea urchins) are assumed to grow logistically (the density is scaled to the carrying capacity) with a relative growth rate of herbivores (r) that is independent of local macroalgal cover (Eqn. 4). Herbivore mortality is represented by a constant fishing pressure (f) (Eqn. 4).

Parameters of the default model without feedbacks are based on the following basic assumptions: 1) the macroalgal growth rate exceeds the coral growth rate, and 2) the mortality rate of macroalgae due to herbivory exceeds the mortality rate of corals, if the herbivore population is at carrying capacity (i.e. no fishing). We used the following default parameters for the illustrated cases: $b_C = 0.3$, $b_M = 0.8$, $i_C = 0.05$, $i_M = 0.05$, $d_C = 0.1$, $r = 1$, $g = 1$.

As in almost all ecological models, negative feedbacks prevent unlimited population growth. A familiar term for this effect is negative density-dependence. In our model, for example, macroalgae and coral cover are limited by space, and the herbivore population size has a carrying capacity (Fig. 4.2). In addition to these negative feedbacks, we incorporated three positive feedbacks in the model, described in detail in Appendix A4 (see also Figure A4.1).

First, we implemented a positive feedback between macroalgal cover and herbivory rate. This feedback arises from a decrease in the herbivory rate (i.e. per unit of algae) as macroalgal cover increases, representing a scenario where consumption by herbivores saturates when algae are abundant (Table 4.1, feedbacks 1-3). To model this 'herbivory-escape feedback', we introduced a Holling type II functional response, with parameter η representing the macroalgae handling time of herbivores (Eqn. 5).

$$\frac{dM}{dt} = \left(i_M + b_M M\right) S - \frac{gHM}{g\eta M + 1} \tag{5}$$

Second, we incorporated a positive feedback arising from the direct negative effects of macroalgae on coral recruitment and growth (Table 4.1, feedbacks 6-7). This 'competition feedback' is based on the classic insight that competition can cause alternative stable states if interspecific competition exceeds intraspecific competition (Volterra 1926; Lotka 1932). The competition effect of macroalgae on coral recruitment and growth is represented by αM (Eqn. 6). If α is zero, coral recruitment and growth

are only indirectly affected by macroalgae through space pre-emption. The value of α between 0 and 1 represents the proportion of macroalgae involved in the direct inhibition of corals.

$$\frac{dC}{dt} = \left(i_C + b_C C\right) S\left(1 - \alpha M\right) - d_C C \tag{6}$$

Third, we considered an indirect positive feedback between corals and herbivores. Herbivores graze on macroalgae, thereby reducing the negative effect of macroalgae on coral. A positive feedback exists if corals promote herbivores, for example by providing habitat and shelter (Table 4.1, feedback 15). We modeled this 'coral-herbivore feedback' by assuming a positive relation between coral cover and herbivore carrying capacity. The strength of this relationship is represented by σ (Eqn. 7). If σ is zero, herbivores are not affected by corals. If σ is 1, coral cover completely determines the carrying capacity of herbivores.

$$\frac{dH}{dt} = rH\left(1 - \frac{H}{\left(1-\sigma\right) + \sigma C}\right) - fH \tag{7}$$

To illustrate how stability properties may change we varied parameters that reflect variation in (a) palatability of macroalgae (McCook and Price 1997) by varying the handling time of macroalgae by herbivores (η), and (b) recruitment levels of corals (Connell *et al.* 1997; Diaz-Pulido and McCook 2003; Ayre and Hughes 2004) by varying the density-independent inflow of coral recruits (i_C). Both factors (a and b) are known to vary widely in nature. For instance, the proportion of unpalatable species varies enormously at multiple scales (e.g. McCook and Price 1997), affecting the food handling time of herbivores (Hoey and Bellwood 2011). Similarly, coral recruitment varies greatly in both space and time (e.g. Connell *et al.* 1997; Hughes and Tanner 2000; Halford and Caley 2009).

Results

In the absence of the specific positive feedbacks we address, the model exhibits a smooth response to fishing pressure (Fig. 4.3a). As fishing increases, the abundance of herbivores declines linearly, causing the grazing rate on macro-algae to decrease incrementally, resulting in a smooth and reversible replacement of corals by macro-algae. There is a single stable state for any given level of fishing pressure. Consequently, the system exhibits the same forward and backward trajectory in abundances of herbivores, macroalgae and corals as fishing pressure is increased or decreased.

Adding each of the weak positive feedbacks to the model individually has scarcely any effect, resulting merely in a slight steepening in the response of corals and macroalgae to fishing pressure (Fig. 4.3b-d). In the default parameter setting, none of the individual feedbacks is strong enough to result in alternative stable states.

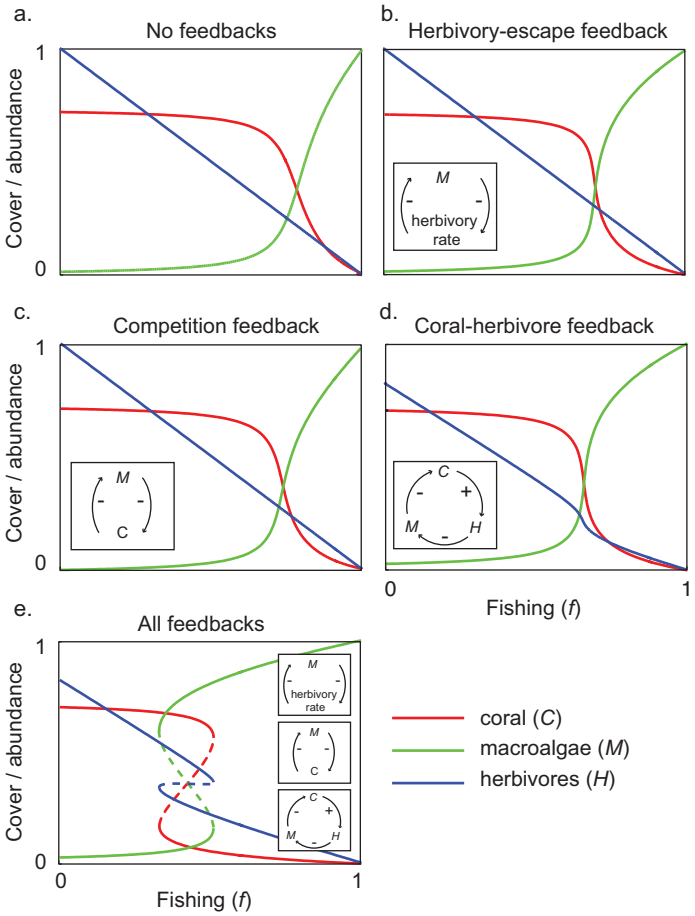

Figure 4.3. The impact of multiple positive feedbacks on the equilibrium response of corals, macroalgae, and herbivores to changing fishing pressure. In **a),** the model has no positive feedbacks, and only a single equilibrium exists for a given level of fishing pressure. In (b)-(d), a single positive feedback is introduced in the model, but each one is too weak to generate hysteresis and alternative stable states: **b)** Herbivory-escape feedback ($\eta = 1$). **c)** Competition feedback ($\alpha = 0.5$). **d)** Coral-herbivore feedback ($\sigma = 0.6$). In **e),** the same three weak feedbacks in panels b, c, and d are combined, generating hysteresis and alternative stable states at an intermediate level of fishing pressure.

By contrast, when the same individually weak feedbacks are allowed to act together a fundamentally different behavior emerges. The model now has alternative stable states over a range of fishing pressures (Fig. 4.3e). Consequently, the threshold in fishing that triggers a collapse of corals is lower than the threshold for the reverse

transition from macroalgae to corals. The system now shows hysteresis, and a gradual change in driver can lead to abrupt shifts between alternative stable states. Similar synergetic effects among feedbacks can occur also in all pairwise combinations of the three feedbacks (Appendix A4, Fig. A4.2).

Whether the response of an ecosystem to a changing driver such as fishing or climate change is hysteretic, or not, obviously depends on the strength of all contributing feedbacks. The strength of these feedbacks depend on local conditions. For instance, commonly observed variation in the species composition of macroalgae, and levels of coral recruitment affect feedbacks in the model. We used the model to illustrate that variations in the parameters affecting the strength of positive feedbacks can cause the equilibrium response to drivers such as fishing pressure to change from smooth to hysteretic (Fig. 4.4). Specifically, these analyses suggest that reefs with a higher proportion of unpalatable macroalgae, or with lower levels of recruitment (e.g.. isolated reefs) are more likely to exhibit alternative stable states.

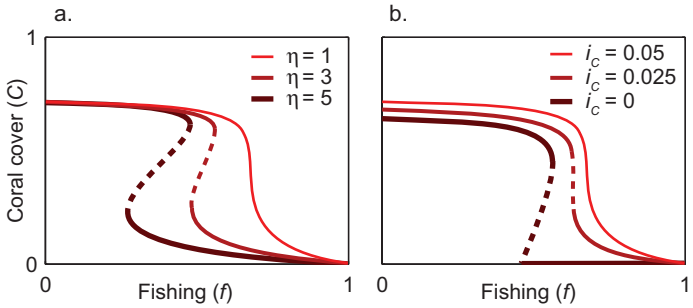

Figure 4.4. The tendency of the system to show hysteresis in response to fishing pressure can be affected by locally varying factors such as: **a)** Low palatability of fully grown algae (high η) (feedback parameters: ($\alpha = 0.2$), ($\sigma = 0$). **b)** Low external recruitment of corals, i_c (feedback parameters: $\eta = 1$, $\alpha = 0.2$, $\sigma = 0$).

Discussion

Multiple causality

Our analyses illustrate that feedback mechanisms that individually have no qualitative effect on stability properties when they are experimentally tested or observed can nonetheless collectively cause an ecosystem to have tipping points. It is well known that reefs are more likely to shift to a degraded state such as a macroalgae-dominated state if stress on corals increases, for example due to climate change, high nutrient run-off, or intensive fishing. However, whether this shift will be gradual or abrupt (Fig. 4.1) will largely depend on the strengths of feedbacks in the ecosystem. Reefs with weakened negative feedbacks or strengthened positive

feedbacks, or, as we have shown here, with multiple weak positive feedbacks are more prone to have critical thresholds where they undergo collapses that are difficult to reverse.

Because the strength of the many commonly-observed feedbacks (Table 4.1) varies from place to place and from time to time (Fig. 4.4), a corollary is that it is impossible to conclude that coral reefs in general will or will not have alternative stable states (Bruno *et al.* 2009; Dudgeon *et al.* 2010; Mumby *et al.* 2013). Consequently, while some coral reefs around the globe may respond smoothly to slowly changing anthropogenic drivers, others can unexpectedly collapse and fail to recover even when drivers are reduced (e.g. Connell 1997; Hughes *et al.* 2010; Graham *et al.* 2011).

Obviously, our model captures only a small part of the complexity of coral reefs. It is tempting to further elaborate and parameterize the model in order to capture more of the complexity and spatial variation found in the field. Indeed, the wish to describe ecosystems as realistically as possible has driven the development of detailed, spatially explicit models, with specified environmental conditions for each location (e.g. Melbourne-Thomas *et al.* 2011). However, although more complex models can be of great help in evaluating the potential role of different processes, they remain challenging to parameterize and fully understand (Oreskes *et al.* 1994). Our model is meant to complement this approach. Rather than aiming to be complete, 'minimal models' such as the one we present may help to understand how non-linear mechanisms may interact to drive complex systems.

Managing ecosystem resilience

Many natural resource management agencies struggle to cope with multiple human impacts that are cumulative and potentially synergistic. Often the response of cash-strapped agencies is to manage "stressors" or drivers without a clear understanding of which interventions are likely to give the best environmental or social outcome. Our analysis illustrates that an understanding of how multiple feedbacks interact is essential to guide management decisions. Even mechanisms that are likely to be dismissed as unimportant, can collectively destabilize an ecosystem. Therefore, efforts to reduce human impacts on reefs need to focus on understanding and managing interactive feedbacks (Bellwood *et al.* 2004; Nyström *et al.* 2012; Graham *et al.* 2013), such as the ones we have highlighted (see also Table 4.1). Our results show that management decisions for protecting coral reefs could be substantially improved by a better understanding of how multiple feedbacks interact to strengthen or weaken hysteresis. Currently, economic and social constraints rather than scientific knowledge often dominate the choice of management action, or inaction (Scheffer *et al.* 2015a).

We conclude that to comprehend ecological resilience and alternative states more fully, and to avoid unwanted critical transitions, will require a new focus on the combined effects of positive and negative feedbacks, measuring the existence and proximity to thresholds, and assessing the strength of hysteresis (e.g. Dakos *et al.* 2012a; Scheffer *et al.* 2012). Importantly, our theoretical exploration of the importance of feedbacks highlights a critical knowledge gap in when and where they occur, how strong or weak they may be, and how they interact to influence the nature of critical transitions.

Appendix A4

References Table 4.1 (main text)

1. May RM. 1977. Thresholds and breakpoints in ecosystems with a multiplicity of stable states. Nature 269: 471–477.
2. Hereu B, Zabala M, Linares C, Sala E. 2004. The effects of predator abundance and habitat structural complexity on survival of juvenile sea urchins. Marine Biology 146: 293–299.
3. Williams ID, Polunin NVC, Hendrick V J. 2001. Limits to grazing by herbivorous fishes and the impact of low coral cover on macroalgal abundance on a coral reef in Belize. Marine Ecology Progress Series 222: 187–196.
4. Hatcher BG. 1984. A maritime accident provides evidence for alternate stable states in benthic communities on coral reefs. Coral Reefs 3: 199–204.
5. Doherty P, Fowler T. 1994. An empirical test of recruitment limitation in a coral reef fish. Science 263: 935–939.
6. Wellington G, Victor BC. 1985. El Niño mass coral mortality: a test of resource limitation in a coral reef damselfish population. Oecologia 68: 15–19.
7. Ledlie MH, Graham NAJ, Bythell JC, Wilson SK, Jennings S, Polunin NVC, Hardcastle J. 2007. Phase shifts and the role of herbivory in the resilience of coral reefs. Coral Reefs 26: 641–53.
8. Hay M, Fenical W. 1988. Marine plant-herbivore interactions: the ecology of chemical defense. Annual review of ecology and systematics 19: 111–45.
9. Fong P, Smith TB, Wartian MJ. 2006. Epiphytic cyanobacteria maintain shifts to macroalgal dominance on coral reefs following ENSO disturbance. Ecology 87: 1162–8.
10. McClanahan TR, Uku JN, Machano H. 2002. Effect of macroalgal reduction on coral-reef fish in the Watamu Marine National Park, Kenya. Marine and freshwater research 53: 223–31.
11. Hoey AS, Bellwood DR. 2011. Suppression of herbivory by macroalgal density: a critical feedback on coral reefs? Ecology letters 14: 267–73.
12. Steneck RS, Leland A, McNaught DC, Vavrinec J. 2013. Ecosystem flips, locks, and feedbacks: the lasting effects of fisheries on Maine's kelp forest ecosystem. Bulletin of Marine Science 89: 31–55.
13. Knowlton N, Lang JC, Keller BD. 1990. Case study of natural population collapse: post-hurricane predation on Jamaican staghorn corals. Smithsonian Contributions to the Marine Sciences 294: 1–25.
14. Eakin CM. 1996. Where have all the carbonates gone? A model comparison of calcium carbonate budgets before and after the 1982–1983 El Nino at Uva Island in the eastern Pacific. Coral Reefs 15: 109–19.
15. McClanahan TR, Maina J, Starger CJ, Herron-Perez P, Dusek E. 2005. Detriments to post-bleaching recovery of corals. Coral Reefs 24: 230–46.
16. Rotjan RD, Dimond JL, Thornhill DJ, Leichter JJ, Helmuth B, Kemp DW, Lewis SM. 2006. Chronic parrotfish grazing impedes coral recovery after bleaching. Coral Reefs 25: 361–8.
17. Coker DJ, Pratchett MS, Munday PL. 2009. Coral bleaching and habitat degradation increase susceptibility to predation for coral-dwelling fishes. Behavioral Ecology 20: 1204–10.
18. Cole AJ, Pratchett MS, Jones GP. 2008. Diversity and functional importance of coral-feeding fishes on tropical coral reefs. Fish and Fisheries 9: 286–307.
19. Cinner JE, Folke C, Daw T, Hicks CC. 2011. Responding to change: using scenarios to understand how socioeconomic factors may influence amplifying or dampening exploitation feedbacks among Tanzanian fishers. Global Environmental Change 21: 7–12.
20. Mackinson S, Sumaila UR, Pitcher TJ. 1997. Bioeconomics and catchability: fish and fishers behaviour during stock collapse. Fisheries Research 31: 11–7.
21. Sumaila UR, Khan A, Watson R, Munro G, Zeller D, Baron N, Pauly D. 2007. The World Trade Organization and global fisheries sustainability. Fisheries Research 88 :1–4.

22. Munro G, Sumaila UR. 2002. The impact of subsidies upon fisheries management and sustainability: the case of the North Atlantic. Fish and Fisheries 3: 233–50.
23. Lotka AJ. 1932. The growth of mixed populations: two species competing for a common food supply. Journal of the Washington Academy of Sciences 22: 461–9.
24. Volterra, V. 1926. Fluctuations in the abundance of a species considered mathematically. Nature 118:558–560.
25. Diaz-Pulido G, Harii S, McCook LJ, Hoegh-Guldberg O. 2009. The impact of benthic algae on the settlement of a reef-building coral. Coral Reefs 29: 203–8.
26. Kuffner I, Walters L, Becerro M, Paul V, Ritson-Williams R, Beach K. 2006. Inhibition of coral recruitment by macroalgae and cyanobacteria. Marine Ecology Progress Series 323: 107–17.
27. Lirman D. 2001. Competition between macroalgae and corals: effects of herbivore exclusion and increased algal biomass on coral survivorship and growth. Coral Reefs 19: 392–9.
28. Tanner JE. 1995. Competition between scleractinian corals and macroalgae: An experimental investigation of coral growth, survival and reproduction. Journal of Experimental Marine Biology and Ecology 190: 151–68.
29. Hughes TP, Rodrigues MJ, Bellwood DR, Ceccarelli D, Hoegh-Guldberg O, McCook L, Moltschaniwskyj N, Pratchett MS, Steneck RS, Willis B. 2007. Phase shifts, herbivory, and the resilience of coral reefs to climate change. Current biology 17: 360–5.
30. Birrell CL, McCook LJ, Willis BL, Diaz-Pulido G. 2008. Effects of benthic algae on the replenishment of corals and the implications for the resilience of coral reefs. Oceanography and Marine Biology: An Annual Review 46: 25–63.
31. Coyer JA, Ambrose RF, Engle JM, Carroll JC. 1993. Interactions between corals and algae on a temperate zone rocky reef: mediation by sea urchins. Journal of Experimental Marine Biology and Ecology 167: 21–37.
32. Jompa J, McCook LJ. 2003. Coral-algal competition: macroalgae with different properties have different effects on corals. Marine Ecology Progress Series 258: 87–95.
33. Jompa J, McCook LJ. 2002. Effects of competition and herbivory on interactions between a hard coral and a brown alga. Journal of Experimental Marine Biology and Ecology 271: 25–39.
34. Smith JE, Shaw M, Edwards RA, Obura D, Pantos O, Sala E, Sandin SA, Smriga S, Hatay M, Rohwer FL. 2006. Indirect effects of algae on coral: algae-mediated, microbe-induced coral mortality. Ecology letters 9: 835–45.
35. Rasher DB, Hay ME. 2010. Chemically rich seaweeds poison corals when not controlled by herbivores. Proceedings of the National Academy of Sciences of the United States of America 107: 9683–8.
36. Nugues MM, Smith GW, Hooidonk RJ, Seabra MI, Bak RPM. 2004. Algal contact as a trigger for coral disease. Ecology Letters 7: 919–23.
37. Littler MM, Littler DS. 1997. Epizoic red alga allelopathic (?) to a Caribbean coral. Coral Reefs 16: 168.
38. Nugues M, Delvoye L, Bak R. 2004. Coral defence against macroalgae: differential effects of mesenterial filaments on the green alga Halimeda opuntia. Marine Ecology Progress Series 278: 103–14.
39. Courchamp F, Berec L, Gascoigne JC. 2008. Allee Effects in Ecology and Conservation. Oxford: Oxford University Press
40. Oliver J, Babcock R. 1992. Aspects of the fertilization ecology of broadcast spawning corals: sperm dilution effects and in situ measurements of fertilization. The Biological Bulletin 183: 409–17.
41. Willis BL, Babcock RC, Harrison PL, Wallace CC. 1997. Experimental hybridization and breeding incompatibilities within the mating systems of mass spawning reef corals. Coral Reefs 16: S53–S65.
42. Omori M, Fukami H, Kobinata H, Hatta M. 2001. Significant drop of fertilization of Acropora corals in 1999: an after-effect of heavy coral bleaching? Limnology and oceanography 46: 704–6.
43. Edmunds P, Elahi R. 2007. The demographics of a 15-year decline in cover of the Caribbean reef coral Montastraea annularis. Ecological Monographs 77: 3–18.

44. Hughes T, Baird A, Dinsdale E, Moltschaniwskyj N, Pratchett M, Tanner JE, Willis BL. 2000. Supply-side ecology works both ways: the link between benthic adults, fecundity, and larval recruits. Ecology 81: 2241–9.
45. Vermeij MJA, Marhaver KL, Huijbers CM, Nagelkerken I, Simpson SD. 2010. Coral larvae move toward reef sounds. PLoS ONE 5: e10660.
46. Baird A, Morse A. 2004. Induction of metamorphosis in larvae of the brooding corals *Acropora palifera* and *Stylophora pistillata*. Marine and freshwater research 55: 469–72.
47. Harrington L, Fabricius K, De'Ath G, Negri A. 2004. Recognition and selection of settlement substrata determine post-settlement survival in corals. Ecology 85: 3428–37.
48. Price N. 2010. Habitat selection, facilitation, and biotic settlement cues affect distribution and performance of coral recruits in French Polynesia. Oecologia 163: 747–58.
49. Babcock R, Mundy C. 1992. Reproductive biology, spawning and field fertilization rates of *Acanthatser planci*. Australian Journal of Marine and Freshwater Research 43: 525–34.
50. Levitan DR. 1991. Influence of body size and population density on fertilization success and reproductive output in a free-spawning invertebrate. Biological Bulletin 181: 261–8.
51. Hutchings JA, Reynolds JD. 2004. Marine fish population collapses : consequences for recovery and extinction risk. BioScience 54: 297–309.
52. Lee SC. 2006. Habitat complexity and consumer-mediated positive feedbacks on a Caribbean coral reef. Oikos 112: 442–7.
53. Friedlander AM, Parrish JD. 1998. Habitat characteristics affecting fish assemblages on a Hawaiian coral reef. Journal of Experimental Marine Biology and Ecology 224: 1–30.
54. Lindahl U, Öhman MC, Schelten CK. 2001. The 1997/1998 mass mortality of corals : effects on fish communities on a Tanzanian coral reef. Marine Pollution Bulletin 42: 127–31.
55. Mumby PJ, Wabnitz CCC. 2002. Spatial patterns of aggression, territory size, and harem size in five sympatric Caribbean parrotfish species. Environmental Biology of Fishes 63: 265–79.
56. Paddack MJ, Reynolds JD, Aguilar C, Appeldoorn RS, Beets J, Burkett EW, Chittaro PM, Clarke K, Esteves R, Fonseca AC, Forrester GE, Friedlander AM, García-Sais J, González-Sansón G, Jordan LKB, McClellan DB, Miller MW, Molloy PP, Mumby PJ, Nagelkerken I, Nemeth M, Navas-Camacho R, Pitt J, Polunin NVC, Reyes-Nivia MC, Robertson DR, Rodríguez-Ramírez A, Salas E, Smith SR, Spieler RE, Steele MA, Williams ID, Wormald CL, Watkinson AR, Côté IM. 2009. Recent region-wide declines in Caribbean reef fish abundance. Current biology 19: 590–5.
57. Öhman MC, Munday PL, Jones GP, Caley MJ. 1998. Settlement strategies and distribution patterns of coral-reef fishes. Journal of Experimental Marine Biology and Ecology 225: 219–38.
58. Halford A, Cheal AJ, Ryan D, Williams DM. 2004. Resilience to large-scale disturbance in coral and fish assemblages on the Great Barrier Reef. Ecology 85: 1892–905.
59. Graham NAJ, Wilson SK, Jennings S, Polunin NVC, Bijoux JP, Robinson J. 2006. Dynamic fragility of oceanic coral reef ecosystems. Proceedings of the National Academy of Sciences of the United States of America 103: 8425–9.
60. Garpe K, Yahya S, Lindahl U, Öhman M. 2006. Long-term effects of the 1998 coral bleaching event on reef fish assemblages. Marine Ecology Progress Series 315: 237–47.
61. Wilson SK, Graham NAJ, Pratchett MS, Jones GP, Polunin NVC. 2006. Multiple disturbances and the global degradation of coral reefs: are reef fishes at risk or resilient? Global Change Biology 12: 2220–34.
62. Syms C, Jones GP. 2000. Disturbance, habitat structure, and the dynamics of a coral-reef fish community. Ecology 81: 2714–29.
63. Vergés A, Vanderklift MA, Doropoulos C, Hyndes GA. 2011. Spatial patterns in herbivory on a coral reef are influenced by structural complexity but not by algal traits. PloS one 6: e17115.
64. Bellwood, DR, Fulton CJ. 2008. Sediment-mediated suppression of herbivory on coral reefs: decreasing resilience to rising sea levels and climate change? Limnology and Oceanography 53: 2695–2701.

65. Birrell CL, McCook LJ, Willis BL. 2005. Effects of algal turfs and sediment on coral settlement. Marine pollution bulletin 51: 408–14.
66. Mascia MB. 2001. Designing effective coral reef marine protected areas. A synthesis report based on presentations at the 9th International Coral Reef Symposium Bali, Indonesia October 2000.

Modeling positive feedbacks

We modeled three positive feedback mechanisms, where the strength of each is determined by one parameter (η, α, and σ) (Fig. A4.1). The feedbacks interact synergetically, as illustrated by the bifurcation plots in Figure A4.2.

Herbivory-escape feedback (Table 4.1, feedbacks 1-3): we assumed that herbivores have a certain handling time when consuming macroalgae (η). If macroalgae availability increases, herbivores can handle less macroalgae, and thus herbivory pressure per macroalga decreases (Fig. A4.1a).

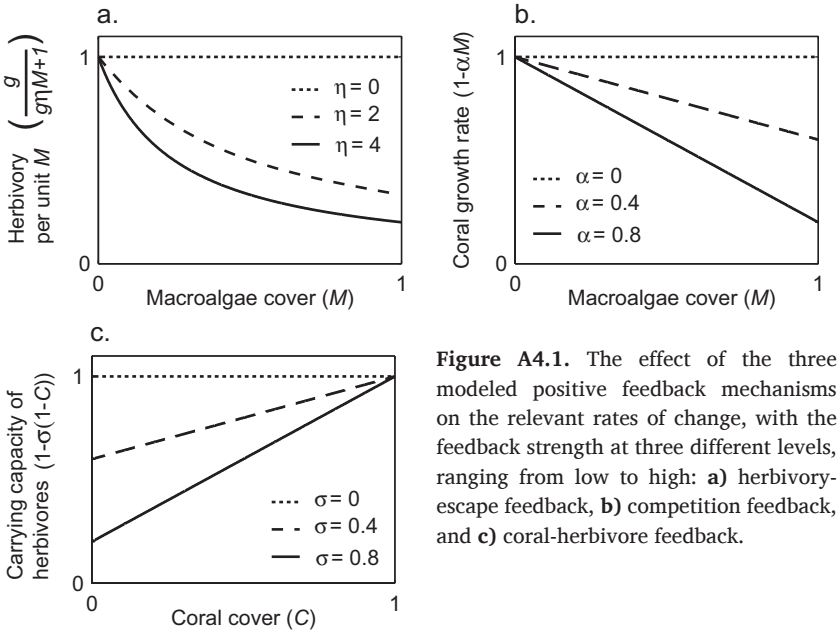

Figure A4.1. The effect of the three modeled positive feedback mechanisms on the relevant rates of change, with the feedback strength at three different levels, ranging from low to high: **a)** herbivory-escape feedback, **b)** competition feedback, and **c)** coral-herbivore feedback.

Competition feedback (Table 4.1, feedbacks 6-7): We assumed that macroalgae can reduce coral recruitment, for example, by pre-empting, shading and overgrowing juvenile corals. The strength of this inhibition is represented by the parameter α. The level of α depends on the macroalgae and coral species present. A lower coral recruitment per unit area of empty space per adult coral occurs if macroalgae cover increases, which leads to a competitive advantage for macroalgae (Fig. A4.1b).

Coral-herbivore feedback (Table 4.1, feedback 15): Herbivores have a positive effect on corals, because they release them from competition with macroalgae. We assumed that corals can also have a positive effect on herbivores by providing shelter (e.g. for *Diadema* or parrotfish) (Fig. A4.1c). The strength of this dependence (σ) will depend on traits of the herbivore and coral species.

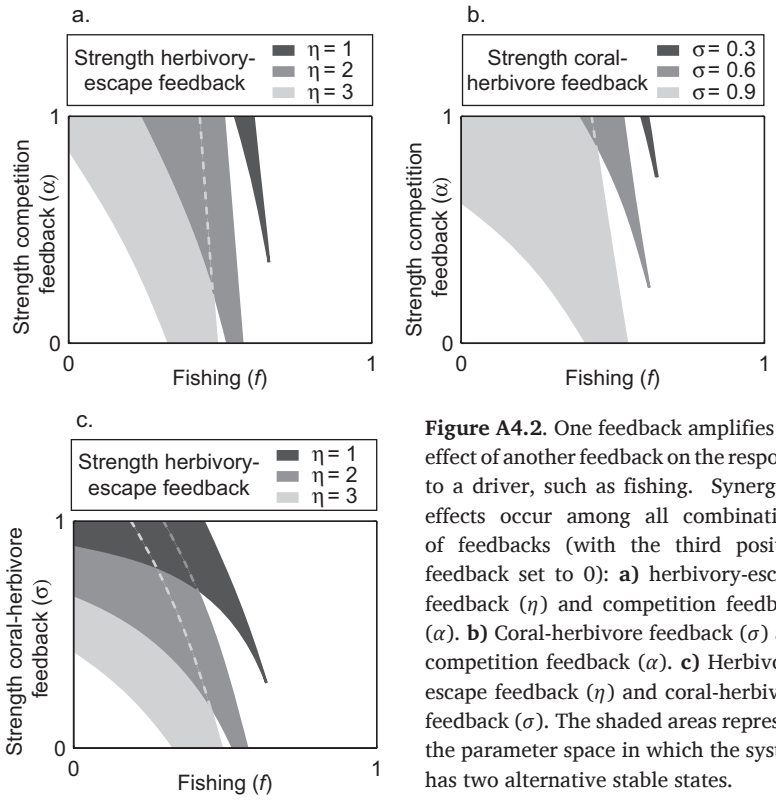

Figure A4.2. One feedback amplifies the effect of another feedback on the response to a driver, such as fishing. Synergetic effects occur among all combinations of feedbacks (with the third positive feedback set to 0): **a)** herbivory-escape feedback (η) and competition feedback (α). **b)** Coral-herbivore feedback (σ) and competition feedback (α). **c)** Herbivory-escape feedback (η) and coral-herbivore feedback (σ). The shaded areas represent the parameter space in which the system has two alternative stable states.

Chapter 5

Anticipating critical transitions: a review

Marten Scheffer,
Steve R. Carpenter,
Tim M. Lenton,
Jordi Bascompte,
William Brock,
Vasilis Dakos,
Johan van de Koppel,
Ingrid A. van de Leemput,
Simon A. Levin,
Mercedes Pascual,
and John Vandermeer

Published in *Science:*

Scheffer M, Carpenter SR, Lenton TM, Bascompte J, Brock W, Dakos V, van de Koppel J, van de Leemput IA, Levin SA, van Nes EH, Pascual M, Vandermeer J. 2012. Anticipating critical transitions. *Science* **338**: 344–8

Abstract

Tipping points in complex systems may imply risks of unwanted collapse, but also opportunities for positive change. Our capacity to navigate such risks and opportunities can be boosted by combining emerging insights from two unconnected fields of research. One line of work is revealing fundamental architectural features that may cause ecological networks, financial markets, and other complex systems to have tipping points. Another field of research is uncovering generic empirical indicators of the proximity to such critical thresholds. While sudden shifts in complex systems will inevitably keep taking us by surprise, work at the crossroads of these emerging fields offers new approaches for anticipating critical transitions.

The current global financial crisis, the HIV pandemic and the Arab revolts are recent reminders of the unpredictable nature of the transitions that occasionally affect humanity. Such defining events are not necessarily negative. About 12,000 years ago, the Earth suddenly shifted from a long harsh glacial episode into the benign and stable Holocene climate that allowed human civilization to develop. On smaller and faster scales, ecosystems occasionally flip to contrasting states. Unlike gradual trends, such sharp shifts are largely unpredictable (Folke *et al.* 2004; Scheffer 2009; Barnosky *et al.* 2012). Nonetheless, science is now carving into this realm of unpredictability in fundamental ways. While the complexity of systems such as societies and ecological networks prohibits accurate mechanistic modeling, certain features turn out to be generic markers of the fragility that may typically precede a large class of abrupt changes. Two distinct approaches have led to these insights. On the one hand, analyses across networks and other systems with many components have revealed that particular aspects of their structure determine whether they are likely to have critical thresholds where they may change abruptly; on the other hand, recent findings suggest that certain generic indicators may be used to detect if a system is close to such a 'tipping point'. We highlight key findings but also challenges in these emerging research areas and discuss how exciting opportunities arise from the combination of these so far disconnected fields of work.

The architecture of fragility

Sharp regime shifts that punctuate the usual fluctuations around trends in ecosystems or societies may often be simply the result of an unpredictable external shock. However, another possibility is that such a shift represents a so-called critical transition (Scheffer 2009; Kuehn 2011). The likelihood of such transitions may gradually increase as a system approaches a 'tipping point' (i.e. a catastrophic bifurcation (Kuznetsov 1995)), where a minor trigger is enough to invoke a self-propagating shift to a contrasting state. One of the big questions in complex systems science is what causes some systems to have such tipping points. The basic ingredient for a tipping point is a positive feedback that, once a critical point is passed, propels change towards an alternative state (Angeli *et al.* 2004). While this principle is well understood for simple isolated systems, it is more challenging to fathom how heterogeneous structurally complex systems such as networks of species, habitats, or societal structures might respond to changing conditions and perturbations. A broad range of studies suggests that two major features are crucial for the overall response of such systems (Levin 2000): (i) the heterogeneity of the components and (ii) their connectivity (Fig. 5.1). How these properties affect the stability depends on the nature of the interactions in the network.

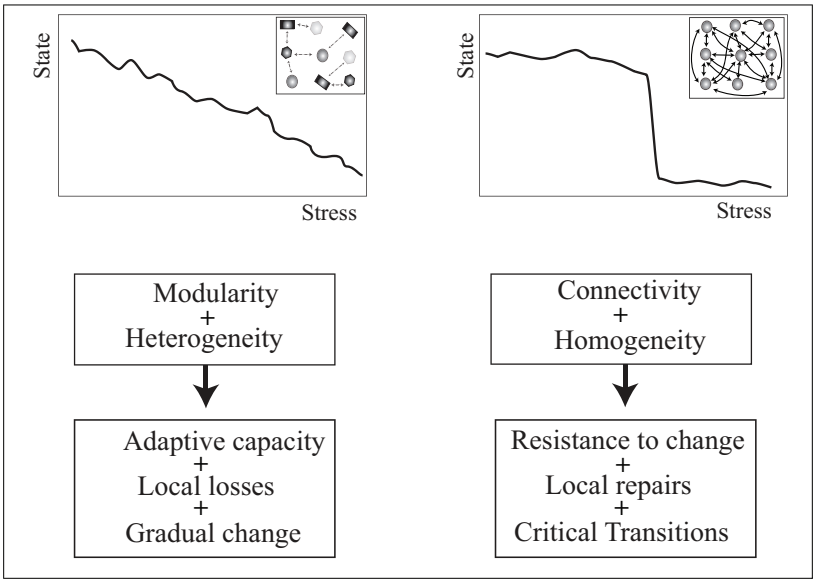

Figure 5.1. The connectivity and homogeneity of the units affect the way in which distributed systems with local alternative states respond to changing conditions. Networks where the components differ (are heterogeneous) and where incomplete connectivity causes modularity tend to have adaptive capacity in the sense that they adjust gradually to change. By contrast, in highly connected networks local losses tend to be 'repaired' by subsidiary inputs from linked units until at a critical stress level the system collapses. As explained in the main text, the particular structure of connections also has important consequences for the robustness of networks, depending on the kind of interactions between the nodes of the network.

Domino effects. One broad class of networks includes those where units (or 'nodes') can flip between alternative stable states and where the probability of being in one state is promoted by having neighbors in that state. One may think, for instance, of networks of populations (extinct or not), or ecosystems (with alternative stable states) or banks (solvent or not). In such networks, heterogeneity in the response of individual nodes and a low level of connectivity, may cause the network as a whole to change gradually---rather than abruptly---in response to environmental change. This is because the relatively isolated and different nodes will each shift at another level of an environmental driver (van Nes and Scheffer 2005). By contrast, homogeneity (nodes being more similar) and a highly connected network may provide resistance to change until a threshold for a systemic critical transition is reached where all nodes shift in synchrony (Dunne *et al.* 2002; van Nes and Scheffer 2005).

This situation implies a trade-off between local and systemic resilience. Strong connectivity promotes local resilience, in the sense that effects of local perturbations can be eliminated quickly through subsidiary inputs from the broader system. For instance, local damage to a coral reef may be repaired by 'mobile link organisms'

from nearby reefs, and individual banks may be saved by subsidiary inputs from the larger financial system (Lundberg and Moberg 2003). However, as conditions change, highly connected systems may reach a tipping point where a local perturbation can cause a domino effect cascading into a systemic transition (van Nes and Scheffer 2005). Importantly, in such connected systems the repeated recovery from small scale perturbations can give a false impression of resilience, masking the fact that the system may actually be approaching a tipping point for a systemic shift. For example, before the sudden large scale collapse of Caribbean coral systems in the 1980s evoked by a sea urchin disease outbreak, the reefs were considered highly resilient systems, as they recovered time and time again from devastating tropical storms and other local perturbations (Bellwood *et al.* 2004). In summary, the same prerequisites that allow recovery from local damage may set a system up for large-scale collapse.

Robustness in different kinds of networks. In addition to the work on systems where units can switch between alternative states in a contagious way, there has been an increasing interest in understanding robustness of webs of other kinds of interactions. For instance, species in ecosystems can be linked through mutualistic (+/+) interactions such as in pollinators and plants, or by competition (-/-) or predation (+/-). Rather than asking what causes the overall systems response to be catastrophic or gradual, most of these studies have so far been focused on what topology of interaction structures makes the overall system less likely to fall apart when components are randomly removed. The answer turns out to depend on the kind of interactions between the units. Overall, networks with antagonistic interactions (e.g. competition) are predicted to be more robust if interactions are compartmentalized into loosely connected modules whereas networks with strong mutualistic interactions (e.g. pollination) are more robust if they have nested structures where specialists are preferentially linked in their mutualism to generalists that act as hubs of connectivity (Pascual and Dunne; Thébault and Fontaine 2010). Empirical studies in ecology suggest that the structures predicted to be more robust are also found most in nature (Bascompte *et al.* 2003; Otto *et al.* 2007; Thébault and Fontaine 2010), but this is an active field of research where new insights are still emerging (Allesina and Pascual 2009) and much remains to be explored.

The challenge of designing robust systems. The work on ecological networks has led to the idea that we might apply our insights in the functioning of natural systems when it comes to designing structures that are less vulnerable to collapse. For instance, about half a year before the collapse of global financial markets in 2008, it was pointed out (May *et al.* 2008) that it could be helpful to analyse the financial system for the generic structural features that were found by ecologists to affect

the risk of systemic failure. Building on such parallels between the architecture of ecological and financial systems, Haldane and May (2011) have made specific recommendations to encourage modularity and diversity in the financial sectors as a way to decrease systemic risk. There are still obvious challenges in bridging from ecosystems and conceptual models to societal structures, and much will be beyond our reach when it comes to 'design'. For instance, the extremely fast global spread of information is an important feature of current social systems, and the worldwide connection of social-ecological systems through markets implies a daunting level of complexity (Adger *et al.* 2009). Nonetheless, this line of thinking about features that affect robustness across systems clearly offers fresh perspectives on the question how we can make the complex networks on which we depend more robust.

Early warning signals for critical transitions

Although such insight into structural determinants of robustness and fragility can guide the design of systems that are less likely to go through sharp transitions, there are so far no ways in which these features can be used to measure how close any particular system really is to a critical transition. A new field of research is now emerging that focuses on precisely that (Scheffer *et al.* 2009).

Critical slowing down near tipping points. One line of work is based on the generic phenomenon that in the vicinity of many kinds of tipping points, the rate at which a system recovers from small perturbations becomes very slow, a phenomenon known as 'critical slowing down' (Fig. 5.2). This happens, for instance, at the classical fold bifurcation, often associated with the term 'tipping point', as well as more broadly in situations where a system becomes sensitive so that a tiny nudge can cause a large change (Scheffer *et al.* 2009). The increasing sluggishness of a system can be detected as a reduced rate of recovery from (experimental) perturbations (van Nes and Scheffer 2007; Veraart *et al.* 2012). However, the slowness can also be inferred indirectly from rising 'memory' in small fluctuations in the state of a system (Fig. 5.2), as reflected for instance in a higher lag-1 autocorrelation (Ives 1995; Dakos *et al.* 2008), increased variance (Carpenter and Brock 2006), or other indicators (Kleinen *et al.* 2003; Livina and Lenton 2007).

Obviously, not all abrupt transitions will be preceded by slowing down. For instance, sharp change may simply result from a sudden big external impact. Also, slowing down of rates can have other causes than approaching a tipping point (e.g. a drop in temperature). Therefore, slowing down is neither a universal warning signal for shifts, nor specific to an approaching tipping point. Instead, slowing down should be seen as a 'broad spectrum' indicator of potential fundamental change in the current regime. Further diagnosis of what might be coming up requires additional information.

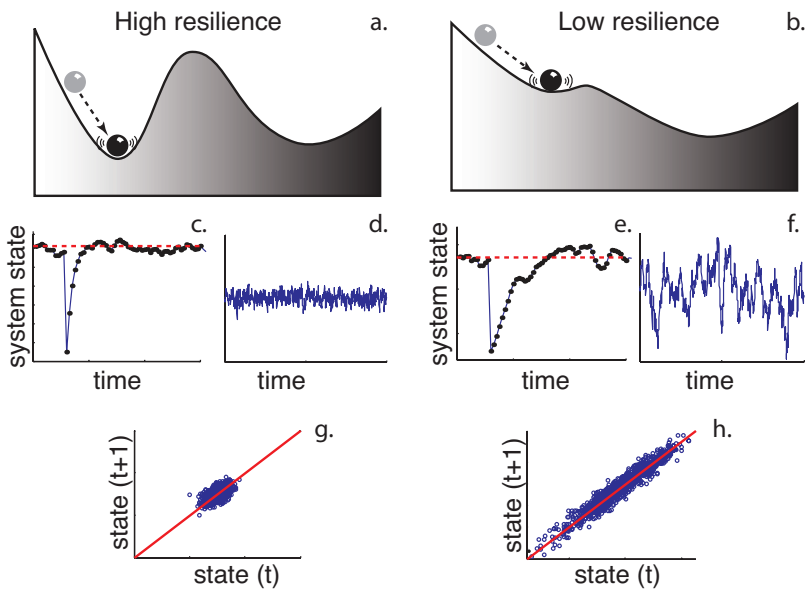

Figure 5.2. Critical slowing down as an indicator that the system has lost resilience in the sense that it may be tipped more easily into an alternative state. Recovery rates upon small perturbations **(panels c and e)** are slower if the basin of attraction is small (right hand panels) than when the attraction basin is larger (left hand panels). The effect of this slowing down may be measured in stochastically induced fluctuations in the state of the system **(panels d and f)** as increased variance and 'memory' as reflected by lag-1 autocorrelation **(panels g and h)**.

Changing stability landscapes in stochastic systems. In highly stochastic systems, transitions will typically happen far from local bifurcation points. This makes it unlikely that in such stochastic situations slowing down is a useful characteristic to measure. On the other hand, the behaviour of systems exposed to strong perturbation regimes can hint at features of the underlying stability landscape. When an alternative basin of attraction begins to emerge, one may expect that in stochastic environments, systems will occasionally flip to that state, a phenomenon referred to as 'flickering' (Scheffer *et al.* 2009). Rising variance can reflect such a change. Moreover, under certain assumptions, the probability density distribution of the state of a system can even be used to estimate how the potential landscape reflecting the stability properties of the system changes over time (Livina *et al.* 2010) or is affected by important drivers (Hirota *et al.* 2011) (Fig. 5.3). The idea behind this approach is that even if stochasticity is large, systems will more often be found close to attractors than far away from them. The scope of this approach is different from that implied in work on critical slowing down. Slowing down suggests an increased probability of a sudden transition to a new unknown state. By contrast, the information extracted from more wildly fluctuating systems suggests a

contrasting regime to which a system may shift if conditions change. Just as in the detection of critical slowing down, patterns in the data should be interpreted with caution. For instance, multimodality of the frequency distribution of states over a parameter range may be caused by non-linear responses to other, unobserved drivers or from a multimodality of the distribution of such drivers. Also, the character of the perturbation regime may have a large effect.

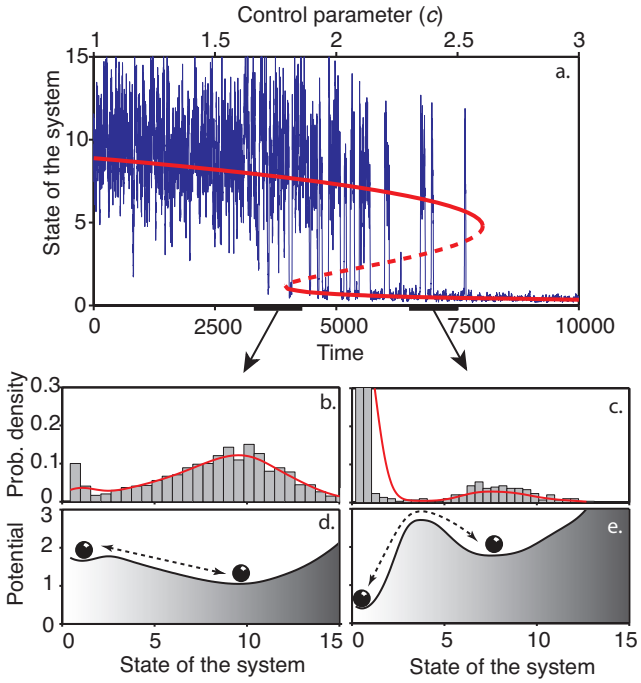

Figure 5.3. Flickering to an alternative state as a warning signal in highly stochastic systems. In such situations, the frequency distribution of states **(panels b and c)** can be used to approximate the shape of the basins of attraction of the alternative states **(panels d and e)**. The data in this example are generated with a model of overexploitation (May 1977): $\frac{dx}{dt}=x\left(1-\frac{x}{K}\right)-\frac{cx}{1+x}$ with different additive and multiplicative stochastic terms (Dakos *et al.* 2012a) (we used K=11).

Prospects, challenges and limitations. Although the work on empirical indicators of robustness and resilience is just emerging, there is already a fast-growing body of modeling as well as empirical work (Table 5.1). Nonetheless, major challenges remain when it comes to developing robust procedures for assessment. One problem is that methods for detection of incipient transitions from time-series tend to require long, high-resolution data (Dakos *et al.* 2008, 2012a). As a picture of a spatial pattern can carry much more information than a single point in a time series, the interpretation of spatial patterns is a potentially powerful option. Just as increased memory in time series, correlation between neighbouring units can reflect slowing

down (Dakos *et al.* 2010). Similarly, spatial data can be used to infer how resilience of alternative states depends on key drivers (Hirota *et al.* 2011). Various aspects of spatial patterns may also change in unique ways as a critical point is near (Solé *et al.* 1996; Holling 2001; Rietkerk *et al.* 2004; Pascual and Guichard 2005; Kéfi *et al.* 2007; Dakos *et al.* 2010), but these patterns and their interpretation differ across systems in ways that are not yet entirely understood.

A fundamental limitation is that the indicators cannot be used for prediction of transitions, as stochastic shocks will always play an important role in triggering transitions before a bifurcation point is reached. Also, interpreting absolute values of indicators as signalling particular levels of fragility so far remains beyond reach. Thus, indicators should be used to rank situations on a relative scale from fragile to resilient. Detecting early-warning signals in monitoring time-series may seem an obvious application. However, this requires the rare situation that we have data of high resolution for a system that moves towards a tipping point gradually (Biggs *et al.* 2009). In addition to such challenges in detection, there are still gaps in our understanding of how indicators will behave in more complex situations. In view of these limitations there is no silver bullet approach. Instead, a diverse collection of complementary indicators and methods of applying them is emerging. A state of the art overview linked to a website with open-source software for data analysis is published elsewhere (Dakos *et al.* 2012a) (www.early-warning-signals.org).

Table 5.1: Studies of early warning indicators for critical transitions in different complex systems (+ denote cases where early warning signals were detected by indicators, 0 cases where transitions were not preceded by indicators, - is unknown or opposite effect)

Field	Phenomenon	Indicator	Signal	References
Chemistry	Critical slowing down	recovery rate/ return time	+	Kramer and Ross 1985
Physics	Critical slowing down	return time/ dominant eigenvalue	+	Tredicce *et al.* 2004
		rate of change of amplitude	+	Lim and Epureanu 2011
Engineering	Critical slowing down	autocorrelation at lag 1	+	Hines *et al.* 2011
Tectonics	Not specified	autocorrelation/ spatial correlation	+	Ramos 2010
Climate	Critical slowing down	autocorrelation at lag 1	+	Dakos *et al.* 2008; Thompson and Sieber 2011; Lenton *et al.* 2012
			0	Ditlevsen and Johnsen 2010; Lenton *et al.* 2012
		detrended fluctuation analysis	+	Livina and Lenton 2007; Lenton *et al.* 2012
			-	Lenton *et al.* 2012
	Increasing variability	variance	+	Lenton *et al.* 2012
			0	Ditlevsen and Johnsen 2010; Lenton *et al.* 2012
	Skewed responses	skewness	0	Guttal and Jayaprakash 2008a
Ecology	Critical slowing down	return time/dominant eigenvalue	+	Wissel 1984; Drake and Griffen 2010; Carpenter *et al.* 2011; Veraart *et al.* 2012
		autocorrelation at lag 1	+	Veraart *et al.* 2012
		spectral reddening	0	Carpenter *et al.* 2011
		spatial correlation	+	Hsieh *et al.* 2006; Beaugrand *et al.* 2008; Drake and Griffen 2010; Carpenter *et al.* 2011

Field	Phenomenon	Indicator	Signal	References
	Increasing variability	variance	+	Hsieh *et al.* 2006; deYoung *et al.* 2008; Drake and Griffen 2010; Carpenter *et al.* 2011
			0	Bestelmeyer *et al.* 2011; Veraart *et al.* 2012
		spatial variance	+	Litzow *et al.* 2008; Hewitt and Thrush 2010; Drake and Griffen 2010; Carpenter *et al.* 2011
	Skewed responses	skewness	+	Drake and Griffen 2010; Carpenter *et al.* 2011
Microbiology	Critical slowing down	autocorrelation at lag 1	+	Dai *et al.* 2012
		variance	+	Dai *et al.* 2012
		return time	+	Dai *et al.* 2012
		skewness	0	Dai *et al.* 2012
Physiology	Critical slowing down	recovery rate/ return time	+	Matsumoto and Kunisawa 1978
Epilepsy	Critical slowing down	correlation	+	Gorban *et al.* 2010; Meisel and Kuehn 2012
	Increasing variability	variance	+	McSharry *et al.* 2003)
Behaviour	Critical slowing down	recovery rate/ return time	+	Kelso *et al.* 1986; Scholz *et al.* 1987
Sociology	Critical slowing down	autocorrelation at lag 1	+/0	Neuman *et al.* 2011
		variance	+/0	Neuman *et al.* 2011; Saavedra *et al.* 2011
		Fisher information	+	Mayer *et al.* 2007
Finance	Not specified	correlation	+	Gorban *et al.* 2010
	Not specified	Shannon index	+	Brida and Punzo 2003
	Not specified	variance	+	Sornette and Woodard 2010

Towards an integrative approach for anticipating critical transitions

So far, research on network robustness and work on empirical indicators of resilience has been largely segregated. However, connecting across these fields opens up obvious new perspectives. First of all, there is complementarity in the existing approaches. The structural features that create tipping points and the different empirical indicators for their proximity offer alternative angles for diagnosis and potential action (Fig. 5.4). A smart combination of approaches in a unified framework may therefore greatly enhance our capacity to anticipate critical transitions.

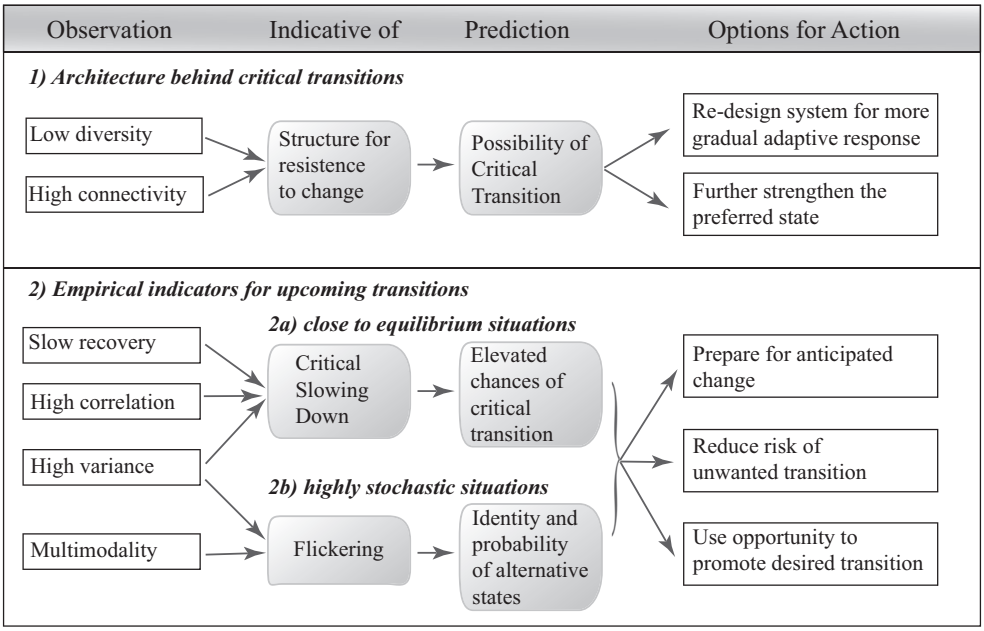

Figure 5.4. Different classes of generic observations that can be used to indicate the potential for critical transitions in a complex system.

At the same time, linking these two vital fields may boost exciting novel directions. For instance, it is an intriguing question how early warning signals for loss of resilience may best be detected in a complex network (e.g. of species, persons or markets). Will particular nodes in the network reveal critical slowing down or other early warning indicators more than others? Can we know *a priori* which nodes would carry such a clear signal? Or would some integrative indicator over the entire network be best? Clearly, this is a wide open area of research, and much may be gained if we develop the different lines of work towards an integrative science for understanding and predicting fragility and transitions in complex systems. There is no doubt that occasional radical transitions will keep taking us by surprise. However, the emerging field of research we sketched may reduce the realm of surprise in fundamental ways when it comes to transitions related to tipping points.

Perhaps the most exciting aspect of this work is that it is uncovering generic features that should in principle hold for any complex system. This implies that we may use these approaches even if we do not understand all details of underlying mechanisms that drive any particular system. This is the rule rather than the exception, as we are far from being able to construct accurate predictive mechanistic models for most, if not all, complex systems. So far, most work on generic indicators of resilience has been carried out in ecology and climate science (Table 5.1). However, social sciences and medicine might well be particularly rich fields for exploration.

Certainly, there are major challenges ahead to develop sound predictive systems based on these generic properties. On the other hand, the potential gains are formidable. Empirically detecting opportunities where positive transitions in social or ecological systems can be invoked with minimal effort may be of great value. When it comes to the risk side, guidelines for designing financial systems that are less prone to systemic failure, or ways to foresee critical transitions ranging from seizures to the collapse of fish-stocks or tipping elements of the Earth climate system certainly rank high when it comes to their relevance for humanity.

Chapter 6

Resilience of alternative states in spatially extended ecosystems

Ingrid A. van de Leemput,
Egbert H. van Nes,
and Marten Scheffer

Published in *PLoS ONE:*

van de Leemput IA, van Nes EH, and Scheffer M. 2015. Resilience of alternative states in spatially extended ecosystems. *PLoS ONE* **10**: e0116859.

Abstract

Alternative stable states in ecology have been well studied in isolated, well-mixed systems. However, in reality, most ecosystems exist on spatially extended landscapes. Applying existing theory from dynamic systems, we explore how such a spatial setting should be expected to affect ecological resilience. We focus on the effect of local disturbances, defining resilience as the size of the area of a strong local disturbance needed to trigger a shift. We show that in contrast to well-mixed systems, resilience in a homogeneous spatial setting does not decrease gradually as a bifurcation point is approached. Instead, as an environmental driver changes, the present dominant state remains virtually 'indestructible', until at a critical point (the Maxwell point) its resilience drops sharply in the sense that even a very local disturbance can cause a domino effect leading eventually to a landscape-wide shift to the alternative state. Close to this Maxwell point the travelling front moves very slow. Under these conditions both states have a comparable resilience, allowing long transient co-occurrence of alternative states side-by-side, and also permanent co-existence if there are mild spatial barriers. Overall however, hysteresis may mostly disappear in a spatial context as one of both alternative states will always tend to be dominant. Our results imply that local restoration efforts on a homogeneous landscape will typically either fail or trigger a landscape-wide transition. For extensive biomes with alternative stable states, such as tundra, steppe and forest, our results imply that, as climatic change reduces the stability, the effect might be difficult to detect until a point where local disturbances inevitably induce a spatial cascade to the alternative state.

Introduction

The magnitude of a perturbation that a system can withstand without being tipped into an alternative stable state has been termed 'ecological resilience' by Holling (1973). Although the idea of alternative attractors and Hollings concept of resilience have become highly influential, most empirical work in ecology comes from relatively small, isolated systems, such as small lakes and ponds (Scheffer 1998), from controlled isolated experiments (Drake and Griffen 2010; Veraart *et al.* 2012), or from small enclosures in large-scale systems (Handa *et al.* 2002; Silliman *et al.* 2005). Here we address the fundamental problem of scaling up insights from such studies to spatially extended ecosystems. We consider a system spatially extended if the landscape is large relative to the scale of the relevant biological interactions, such that the system should not be considered well-mixed.

Fundamental aspects of stability of spatially extended systems with local alternative states have been addressed so-far mainly in theoretical literature from a rather abstract mathematical point of view (Bel *et al.* 2012). Yet, the issue is highly relevant from a practical perspective in ecology. One may, for instance ask under which conditions local restoration efforts could flip a system to an alternative state that would remain stable despite an open connection to the rest of the landscape. Similarly, one may ask under which conditions climatic change would result in a patchwork of local shifts between alternative states such as forest and savanna (Higgins and Scheiter 2012), or invoke large scale synchronous shifts in tropical (Hirota *et al.* 2011) or boreal biomes (Scheffer *et al.* 2012b). In essence, such problems boil down to the question under which conditions two alternative states may persist side by side in open connection.

This question has been specifically addressed in the context of invasion dynamics of species with a strong local Allee effect (Keitt *et al.* 2001; Holt *et al.* 2005; Taylor and Hastings 2005). These modeling studies show that alternative stable states may co-exist side-by-side provided that the landscape consists of discrete units. Discrete units can clearly be distinguished in certain ecosystems, such as coral reefs connected through larval exchange (Kool 2009; Steneck *et al.* 2009) or shallow ponds connected through overflows (van Geest *et al.* 2003; Cottenie and De Meester 2003). However, some systems have contrasting states co-existing in apparently continuous and homogeneous landscapes (e.g. Fig. 6.1). For example, within shallow lakes we can find sharp boundaries between clear water with submerged plants, and turbid water with no vegetation (Scheffer *et al.* 1994) (Fig. 6.1a). In marshlands, patches of vegetation can be found adjacent to non-vegetated mudflat (van Wesenbeeck *et al.* 2008) (Fig. 6.1b). Distinct boundaries are also found between mussel beds and bare soil in intertidal zones (Robles *et al.* 2010; Donahue *et al.* 2011) (Fig. 6.1c). Other

examples include boundaries between forest, savanna and grasslands (Sternberg 2001; Warman and Moles 2009), or between kelp beds and bare ocean floor covered by sea urchins (Konar and Estes 2003; Gagnon *et al.* 2004).

Figure 6.1. Example systems with alternative stable states in space. **a)** Shallow lake: clear water with Chara vegetation vs. turbid water (photo by Ruurd Noordhuis). **b)** Salt marsh: vegetation vs. bare marshland (photo by Johan van de Koppel). **c)** Musselbed: mussels vs. bare soil (photo by Andre Meijboom).

Could such apparent co-existence of alternative states be truly stable, or would it rather be a transient situation towards dominance by either of the states (van Wesenbeeck *et al.* 2008)? Clearly experimentation on relevant landscape scales is difficult, but there are even few spatially explicit theoretical studies on alternative stable states (van de Koppel *et al.* 2002; van Nes and Scheffer 2005; Guttal and Jayaprakash 2008b; Dakos *et al.* 2010; Hilt *et al.* 2011; Bel *et al.* 2012).

Here we use simple models in an effort to help narrowing the gap between our understanding of local alternative states and patterns in spatially extended systems. We systematically analyze the behavior of a spatially explicit model with local alternative stables states. We consider spatial exchange of the key species, and investigate the behavior of the system on a large landscape. First, we show how theoretical insights from physics literature as recently reviewed by Bel *et al.* (2012) can help to understand resilience of spatially extended systems, defined as the capacity to recover upon a disturbance (Holling 1973), and hysteresis, defined as the tendency of a system with alternative stable states to stay in the same state despite changes in external conditions (Scheffer 1998). Second, we investigate under which conditions alternative stable states may co-exist in space. We show how dispersal barriers and heterogeneity of other environmental conditions can lead to stable co-existence.

Methods

The model

Our model consists of a reaction-diffusion equation including a growth term ($f_N\left(N\right)$), and a spatial explicit diffusion term ($f_D\left(N,x\right)$) (Eqn. 1):

$$\frac{\partial N(x)}{\partial t} = f_N\left(N\right) + f_D\left(N,x\right) \tag{1}$$

For the growth term, we here use one of the simplest models with alternative stable states, the classical resource harvesting model. In this model, a resource species, *N*, is growing logistically, and is being harvested following a sigmoidal functional response (Eqn. 2).

$$f_N\left(N\right) = rN\left(1-\frac{N}{K}\right) - \frac{cN^2}{N^2+H^2} \tag{2}$$

The logistic growth is described by r as the maximal growth rate, and K as the maximum local biomass species N can reach. Mortality as a result of harvesting is described by c as the maximal mortality rate if N is high, and H as the half saturation level of the functional response. The modeled species can have two alternative stable states for a range of parameter settings: a low biomass state, for which high mortality rates prevent further growth, and a high biomass state, for which growth is limited by available food or space. In the non-spatial model, the size of the basin of attraction (i.e. ecological resilience) of each state varies with parameters such as the maximal mortality rate c, which we here assume to be the landscape-wide driver. Default parameters used for the growth-term are: $r = 1$ d^{-1}, $K = 10$ g m^{-1}, $c = 2.4$ g m^{-1} d^{-1}, $H = 1$ g m^{-1}. This model has been introduced as an overexploitation model (Noy-Meir 1975; May 1977). More in general, it describes the dynamics of a population that has high per capita mortality rates at low biomass, and low per capita mortality rates at high biomass. Potential mechanisms for this are saturation of the predator, or decreased palatability or capture rate at high biomass. From a dynamical systems perspective the essence is the existence of a positive feedback mechanism that can cause a self-amplification of the effect of a disturbance around a critical threshold. For instance, if the biomass of the population in our model is depressed beyond a critical point, an increase in per capita mortality can lead to a further decrease and prevent the population to re-establish. We explored three other models in the Appendix A2 (Table A6.1) to show that our results are not specific to the model we use, as long as there is a local positive feedback that is strong enough to cause alternative stable states locally.

Space is represented by a one-dimensional continuum without discrete spatial units. Diffusion is the simplest form of modeling spatial exchange of the modeled species. As examples for spatial exchange one may think of clonal growth if the population represents vegetation, random movement if it represents a relatively sessile animal, or mixing if it represents water or dissolved nutrients (Eqn. 3):

$$f_D(N,x) = D\frac{\partial^2 N}{\partial x^2} \tag{3}$$

with D as the diffusion rate, and x representing distance. This is the most straightforward way to model the scale at which feedbacks act. If D is high relative to the size of the landscape, local biomass differences are quickly smoothened out, such that feedbacks resulting from biomass differences practically affect the entire landscape. However, if D is low relative to the size of the landscape, local biomass differences remain for a relatively long period, such that the feedbacks act locally (see Appendix A6.1 for the non-dimensional form of the model, in which the spatial scale is scaled to the diffusion rate).

Additionally, we simulated dynamics on a heterogeneous landscape. We modeled heterogeneity in conditions, simply by assuming a landscape gradient of the growth rate r. We also simulated a landscape in which the diffusion rate (D) is varied randomly but smoothly in space. In order to simulate such smooth heterogeneous landscape, we first generated spatially auto-correlated stochastic diffusion rates on a one-dimensional grid of 30 cells (Eqn. 4):

$$D_{i+1} = 0.3D_i + 0.7D_0 + Rnd_i \tag{4}$$

with D_i as the diffusion rate at grid cell i, D_0 as the diffusion rate at x=0, Rnd_i as a random number from a normal distribution, with mean 0 and standard deviation s. Then, from these discrete values we made a landscape with smoothly varying diffusion rates over space using a Gaussian kernel smoothing function, by interpolating between these 30 cells (Bowman and Azzalini 1997) (Eqn. 5):

$$f_D(N,x) = \frac{\partial}{\partial x}\left(\left(\frac{1}{n}\sum_{i=1}^{30} G_h(x - x_i)\right)\frac{\partial N}{\partial x}\right) \tag{5}$$

with G_h as a Gaussian kernel, and h as the bandwidth of the kernel-smoothing window. Default parameters used for the diffusion equations are: D=1 $m^2\,d^{-1}$, D_0=1 $m^2\,d^{-1}$, s=1.6 $m^2\,d^{-1}$, h=0.05m.

Computational approach

In order to test for the possibility of stable co-occurrence of alternative stable states in space, we initialized the studied landscape such that the left half of the landscape was in the high biomass state, and the right half in the low biomass state. To explore the effect of strong but local disturbances, we initialized the system such that the entire landscape was in one state. Then, we simulated a local disturbance by shifting a small section on one side of the landscape to the alternative stable state.

We used the *pdepe* solver in Matlab to solve the partial differential equations (Skeel and Berzins 1990). Boundaries were defined to be reflective. To check that our results were not influenced by the spatial discretization method used in *pdepe*, we repeated all simulations for 100, 1000 and 5000 grid cells.

Results

We first show how the resilience of alternative stable states in homogeneous spatially extended systems differs from the classical well-mixed systems. At first, we initialized the landscape such that the population was in the high biomass state on one half of the landscape, and in the low biomass state on the other half. On either side of the created boundary the local dynamics driven by diffusion (f_D) have an equalizing effect, while the growth and mortality dynamics (f_N) drive the system back to each equilibrium state. The net effect around the front $\left(\frac{\partial N}{\partial t}\right)$drives the system locally towards one of the states (Fig. 6.2). This shift propagates further through the landscape resembling a domino effect. Such moving front is called a 'travelling front' (Bel *et al.* 2012).

Assuming other conditions to be constant, the maximal mortality rate c determines the direction of the travelling front. If the maximal mortality rate is low, a front of high biomass propagates through the landscape, leaving the entire system in the high biomass state (Fig. 6.2a). If the maximal mortality rate is high, the low biomass state is the one that propagates through the landscape (Fig. 6.2c).

There is a single critical value of the mortality rate at which the resilience of both states is equal. At this specific parameter setting, the front speed is zero (Fig. 6.2b). This point is called the Maxwell point (Pomeau 1986; Bel *et al.* 2012), where both states have the same potential energy, and therefore the base level in a stability landscape should be the same for both basins of attraction (Strogatz 1994). At the Maxwell point, the dynamics driven by local growth and mortality exactly compensate for the local dynamics driven by diffusion (Fig. 6.2b, Appendix A6.2, Fig. A6.1). For single-variable models with local alternative stable states, the set of

conditions for the Maxwell point can be mathematically derived from the growth function (Appendix A6.2) (Aronson and Weinberger 1975; Fife 1979; Pomeau 1986), and is generic for any single-variable model with local alternative stable states and diffusion (Fig. A6.2a-d).

The key result is that if either side of the landscape is in one alternative state, a travelling front always leaves the system in the state with the highest resilience (or more precisely in the state with the lowest potential energy). As a result, in such a simple system we have described, alternative stable states cannot co-exist in a homogeneous landscape. In our single-variable model, the conditions for the Maxwell point are independent of the diffusion rate. However, in a multi-variable model, such as the well-known macrophyte-turbidity model representing shallow lakes dynamics (Fig. A6.2e-f), the rates of exchange of each variable can be different, which has an effect on the stability of either state. For instance in the shallow lakes example, the macrophyte-dominated state will become more resilient against local perturbations if the dispersal rate of macrophytes increases (Fig. A6.3). Most importantly however, for multi-variable models with local alternative stable states and random dispersal of key species or diffusion of nutrients, the same key result holds.

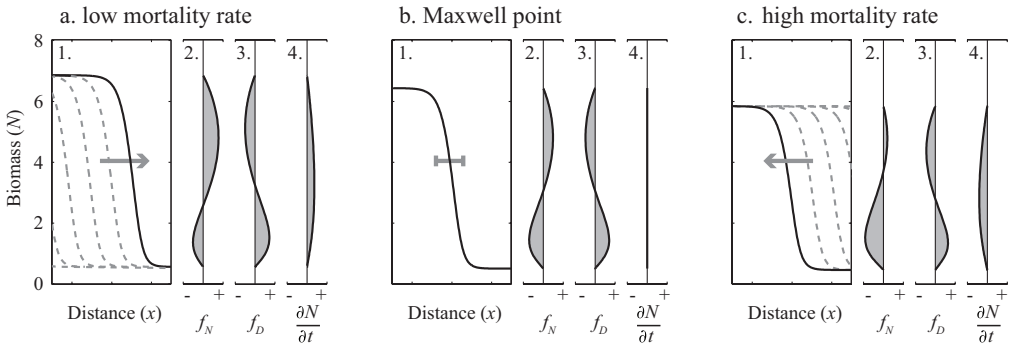

Figure 6.2. Simulations in a homogeneous landscape with local alternative states and diffusion of the modeled species. Initially, the left side of the landscape is set to the high biomass state, and the right side to the low biomass state. With these initial conditions a moving front establishes, shifting the entire landscape to the state with the highest resilience **a)** $c = 2.2$, **b)** $c = 2.3487$, **c)** $c = 2.5$ (g m^{-1} d^{-1}). The four figures in each panel represent: 1) snapshots of the moving front with the grey arrows indicating the shifting direction (scale = 30 m), 2) the local change in biomass per day due to growth and mortality (f_N), 3) the local change in biomass per day due to diffusion (f_D), and 4) the net local change in biomass per day $\left(\frac{\partial N}{\partial t} = f_N + f_D\right)$. Note that local dynamcs and diffusion precisely cancel out if conditions are such that the modeled system is at the Maxwell point (panel b). The scale of all change-in-biomass plots ranges from -0.5 to 0.5 (g m^{-1} d^{-1}).

On an 'infinitely' sized landscape, the most resilient state is thus 'indestructible', in the sense that no local disturbance, independent of the size of the disturbance, is

able to propagate through space, because conditions are such that a travelling front in the direction of dominance of the least resilient state cannot occur (Fig. 6.2). However, if conditions change, such that the system crosses the Maxwell point, the system becomes vulnerable to local disturbances, ending this indestructibility. Environmental conditions will thus determine whether a strong local disturbance in a spatial system can potentially propagate or not.

Moreover, for a travelling front to develop, a critical area needs to be disturbed to the alternative state. The actual critical size of this disturbed area (Δx) increases towards the Maxwell point (Fig. 6.3a). The asymptotic speed of a travelling front between alternative states is constant on a homogeneous landscape (Murray 2002), and approaches zero towards the Maxwell point (Fig. 6.3b). A non-dimensional version of our model (see Appendix A6.1) shows that an n-fold increase in diffusion rate D leads to a $\sqrt{n}$-fold increase in both Δx and in front speed (see Fig. A6.4). Importantly, once the system has shifted to the alternative state, a front travelling backwards cannot establish, so the new state is on its turn indestructible against local disturbances to the other state. Note that if a system is indestructible against local disturbances, such as fires or storms, it is not indestructible against disturbances that affect the entire landscape, such as periods of drought.

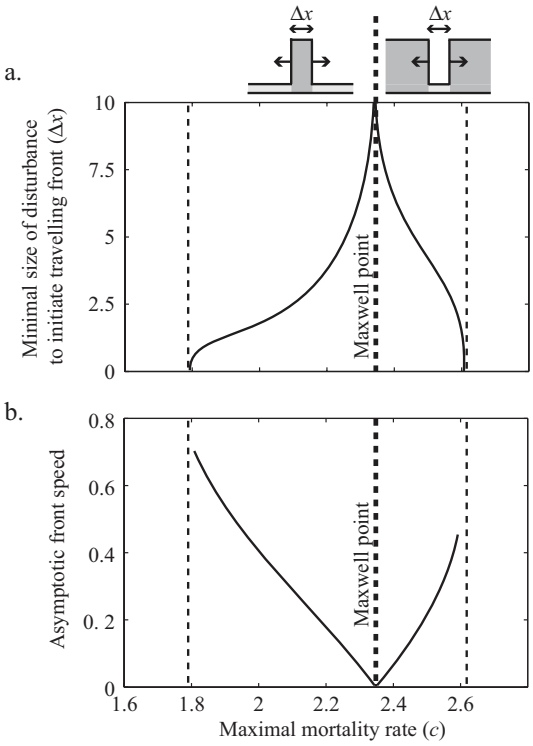

Figure 6.3. Critical size of a local disturbance and the speed of a travelling front as a function of the maximal mortality rate c. **a)** On an infinitely sized landscape, disturbances smaller than the critical size Δx (in m) are repaired, while larger disturbances will initiate a propagating front that travels through the landscape with **b)** a constant front speed (in m d^{-1}). The thick dashed line represents the Maxwell point. The thin dashed lines represent the two fold bifurcations in a non-spatial system. Left of the Maxwell point the entire landscape was initially set to the low biomass state, and the disturbance was set to the high biomass state. Right of the Maxwell point the landscape was initially set to the high biomass state, and the disturbance was set to the low biomass state (indicated by the small upper panels). In this model, an n-fold increase in diffusion rate leads to a $\sqrt{n}$-fold increase in both critical disturbance size and front speed.

So far, we considered a landscape without borders, to rule out any edge effects. We now turn to the more realistic case of finite landscapes. In case the landscape is small (or diffusion is high, which is mathematically the same) the system does in practice behave like a well-mixed system (Fig. 6.4b). Consequently, shifts will occur almost simultaneously across the landscape. In contrast, if the landscape is large, a local disturbance can cause a travelling front that propagates through space, always in the direction of the least stable state. A relatively small disturbance can therefore already lead to systemic collapse (Fig. 6.4c). As a result, spatial resilience, here defined as the capacity to recover upon a local disturbance, of the alternative states changes abruptly around the Maxwell point (Fig. 6.4e, see Fig. A6.2 and Table A6.1 for other models). As stress on the dominant state increases (e.g. through the mortality rate in our model), resilience to local disturbances remains unaltered in the sense that the system will recover, even from large disturbances, until a critical point is reached (the Maxwell point) where resilience sharply drops to a point where even a local disturbance can induce a traveling front that will eventually bring the entire landscape in the alternative state. This is quite unlike the gradual decrease of resilience on a small landscape (Fig. 6.4d), corresponding to the classical well-mixed situation.

In contrast to the resilience as defined by Holling (1973), the recovery rate of a local disturbance (i.e. 'engineering resilience') does decrease gradually in a spatially extended system (Fig. 6.4g). In that case, recovery from a local disturbance slows down if conditions are close to the Maxwell point. The recovery rate is slowest just before the point at which the disturbance will trigger a travelling front of expansion towards the alternative state (Fig. 6.4g). While this point lies beyond the Maxwell point for small disturbances, for large disturbances a front will be triggered as soon as the Maxwell point is crossed. Importantly, the same key result holds: once a spatially extended system has shifted to a degraded state, it is extremely difficult to re-establish the original desired state without changing global conditions. For example, in the scenario with a large landscape in Figure 6.4, one needs to bring more than 90% of the landscape back into the desired state; otherwise the remaining degraded patch will, although slowly, expand again (Fig. 6.4e).

In all scenarios we examined so far, the spatially extended system eventually ends up in one state. Situations in which the alternative states occur side-by-side in a homogeneous landscape can be induced by strong local perturbations, but are transient. For stable co-existence of alternative stable states we need to relax the assumption that the environmental conditions determining growth and mortality parameters as well as diffusion rates are entirely homogeneous in space.

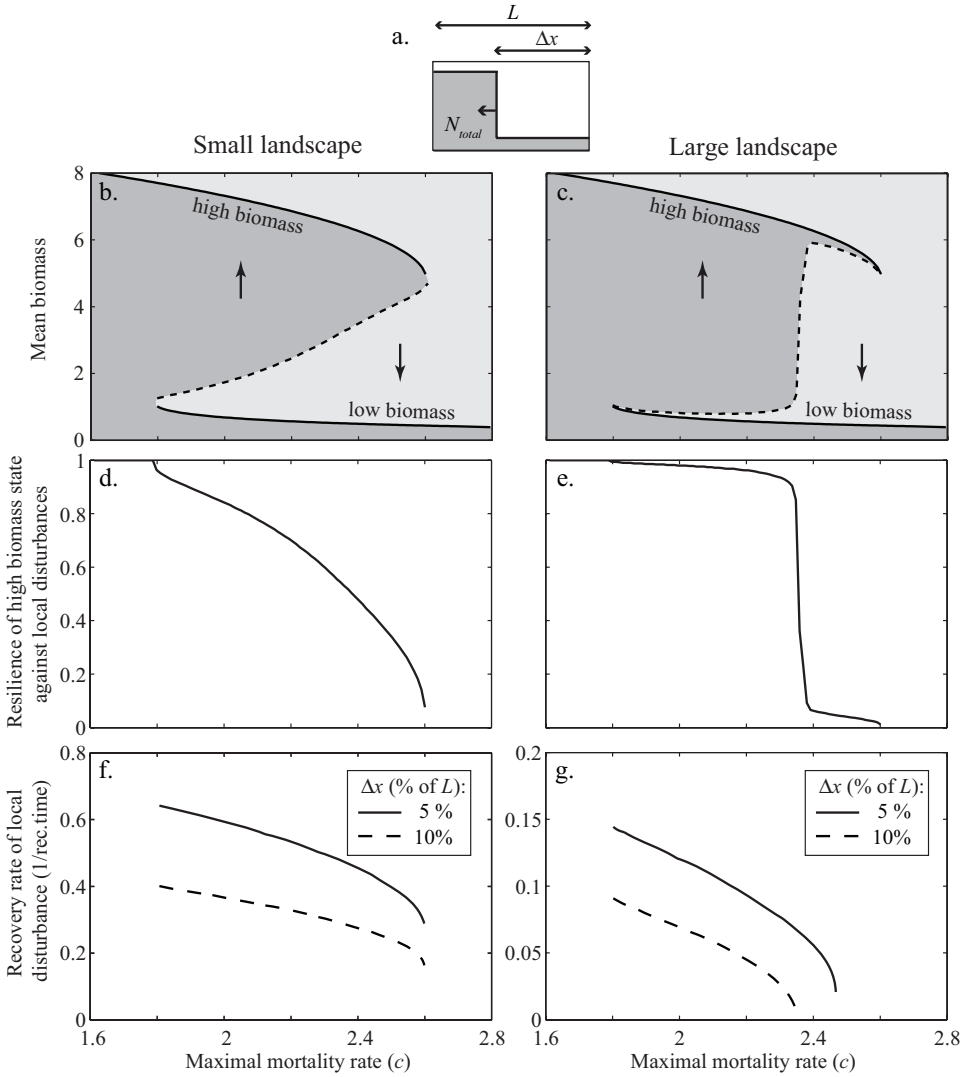

Figure 6.4. Resilience to local disturbances on a small and a large landscape. **a)** Local disturbances to the alternative stable state (i.e. the low biomass state) were performed on one side of the landscape, in order to have a symmetrical landscape. **b)** Mean biomass on the landscape in equilibrium (N_{total}/L) as a function of the maximal mortality rate for a system on a relatively small landscape ($L = 5$ m). The solid parts of the curve represent the two stable landscape-wide equilibria. The dashed part of the curve represents the disturbance threshold, i.e. the size of the disturbed patch needed to induce a systemic shift to the alternative stable landscape-wide state. **c)** The same as panel b but for a system on a large landscape ($L = 50$ m). Note that the disturbance threshold remains very close to the less resilient of the two stable equilibria implying that only a small disturbance is needed to induce a shift to the more resilient landscape-wide state. **d)** Resilience of the high biomass state, in terms of the fraction of the landscape that needs to be perturbed to the alternative state to trigger a shift ($\Delta x/L$), for a system on a small landscape. **e)** The same as panel d but for a system on a large landscape. Note that resilience shows a steep drop. **f)** Engineering resilience of the high biomass state, in terms of the recovery rate of a local disturbance to the low biomass state, for a system on a small landscape. **g)** The same as panel f, but for a system on a large landscape.

We first simulated landscapes with spatially variable diffusion rates (Fig. 6.5). This can be seen as an intermediate between two simplified spatial models: a spatially discrete model with exchange between patches and a continuous model with homogeneous diffusion (see Appendix A6.3 and Fig. A6.5). The results show that a travelling front can slow down and can come to a halt, if it meets an area of *increasing* diffusion rates (Fig. 6.5a). Whether a travelling front comes to a halt, so-called 'pinning', depends on three factors. Pinning is more likely if i) the actual level of increase in diffusion (D_{plus}) is high (Fig. 6.5b), ii) the scale on which the increase in diffusion occurs is low, i.e. the steepness of the diffusion function (set by p in the sigmoidal function described in the caption of Figure 6.5) is high (Appendix A6.3, Fig. A6.6), and iii) there is little difference between the resilience of the alternative states, causing the system to be close to the Maxwell point (Fig. 6.5b). Thus even if growth and mortality rates are homogeneous, spatial variation in exchange or dispersal rates can allow spatial co-existence of alternative stable states.

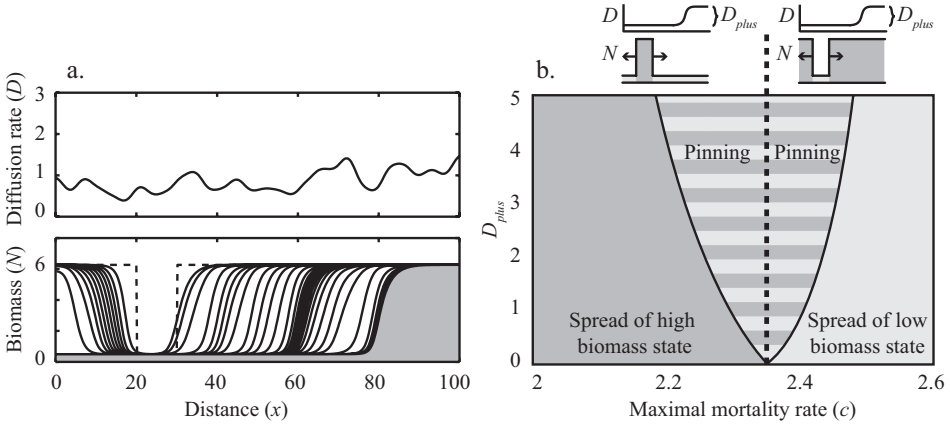

Figure 6.5. The effect of spatially heterogeneous diffusion. A travelling front of collapsing biomass triggered by a disturbance can come to a halt if it meets an area of increased diffusion rates. **a)** The effect is illustrated in a simulated landscape with heterogeneous diffusion rates ($c = 2.4$ g m^{-1} d^{-1}) (upper panel). The dashed line in the lower panel represents the initial disturbance and the solid lines depict the transient situation every 40 days. The shaded area depicts the final stable configuration. This configuration is stable, as long as the system does not suffer from other local disturbances. **b)** In order to understand the conditions for pinning, we introduced a local disturbance in a landscape with a single spatial gradient in diffusion rate, representing a change from an area with low diffusion (D_0) to an area with high diffusion ($D_0 + D_{plus}$) (visualized in the small upper panels). The landscape was created by a sigmoidal function: $f_D(N,x) = \frac{\partial}{\partial x}\left(\left(D_0 + D_{plus}\frac{x^p}{x^p + (L/2)^p}\right)\frac{\partial N}{\partial x}\right)$ ($D_0 = 1$ m^{2}d^{-1}, $p = 50$, $L = 100$ m). The main panel represents the occurrence of pinning for different combinations of maximal mortality rate c and the level of increase in diffusion rate D_{plus}. Importantly, pinning only occurs if a traveling front meets an area in which diffusion is higher. The thick black dashed line indicates the Maxwell point.

Next, we simulated heterogeneity in environmental conditions in the most straightforward manner, using a spatial gradient of growth rate r (Fig. 6.6). One can for example imagine a gradient in water availability related to distance to water source, or precipitation and temperature gradients related to latitude. With a smooth spatial gradient in the growth rate, a sharp boundary between two states is formed simply wherever conditions cross the Maxwell point. If both sides of the landscape are connected to an area in which the system has only one stable state, this configuration is completely independent of initial conditions (Fig. 6.6). As a consequence, as long as diffusion rates are homogeneous, and there is a smooth gradient in environmental conditions, there will be no local nor large-scale hysteresis effects in the response to a changing environmental variable. If global conditions change gradually, the location of the spatial shift will also shift in a gradual manner.

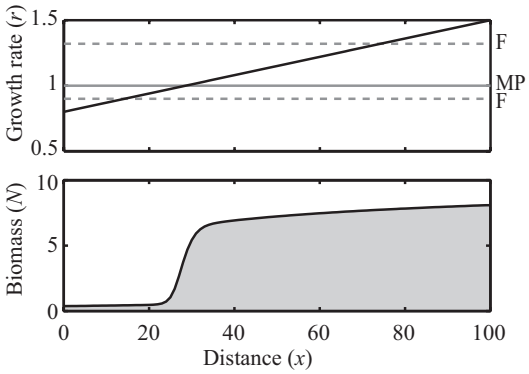

Figure 6.6. The effect of spatially heterogeneous conditions. A gradual increase in growth conditions in space (e.g. north-south gradient in temperature) results in a distinct shift in space from the low biomass state to the high biomass state (i.e. a stable standing front) on the location where conditions cross the Maxwell point. Upper panel: The solid black line represents the local growth rate r on the landscape. The solid grey line indicates where the conditions cross the Maxwell point (MP), and the two dashed grey lines indicate where the two fold bifurcations (F) are crossed. Lower panel: The shaded area represents the stable end configuration of biomass for any initial configuration ($c = 2.35$ g m^{-1} d^{-1}).

In natural systems, however, one would expect environmental conditions to be more heterogeneous than along a simple gradient. In that situation, a slow, gradual change in global conditions would likely lead to incidental 'local fronts' of change (see Appendix A6.4, and Fig. A6.7). These local fronts would cause a reverse change if global conditions are reversed. In contrast, if exchange or dispersal rates are heterogeneous is space, a slow, gradual reversal in conditions would not simply cause a reverse change in the landscape as a local increase in exchange or dispersal of a key variable in one direction would not lead to 'pinning' in the other direction (Fig. 6.5).

Discussion

Our results illustrate that even for entirely homogeneous landscapes, stability properties of a spatially extended ecosystem can differ profoundly from those of a simple, well-mixed ecosystem. Differences are especially intriguing when it comes to ecological resilience, generally defined as the maximum disturbance that a system can tolerate without switching to the alternative stable state (Holling 1973). Here, we specify this definition to local disturbances, and define ecological resilience as the size of the area of a strong local disturbance needed to trigger a shift. If the ecosystem is spatially extended, the least resilient state tends to be always fragile (Fig. 6.4c) in the sense that a strong local disturbance can already trigger a domino effect in the form of a travelling front (Fig. 6.2) that leaves the landscape in the alternative more resilient state. Importantly, as environmental conditions change, there is a sudden drop in resilience at the point where one state becomes more resilient than the other (i.e. at the Maxwell point) (Fig. 6.4e), rather than the classical gradual decrease towards the fold bifurcation (Fig. 6.4d). In fact, this class of systems may hardly have hysteresis in practice as only a small patch needs to be in the most stable state to trigger a system wide shift, and the new state is stable against local disturbances (Fig. 6.4c). Mathematically, these results on travelling fronts and the Maxwell point are not new (Bel *et al.* 2012), and have been discussed in the context of populations with an Allee effect (Keitt *et al.* 2001; Holt *et al.* 2005; Taylor and Hastings 2005). However, surprisingly, the connection to the concepts of resilience and hysteresis has not been made so far.

Effectively, a spatially extended system in our model means that a positive feedback acts on a small scale relative to the size of the landscape, which is often the case in ecosystems. For example, foundation species such as *Spartina* (cordgrass) on intertidal flats facilitate vegetation development, by locally lowering erosion levels (Altieri *et al.* 2007). Seagrass facilitates neighboring seagrass development by trapping sediment leading to increased light conditions (van der Heide *et al.* 2011) and decreased erosion levels, but it will depend on the water mixing rate how far this effect can reach. Similarly, but on a much larger scale, local development of forest suppresses wildfire propagation (Staver *et al.* 2011a), but has no effect on fires at a longer distance. Our results suggest that ecosystems that have alternative stable states in small-scale experiments or on a small landscape, could, on a larger landscape, be surprisingly resilient (Fig. 6.4e). This may explain why, after a large-scale die-off of *Spartina* due to drought, snail grazing, and fungal infections (Angelini and Silliman 2012), remnant *Spartina* patches (if large enough) could slowly expand into die-off areas. Survival is possible, because *Spartina* facilitates expansion locally. On the other hand, once the Maxwell point has passed, the degraded (or undesired)

state will also be surprisingly resilient. This could explain the persistent failure of local restorations in certain systems, such as the lack of survival of planted seagrass patches in the Wadden sea where this plant used to dominate (van Katwijk *et al.* 2009).

It is important to note that the systems we studied are different from those with self-organized Turing patterns (Rietkerk and van de Koppel 2008). Such patterns can arise in situations where local positive feedbacks are associated to a depletion of resources or increased stress levels (i.e. erosion) at a distance. For instance, vegetated patches in an arid landscape can locally increase soil permeability, which has a positive effect on local plant growth. However, at a distance from the patch this may lead to water depletion, and thus to unfavorable plant growth conditions (Rietkerk *et al.* 2002). Similarly, mussels or diatoms may locally protect themselves and their neighbors from wave action and erosion, but by doing this they increase these stress levels at a distance (van de Koppel *et al.* 2008; Weerman *et al.* 2010). The combination of a local positive feedback, and a sufficiently strong long-range negative feedback can, without intrinsic heterogeneity in abiotic conditions, lead to regular spatial patterns (i.e. spots, labyrinth, gaps) (Rietkerk and van de Koppel 2008).

The conspicuously regular patterns of contrasting states in such self-organized systems tend to be very robust. By contrast, our analysis suggests that stable coexistence of alternative states (without a long-range negative feedback) in a homogenous landscape might be unlikely, even though the movement of the front between states can be slow in practice. Indeed, field observations do suggest that some sharp borders between alternative states may represent transient situations rather than stable states. For instance, following improved water quality, patches of clear water with submerged water plants arose during the summer of 1993 in the Dutch lake Veluwe. At that time, this was thought to be an indication of stable co-existence of alternative stable states (Scheffer *et al.* 1994). However, over the years, these patches of clear water with submerged water plants have gradually spread to a patch as large as almost the entire lake (Fig. 6.7). Similarly, van Wesenbeeck *et al.* (2008) describe the slow spatial spread of vegetation cover in saltmarsh pioneer zones as being non-stable at longer timescales.

In the context of our model analyses it becomes clear from such observations that the existence of a sharp border between ecosystem states in an otherwise homogeneous landscape should be interpreted with care when it comes to the framework of alternative stable states. Close to the Maxwell point, borders may simply move very slowly (Fig. 6.4g) (Bel *et al.* 2012), resulting in apparent co-existence at shorter timescales, even if one state may eventually dominate. It is also important to note

that if an ecosystem is subject to occasional stochastic disturbances or recurrent temporal change (e.g. seasons), the slowness of the movement of fronts would allow the existence of a permanent (albeit spatially unstable) patchwork of alternative states (Bertness *et al.* 2002).

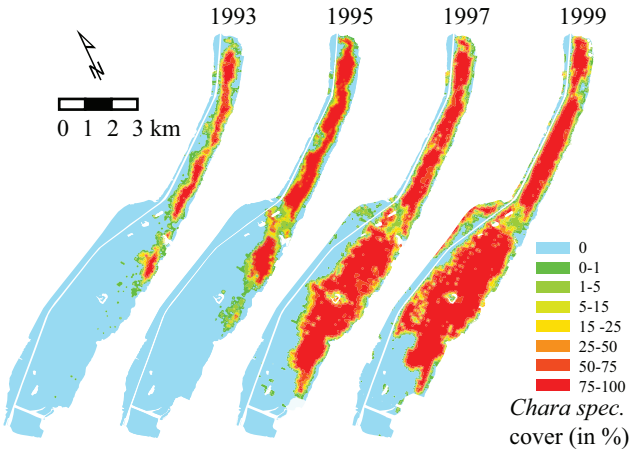

Figure 6.7. Travelling front-type of spread of aquatic vegetation (*Chara spec*). Lake Veluwe, the Netherlands, from 1993 to 1999 (from: Monitoring of aquatic vegetation of the IJsselmeer Area by Rijkswaterstaat, an Agency of the Ministry of Infrastructure and the Environment, The Netherlands).

Clearly, situations with sharp borders between alternative states may often occur in a stable way along smooth environmental gradients (Fig. 6.6). Such situations do in a sense represent critical transitions in space. This is analogous to classical critical transitions in time, except that environmental conditions now change over space rather than over time (e.g. Wilson and Nisbet 1997; van de Koppel *et al.* 2005b). At the established border the positive feedback is too weak to trigger a local shift towards the other state, leading to a dynamic equilibrium. This type of dynamics has, for example, been suggested to be the underlying mechanism for sharp borders of clear vegetated water in a river stretch with increasing background turbidity (Hilt *et al.* 2011), sharp mussel bed borders on an intertidal flat with increasing wave exposure (Donahue *et al.* 2011), and northern boreal forest boundaries as a result of latitudinal gradients in temperature (Scheffer *et al.* 2012b).

Interestingly, our model analysis also suggests that even if environmental conditions for growth and survival are homogeneous, spatial coexistence of alternative states can still be stable if diffusion rates are not entirely homogeneous through space (Fig. 6.5 and Fig. A6.6). One may think for example of internally mixed lakes that are connected through channels (Cottenie and De Meester 2003), or natural areas fragmented by roads or other landscape elements that limit dispersal of species. The mechanism behind this particular case of co-existence of alternative states is that a

local increase in exchange rates causes the area from which each of the states draw for additional inputs (the 'hinterland') to vary from place to place, thus effectively causing the strength of the positive feedback to vary over space. As a consequence, expansion can be halted allowing stable co-existence of the low and high biomass state (Fig. 6.5). From a modeling point of view, this result demonstrates that stable co-occurrence of alternative stable states in space is not an artifact of using discrete space models (Keitt *et al.* 2001) (see Fig. A6.5). Rather, the fact that such co-existence is impossible in idealized continuous space models may be seen as an artifact of neglecting the possibility of heterogeneity in dispersal rates. Obviously, animals and plants can have more complex dispersal strategies than simple random dispersal. The potential for co-existing alternative stable states is expected to be lower with long-distance seed dispersal, or active dispersal towards unoccupied areas, since dispersal barriers can be crossed more easily.

Implications

Clearly it is challenging to bridge the gap between our fundamental understanding of alternative stable states on small scales, and the dynamics of spatially extended ecosystems. Our results are limited to basic principles derived from simple models. Nonetheless, they help to see why scale can prohibit restoration of spatially extended homogeneous ecosystems such as estuaries or very large lakes. Petraitis and Latham (Petraitis and Latham 1999) already hypothesized that 'the spatial and temporal window of opportunity of a perturbation must be large enough to gain a foothold and initiate pivotal positive feedback processes'. Indeed, our model predictions are in line with findings that local restoration efforts must be large enough to gain momentum for a travelling front to establish. On the other hand, our results also imply that even if the desired state is stable in an isolated system (e.g. mesocosms or enclosures) it may not be able to spread through space.

In addition to providing a framework for understanding resilience and restoration of spatially extended systems, our results suggest mechanisms leading to entirely different ways in which major biomes might reorganize in response to climate change. Tropical and boreal forests are the two largest biomes on Earth. As climate changes, the regions dominated by these two types of forest will likely change, but the character of the transitions is unclear. Recent studies suggest that, under certain conditions, tropical forest and savanna are alternative stable states (Hirota *et al.* 2011; Staver *et al.* 2011b) and the same may be true for boreal forest and tundra, and tundra and steppe (Scheffer *et al.* 2012b). It has been suggested that more or less stochastic local switches may give the range shift of tropical forest an overall gradual character (Higgins and Scheiter 2012). Our results suggest that this scenario is indeed likely if environmental heterogeneity follows a smooth gradient (e.g.

temperature gradient related to latitude), as in Figure 6.6. On the other hand, one could speculate that over large homogeneous areas, a massive shift to an alternative biome might occur once a tipping point is reached (see Appendix A6.4 and Fig. A6.7). If we assume that currently homogeneous systems signal a tendency to a winner-takes-all situation, our results suggest that such biomes might be likely to shift to an alternative state through massive traveling fronts, called 'gradual regime shifts' by Bel *et al.* (2012), to differentiate them from abrupt landscape-wide shifts. However, the speed of such fronts would depend among other things upon the rate at which states disperse. For example, the spread of boreal trees into the tundra may be limited by seed dispersal (MacDonald *et al.* 2008). On the other hand, the rate of disappearance of boreal forest at the Southern end of its range as temperatures rise could be dictated by massive wildfires and insect outbreaks as already observed (Wolken *et al.* 2011).

Conclusion

Our analysis illustrates that the resilience of spatially extended ecosystems will differ markedly from those of small isolated parts of such systems. Even if a positive feedback causes a system to have alternative stable states on small scales over a range of conditions, this hysteresis will tend to disappear in a larger spatial context. This is because in a spatially extended system one of both alternative states will tend to be dominant in the sense that it is highly resilient against local disturbances. By contrast, in the alternative (subdominant) state, even a small local disturbance will tend to invoke a shift to the dominant state that spreads through the entire landscape as a travelling front. Environmental conditions determine the resilience of both the dominant and subdominant state and at the so-called Maxwell point the dominance shifts between the states. Close to this point the travelling front moves very slow. This allows long transient co-occurrence of alternative states side-by-side, and also implies that even minor spatial barriers can lead to stagnation of a travelling front and thus to permanent co-existence of alternative states in space.

Obviously model studies as the ones presented in this paper can only hint at potential classes of mechanisms and dynamics. Combinations of field experiments, elaborate models and analyses of field patterns will be required to reduce the uncertainty we have about the mechanisms that rule the large scale dynamics of spatially extended systems. In any case our results illustrate that stability properties on large scales cannot be deduced from small-scale experiments alone.

Appendix A6

Appendix A6.1. The Maxwell point in a range of bistable models

Mathematically, one can describe the set of conditions at which the Maxwell point is found as follows (Aronson and Weinberger 1975; Fife 1979; Pomeau 1986):

$$\int_{\overline{N_1}}^{\overline{N_2}} f_N\left(N\right) dN = 0$$

with $f_N\left(N\right)$ as the reaction part of the reaction-diffusion equation (e.g. Eqn. 2, main text), and $\overline{N_1}$ and $\overline{N_2}$ as the two alternative equilibria. To illustrate this, the reaction part (i.e. the growth function) of the exploitation model described in the main text is depicted in Figure A6.1. At the Maxwell point, the shaded areas are of equal size, so both states in the spatially extended system are equally resilient. If the mortality rate is lower, the high biomass state is more resilient, and a travelling front may be triggered to this state. Similarly, if the mortality rate is higher, the low biomass state is more resilient, and a travelling front may be triggered to this state.

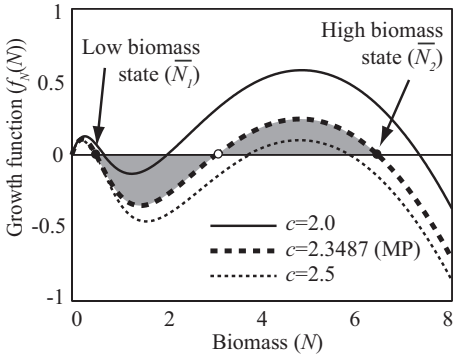

Figure A6.1. Conditions for the Maxwell point in relation to the growth function. The shape of the growth function determines the direction and speed of the travelling front. Front speed is zero when the shaded areas on both sides of the unstable equilibrium have equal size (here at $c = 2.3487$, *MP* = Maxwell point).

The condition for the Maxwell point is generic for models with local alternative stable states and diffusion (Fig. A6.2). Related to the existence of a Maxwell point is the effect that resilience drops at conditions equal to the Maxwell point if the size of the landscape is large (Fig. A6.2). We used three different ecosystem models to illustrate this generality (Table A6.1): 1) a model with one state variable describing the eutrophication level in lakes. Nutrient dynamics are assumed to depend on nutrient input, loss (e.g. sedimentation, outflow), and recycling (e.g. from sediment or consumers) following a sigmoid function of the nutrient level (Carpenter *et al.* 1999) (Figs. A6.2a and b), 2) a model with one state variable describing a

population with an Allee effect (Keitt *et al.* 2001), that is being harvested with a type I functional response (Figs. A6.2c and d), and 3) a well-developed model with two state variables describing the dynamics of aquatic vegetation and vertical light attenuation in shallow lakes. Aquatic vegetation is assumed to have a positive feedback on its own growth, by reducing turbidity, which enhances vegetation growth (Scheffer 1998) (Figs. A6.2e and f).

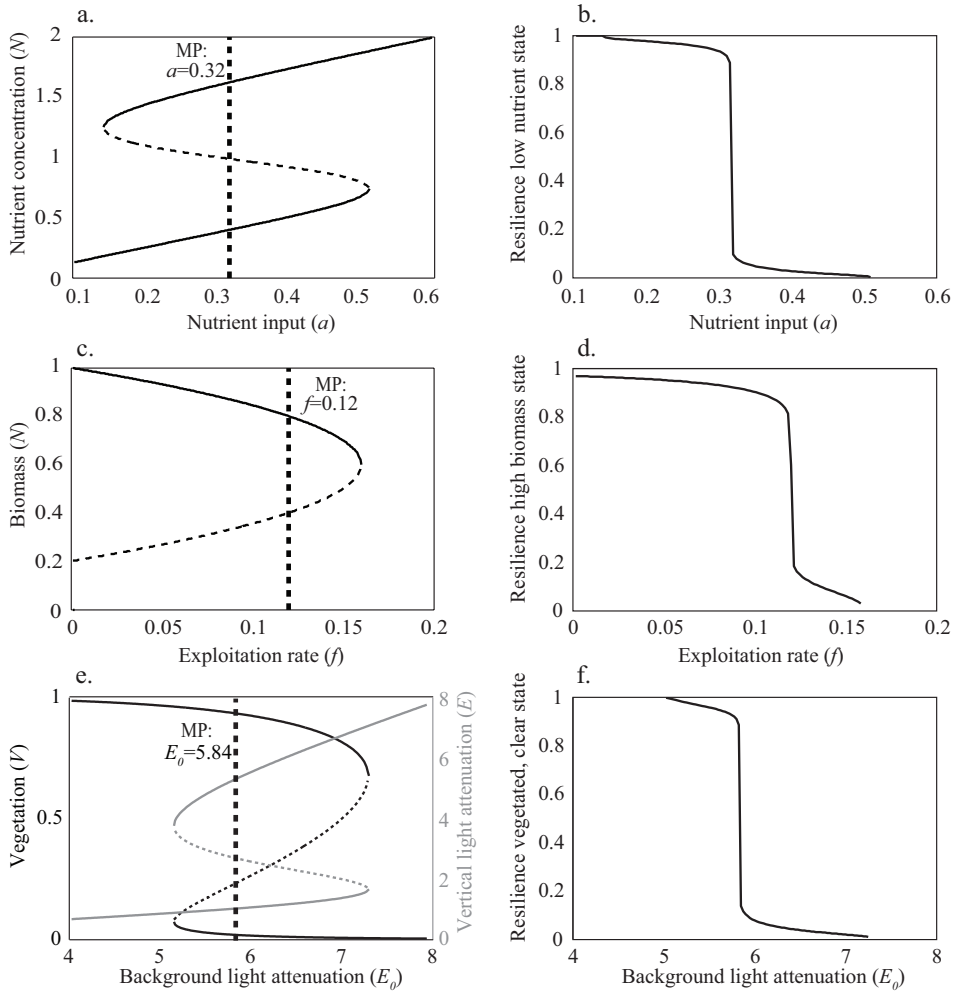

Figure A6.2. The Maxwell point and resilience of three models with local alternative stable states (see Table A6.1). **a-b)** eutrophication model with nutrient input a as the control parameter; **c-d)** Allee effect model with exploitation rate f as the control parameter; and **e-f)** vegetation and light attenuation model with background light attenuation level E_0 as the control parameter. The thick dashed line in the left panels indicates the level of the control parameter at the Maxwell point (MP). The right panels show the resilience, in terms of the fraction of the landscape that needs to be perturbed (i.e. with a strong local perturbation) to trigger a shift to the alternative stable state of the low nutrient state in the eutrophication model (panel b); the high biomass state in the Allee effect model (panel d); and the vegetated, clear state in the vegetation – light attenuation model (panel f). For all three models, the size of the landscape (L) is 100 m.

Table A6.1. Model equations and parameters of three models with alternative stable states.

Models	State variables and parameters		Value
Eutrophication model (Carpenter *et al.* 1999) $\frac{dN}{dt} = a - bN + \frac{rN^p}{N^p + 1} + D\frac{\partial^2 N}{\partial x^2}$	N	Local nutrient concentration (state variable)	
	a	Nutrient loading rate	0.1-0.6
	b	Nutrient loss rate	0.8
	p	Hill coefficient	8
	r	Maximal recycling rate	1
	D	Nutrient mixing rate	10
Allee effect model (Keitt *et al.* 2001) *with harvesting* $\frac{dN}{dt} = rN\left(1 - \frac{N}{K}\right)\left(\frac{N}{K} - \frac{C}{K}\right) - fN + D\frac{\partial^2 N}{\partial x^2}$	N	Local population size (state variable)	
	C	Allee threshold	0.2
	f	Exploitation rate	0-0.2
	K	Local carrying capacity	1
	r	Maximal growth rate	1
	D	Dispersal rate	10
Vegetation-turbidity model (Scheffer 1998) $\frac{dE}{dt} = E\left(1 - \frac{E}{E_0}\frac{h_v + V}{h_v}\right) + D_E\frac{\partial^2 E}{\partial x^2}$ $\frac{dV}{dt} = \frac{r_V}{r_E}V\left(1 - V\frac{{h_E}^p + E^p}{{h_E}^p}\right) + D_V\frac{\partial^2 V}{\partial x^2}$	V	Local vegetation cover (state variable)	
	E	Local vertical light attenuation (state variable)	
	E_0	Local vertical light attenuation without vegetation	4-8
	r_V	Growth rate of vegetation	0.05
	r_E	Growth rate of vertical light attenuation	0.1
	h_E	Vertical light attenuation at which local vegetation cover is reduced by half	2
	h_V	Vegetation cover at which local vertical light attenuation is reduced by half	0.2
	p	Hill coefficient	4
	D_V	Dispersal rate vegetation	0.1
	D_E	Mixing rate turbidity	1

Interestingly, in contrast to models with one state variable, for models with two state variables the conditions for the Maxwell point change with diffusion rate. More specifically, in the vegetation-light attenuation model, the conditions for the Maxwell point depend on the dispersal rate of vegetation relative to the mixing rate of turbid water (Fig. A6.3). Under the assumption that clonal expansion rate of aquatic plants is much lower than mixing of turbidity (i.e. $D_V / D_E < 1$), one may conclude that the resilience of the macrophyte-dominated state against local removal of vegetation in a large lake is not only lower than predicted by well-mixed models (see main text), but it is also lower than predicted by models that assume equal diffusion rates. Therefore, an increase in clonal expansion rate would lead to an increase in resilience of the macrophyte-dominated state.

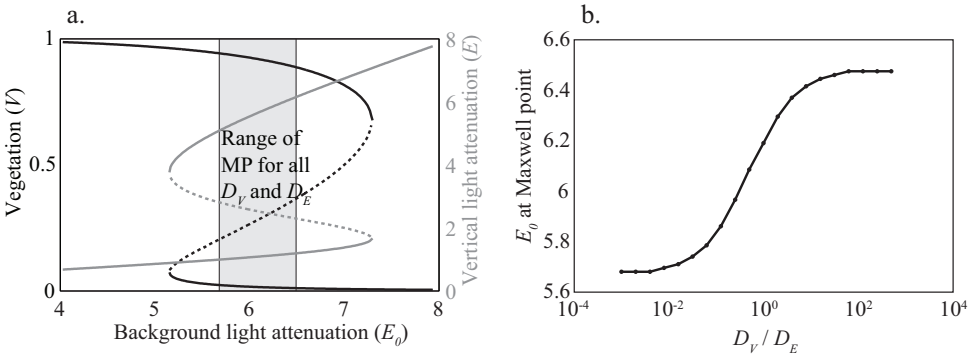

Figure A6.3. The Maxwell point in the vegetation-light attenuation model. **a)** The range of conditions holding the Maxwell point. The actual conditions for the Maxwell point depend on **b)** the ratio between the dispersal rate of vegetation and the mixing rate of turbidity (D_V / D_E). Note that the location of the Maxwell point influences the resilience of the two global states against local perturbations.

Appendix A6.2. Non-dimensional model

We reduced the number of parameters by rescaling the model described in the main text:

$$\frac{\partial N^*}{\partial t^*} = N^*\left(1 - N^*\right) - \frac{\sigma\left(N^*\right)^2}{\left(N^*\right)^2 + \mu^2} + \frac{\partial^2 N^*}{\partial\left(x^*\right)^2}$$

With new, dimensionless variables: $t^* = rt$, $N^* = \frac{N}{K}$, $x^* = x\sqrt{\frac{r}{D}}$, $L^* = L\sqrt{\frac{r}{D}}$ and parameters: $\sigma = \frac{c}{rK}$, $\mu = \frac{H}{K}$.

In this rescaled, non-dimensional model, the population size is scaled to the carrying capacity, the timescale is scaled to the growth rate of the species, and the spatial scale is scaled to the diffusion rate. Using such formulation, one can predict generic patterns independent of population size, temporal scale, and spatial scale. However, it is often more difficult to understand the abstract variables and parameters.

The non-dimensional model allows us, for example, to generalize the minimum size of a disturbance needed to trigger a travelling front (as in Figure 6.3a, main text), in terms of the rescaled, non-dimensional perturbation size Δx^* (Fig. A6.4a). It also allows us to draw the hysteresis plot in terms of the rescaled landscape size L^* (Fig. A6.4b, as in Figure 6.4b and 6.4c, main text).

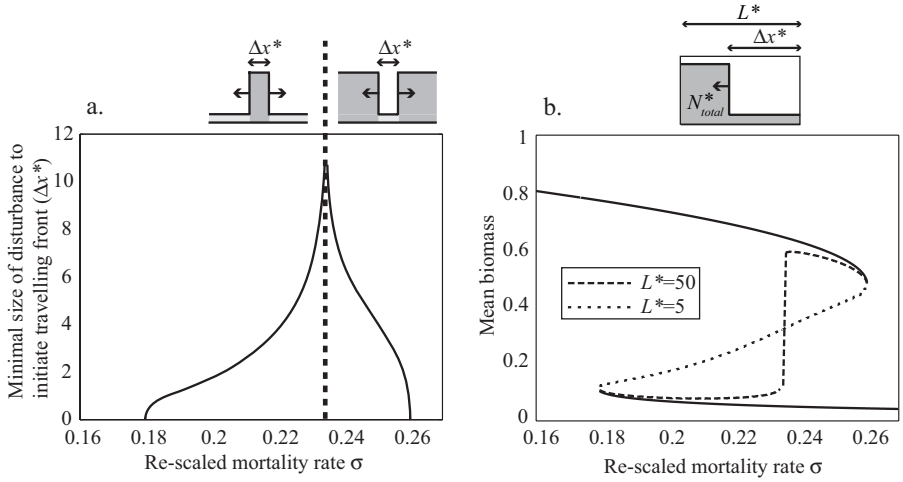

Figure A6.4. Critical size of disturbance and front speed as a function of the re-scaled mortality rate σ. **a)** Critical size of a local disturbance as a function of the re-scaled maximal mortality rate σ. Disturbances smaller than the critical size are repaired, while larger disturbances propagated through the landscape, shifting the entire landscape to the alternative state. The thick dashed line represents the Maxwell point. Left of the Maxwell point the entire landscape was initially set to the low biomass state, and the disturbance was set to the high biomass state. Right of the Maxwell point the landscape was initially set to the high biomass state, and the disturbance was set to the low biomass state (indicated by the small upper panels). **b)** Mean biomass on the landscape in equilibrium (N^*_{total} / L^*) as a function of the re-scaled maximal mortality rate for two systems with landscape size L^*. The solid parts of the curve represent the two stable landscape-wide equilibria. The dashed parts of the curve represent the disturbance thresholds, i.e. the size of the disturbed patch needed to induce a systemic shift to the alternative stable landscape-wide state.

Appendix A6.3. Co-existence of alternative stable states

Alternative stable states can co-exist in space, if the landscape consists of patches (Fig. A6.5), or if there is some level of heterogeneity in the dispersal rate or mixing rate of the state variable (Fig. A6.6).

Landscapes are often modeled by means of a lattice differential equation (LDE) (Chow *et al.* 1996). For an LDE, one models the landscape as a grid with discrete grid cells. Dispersal is represented by an exchange of biomass between neighboring grid cells. This method is often used to mimic a continuous landscape, using sufficiently small grid cells relative to the diffusion rate, to avoid potential side effects of the 'artificial' grid cells. LDEs may also be used to simulate a patchy system, in which the grid cells represent individual patches, or islands. We made a simple LDE version of our model with ten grid cells, using:

$$\frac{dN_j}{dt} = rN_j\left(1-\frac{N_j}{K}\right) - \frac{cN_j^{\,2}}{N_j^{\,2}+H^2} + \frac{D}{(\Delta x)^2}\left(N_{j-1}+N_{j+1}-2N_j\right) \qquad j = 1\ldots10$$

Using an LDE, it is possible to have areas with low biomass coexisting with areas with high biomass. Between both states there is a stagnant gradient in the biomass (Fig. A6.5a). Such coexistence is only possible for intermediate mortality rates and low dispersal rates between the grid cells (Fig. A6.5a)(van Nes and Scheffer, unpublished manuscript). The range of co-existence decreases with high dispersal. In contrast, if we model continuous space by means of a PDE (as in the main text), co-existence of alternative stable states is not possible for any parameter setting (Fig. A6.5b). A travelling front with a constant rate of spread always emerges, leaving the entire system in the state with the highest resilience (main text).

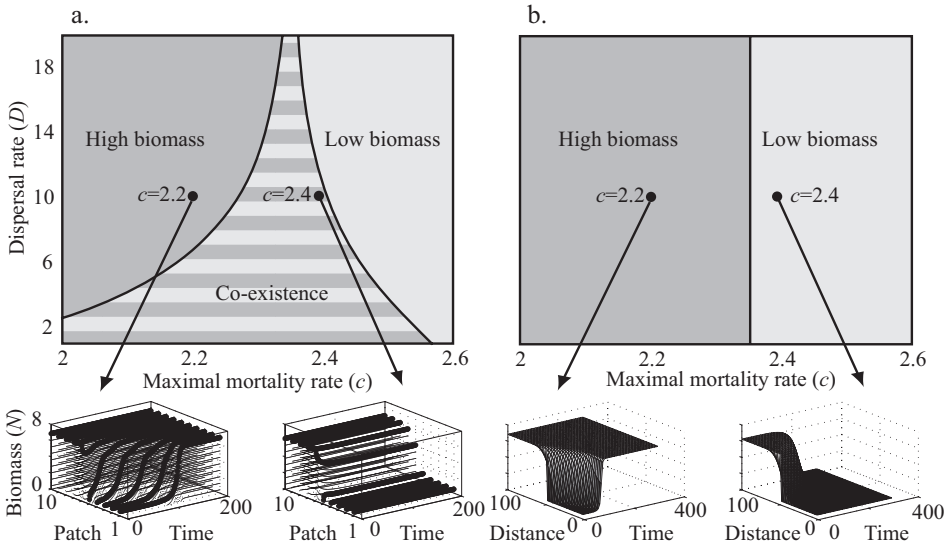

Figure A6.5. Comparison of a spatially discrete and a spatially continuous model with local alternative stable states. Stable end configurations of the entire landscape in the high biomass state, the entire landscape in the low biomass state, or stable co-existence of both alternative states in space, as a function of the maximal mortality rate and the dispersal rate of species N. The initial landscape was set at one half in either of the alternative states in: **a)** a one-dimensional lattice with discrete grid cells; and **b)** a homogeneous, spatially continuous landscape. Note that alternative states can co-occur in space on a landscape with patches (panel a), while in a spatially continuous system, a travelling front will always move the entire system to one of the states (panel b) (main text). The example simulations below are space-time-plots for $c = 2.2$ and $c = 2.4$ ($D = 10$).

The prediction that alternative stable states cannot co-exist in space holds only for the limit case where exchange rates are completely homogeneous in space. Co-existence of alternative stable states in continuous space may happen when a travelling front meets an area of increased diffusion, such that the processes that stabilize the alternative state locally have a higher impact. This effect is most pronounced close to the Maxwell point, if processes that trigger the travelling front are weak. Obviously, the more spatially heterogeneous the exchange rates or other spatial processes are, the larger the scope for such 'wave-pinning' situations (Fig. A6.6).

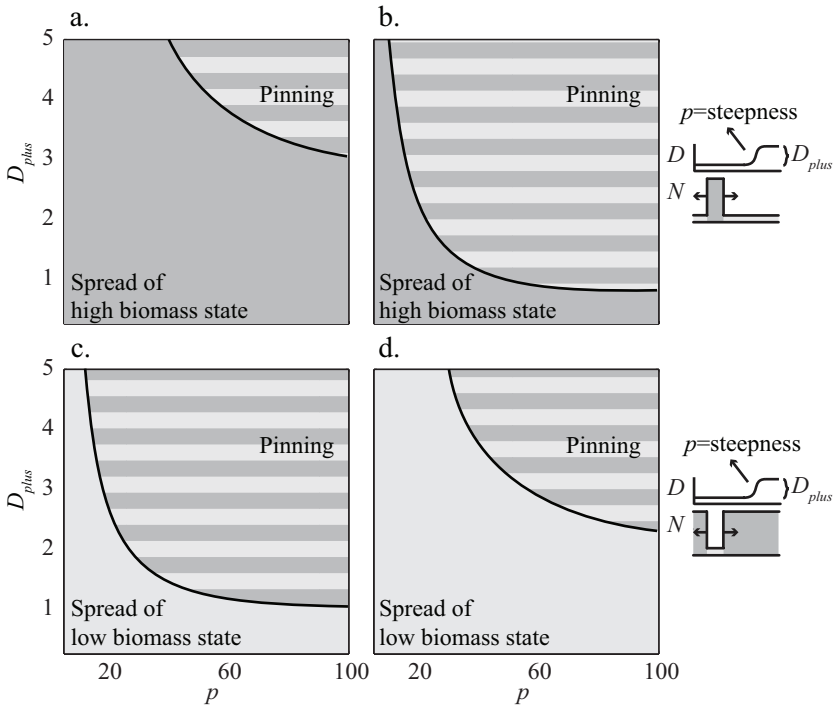

Figure A6.6. The effect of spatially heterogeneous diffusion. A travelling front of collapsing biomass triggered by a disturbance can come to a halt if it meets an area of increased diffusion (D_{plus}). The probability of this so-called pinning increases if the shift in diffusion becomes less gradual, thus if the steepness of the shift (p) increases. Maximal mortality rate: **a)** $c = 2.2$; **b)** $c = 2.3$; **c)** $c = 2.4$ **d)** $c = 2.45$. As shown by Figure 6.5 (main text), the likelihood of pinning is high if the maximal mortality rate is close to the Maxwell point (e.g. panels b and c).

A corollary of this result is that spatial coexistence of alternative stable states in finite element models (Fig. A6.5a) is not simply an artifact of the discretization of space (Fáth 1998; Keitt *et al.* 2001; Holt *et al.* 2005; Taylor and Hastings 2005), but a consequence of heterogeneous local exchange rates. This is important, as discrete models are much easier to implement computationally.

Appendix A6.4. Gradual shifts in heterogeneous spatially extended systems

Abrupt shifts of alternative stable states in space may be expected if environmental conditions (here represented by the maximal growth rate r) change gradually in space (Fig. A6.7). In such situation, a travelling front triggered by a local disturbance will come to a hold if it hits environmental conditions that correspond to the Maxwell point (Fig. A6.7). One may wonder what happens to the location of the spatial shift if global conditions change. We simulated the effect of an increasing globally changing driver (here represented by the maximal mortality rate c) in various

spatially extended landscapes (Fig. A6.7). A smooth environmental gradient of the maximal growth rate will simply result in a smooth range shift (Fig. A6.7b), while a system with healthy edges may recolonize from these refuges (Fig. A6.7a) as soon as the Maxwell point is crossed. In general, heterogeneity in spatially extended systems with local alternative states will lead to an overall smooth response to gradually changing conditions, with some larger waves of collapse or repair, when crossing more vulnerable, or healthy parts of the landscape (Figs. A6.7c and A6.7d). The Maxwell point plays an important role, as it is the point at which the direction of the travelling front shifts: it determines the borders of spatial co-existence of alternative stables states.

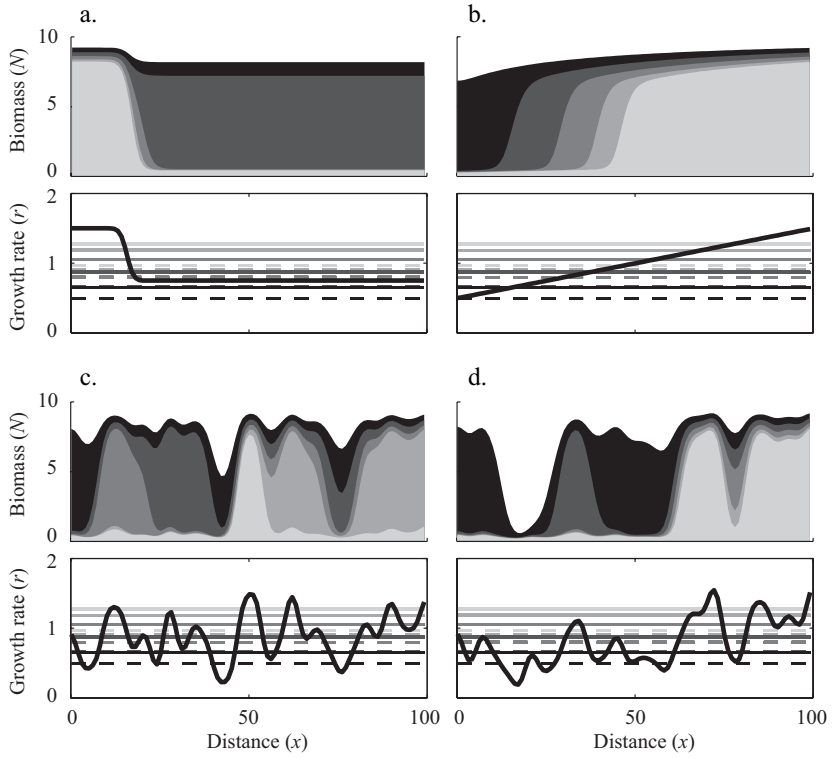

Figure A6.7. The effect of spatially heterogeneous environmental conditions. Example simulations of recovery, following a gradual decrease in maximal mortality rate, on a landscape with local alternative stable states in: **a)** a generally homogeneous landscape with one edge at which the growth rate is locally high (a refuge); **b)** a landscape with a linear gradient in growth rate; and **c)** and **d)** two landscapes with random heterogeneity in growth rate. The thick black line in the lower panels represents the local growth rate r. The maximal mortality rate is changed from 2.36 to 1.96, and the simulation results are depicted for steps of 0.02. The stable end configurations of biomass are depicted in the upper panels as shaded areas, ranging from light gray to black. For each parameter setting, the grey solid lines in the lower panels represent the upper fold bifurcation, and the grey dashed lines the Maxwell point. When the growth rate at a point in space exceeds the fold bifurcation, there is locally only one stable state.

When the growth rate locally exceeds the Maxwell point, a travelling front towards the higher biomass could be triggered, provided that the area that initiates the front is sufficiently large. Note that in an environment with an environmental gradient (panel *b*), the location of a standing front directly follows changes in global conditions (no hysteresis), while in an environment with random heterogeneity, the location of the standing front changes stepwise, which can result in hysteresis if the maximal mortality rate decreases again.

Chapter 7

Slow recovery from local disturbances as indicator for loss of ecosystem resilience

Ingrid A. van de Leemput,
Vasilis Dakos,
Marten Scheffer,
and Egbert H. van Nes

Submitted to Ecosystems

Abstract

A range of early-warning signals have been proposed for identifying elevated risk of critical transitions in ecosystems. Most indicators are based on the idea that critical slowing down can be inferred from changes in statistical properties of natural fluctuations and spatial patterns. However, identifying these signals in nature has remained challenging. An alternative approach is to infer changes in resilience from differences in standardized experimental perturbations. However, system-wide experimental perturbations are rarely feasible. Here we evaluate the potential to infer the risk of large-scale systemic transitions from local experimental or natural perturbations. We use models of spatially explicit landscapes to illustrate how recovery rates upon small-scale perturbations decrease as an ecosystem approaches a tipping point for a large-scale collapse. We show that the recovery trajectory depends on: (1) the resilience of the ecosystem at large scale, (2) the dispersal rate of organisms, and (3) the scale of the perturbation. In addition, we show that recovery of natural disturbances in a heterogeneous environment can potentially function as an indicator of resilience of a large-scale ecosystem. Our analyses reveal fundamental differences between large-scale weak and local-scale strong perturbations, leading to an overview of opportunities and limitations of the use of local disturbance-recovery experiments.

Introduction

The idea that we might detect loss of resilience as an early-warning signal for critical transitions in ecological systems has attracted much attention (Scheffer *et al.* 2012a; Dakos *et al.* 2015). It can be mathematically shown that close to a broad class of tipping points (namely zero-eigenvalue bifurcations) systems become slower in recovering from small perturbations (Wissel 1984; Strogatz 1994). A straightforward consequence of this 'critical slowing down' is that, if we can measure the time it takes for a system to return to its original state after a small disturbance, we may indicate the proximity of the system to a catastrophic shift (van Nes and Scheffer 2007). A range of indicators has been proposed that may reflect such slowing down in natural fluctuations or in spatial patterns (Scheffer *et al.* 2012a; Dakos *et al.* 2015). In particular, rising temporal autocorrelation and variance have received much attention as indicators of loss of resilience before a transition. For instance, variance of phosphorus concentration in a lake is predicted to increase as conditions reach a threshold at which the lake shifts from an oligotrophic to a eutrophic state (Carpenter and Brock 2006). Similarly, temporal autocorrelation in vegetation biomass may rise before the ecosystem collapses to a desert state due to overgrazing (Dakos *et al.* 2011). Other proposed early-warning signals include increasing spatial correlation (Dakos *et al.* 2010), increasing skewness (Guttal and Jayaprakash 2008a), changing frequency spectra (Kleinen *et al.* 2003), deviations in pattern formation (Rietkerk *et al.* 2004), and truncated power law distributions (Kéfi *et al.* 2007).

In theory, these early warnings may well indicate a nearby tipping point. However, detecting them in practice remains difficult. Timely and robust identification of early warnings requires long, high-resolution records with low measurement error that are simply unavailable in most ecological systems. Thus, it is not surprising that the best reported cases for detecting early warnings before shifts come from controlled experiments in the lab where short-lived and easy-to-monitor single species populations are used (Drake and Griffen 2010; Veraart *et al.* 2012; Dai *et al.* 2012, 2013). The only ecological study that identified indicators of reduced resilience before a catastrophic shift in the field is a lake trophic cascade experiment that relied on the exceptional case of comparing dynamics between a manipulated and a control lake (Carpenter *et al.* 2011).

Part of the difficulty stems from the fact that the discussed indicators are mostly indirect measures of critical slowing down. Such proxies have a number of issues that ultimately limit their potential to unequivocally detect if critical slowing down is at play (Brock and Carpenter 2010; Dakos *et al.* 2012b, 2015). For instance, strong environmental stochasticity could muffle any rising pattern in variance caused by critical slowing down. False positive trends in both variance and autocorrelation

might be driven by changes in the pattern of environmental fluctuations rather than by the proximity to a nearby transition (Dakos *et al.* 2015). Overall, the most reliable way to identify critical slowing down is to directly measure the time (or alternatively rate) it takes for a system to recover after a small experimental disturbance (van Nes and Scheffer 2007).

In its simplest form, one applies a homogeneous (system-wide), weak perturbation (e.g. by removing 5% of the biomass) and measures the time it takes to recover to the pre-disturbance state. However, most ecosystems are 'spatially extended', in the sense that the size of the landscape is large compared to the scale at which important processes and interactions are acting. Examples of spatially extended ecosystems with critical transitions between alternative stable states include kelp forests (Konar and Estes 2003), coral reefs (McManus and Polsenberg 2004; Elmhirst *et al.* 2009), semi-arid vegetation (Rietkerk and van de Koppel 1997), mud-flats (van de Koppel *et al.* 2001), and lake vegetation in large lakes (Scheffer 1998). Homogeneous (system-wide) disturbance experimentation could be problematic in practice, either due to cost and management restrictions (e.g. protected habitats), or because experiments are simply impossible to perform on the scale of the entire ecosystem. For instance, one simply cannot remove a certain percentage of coral cover on an entire reef to measure its recovery. In addition, the effects of a weak disturbance might be difficult to measure in a naturally stochastic environment, while a too strong system-wide pulse experiment might "accidentally" push the ecosystem to an undesirable state. Thus, such large-scale approaches do not always belong to the fail-safe experimentation that would be appropriate for measuring resilience (Holling and Meffe 1996).

In practice, it will be more feasible to perform a *strong local* perturbation, for instance by removing all vegetation in a small area in the middle of a vegetated area. However, this perturbation type is different from a system-wide perturbation, since spatial interactions and dispersal play a role in the recovery. Here, we study whether recovery rate from strong but local disturbances in spatially extended ecosystems can be used to infer *system-level* proximity to a tipping point. We show that both in continuous landscapes (e.g. a single large lake or forest), and in patchy landscapes (e.g. a set of connected ponds or forest patches) recovery rates upon local disturbances should be expected to reflect the proximity of a threshold for system-wide collapse, but also depend on factors such as the dispersal rate of organisms, and the scale of perturbations.

Methods

Model

To test whether recovery time upon strong local perturbations can, theoretically, be used as an indicator for loss of resilience in large-scale ecosystems, we adapted a harvesting model with alternative stable states (Noy-Meir 1975) to make it spatially explicit. The basic model describes the logistic growth of a resource N that is harvested following a sigmoidal functional response. This model has been extensively used to study overexploitation (May 1977). For a range of parameters, resource biomass can be in two alternative states: a high biomass (underexploited) state, and a low biomass (overexploited) state. Growth rate of resource N is given by equation 1:

$$f(N) = rN\left(1 - \frac{N}{K}\right) - c\frac{N^2}{N^2 + H^2} \quad (1)$$

in which r (1 day^{-1}) is the local maximum growth rate of resource N (in g m^{-2}), K (10 g m^{-2}) is the local carrying capacity of resource N, c (ranging from 1.8 – 2.8 g m^{-2} day^{-1}) is the maximum harvest rate, and H (1 g m^{-2}) is the half saturation of the functional response of harvesting. An increase in harvest rate c (stress driver) leads to a decrease in stability of the underexploited, high biomass state and eventually pushes the system to the overexploited, low biomass equilibrium state.

We considered two representative spatially extended ecosystems: a 'continuous landscape' and a 'patchy landscape' (Table 7.1, Fig. 7.1). In a continuous landscape, we assumed that the resource disperses randomly through the landscape with constant dispersal rate D (i.e. modeled as diffusion) (Table 7.1, Fig. 7.1a). A patchy landscape was defined as a random network of 100 patches with 0.04 connectivity (i.e. there is 4% probability that there is an edge between two patches in the network) (Fig. 7.1b). We assumed that resource biomass is well mixed within each patch, whereas dispersal occurs between connected patches with a constant rate f_d (Table 7.1). For consistency with the continuous model, we assume that all patches are of the same size (1 m^2). The parameters D in the continuous landscape, and f_d in the patchy landscape thus represent the level of mixing of the resource N across the landscape.

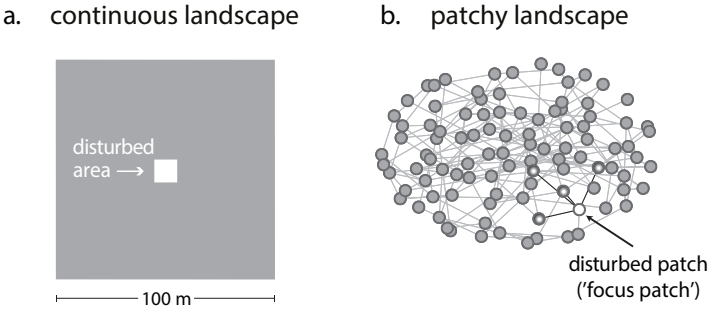

Figure 7.1. Representation of disturbance-recovery experiments in our spatially extended ecosystems. **a)** A continuous landscape is defined as a fully connected landscape. We performed a local strong disturbance by removing all resource biomass from an area in the center of the landscape, indicated in white. **b)** A patchy landscape is defined as a sparsely connected landscape: that is a network of patches that are randomly connected to other patches in the landscape. We performed a local strong disturbance by removing resource biomass from one patch, the so-called focus patch, indicated by the white dot. The focus patch used for the simulations is connected to four other patches, indicated by the shaded dots.

Table 7.1. Different dispersal and disturbance levels applied in the recovery time experiments for continuous and patchy landscapes. A two-dimensional partial differential equation describes the dynamics of the continuous landscape, and a sparse lattice differential equation describes the dynamics of the patchy landscape. The parameter m_i represents the number of patches that are connected with patch *i*.

	Continuous landscape	**Patchy landscape**
	$N' = f(N) + D\left(\frac{\partial^2 N}{\partial x^2} + \frac{\partial^2 N}{\partial y^2}\right)$	$N_i' = f(N_i) + f_d\left(\sum_j^{m_i} N_j - m_i N_i\right)$
Landscape size	100 x 100 m	100 patches
Low dispersal	D = 2.5 m^2 day^{-1}	f_d = 0.02 day^{-1}
High dispersal	D = 12.5 m^2 day^{-1}	f_d = 0.1 day^{-1}
Small disturbance (1%)	10 x 10 m	1 patch
Large disturbance (5%)	~22.4 x 22.4 m	5 patches

Simulations

We started all experiments with the entire landscape in the underexploited (high resource biomass) equilibrium state. We performed a strong, local disturbance by removing all biomass ($N_{i,t0}$= 0) either in a square in the center of the continuous landscape or in a patch of the patchy landscape (where *i* denotes the local area, or patch disturbed). We compared effects for a 'small' versus a 'large' disturbed area. A small-disturbed area was defined as an area equal to 1% of the landscape (expressed in m^2) whereas a large disturbed area was equal to 5% (Table 7.1). In the patchy landscape, perturbations were initially performed on one specific focus patch in the network. In the modeled network, this particular focus patch is connected to four

other patches in the network (i.e. the degree of the focus patch is four). Complete biomass removal in the focus patch was called a small disturbance (1% of the total landscape), whereas for a large disturbance both the focus patch and its four connected patches were set to zero biomass (5% of the landscape) (Table 7.1).

We defined recovery time upon local disturbance as the time it takes ($t - t_0$) for the resource biomass $N_{j,t}$ to recover to the pre-disturbed state $N_{j,t0}$ (where j denotes the center of the disturbed area i, or patch i). The disturbance was assumed to be recovered, if the difference between $N_{j,t0}$ and $N_{j,t}$was smaller than 0.1 g m^{-2}. We investigate how recovery rate (defined as 1/recovery time) changes with the distance to the tipping point by changing the harvest rate c, using the standardized disturbances described above.

Strong local disturbances do not always recover (Keitt *et al.* 2001; van de Leemput *et al.* 2015). There are two other possibilities. A local strong disturbance can either trigger a systemic collapse to the overexploited state (we call this 'induced collapse'), or the effect of the disturbance can persist, that means that it neither recovers nor triggers a systemic collapse (we call this 'no recovery'). As recovery time cannot be defined for such cases, we reported recovery rates only when there was actual recovery. Overall, we estimated recovery rate upon local disturbances for different scenarios that are summarized in Table 7.1; at low and high dispersal rates, and for small and large disturbed areas.

In the baseline scenarios we assumed a homogenous landscape (i.e. the same parameters across space) and standardized disturbances (i.e. same size and location of the disturbed area). In addition, we performed experiments in the presence of spatial heterogeneity and with randomly located, not standardized disturbances. We introduced spatial heterogeneity in both landscapes by varying the maximal growth rate of the resource (r). To create heterogeneity in the continuous landscape, we first split the landscape in 25 equally-sized squares, and assigned growth rates from a uniform distribution ($r \sim U[0.8, 1.2\ \text{day}^{-1}]$). Next, we smoothened the generated variability over the entire space with a Gaussian smoothing function (Bowman and Azzalini 1997). In the patchy landscape, growth rates were randomly assigned to patches following the same uniform distribution ($r \sim U[0.8, 1.2\ \text{day}^{-1}]$).

Randomly located, not standardized disturbances were introduced as follows. In the continuous landscape, the size of each disturbance (as percentage of the total area) was drawn from a uniform distribution (size ~ $U[0.01, 0.05]$, whereas the location of the disturbance was determined randomly in the landscape. In the patchy landscape, we selected one patch at random for each simulation (patch ~ $U[1,100]$). Due to the network topology, the disturbed patches differ in their number of neighbors (i.e. degree). We define a single 'recovery rate experiment' as a collection

of simulations with one random disturbance per simulated level of harvest rate c. To get an estimate of the variability in recovery rate, we simulated 100 recovery rate experiments. We report the mean recovery time (1/recovery time), and the 10th and 90th percentiles for each level of the harvest rate c. Moreover, we report the percentage of simulations that yield 'no recovery'. The indicator can be improved if other variables related to the disturbances are known. As an example, we corrected for the size of disturbance A (in m^2) in a continuous landscape, and the degree of the disturbed node k in a patchy landscape. For each recovery rate experiment, we performed a regression analysis of recovery rate $\frac{1}{\Delta t}$ against perturbation size A in case of a continuous landscape, and degree of perturbed node k in case of a patchy landscape, yielding an estimated recovery rate for each perturbation $\left(\frac{\bar{1}}{\Delta t}\right)$. Finally, we reported the residuals $\left(\frac{1}{\Delta t}-\frac{\bar{1}}{\Delta t}\right)$, and the 10th and 90th percentiles of the residuals. For all analyses we used Grind for Matlab (accessed at http://www.sparcs-center.org/grind). We approximated a continuous landscape using the finite difference method where we discretized space in a lattice, while making sure that cells were sufficiently small to approximate continuous space for the parameters we used. This resulted in a 50x50 cells lattice. Importantly, a finer-meshed lattice did not alter the resulting dynamics for the parameters we used. Note that one should always be aware of situations of no recovery due to the discretization method used (Keitt *et al.* 2001; van de Leemput *et al.* 2015). All differential equations were solved using an explicit Runge-Kutta (4,5) solver with adaptive step-size.

Results

In both our spatial systems (Fig. 7.1), increasing the harvest rate caused a gradual decrease in resource biomass up till the tipping point at which the ecosystem collapsed to the alternative overexploited state (the fold bifurcation point in Figure 7.2a). In line with previous results (van Nes and Scheffer 2007), the time of the system to recover upon a weak global perturbation becomes longer as the system is closer to the bifurcation point (Fig. 7.2b).

Slowing down is also observed in the time to recover from resource biomass removal in a small area (Fig. 7.2c). Note, though, that close to the systemic tipping point the local recovery trajectory is not exponential due to the nonlinear dynamics involved (Fig. 7.2c). The total biomass on the landscape even decreases prior to recovery (see Fig. A7.1). This is because the low biomass state is actually stronger than the high biomass state under these conditions. However, the perturbation is too small to create an actual travelling front of an expanding perturbation (see van de Leemput *et al.* (2015)). While the system does recover eventually, such non-

exponential recovery trajectory obviously hints at the proximity of the system to a runaway cascading collapse of the landscape. The decrease in resilience of the high biomass state is indeed reflected in the local recovery time (Fig. 7.2c). In addition, the size of the area that is affected by the perturbation could be considered an indicator of resilience (see also Dai *et al.* (2013) for a similar measure of recovery length). Systematic analysis of the size of the affected area suggests that it may be an appropriate metric that does rise steadily as the system approaches critical conditions for systemic collapse (see Fig. A7.2). In what follows, we limited our further analysis to recovery rate of the perturbed site itself.

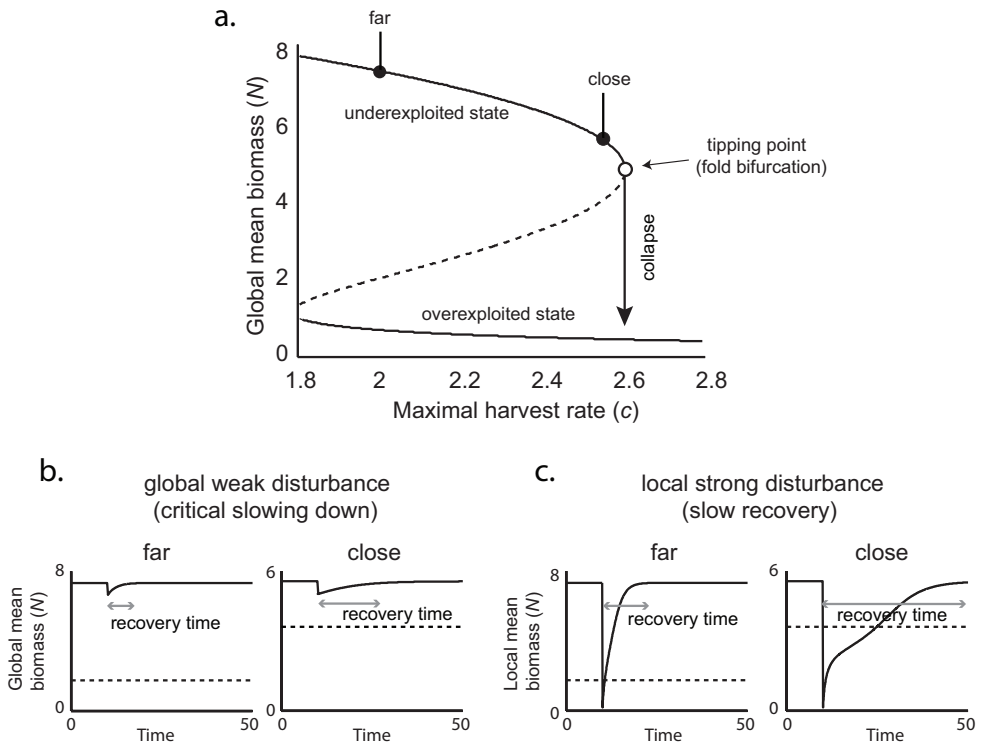

Figure 7.2. The collapse of resource biomass under increasing harvesting and two distinct disturbance-recovery experiments in a spatially continuous ecosystem. **a)** Bifurcation diagram of resource biomass. Increasing harvest rate c pushes the resource (mean biomass) towards the tipping point to overexploitation. Continuous lines indicate the two alternative equilibria. The dashed line indicates the unstable equilibrium that divides the two alternative basins of attraction. **b)** We performed a weak global disturbance (by removing 10% of standing biomass) far ($c = 2$) and close ($c = 2.55$) to the transition, and monitored an increase in recovery time due to critical slowing down. **c)** We performed a strong local disturbance (by removing all standing biomass in an area comprising 1% of the landscape) far ($c = 2$) and close ($c = 2.55$) to the transition, and monitored an increase in recovery time. Note this increase is not strictly due to critical slowing down. Dashed horizontal lines indicate the threshold between the basins of attraction of the two alternative states. For all simulations, dispersal rate is low ($D = 2.5$ m^2 day^{-1}).

In general, we found that recovery rate (i.e. 1/recovery time) decreased smoothly as increased harvest rates brought the system closer to the tipping point for a systemic collapse. This was true in both continuous and patchy landscapes (Fig. 7.3a, b). As the perturbed area was larger it invoked a systemic collapse at lower harvest rates ('induced collapse') (Fig. 7.3a vs. 3c and 3b vs. 3d).

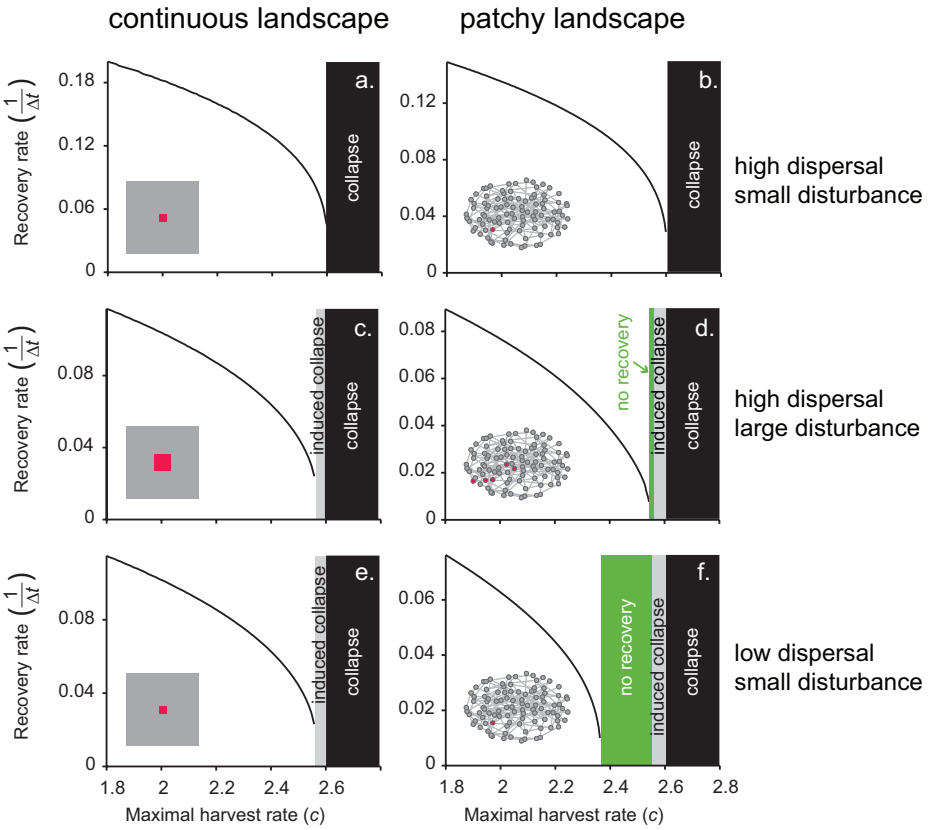

Figure 7.3. Strong local disturbance-recovery experiments for measuring recovery rate (as 1/recovery time) as an indicator for ecosystem-level resilience. **a)** Recovery rate upon a local disturbance -a zero-biomass area in the middle of a homogeneous high-biomass landscape (indicated by the red area)- as a function of harvest rate *c* up to the crossing of the critical transition. **b)** Recovery rate upon a local disturbance -a zero-biomass patch in a patchy high-biomass landscape (indicated by the red focus patch)- as a function of harvest rate c up to the crossing of the critical transition. **c and e)** In a continuous landscape, a large disturbance in a system with high dispersal or a small disturbance in a system with low dispersal rate may induce a "premature" systemic collapse (grey area). This means that a transition of the global ecosystem takes place before the actual fold bifurcation point (black area). **d and f)** In a patchy landscape, a local disturbance may also induce a systemic collapse (grey area), but can also lead to no recovery (green area) especially when dispersal is low.

However, results depend on the dispersal rates too. If dispersal was low, even small-scale perturbations could provoke such premature systemic collapses in the continuous landscape (Fig. 7.3e). In a patchy landscape there was also a range of conditions at which a local disturbance persisted without expanding or recovering ('no recovery', Fig. 7.3d, f). This range was larger when dispersal was lower (Fig. 7.3f). Not surprisingly, when on top of low dispersal we imposed a large disturbed area, the probability of a premature collapse or no recovery increases even more (Fig A7.3). In spite of those differences, recovery rates always decreased as the harvest rates approached the critical point where a premature collapse or 'no recovery' situation occurred (Fig. 7.3c-f). Thus rather than the distance to the generic bifurcation point, a drop in recovery rates signaled the decreased capacity of the ecosystem to recover from the prescribed local perturbations.

So far, we assumed that environmental conditions across the landscape were homogeneous. As a next step we consider a situation where conditions (represented by the maximum growth rate r, see methods) vary spatially (Fig. 7.4). To analyze the properties of such heterogeneous landscapes we performed multiple experiments in which we simulated disturbances of random size at random locations. There is a clear decreasing trend in such average recovery rates as increasing harvest brings the landscapes closer to the systemic collapse (Fig. 7.4, see Fig. A7.4 for high dispersal). Still, variability is relatively large, which is due to 1) the location of the disturbance in the heterogeneous landscape, and 2a) the variation in size of disturbance in a continuous landscape, or 2b) number of neighbors (degree) of the disturbed node in the patchy landscape. Importantly, if data is available on any of these variables, one might be able to reduce the variability in recovery rates (Fig. 7.4c, d, Fig. A7.4), and therefore strengthen the resilience indicator. In the patchy landscape, the probability of local no-recovery upon perturbations strongly increased towards the systemic collapse (Fig. 7.4b), which is much less if dispersal is high (Fig. A7.4).

Discussion

Our analyses suggest that in spatially extended ecosystems, reduced recovery rates upon local perturbations may signal that the ecosystem is approaching a system-wide transition. At the same time our results show that local recovery rates depend strongly on landscape connectivity (i.e. continuous vs. patchy), dispersal rates and the scale of local perturbations. Although these findings may seem straightforward at first sight, the link to practical implications as well as the more fundamental underlying theory is not so clear.

Signals from strong local disturbance vs. weak global disturbance experiments

Although our results resemble the patterns found by measuring recovering rate upon a small perturbation in a well-mixed system (van Nes and Scheffer 2007; Dakos *et al.* 2011) they are not directly related to the same phenomenon of critical slowing down. Critical slowing down is defined for weak disturbances close to equilibrium (Fig. 7.2b) where recovery is approximately exponential. In our strong local disturbance experiments, we pushed a local area to the alternative equilibrium (Fig. 7.2c). Therefore the nonlinearity of the system will play a role in the recovery. As the disturbed area lies in the basin of attraction of the alternative state, it will not recover by itself. Inflow of biomass from the neighboring undisturbed parts of the system is needed. The capacity for this recovery process depends on the resilience of the ecosystem. Phrased loosely, a low resilient (highly stressed) system will recover from local damage slower because the neighboring area has a low capacity to "pull" the disturbed area back to the pre-disturbed state. On a more fundamental level, this change in the relative resilience and reduction of the recovery capacity of spatially extended systems is related to the crossing of a Maxwell point (Keitt *et al.* 2001; Bel *et al.* 2012). At this point both equilibria are equally "strong" (i.e. they have the same potential (Strogatz 1994)) and large spatial perturbations will neither recover nor expand (van de Leemput *et al.* 2015).

Regardless of the fundamental aspects, our results have marked practical implications. They suggest that a local scale experiment can provide information for the resilience of a large-scale ecosystem. This is important as performing a small-scale disturbance experiment is much more realistic than applying a large-scale disturbance. For example, instead of facing the daunting task of removing 10% of submerged vegetation in a whole shallow lake, one may probe the resilience of the lake by removing all vegetation from just a small area. Moreover, the detectability of local recovery rates should be stronger when compared to recovery rates from weak global perturbations under noisy conditions (Appendix A7.3).

Our results also suggest that detecting altered local recovery rate may be feasible for random disturbances in a heterogeneous environment (Fig. 7.4). Obviously, this approach still requires having sufficient replicates of the disturbance experiments to get accurate results. Importantly, one can reduce some of the observed variability in recovery rates if one has relevant information on the disturbances (Fig. 7.4c, d), such as the size of the disturbance, the degree of the disturbed node, or the conditions at the location of the disturbance.

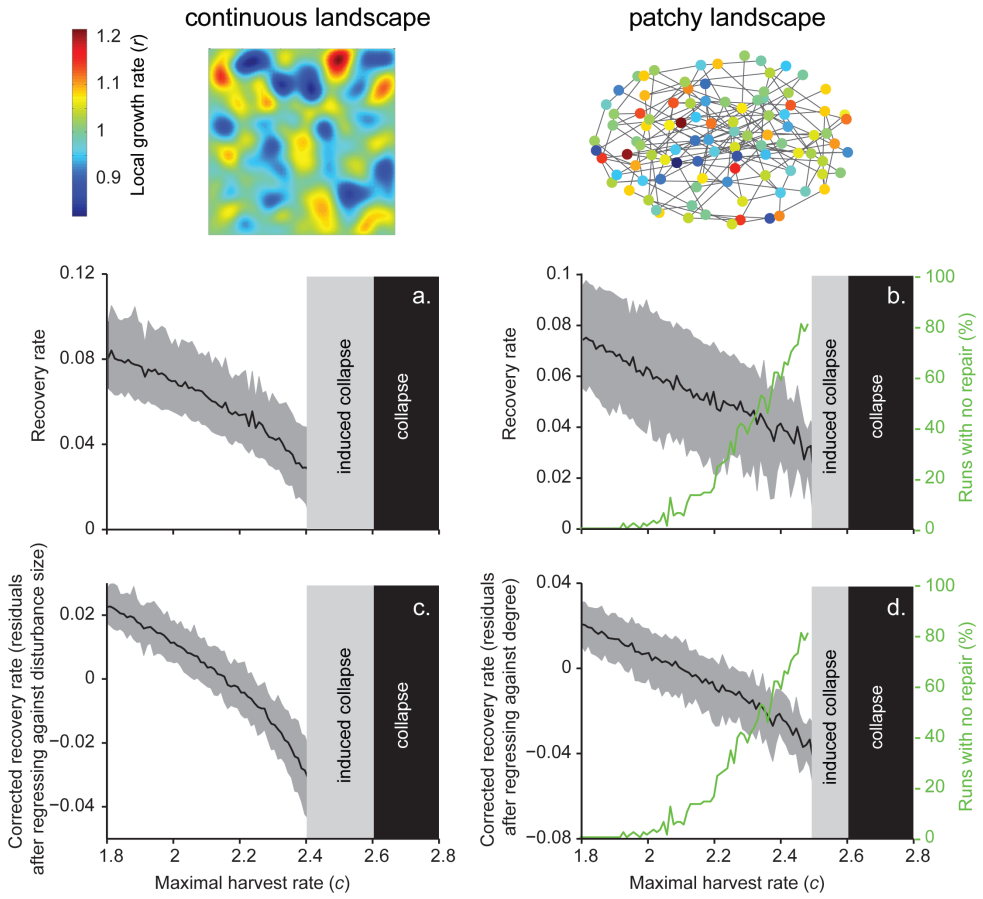

Figure 7.4. Effects of random disturbance experiments in landscapes with spatially heterogeneous conditions, and low dispersal. We randomly disturbed areas of different size on a continuous landscape and different patches in a patchy network for each level of resilience (in terms of maximal harvest rate) and measured recovery rates. **a-b)** Average recovery rates decrease in all situations as the system approaches the critical harvest rate for collapse. Black lines represent the average recovery rate, while the grey shaded lines show the 10th and 90th percentile, based on experiments per simulated harvest rate. In a patchy landscape (panel b), the percentage of experiments followed locally by no-recovery (green lines) increases as the harvest rate increases. This occurs especially when dispersal is low (see Appendix A7.2 for high dispersal). **c-d)** Average residual recovery rates after being corrected for the size of the disturbance (panel c), or the degree of the disturbed node (panel d). Note that the variance in recovery rates is lower after the correction.

Designing experiments

Clearly, our models are quite abstract, and bridging from our results to any particular field situation is a challenge. Nonetheless, our results suggest some aspects to ponder when it comes to designing experiments. First of all, the domino effects we show indicate that disturbance experiments are never completely free of risk. The

likelihood of an induced system-wide collapse depends on the spatial extent of the perturbation, the overall ecosystem resilience (i.e. the level of the stress driver), and on the strength of dispersal (see Appendix A7.4). It also depends on the connectivity in the landscape, so whether the landscape can be considered continuous or patchy (Fig. 7.1). Even a very local perturbation can theoretically trigger a collapse in a continuous landscape that is close to a tipping point, provided that the dispersal rate is low (Fig. 7.3e). This is because at low dispersal rates, the capacity of the landscape at larger scales to recover from a local disturbance is reduced. As a result, the local effect may persist long enough to kick-off a domino effect leading to an expanding collapse (van de Leemput *et al.* 2015).

Obviously, spatial interactions that are relevant to recovery are typically more complex than the simple diffusion mechanism in the model. Plants may enter through seed dispersal or root expansion depending on species and conditions, and animals may move directionally in or out of damaged patches. For example, clearing part of seagrass meadows creates open spaces attracting swans that delay or prohibit the regrowth of seagrass (van der Heide *et al.* 2012). Also, other processes may play a role in the recovery of local disturbances. For example, regrowth of vegetation patches may not occur from the side of a cleared patch, but simply from overwintering structures belowground. Typically researchers in any particular ecosystem will have a good intuition about the type and size of experimental perturbation that will yield a clear recovery signal, while not posing a risk of inducing a spreading collapse. We summarize the opportunities and limitations of recovery of local disturbances as an indicator of resilience in Table 7.2.

Table 7.2. Opportunities and limitations for performing local disturbance-recovery experiments in spatially extended ecosystems in order to indicate system-wide resilience.

Local recovery time experiments	
opportunities	*limitations*
• are feasible to perform	• can accidentally induce a collapse
• are easy to monitor	• might not reflect system-level resilience (under extreme landscape heterogeneity)
• provide a strong signal even under stochastic conditions	• require multiple experiments for averaging out local differences
• natural disturbances can be used as proxy experiments	• require information on dispersal rates and landscape heterogeneity • variability in dispersal and perturbation size can muffle the effect of resilience
• can be performed at different spatial scales	• may initiate other processes that lead to alternative outcomes

Although replicated prescribed experiments are the cleanest way to monitor change in recovery rates, natural local disturbances may offer an alternative in some situations. Recovery from events such as disease outbreaks, wildfires and bleaching have been studied in ecosystems ranging from grasslands (Tilman and Downing 1994) and marine kelp ecosystems (Dayton *et al.* 1992) to forests (Cole *et al.* 2014) and coral reefs (Houk *et al.* 2014). Especially if data on many repeated events are available, differences in recovery rates may hint at differences in resilience.

Restoration; a flipped perspective

In our model of a patchy landscape there is the possibility that a disturbed patch does not recover without causing the entire landscape to shift to the other state (i.e. it has an infinite recovery time, so-called 'pinning' (Keitt *et al.* 2001; van de Leemput *et al.* 2015). Also, in heterogeneous landscapes we can have a partial transition of the landscape (van de Leemput *et al.* 2015). In practice, lack of recovery or partial transitions of a landscape may be more common than all-or-non transitions, as even modest heterogeneity of conditions or dispersal rates can allow spatial coexistence of alternative stable states (van de Leemput *et al.* 2015). How one looks at such transitions depends on the context. Clearly, the words 'collapse' and 'recovery' we used are value laden, suggesting that the current state of the landscape is preferred over the potential alternative state. However, one may flip the perspective and frame our results thinking of the transition to the alternative state as a 'restoration', that brings the system in a preferred state. For instance, one may try to eradicate an invasive species, or promote the return of a species or vegetation that originally dominated the landscape. Importantly, the same principles hold for the backward shift, so if the ecosystem is initially in the state with low biomass, and one 'perturbs' the system by adding a patch with high biomass. In such situations, the 'no-recovery' results may correspond to successful restorations of parts of the landscape. A cascading 'collapse' would be a large-scale success, and 'recovery' would be a failure, as the effects of the local restoration effort do not last long. The same results then illustrate that depending on the tendency of species to spread (our dispersal rate) a sufficiently large scale of restoration efforts can be critically important, especially in homogeneous landscapes (van de Leemput *et al.* 2015). Importantly, the interpretation of 'recovery rate' (i.e. rate at which the system returns to the original state after a restoration attempt) as an indicator of resilience remains equally relevant, as it may be used to probe if a system may easily be restored or not. Areas with the lowest recovery rates may in that perspective be the most promising places for restoration efforts, and the effect of the perturbed initial patch on recovery rates may give an indication of the critical scale needed for successful restoration.

Prospects

The analysis of recovery rates in spatially extended ecosystems is an almost unexplored territory. Our results suggest a number of ways forward. It is easy to see the scope for prescribed replicated experiments along environmental gradients where the system is known to approach a critical transition. On small scales such as laboratory systems or herbaceous vegetation this may be quite feasible. For instance, strikingly clean results can been found in elegant experiments with yeast populations growing in a set of flasks where spatial interactions are simulated by manually dispersing yeast between flask cultures on a daily basis (Dai *et al.* 2013). On larger scales it may be possible to interpret the response to frequent human-induced or natural perturbations. For instance, remotely sensed recovery of tropical forests from wildfires or clearing could indicate spatial variation or long-term trends in resilience.

Also, on the theoretical side there is much scope for further exploration. We have only briefly touched upon the transient spatial expansion of a disturbance as an indicator of resilience. A related suggestion has been done for the slightly different situation of a press perturbation (e.g. a continuous local harvest of biomass instead of a one-time removal). Here recovery time is no relevant measure, as the system is not allowed to recover. Instead the size of the area impacted by the disturbed region, termed 'recovery length' indicates the resilience of the system (Dai *et al.* 2013).

Clearly, the combination of the spatial and temporal dimensions of the response to local perturbations contains most information. The two are not redundant, as the extent of spatial expansion carries information on spatial processes that cannot be inferred from the local response alone. Thus the combination may allow separating the relative importance of intrinsic dynamics and spatial interactions. Developing and testing indicators based on the spatio-temporal response may be an exciting and promising way forward.

Appendix A7

Appendix A7.1: Spatial extent of local strong disturbances in continuous landscapes as indicator of resilience

Our model simulations show that the recovery trajectory of a local perturbation in a continuous landscape can under certain conditions (i.e. low resilience and low dispersal) comprise several phases of recovery (see for example Figure 7.2c in the main text). Such recovery trajectories can be explained by an initial spatial expansion of the disturbance (see Movies A1). Figure A7.1a and b show the landscape-wide recovery trajectories for the same simulation in Figure 7.3c (main text). Figure A7.1b shows that the total biomass on the landscape decreases after the perturbation, but recovers eventually.

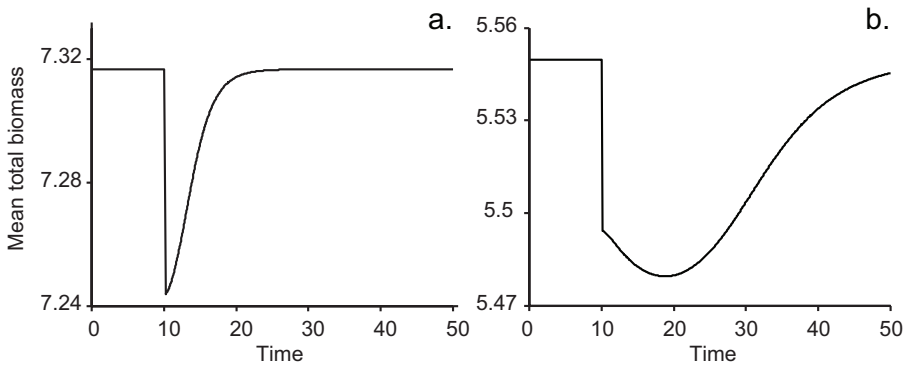

Figure A7.1. Landscape-wide recovery trajectories of a strong local disturbance by removing all standing biomass in an area comprising 1% of the landscape **a)** far (c =2.0), and **b)** close (c =2.55) to the transition in a continuous landscape with low dispersal (D = 2.5 m^2 day^{-1}).

We also calculated the size of the affected area of a local strong perturbation. This alternative measure is related to the concept of 'recovery length' which has been introduced as an indicator of system resilience by Dai *et al.* (2013). While the authors use a local *press perturbation*, we calculate the extent of spatial expansion of a local *pulse perturbation*. Our aim is to map the spatial expansion of a disturbance as the system is approaching a critical transition. For the calculations, we used a one-dimensional version of the model described in the main text (with L = 100 m, low dispersal D=2.5 m^{2}day^{-1}, and high dispersal D=12.5 m^2 day^{-1}, and a disturbance size of 5% of the landscape (= 5 m)). As a first measure, we monitored the size of the affected area at a specific time after the disturbance (Δt). The affected area is defined as the size of the area in which local biomass is below 90% of the biomass before the disturbance.

Our results show that the longer the time interval, the less detectable the recovery length far from the transition (Fig. A7.2a,c). For instance at Δt=20 days, changes in recovery length are detectable after harvest rate has crossed 2.4 g m^{-2} day^{-1}, which is close to the area of induced collapse (red area Fig. A7.2a,c). On the other hand, for short time intervals of Δt=5 days, recovery length is detectable far from the transition, however the differences between the extent of spatial expansion are small for different harvest rates. It is only at intermediate time intervals where changes in recovery length can be used as a detectable indicator. If that optimal time interval is known, the practical advantage of measuring spatial expansion at a specific time after the disturbance is that one has to visit the disturbed area only once. As a second measure, we determined the maximum size of the affected area during the recovery phase (Fig. A7.2b,d). This shows to be a good alternative for recovery rate as an indicator of system-wide resilience, especially if dispersal is low (Fig. A7.2b). However, in practice, similar to recovery rate, one needs to continuously monitor the entire recovery phase to get a good measure. The maximal spatial extent can however be a good indicator in ecosystems for which biomass decrease leaves a well-detectable trace (e.g. waste product).

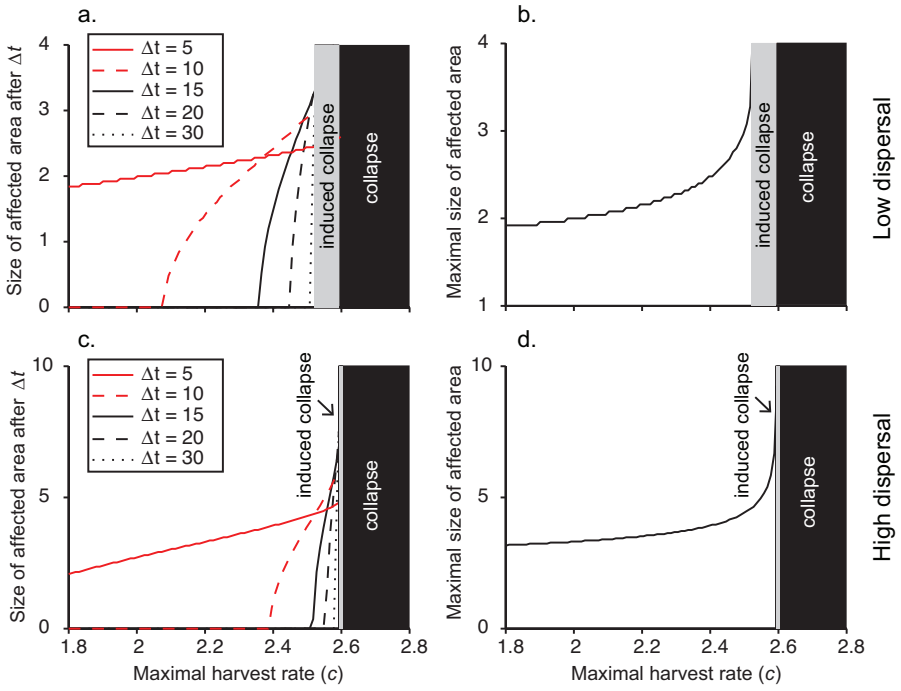

Figure A7.2. The size of the affected area after a local perturbation of 5 m, in a one-dimensional continuous landscape. If local biomass is below 90% of the biomass before the disturbance, the location is defined 'affected'. The left panels show the size of the affected area at a single point in time after the disturbance. The right panels show the maximal size of the affected area during the period after the disturbance. **a-b)** Low dispersal (D = 2.5 m^2 day^{-1}), **c-d)** High dispersal (D = 12.5 m^2 day^{-1}).

Appendix A7.2: Recovery rate of local disturbances

We experimented with large disturbances in continuous and patchy landscapes where the resource has a low dispersal rate. We induced a disturbance comprising 5% of the landscape with a dispersal rate of 2.5 m^2 day^{-1} in the continuous landscape (Fig. A7.3a), and a dispersal rate between nodes of 0.02 day^{-1} in the patchy landscape (Fig. A7.3b). Under these conditions the chances for inducing a collapse or having no recovery after a disturbance are high. Indeed, we found that the range of induced collapse in the continuous landscape considerably increased when compared to conditions of high dispersal but small-scale disturbance (Fig. 7.3c main text), or small-scale disturbance but low dispersal (Fig. 7.3e main text, Fig. A7.3a). Similarly, the range of induced collapse and no recovery in the patchy landscape considerably increased when compared to conditions of high dispersal but small-scale disturbance (Fig. 7.3d main text), or small-scale disturbance but low dispersal (Fig. 7.3f main text).

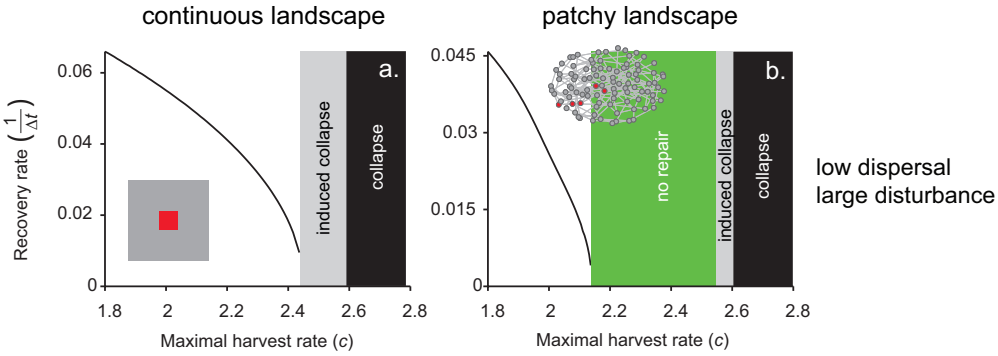

Figure A7.3. Recovery rate (as 1/recovery time) upon a large (5% of the landscape) local disturbance -a zero-biomass area in the middle of a homogeneous high-biomass landscape (indicated in red) as a function of harvest rate c up to the crossing of the critical transition in **a)** a continuous landscape with low dispersal rate ($D = 2.5$ m^2 day^{-1}), and **b)** a patchy landscape with low dispersal rate between patches ($f_d = 0.02$ day^{-1}). The disturbed area in panel a, and the disturbed patches in panel b are indicated in red. Note that in a continuous landscape (panel a), the large disturbance can induce a systemic collapse (grey area) far before the actual fold bifurcation point (black area). In a patchy landscape (panel b), the large disturbance may also induce a systemic collapse (grey area), but far before that point the disturbance leads to no recovery, i.e. partial collapse (green area).

We also experimented with local disturbance-recovery experiments in a heterogeneous landscape with variable size of the disturbed area and a high dispersal rate (Fig. A7.4). All parameters and simulations are the same as for Figure 7.4 in the main text, only the dispersal rate is high.

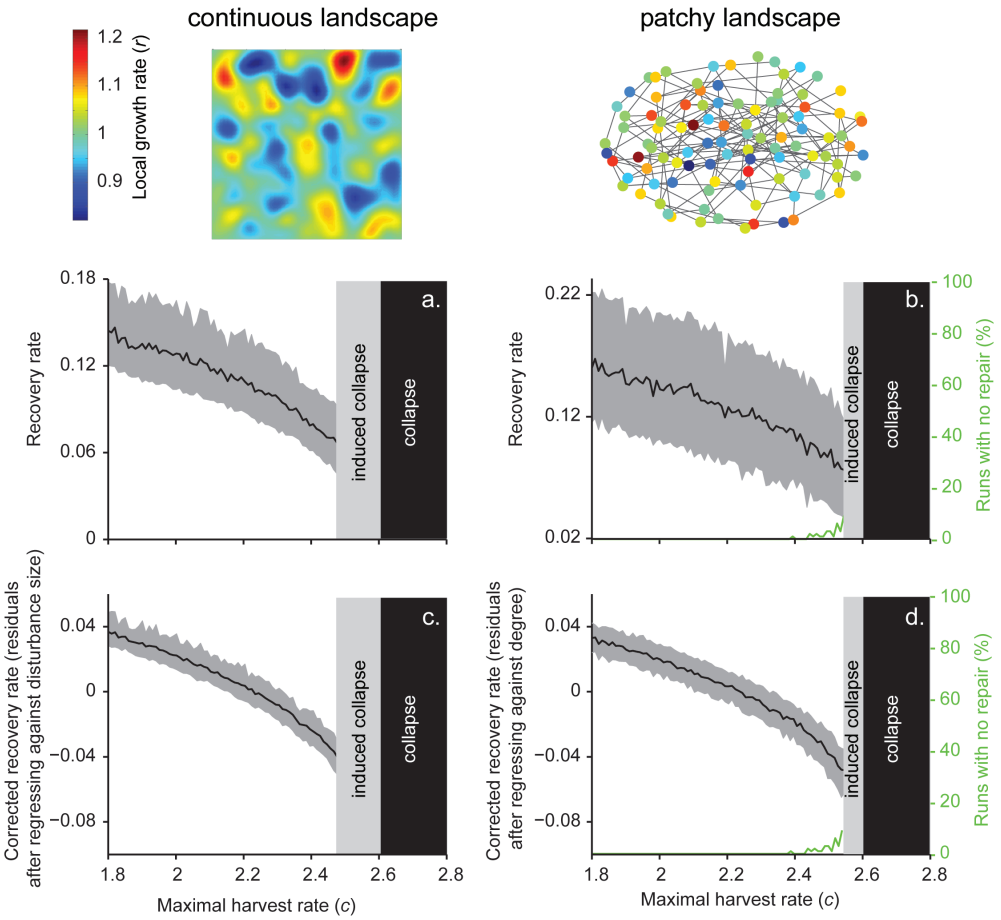

Figure A7.4. Effects of random disturbance experiments in landscapes with spatially heterogeneous conditions, and high dispersal. We randomly disturbed areas of different size on a continuous landscape and different patches in a patchy network for each level of resilience (in terms of maximal harvest rate) and measured recovery rates. **a-b)** Average recovery rates decrease in all situations as the system approaches the critical harvest rate for collapse. Black lines represent the average recovery rate, while the grey shaded lines show the 10th and 90th percentile, based on experiments per simulated harvest rate. In a patchy landscape (panel b), a small percentage of simulations show no recovery (green lines), which increases as the harvest rate increases. **c-d)** Average residual recovery rates after being corrected for the size of the disturbance (panel c), or the degree of the disturbed node (panel d). Note that the variance in recovery rates is lower after the correction.

Appendix A7.3: Recovery time after strong local disturbances in the presence of environmental stochasticity

We compared recovery time after a global weak disturbance to recovery time after a local strong disturbance in the presence of environmental stochasticity. We did this by adding environmental noise to the continuous landscape as a random normally distributed variable $E_t \sim N(0,\sigma^2)$ with standard deviation σ (0.8) applied every Δt (0.1 days) timesteps ($N_{i,t+\Delta t}=N_{i,t}+E_t$). Figure A7.5 (panels a, c) show that it is difficult to distinguish measurable changes in recovery time after a global but weak disturbance. Instead, a local strong disturbance is more easily distinguished from background stochasticity (Fig. A7.5b,d).

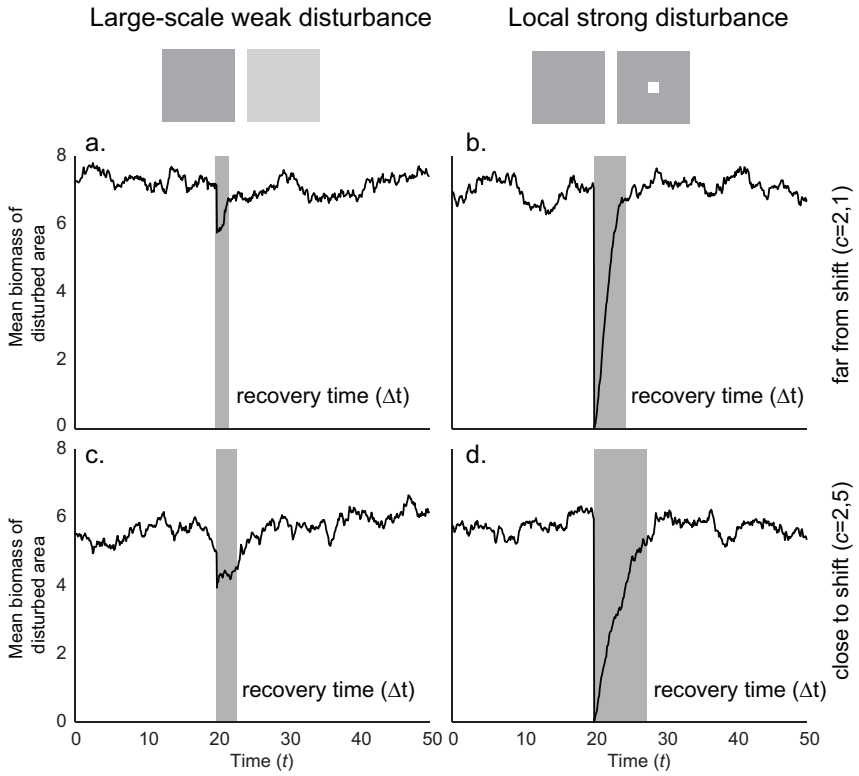

Figure A7.5. The effect of random fluctuations on system-wide and local disturbance-recovery experiments in a continuous landscape **a-b)** far from the fold bifurcation, and **c-d)** close to the fold bifurcation. Stochasticity in a homogeneous landscape may muffle the accuracy of the signal of a large-scale weak perturbation (panels a and c), while a local, strong perturbation can more easily be distinguished from background noise (panels b and d). For all simulations, we removed 2.5 % percent of the total biomass on the landscape, and dispersal rate was assumed to be high ($D = 12.5$ m^2).

Appendix A7.4: The role of dispersal, resilience and disturbance size on 'induced collapse' and 'no recovery' in spatially extended ecosystems

We explored how the three responses after a strong local disturbance we presented in the main text are affected by dispersal, resilience and disturbance size. For this, we simulated the overharvesting model on a square lattice of discrete patches where each patch was connected to its 4 neighbors. We did this as this version is a hybrid between the continuous and the patchy (network) landscapes and summarizes the dynamics of both landscape types. We assumed that all parameters were equal in all patches. Dispersal was defined as a local exchange between patches. We used a lattice with 50x50 patches.

$$N_{i,j}' = f(N) + d\left(N_{i+1,j} + N_{i-1,j} - 2N_{i,j}\right) + d\left(N_{i,j-1} + N_{i,j+1} - 2N_{i,j}\right)$$

We defined the three different model behaviors that we observed as presented in the main text: (1) recovery: the disturbed area returns to the pre-disturbed state, (2) no recovery: the disturbed area remains stable, and (3) induced collapse: the disturbed area expands gradually, pushing the whole system eventually to the alternative stable state. We mapped all different behaviors for a set of 25x100 parameter combinations of dispersal rate d, resilience (harvest rate c), and size of disturbance. The presented 2D bifurcation plots were sketched manually on the basis of the simulation results using an overlay graph.

We first checked which of these behaviors occur at different harvest rates and dispersal rates (Fig. A7.6a). The harvest rate affects the resilience (*sensu* Holling 1973) of the undisturbed state compared to the state in the disturbed patch. At high harvest rates it becomes more likely that a global shift to the perturbed state occurs ("induced collapse"), but there is no single critical harvest rate above which this always happens. More interesting is the effect of the dispersal. If dispersal is low, it becomes likely that the system neither recovers nor collapses as a consequence of the disturbance. This is because the landscape becomes similar to a patchy landscape (i.e. connectivity between cells is low): the exchange between the disturbed area and the neighboring undisturbed area is insufficient to cause a shift of either of them to the other state. As illustrated by our analysis, it is the interplay of resilience (in our case determined by the harvest rate) and dispersal that determines what will happen. At intermediate harvest rates, the probability of no recovery increases for the obvious reason that the resilience of both states is comparable. In addition to resilience and dispersal, the *size* of the disturbed area is also important in determining whether a disturbance will recover (Fig. A7.6b). In general, a larger size perturbation increases the probability of expansion to a systemic shift. Again, if dispersal is low, no recovery is more likely. An important overall result is that the probability of an

induced global collapse is highest at intermediate levels of dispersal (Fig. A7.6a,b). At low dispersal there are increased chances of no recovery. At higher dispersal the chances of recovery increase. This is because the disturbed area effectively interacts stronger with the neighboring area and the disturbed area is rapidly 'diluted' over the rest of the landscape.

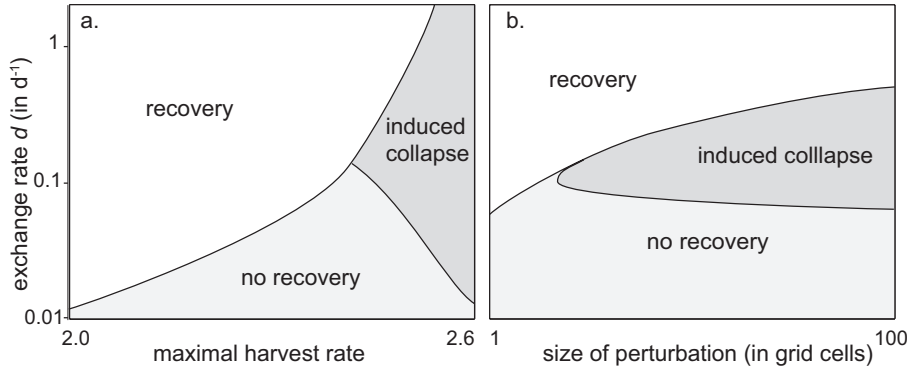

Figure A7.6. Recovery of local disturbance experiments in a lattice with local exchange between grid cells and their four neighboring cells. **a)** Combined effects of resilience (in terms of the maximal harvest rate (c)) and local exchange rate d (with a fixed perturbation size: 7x7 cells) **b)** Combined effects of perturbation size and local exchange rate d (with a fixed harvest rate c = 2.45 d^{-1}). Note that the dispersal rate is on a log scale.

Movies A7.1:

https://www.dropbox.com/sh/bubrdemy22o8blw/AACy1HIgvlW9CYHyfdMut3cRa?dl=0

Chapter 8

Critical slowing down as early warning for the onset and termination of depression

Ingrid A. van de Leemput, Marieke Wichers,
Angelique O.J. Cramer, Denny Borsboom,
Francis Tuerlinckx, Peter Kuppens,
Egbert H. van Nes, Wolfgang Viechtbauer,
Erik J. Giltay, Steven H. Aggen,
Catherine Derom, Nele Jacobs,
Kenneth S. Kendler, Han L.J. van der Maas,
Michael C. Neale, Frenk Peeters,
Evert Thiery, Peter Zachar,
and Marten Scheffer

Published in *Proceedings of the National Academy of Sciences* (PNAS):

van de Leemput IA, Wichers M, Cramer AOJ, Borsboom D, Tuerlinckx F, Kuppens P, van Nes EH, Viechtbauer W, Giltay EJ, Aggen SH, Derom C, Jacobs N, Kendler KS, van der Maas HLJ, Neale MC, Peeters F, Thiery E, Zachar P, Scheffer M. 2014. Critical slowing down as early warning for the onset and termination of depression. *Proc Natl Acad Sci USA* **111**: 87–92.

Abstract

About 17% of humanity goes through an episode of major depression at some point in their lifetime. Despite the enormous societal costs of this incapacitating disorder, it is largely unknown how the likelihood of falling into a depressive episode can be assessed. Here, we show for a large group of healthy individuals and patients that the probability of an upcoming shift between a depressed and a normal state is related to elevated temporal autocorrelation, variance, and correlation between emotions in fluctuations of autorecorded emotions. These are indicators of the general phenomenon of critical slowing down, which is expected to occur when a system approaches a tipping point. Our results support the hypothesis that mood may have alternative stable states separated by tipping points, and suggest an approach for assessing the likelihood of transitions into and out of depression.

Introduction

Depression is one of the main mental health hazards of our time. It can be viewed as a continuum with an absence of depressive symptoms at the low endpoint and severe and debilitating complaints at the high end (Hankin *et al.* 2005). (Throughout this manuscript, the term "depression" refers to this continuum of depressive symptoms.) The diagnosis Major Depressive Disorder (MDD) defines individuals at the high end of this continuum. Approximately 10 to 20% (Bijl *et al.* 1998) of the general population will experience at least one episode of MDD during their lives, but even subclinical levels of depression may considerably reduce quality of life and work productivity (Rodríguez *et al.* 2012). Depressive symptoms are therefore associated with substantial personal and societal costs (Kessler *et al.* 1994; Lopez *et al.* 2006). The onset of MDD in an individual can be quite abrupt, and similarly rapid shifts from depression into a remitted state, so-called sudden gains, are common (Aderka *et al.* 2012). However, despite of the high prevalence and associated societal costs of depression, we have little insight into how such critical transitions from health to depression (and vice versa) in individuals might be foreseen. Traditionally, the broad array of correlated symptoms found in depressed people (e.g. depressed mood, insomnia, fatigue, concentration problems, loss of interest, suicidal ideation etc.) was thought to stem from some common cause, much as a lung tumor is the common cause of symptoms such as shortness of breath, chest pain and coughing up blood. Recently, however, this common-cause view has been challenged (Cramer *et al.* 2010; Kendler *et al.* 2011; Borsboom *et al.* 2013). The alternative view is that the correlated symptoms should be regarded as the result of interactions of components of a complex dynamical system (Hayes and Strauss 1998; Huber *et al.* 1999; Heiby *et al.* 2003; Kendler *et al.* 2011). Consequently, new models of the etiology of depression involve a network of interactions between components, such as emotions, cognitions and behaviors (Cramer *et al.* 2010; Borsboom *et al.* 2013). This implies, for instance, that a person may become depressed through a causal chain of feelings and experiences, such as *stress → negative emotions → sleep problems → anhedonia* (Wichers *et al.* 2007; Borsboom *et al.* 2013; de Wild-Hartmann *et al.* 2013; Wichers 2014). However, the network view also implies that there can be positive feedback mechanisms between symptoms, such as *worrying → feeling down → more worrying* or *feeling down → engaging less in social life → feeling more down* (Bringmann *et al.* 2013). It is easy to imagine that such vicious circles could cause a person to become trapped in a depressed state.

The plausibility of this theoretical framework with regard to MDD is supported in at least four ways. First, intra-individual analyses of multivariate time series of variables related to MDD symptomatology show clear interactions between these

variables (Tzur-Bitan *et al.* 2012; Bringmann *et al.* 2013; Wichers 2014). Second, MDD symptoms display distinct responses to different life events (Keller *et al.* 2007; Cramer *et al.* 2012a) and are differently related to other external variables and disorders (Lux and Kendler 2010), which is consistent with a network view of interacting variables related to MDD symptomatology, but not with a classical disease model that postulates the existence of a common cause (Cramer *et al.* 2012b). Third, when asked how MDD symptoms are related, clinical experts report a dense set of causal relations between them (Kim and Ahn 2002; Borsboom *et al.* 2013). Fourth, using recently developed self-report methods, it has been shown that individuals with elevated symptom levels typically report causal interactions between their symptoms, including those of MDD (Frewen *et al.* 2012, 2013).

Thus, there is ample evidence to support the thesis that MDD is characterized by causal interactions between its 'symptoms'. From dynamical systems theory it is known that positive feedback loops among such causal interactions can cause a system to have alternative stable states (Scheffer 2009). This has profound implications for the way a system responds to change. For example, gradually changing external conditions may cause a system to approach a tipping point. Close to such a point the system typically loses resilience, that is, increasingly small perturbations may suffice to cause a shift to an alternative stable state (Scheffer 2009). In the mood system, characterized by the 'mood state' of an individual that may range from normal to severe depression, stressful conditions may bring the system to such a fragile state (Patten 2013). For example, a chronically unpleasant working situation may reduce resilience of the 'normal state' by precipitating insomnia and other related symptoms. Then, only a slight additional perturbation (e.g. an unpleasant phone call with mother-in-law) may be enough to trigger a chain of symptoms that causes the system to shift from a stable 'normal state' into an alternative 'depressed state'.

In this paper, we analyze time series of four emotions as the observed variables of the mood system in healthy persons and depressed patients providing support for the view that the mood system can have tipping points. Specifically, we show indicators of critical slowing down (Scheffer *et al.* 2009), which have recently been shown to be linked to tipping points in a range of complex systems (Dakos *et al.* 2008; Carpenter *et al.* 2011; Scheffer *et al.* 2012a). These indicators can be used as early warning signals that can help assess the likelihood that an individual will go through a major transition in mood. Before moving to the empirical evidence, we briefly introduce the generic phenomenon of critical slowing down, using a simple model of the mood system as an illustration.

Results and Discussion

Theory of critical slowing down

Marked transitions from one dynamical regime to a contrasting one are observed in complex systems ranging from oceans, the climate and lake ecosystems to financial markets. Such 'regime shifts' (Carpenter 2003) can simply be the result of a massive external shock, or stepwise change in the conditions. However, it is also possible that a slight perturbation can invoke a massive shift to a contrasting and lasting state. It is intuitively clear that this can happen to an object such as a chair or a ship when it is close to a tipping point, but complex systems such as the climate or ecosystems can also have tipping points (Scheffer 2009). The term tipping point in such systems is informally used to refer to a family of catastrophic bifurcations in mathematical models (Strogatz 1994), which in turn are simplifications of what characterizes the stability properties of real complex systems (Scheffer 2009).

As tipping points can have large consequences, there is much interest in finding ways to know whether a catastrophic bifurcation is near. In principle this could be computed if one has a reliable mechanistic model. However, we have little hope of having sufficiently accurate models for complex systems such as lakes or the climate, let alone psychiatric disorders. A recent alternative approach is to look for indicators of the proximity of tipping points that are generic in the sense that they do not depend on the particular mechanism that causes the tipping point. A possibility that has attracted much attention is that across complex systems, the vicinity of a tipping point may be detected on the basis of a phenomenon known as 'critical slowing down' (Strogatz 1994; van Nes and Scheffer 2007). Specifically, critical slowing down happens as the dominant eigenvalue, characterizing the return rate to equilibrium upon small perturbations, goes to zero in tipping points related to zero-eigenvalue bifurcations. On an intuitive level this can be understood from a ball-in-a-cup diagram (Fig. 8.1a-b). As the slope represents the rate of change, close to the tipping point where the basin of attraction becomes shallower, return to equilibrium upon small perturbations will become slower. Although critical slowing down has been known for a long time in mathematics, the idea of using it as a way to detect tipping points in real complex systems is unique, and slowing down at tipping points has only recently been demonstrated experimentally in living systems (Veraart *et al.* 2012; Dai *et al.* 2012).

For most systems it is either impractical or unethical to experimentally perturb them in order to find out if they are close to a tipping point. However, any system, including mood, is continuously subject to small natural perturbations. One can

imagine the effect as a combination of direct impacts on the ball (in models this corresponds to so-called additive noise) and fluctuations in the shape of the stability landscape (multiplicative noise). A range of modeling studies, laboratory experiments and field studies now suggests that under such stochastic conditions, critical slowing down typically causes an increase in the variance and temporal autocorrelation of fluctuations in the system elements (Carpenter and Brock 2006; Dakos *et al.* 2008; Drake and Griffen 2010; Carpenter *et al.* 2011; Veraart *et al.* 2012; Dai *et al.* 2012). Besides, in a network of fluctuating elements, one expects an increase in cross-correlation between elements that will shift together (Chen *et al.* 2012). This implies the possibility that elevated variance and correlation may be used as indicators of critical slowing down and therefore as early warning signals that may reveal the loss of resilience in the proximity of a tipping point (Scheffer *et al.* 2009).

Minimal models of mood

Critical slowing down will occur independently of the specific mechanisms involved in bringing about a tipping point. However, to illustrate how indicators of critical slowing down might signal the proximity of a tipping point in mood, we use a simple dynamical model, based on the classical and well-studied Lotka-Volterra equations (see methods). This is about the simplest way of modeling positive and negative interactions between dynamically varying entities such as populations of organisms. Specifically, we model four emotions as variables of the mood system (reflecting the four quadrants of the affective circumplex: cheerful, content, sad and anxious; see Russell (2003)), and assume that emotions with the same 'valence' (positive or negative) promote each other, while emotions of opposite valence tend to compete (Appendix A8, Fig. A8.1). This is of course an overly simple representation of the mood system, but consistent with the empirical observations that same-valenced emotions tend to augment and opposite-valenced emotions tend to blunt each other (Pe and Kuppens 2012; Bringmann *et al.* 2013), and that this dynamic interplay has relevance for the course of depression (Wichers *et al.* 2012). Also on theoretical grounds, it stands to reason that emotions that show large overlap in terms of their underlying components (such as appraisals; see Pe and Kuppens (2012)) would augment each other, while emotions that diverge in these components, would counteract each other (Pe and Kuppens 2012). Given suitable parameter settings, the model has two alternative stable states over a range of conditions: one state dominated by strong positive emotions, the 'normal state', and the second dominated by strong negative emotions, the 'depressed state' (Appendix A8, Fig. A8.1).

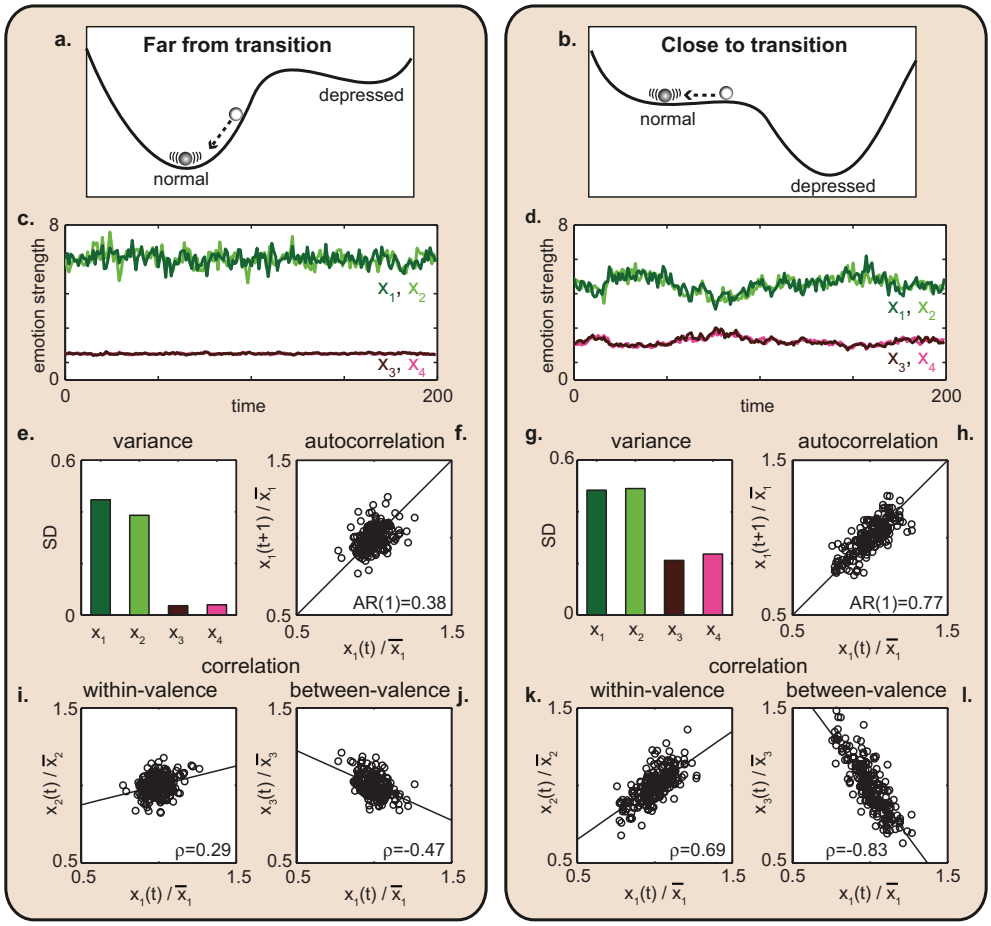

Figure 8.1. Model simulations illustrating generic indicators of proximity to a tipping point from a normal to a depressed state. The stability of a healthy person may become more fragile close to a transition towards depression, which can intuitively be understood from a ball-in-a-cup diagram **(b versus a)**. This fragility would lead to critical slowing down in a system with tipping points between alternative stable states, illustrated by model simulations. Under a permanent regime of stochastic perturbations on the strength of each emotion **(c and d)**, slowing down near the tipping point results in higher variance (SD = standard deviation) in emotion strength **(g versus e)**, higher temporal autocorrelation (AR(1) = lag-1 autoregression coefficient) in emotion strength **(h versus f)**, and stronger correlation (ρ = Pearson correlation coefficient) between emotion strength of emotions with the same valence **(k versus i)**, and between emotions with different valence **(l versus j)**. Positive emotions are represented by x_1 and x_2, and negative emotions by x_3 and x_4. Parameters: left panels $r_3 = r_4 = 0.5$, right panels $r_3 = r_4 = 1.18$.

To mimic the stochastic environment, we expose the model to a regime of random perturbations (Fig. 8.1c and d). The resulting fluctuations in the strength of the four modeled emotions show signs of critical slowing down as expected from the generic theory (Scheffer *et al.* 2009). Specifically, close to the tipping point towards depression, the fluctuations have a higher variance (Fig. 8.1g versus e), and temporal autocorrelation (Fig. 8.1h versus f). Also, the cross-correlations between the strength

of the modeled emotions become stronger in the vicinity of the tipping point (Fig. 8.1k and l versus i and j). Note that positive correlations between emotions within the same valence will tend towards 1 (Fig. 8.1k), whereas negative correlations between opposed valence emotions will tend towards -1 (Fig. 8.1l). Similarly, once the model system is in the depressed state, we see elevated variance and correlations close to the critical point of recovery (Appendix A8, Fig. A8.2).

Although the view of mood as consisting of interactions between its various components (e.g. cheerful and sad) fits well with recent theories regarding the pathology of MDD (Cramer *et al.* 2010; Kendler *et al.* 2011), one could argue that such mood variables (unlike for instance populations of animals) are not on equal par with true physical quantities. Rather, emotions such as feeling cheerful or anxious seem to be the result of complex interactions between biology (including genetics), previous life experiences and current contextual influences. We will probably never be able to assess and understand the full complexity of this system. However, psychologists work with emotions because they are thought to reflect meaningful aspects of the mood system (Watson *et al.* 1988; Russell 2003). In fact, the subjective experience component of emotions is thought to function as a monitoring tool for organisms to detect important changes in the complex mood system (Russell 2003). Given that emotions are unitless subjective measures that are not governed by any laws of conservation, one could wonder if they should still be expected to reflect critical slowing down if that underlying system approaches a tipping point. To explore this, we made a model of a complex network of interactions between 20 variables, representing (in principle) objectively measurable components of mood (e.g. elements ranging from neurotransmitter and hormone concentrations to physical activity modes and social interactions). We created the model such that it has tipping points. Then, we mimicked the strength of emotions as indirect indicators of the state of the highly complex network by using Principal Components (principal component analysis (PCA) axes) (Appendix A8.1). Analyses of this model illustrate that critical slowing down remains clearly reflected in the PCA based indicators (Appendix A8.1, Figs. A8.3-5).

Clearly, many other dynamical models of the mood system could be conceived. However, the examples we analyzed may serve to illustrate the general phenomenon that indicators of critical slowing down can be found at tipping points independently of the precise underlying complex mechanisms involved, and on the way the variables are measured (Scheffer *et al.* 2009, 2012a; Dakos *et al.* 2012a). Thus, even if we cannot attain a complete understanding of the complex array of mechanisms that are involved in regulating mood, we may expect that if transitions in mood are related to the proximity of tipping points, the likelihood of such shifts to happen should be evident in indicators of critical slowing down.

Patterns in recorded mood dynamics

To explore whether mood dynamics do indeed display such indications of critical slowing down prior to tipping points in depression, we analyzed time series of four emotions (cheerful, content, sad and anxious) as observed variables of the overall 'mood state' obtained through the Experience Sampling Method (ESM, see methods), in which subjects have monitored, for each emotion, their position on an emotional scale during five to six consecutive days. We refer to this as their 'emotion score' at a certain time. We studied a general population sample that varies in the development of depressive symptoms over time. Some subjects shifted upward along the continuum of depression and some downward. A fraction of this group (13.5%), showed a transition from a normal state to a DSM-IV clinical diagnosis of MDD. We investigated in this general population sample whether indicators of critical slowing down are associated with elevated risk of future shifts towards depression. In addition, we analyzed ESM data from a population sample of depressed patients to see whether critical slowing down is related to the probability of upcoming recovery (for sample descriptions see Appendix A8, Table A8.1).

Both temporal autocorrelation (i.e. the autoregression coefficient) and variance of fluctuations in emotion scores were higher in individuals with upcoming transitions (Fig. 8.2 and Appendix A8, Tables A8.2 and A8.3). For an impending worsening of depressive symptoms, these signals are strongest for negative emotions (Fig. 8.2a and c), whereas for an upcoming improvement in depressive symptoms in individuals with current MDD, these signals are strongest for positive emotions (Fig. 8.2b and d) compared to the other emotions (Appendix A8, Fig. A8.6). Also, correlations between emotion scores were consistently stronger for individuals who experienced a future transition upward on the continuum of depression (Fig. 8.3a and c) as well as in depressed patients who were moving downward on the continuum within the study period (Fig. 8.3b and d) (Appendix A8, Table A8.4). Note that the main structure of our model of positive and negative interactions is consistent with the data: emotions of opposite valence affect each other negatively whereas emotions with the same valence are positively correlated (Fig. 8.3).

The rise in temporal correlations and cross-correlations is likely a more direct indicator than the rise in variance. This is because change in variance can be confounded by several mechanisms (Dakos *et al.* 2012b). For instance, a trend in variance may be related to a trend in the mean. Indeed, such a coupling of variance to mean may partly explain the trends we observe in upcoming emotions (Appendix A8, Fig. A8.6). However, an analysis of trends in the coefficients of variation illustrates that especially in the general population, rising variability in all emotions may be an observable indicator of critical slowing down associated with an elevated risk of an impending depression (Appendix A8, Fig. A8.7). Also, one could

argue that the observed effect in variance might be an effect of increased external perturbations ('noise' in the model), and not a result of critical slowing down. As temporal autocorrelation and cross-correlations are independent of the means as well as the amplitude of noise (Dakos *et al.* 2012b), the trends in correlations may be our most robust indicator of critical slowing down.

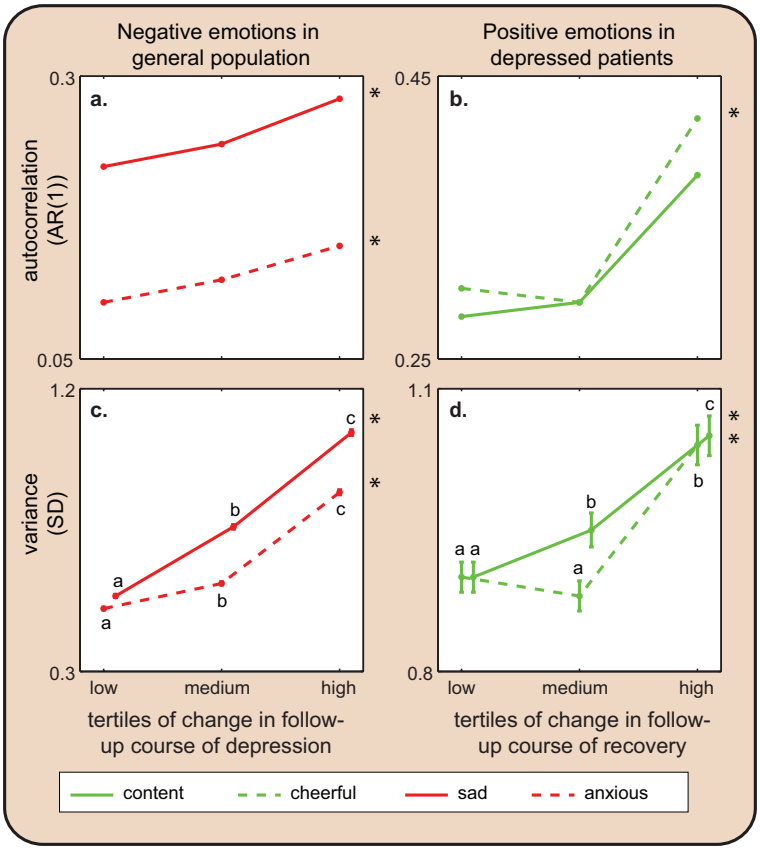

Figure 8.2. Temporal autocorrelation and variance of emotion scores as a function of future symptoms. Increasing autocorrelation (AR(1) = mean lag-1 autoregression coefficient) **(a-b)** and variance (SD = mean standard deviation) **(c-d)** of negative emotions according to tertiles of development of future depressive symptoms in a general population (n = 535) **(left panels)**, and of positive emotions according to tertiles of future recovery in depressed patients (n = 93) **(right panels)**. For temporal autocorrelation (panels a-b), we present data according to tertiles of change in follow-up course for illustrative purposes only, however, note that in the statistical analyses continuous variables were used. Asterisks indicate a significant upward trend in temporal autocorrelation (positive interaction effect of future symptoms: $p < 0.05$). For variance (panels c-d), error bars represent standard errors (SEs). Note that the SEs in panel c are very small. Asterisks indicate an overall significant upward trend in variance (overall tests: $p < 0.05$). Mean values represented by different letters within emotions are significantly different (post-hoc tests: $p < 0.05$).

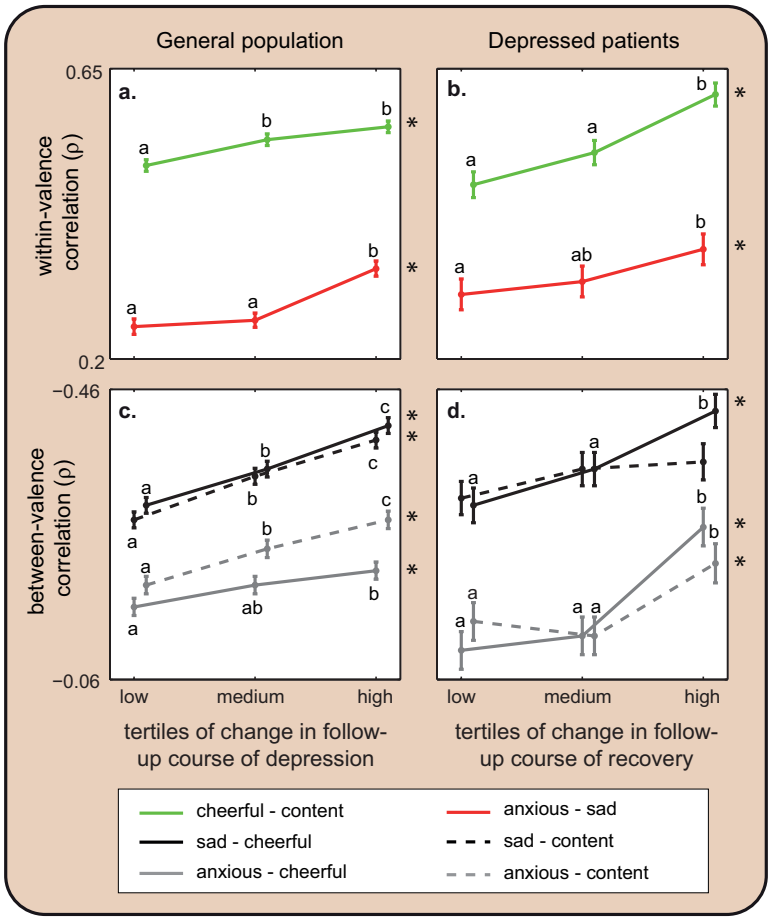

Figure 8.3. Correlations between emotion scores as a function of future symptoms. Strengthening correlations between emotions of the same valence **(a-b)**, and between emotions of different valence **(c-d)** according to tertiles of the development of future depressive symptoms in a general population (n = 535) **(left panels)**, and to tertiles of future recovery in depressed patients (n = 93) **(right panels)**. Error bars represent standard errors (SEs). Asterisks indicate an overall significant strengthening trend in correlation (overall tests: $p < 0.05$). Mean values represented by different letters within emotions are significantly different (post-hoc tests: $p < 0.05$).

Taken together, our results suggest that there is an elevated chance of upcoming shifts between a depressed and a normal mood state in persons that show indications of critical slowing down in their emotion scores. This is consistent with the idea that such transitions tend to happen when a subject is close to a tipping point. The relationship between elevated temporal correlations and upcoming transitions we detected is also consistent with independent earlier studies, showing that 'emotional inertia' (slower rates of change in emotion scores) is associated with future transition into a more depressed state (Kuppens *et al.* 2010, 2012). Moreover, the corresponding view of depression as an alternative stable state is in line with the

finding of reinforcing feedbacks between emotions, and with the sudden character of shifts to depression and recovery (Aderka *et al.* 2012).

Importantly, this body of evidence does not imply that *all* persons would have such tipping points. It seems more likely that while some persons abruptly shift between a normal and a depressed state, for others, certain positive feedback mechanisms (e.g. *feeling down → engaging less in social life → feeling more down*) remain too weak to cause alternative stable states. Such persons would be expected to move more gradually between a normal and a depressed state, experiencing intermediate states to be stable as well. Indeed, dynamical systems with tipping points will often respond more smoothly if the positive feedback responsible for this feature becomes weaker (Appendix A8, Fig. A8.8). Hints of slowing down may still be detected for persons without alternative stable states in case their mood responds relatively strongly to a gradual change in conditions. This is because some slowing down (albeit not full-blown critical slowing down, where recovery rate upon perturbation reaches zero) is expected across a wide range of situations where systems respond relatively sensitively around a threshold (Kéfi *et al.* 2012).

Implications

Clearly, the effects of stressors may differ widely between persons and contexts depending on a complex set of interacting factors shaped by genes and history (e.g. genetic variants, epigenetic regulation, early life events, and connection strength between neurons which are changed by experience). This makes it unlikely that we would ever be able to obtain accurate individual predictions of risk for relapse or recovery based on a mechanistic insight into the mood regulation system. However, if the mood system, as our results suggest, shows signals of critical slowing down, we may use this generic feature to improve our ability to anticipate clinically relevant mood shifts, even in the absence of a full understanding of the complex underlying system that is responsible for such shifts. Clearly such mechanistic insight may be important to develop better treatment strategies. However, when it comes to risk stratification, the indicators of critical slowing down may be a powerful and independent addition to our clinical toolkit.

This has important implications for treatment. Mood data suitable for analysis of critical slowing down are now easy to assess and monitor, for instance through an app on a smartphone. Furthermore, web-applications are able to provide user-friendly feedback to patients and clinicians on the patient's critical slowing down patterns. The ability to anticipate transitions (e.g. a shift upward on the continuum of depression for a person at risk, or a shift downward on the continuum for a patient with current MDD) could prove beneficial in terms of the timing and magnitude

of treatment interventions. This information may prove especially valuable in optimizing health care and in reducing mental health care costs. Hence, in terms of understanding and treating psychiatric disorders like depression, the potential gains associated with our approach are considerable. Therefore, our central hypothesis – that symptomatology like depression should be conceptualized as alternative states of complex dynamical systems – is not an endpoint; rather, it should mark the beginning of novel research programs.

Materials and Methods

Samples. We analyzed data from i) the general population (females; n = 621) and ii) depressed patients eligible for treatment (n = 118, for sample description see Appendix A8, Table A8.1). The first sample was recruited from a population-based sample of the East-Flanders Prospective Twin Survey (Belgium). The data of depressed patients came from two studies. Both included baseline Experience Sampling Method (ESM) measurements followed by an intervention (either a combination of pharmacotherapy and supportive counseling or allocation to either imipramine or placebo) and follow-up assessments of depressive symptoms. For details on inclusion criteria and final set of participants see supplementary methods (Appendix A8.2). A total of 535 individuals from the general population and 93 depressed patients were included in the final analyses.

Experience Sampling Method. In order to calculate early warning signals for transition, the four emotions were measured repetitively and prospectively using the ESM. This structured diary technique prospectively assesses individual experience in the context of daily life (Csikszentmihalyi and Larson 1987; Myin-Germeys *et al.* 2009). Subjects received a digital wristwatch and a set of ESM self-assessment forms collated in a booklet for each day. The wristwatch was programmed to emit a signal ('beep') at an unpredictable moment in each of ten 90-min time blocks between 07:30 and 22:30, on five or six consecutive days, depending on the study. After each beep, subjects were asked to fill out the ESM self-assessment forms, including emotion scores on seven-point Likert scales. This resulted in a maximum of 50 or 60 measurements, depending on the study.

Design. All participants underwent a baseline period of ESM. In the depressed patients follow-up course of depression was measured with the Hamilton Depression Rating Scale (HDRS-17) at 6-8 weeks following start of treatment. In the general population the Symptom Checklist 90 (SCL-90-R) was completed at baseline and at 4 follow-up measurements, approximately 3 months apart from each other. Follow-up depression score was based on the average of the four follow-up measurements.

Analyses. The aim was to analyze whether the hypothesized early warning signals (autoregression coefficients, variance and correlation between emotions as derived from the repeated ESM measures) are associated with follow-up course of depression in both samples. Analyses were performed for four emotions which were a priori chosen to represent each quadrant of the affective space defined by valence and arousal (Russell 2003): feeling cheerful (positive valence, high arousal), content (positive valence, low arousal), anxious (negative valence, high arousal), and sad (negative valence, low arousal). Data on these four emotions were available in both samples. Because the ESM data have a hierarchical structure (in which the four emotions are clustered within measurement moments (about 50 to 60 'beeps') and measurement moments are clustered within persons), a statistical model needs to be used that deals appropriately with the hierarchical structure. These models are known as multilevel models. Two different models were used (see below). All multilevel models included modeling of random intercept and slope. Data were analyzed using STATA 12.1 (StataCorp 2009) and most analyses were replicated independently in R (R Development Core Team 2005). See supplementary methods for details on heteroscedasticity and normality (Appendix A8.2). The R code is published online (http://www.pnas.org/content/suppl/2013/12/04/1312114110.DCSupplemental/sd01.pdf).

Multilevel model 1: Autocorrelation. To extract the information on autocorrelation, we analyzed each emotion separately. A multilevel model was set up in which the emotion score at time t (e.g. anxious at time t) is predicted by the emotion score at time t-1 (e.g. anxious at time t-1). The regression coefficient of the emotion scores at time t-1 on emotion scores at time t is the autoregression coefficient. In the model we additionally included an interaction between the emotion scores at time t-1 and follow-up course of depression. This means that in this model the size of the autoregression coefficient for a person depends on the continuous follow-up course of depression score. Thus, the autoregression coefficient (and henceforth the autocorrelation) may differ between people with a different follow-up course of depression score. In this way, we are able to test whether persons whose depression score shows a large change over time, will have a higher autoregression coefficient while persons whose depression score shows little change, will have a lower autoregression coefficient (this being the phenomenon of critical slowing down). However, the follow-up in course of depression score is probably not the only variable that is related to differences in autoregression coefficients between persons. A multitude of other variables may contribute to the individual differences in the autoregression coefficient. For this reason, a person-specific deviation is added to the regression coefficient of the person which is drawn from a normal distribution with zero mean and a to-be-estimated variance, which makes the model formally a

multilevel regression model. (Note that also the intercept of the regression model is assumed to be random.) In this way, we are able to examine the association between autoregression coefficients of the four emotions and follow-up course of depression. This multilevel approach enables us to assess this so-called interaction effect between emotion scores at time t-1 and the follow-up course of depression, while respecting the hierarchical structure of the data. Note that for the purpose of visualization tertiles of depression scores were used in Figures 8.2 and A8.6 (see multilevel model 2 for the definition of the tertile groups).

Multilevel model 2: Variance and correlations. In this second multilevel model, we examined the extent to which variance and correlations differ with follow-up course of depression. In contrast to the autocorrelation analysis, we first clustered the individuals into discrete tertile groups according to follow-up course of depression score and used these tertile groups in our analysis (instead of the continuous score). Those individuals in the general population with the lowest level of depressive symptoms (33%) at follow-up were classified as group 1, those in the middle (33%) as group 2, and the highest 33% as group 3. Similarly, patients with the lowest decrease in symptoms over course of treatment were classified as group 1, those in the middle as group 2, and those with the highest decrease as group 3. Ideally, we would have liked to model the variances and correlations in some (non-)linear way as a function of the covariate (future depressive symptoms) in the context of a multilevel model directly, but appropriate models for such an analysis have not been fully developed and tested yet. In the analyses, all four emotions were simultaneously considered. This creates a three-level structure: emotions nested in measurement moments nested in persons. For each tertile group, a multilevel regression model was fitted with emotion score as the dependent variable and dummy codes for the four emotions as independent variables. Random effects corresponding to these dummy-coded variables were added at the person and at the measurement level. These random effects were allowed to have different variances for the four items and their correlations were estimated freely. Therefore, no structure was imposed on the model, making this a saturated model (i.e. the model with the most complex covariance structure possible for the data at hand; (Hox 2010)). The estimated variation in these random effects was used to estimate variance in emotion scores at the measurement level. Correlations between these random effects were used to estimate correlations between emotions at the measurement level. Wald-type tests were used to test for overall differences in the variances and correlations between the three groups.

The dynamical systems model. We analyzed a minimal model, simulating interactions between four modeled emotions in a person as a stochastic differential equation (inspired by the Lotka-Volterra models, as in van Nes *et al.* (2004)):

$$\frac{dx_i}{dt} = \left(r_i + \varepsilon_r\right)x_i + \sum_j^4 C_{i,j}x_j x_i + \mu$$

where x_1 and x_2 signify the strength of positive emotions (such as cheerful and content), and x_3 and x_4 the strength of negative emotions (such as sad and anxious). The maximum rate of change of the positive emotions, r_1 and r_2, was set to 1, while the maximum rate of change of the negative emotions, r_3 and r_4, was assumed to be stress-related, ranging between 0.5 (low stress) and 1.5 (high stress). The matrix C represents the interaction network between the emotions.

$$C = \begin{pmatrix} -0.2 & 0.04 & -0.2 & -0.2 \\ 0.04 & -0.2 & -0.2 & -0.2 \\ -0.2 & -0.2 & -0.2 & 0.04 \\ -0.2 & -0.2 & 0.04 & -0.2 \end{pmatrix}$$

Each term of this interaction network describes the strength and direction of the interaction. Negative terms mean that these emotions suppress each other and positive terms imply enhancement. The maximum rate of change (r_i) of each emotion was subjected to a noise term (ε_r) representing short-term fluctuations in the rate of change of each emotion. ε_r is represented by a Gaussian white noise process of mean zero and intensity σ^2/dt (σ=0.15). Effectively, this means that the system is subject to multiplicative noise. Independent of the strength of the emotions their value increases by a fixed amount (μ=1) to prevent emotion levels to be close to zero. The model was solved using a Euler-Maruyama scheme in Matlab.

Appendix A8

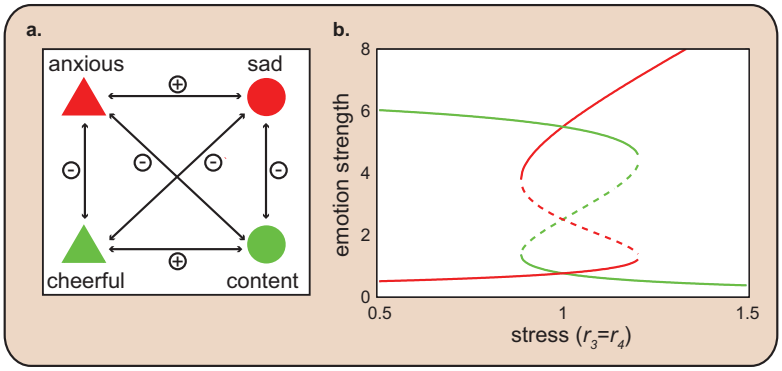

Figure A8.1. The model. **a)** A graphical representation of our simple dynamical model of four emotions. Emotions with the same valence have a positive effect on each other, while emotions of different valence have a strong negative effect on each other. **b)** The stability properties of the deterministic part of the model (i.e. without noise) change if stress levels, represented by the growth rate of the two negative emotions (r_3 and r_4), change. Green lines represent positive emotions (x_1 and x_2), red lines represent negative emotions (x_3 and x_4). Solid lines represent stable states, and dashed lines unstable states. Far from the tipping point, at low stress levels, the network has only one stable state with high levels of positive emotions, and low levels of negative emotions. If stress levels increase, the network has two stable states: a 'normal state', and a 'depressed state', while at even higher stress levels, the system reaches a tipping point, at which the normal state disappears, and only one stable depressed state remains. Note that once the system is in the alternative depressed state, stress levels need to be decreased tremendously to trigger a backward shift.

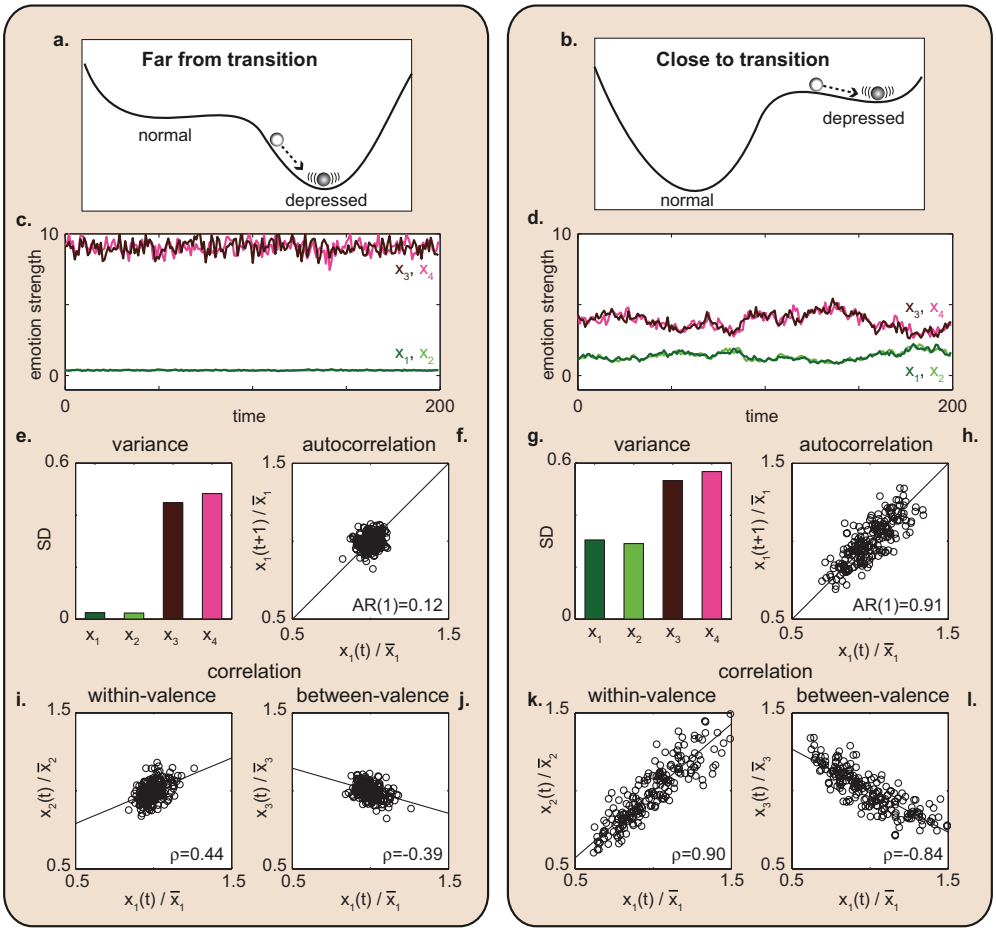

Figure A8.2. Model simulations illustrating generic indicators of proximity to a tipping point from a depressed to normal state. Our model shows that the generic early warning signals that signal the proximity of a shift from a normal state towards a depressed state are also valid for the backward shift from a depressed state towards recovery. In that case, the stability of a depressed person may become more fragile close to the transition towards recovery **(b versus a)**. Under a permanent regime of stochastic perturbations **(c and d)**, slowing down near the tipping point results in higher variance (SD= standard deviation) **(g versus e)**, higher temporal autocorrelation (AR(1)= lag-1 autoregression coefficient) **(h versus f)**, and stronger correlation (ρ= Pearson correlation coefficient) between emotions with the same valence **(k versus i)**, and between emotions with different valence **(l versus j)**. Positive emotions are represented by x_1 and x_2, and negative emotions by x_3 and x_4. Parameters: left panels r_3= r_4=1.5, right panels r_3= r_4=0.9.

Appendix A8.1. Network model of latent variables

We developed a network model that serves as a hypothetical representation of the complex neurobiological system underlying the mood of an individual person. The network consists of twenty interacting latent variables. Each network variable represents one (unknown, but in principle measurable) component of the neurobiological system of that individual. Emotions are not represented directly as variables but are computed as principal components of simulation results of clusters of the network. In contrast with the simple model in the main text, they do not interact directly with each other. We demonstrate that such indirect indicators show the same behaviour in terms of early warning signals.

The network model was also based on the Lotka-Volterra model, describing the dynamics of interacting variables, representing the components of the neurobiological system:

$$\frac{dN_i}{dt} = r_i N_i + \sum_j^{20} C_{i,j} N_j N_i + \varepsilon_N + \mu$$

where N_i represents the strength of network variable i, r_i represents the maximum rate of change of network variable i, C represents a matrix of interactions between network variables, μ represents a small continuous increase of the strength of a network variable (independent of their state) (μ=1), and ε_N is the stochastic part of the model represented by a Gaussian white noise process of mean zero and intensity σ^2/dt (σ=0.1) (i.e. additive noise).

We parameterized the network such that the system has two main clusters: network variables that are in the same cluster have a positive effect on each other, while variables of different clusters have a negative effect. The interaction strengths $C_{i,j}$, as well as the maximum rate of change (r_i), were randomly drawn from two uniform distributions. Positive interactions between network variables within a predefined cluster ranged from 0.003 to 0.005. Similarly, the negative interactions between variables of different clusters were drawn in a range between -0.002 and -0.004. The maximum relative rates of change (r_i) of the individual variables were assumed to be stress-dependent, following:

$$r_i = r_{0,i} + r_\rho \rho_i$$

Maximum rates of change of network variables in a state without stress (r_0) are set to differ between the two clusters. In cluster 1 r_0 ranges from 0 to 1, while in cluster 2 r_0 ranges from 0 to 0.5. Stress is assumed to influence the maximum rates by a factor r_ρ. Each network variable has a different sensitivity (ρ) to this stress factor. The sensitivity of variables in cluster 1 is assumed to be 0, while the sensitivity of variables in cluster 2 ranges from 0 to 1. For these parameter settings, this complex network has alternative stable states (Fig. A8.3).

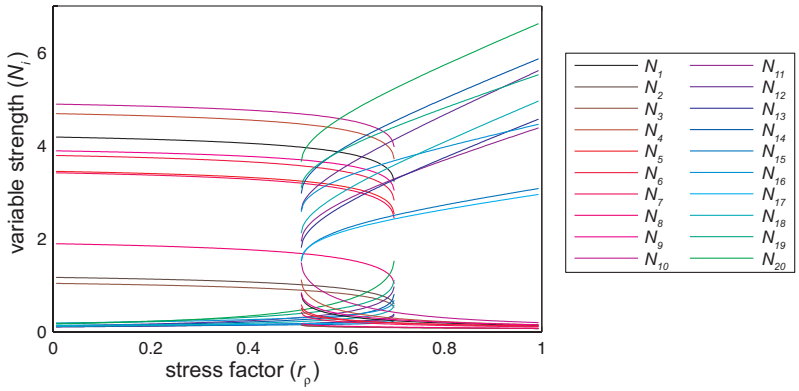

Figure A8.3. Response of the network model to stress. The stability properties of the deterministic part of the model (i.e. without noise) change if stress levels, represented by r_p, change. Solid lines represent stable states, unstable states are not depicted. Far from the tipping point, at low stress levels, the network has only one stable state with one dominant cluster of network elements: the 'normal state'. If stress levels increase, the network has two stable states. Next to the 'normal state', another cluster can be dominant under the same conditions: the 'depressed state'. At even higher stress levels, the system reaches a tipping point, at which the normal state disappears, and only one stable depressed state remains.

In order to define four relevant indicators of dynamics in the network, we assume that each emotion is influenced by the dynamics of a subcluster of the network: each positive emotion is determined by seven of the ten variables of cluster 1, while each negative emotion is determined by seven of the ten variables of cluster 2 (Fig. A8.4). The subclusters that define the new variables contain overlapping network variables. Therefore, we simulated two time series with a different dominant cluster. We used each time series to perform two PCA analyses on seven variables of the dominant cluster. We used the first principal component ($PC1$) of each analysis to define the dynamics of the four new variables (x). For instance, the first variable (x_1) is defined as follows:

$$x_1 = \sum_j^7 PC1_j N_j$$

We simulated the dynamics of the complete model, and used the data of the four variables as input for the early warning signal analysis, as in the main text.

Importantly, in our network model, the four variables representing emotion strength (x) do not directly affect each other, they are simply indicators of the dynamics of a complex underlying network (Fig. A8.4). Our analyses show that the same early warning signals are expected if the variables are indirect indicators of a complex underlying system with tipping points between alternative stable state (Fig. A8.5). The predictions of critical slowing down are thus robust against this oversimplified way of representing emotions in the model of the main text.

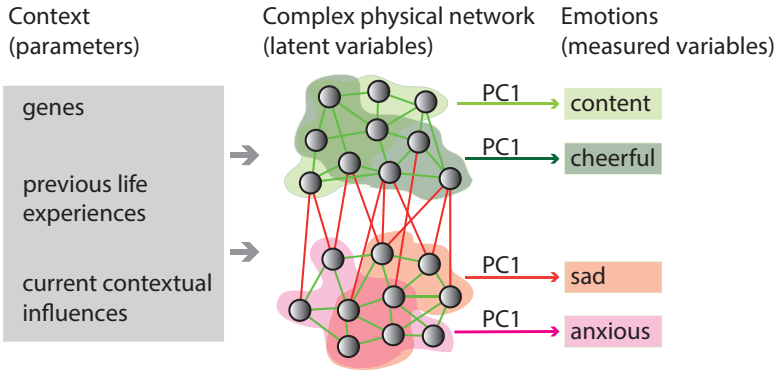

Figure A8.4. Illustration of the relation between the context, the complex physical network model (e.g. elements ranging from neurotransmitter and hormone concentrations to physical activity modes and social interactions) and the four newly defined variables. Note that the four variables are indirect indicators of parts of the complex system.

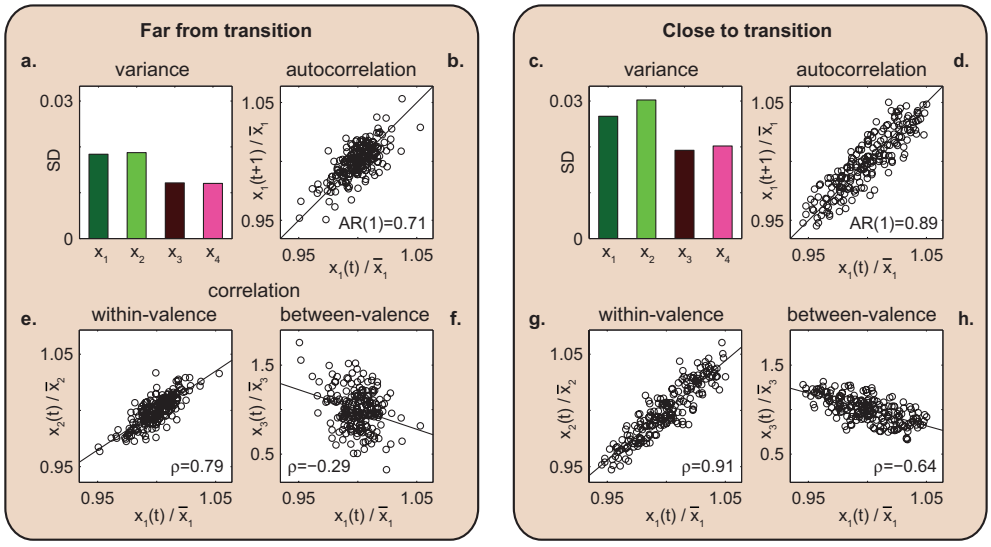

Figure A8.5. Early warning signal analysis of model simulations of the four indirect indicators of the complex network. As for the four-component model with direct interactions, under a permanent regime of stochastic perturbations, slowing down near the tipping point results in higher variance (SD = standard deviation) **(a versus c)**, higher temporal autocorrelation (AR(1) = lag-1 autoregression coefficient) **(b versus d)**, and stronger correlation (ρ = Pearson correlation coefficient) between emotions with the same valence **(e versus g)**, and between emotions with different valence **(f versus h)**. Positive emotions are represented by x_1 and x_2, and negative emotions by x_3 and x_4. Parameters: left panels r_ρ=0.1, right panels r_ρ=0.68.

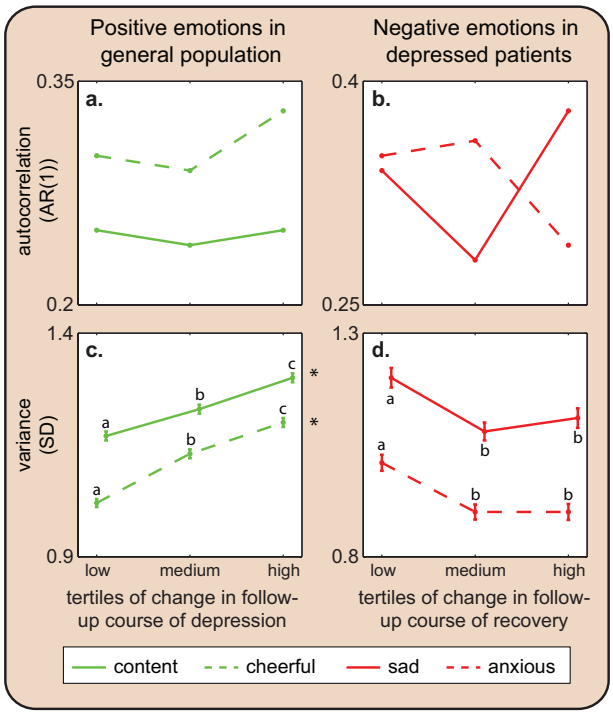

Figure A8.6. Temporal autocorrelation and variance as a function of future symptoms. Increasing autocorrelation (AR(1) = mean lag-1 autoregression coefficient) **(a and b)** and variance (SD = mean standard deviation) **(c and d)** of positive emotions according to tertiles of development of future depressive symptoms in a general population **(left panels)**, and of negative emotions according to tertiles of future recovery in depressed patients **(right panels)**. For autocorrelation (panels a and b), we present data according to tertiles of change in follow-up course for illustrative purposes only, however, note that in the statistical analyses continuous variables were used. There are no significant trends in autocorrelation (positive interaction effect of future symptoms: $p < 0.05$). For variance (panels c and d), error bars represent standard errors (SEs). Note that variance of negative emotions in the depressed population goes down with future recovery. This may be explained by differences in the mean (see Fig. A8.7). Asterisks indicate an overall significant upward trend in variance (overall tests: $p < 0.05$). Mean values represented by different letters within emotions are significantly different (post-hoc tests: $p < 0.05$).

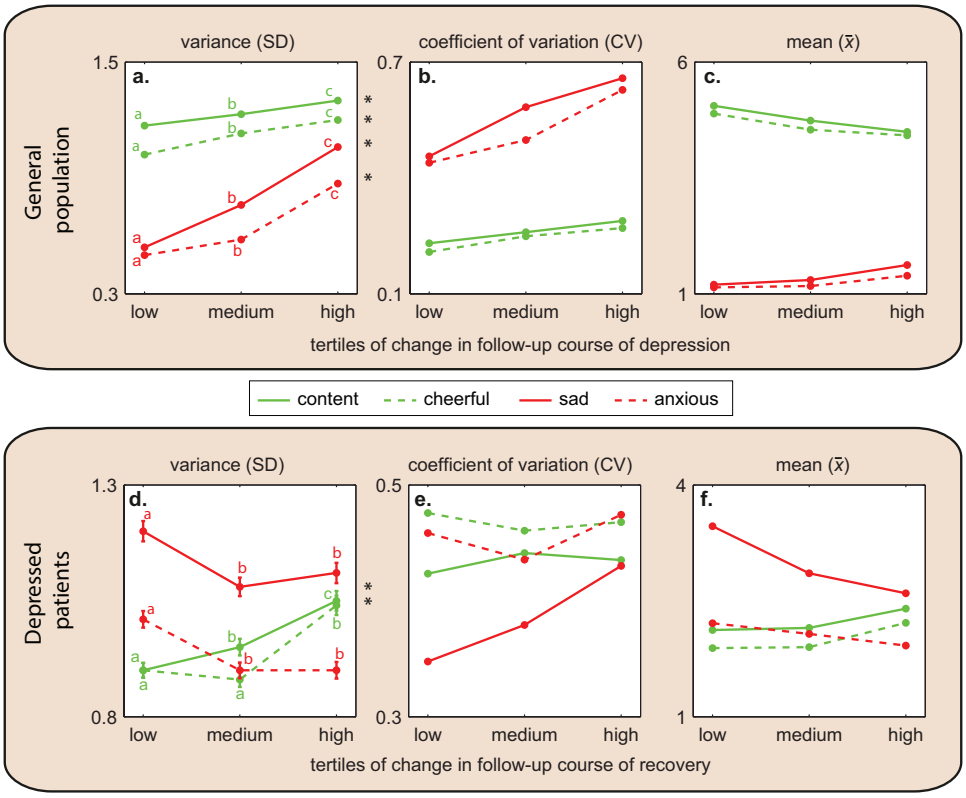

Figure A8.7. The effect of critical slowing down on variance can be confounded by a change in the means. Variance ($SD =$ mean standard deviation) **(a and d)**, coefficient of variation $\left(CV = SD / \bar{x}\right)$ **(b and e)**, and mean affect level $\bar{x}$ **(c and f)** according to tertiles of development of future depressive symptoms in a general population (n = 535) **(upper panels)**, and according to tertiles of future recovery in depressed patients (n = 93) **(lower panels)**. Note that for the general population, higher variance in individuals with higher future recovery is robust if corrected for the means, while for the depressed population, both higher variance of positive emotions, and lower variance of negative emotions, are not robust.

Appendix A8.2. Supplementary methods

Inclusion criteria and final set of participants. Inclusion criteria in both studies were a DSM-IV diagnosis of major depressive disorder (MDD), age between 18 and 65 years, and a baseline score of ≥ 18 on the 17-item HDRS. Patients using psychotropic medications, other than low dose benzodiazepines, were excluded (Barge-Schaapveld *et al.* 1995; Peeters *et al.* 2003). Of the 621 individuals of the general population sample, only 610 participated in ESM. Of this group 31 were excluded because of too few valid ESM measurements (Delespaul 1995). Forty-four participants had missing data either at baseline or follow-up resulting in 535 individuals. In the depressed sample 118 were eligible to participate. Of those, six were excluded because of too few valid ESM measurements and 1 because of unavailability of emotion ratings in

ESM. Additionally, 1 had missing baseline data and 17 had missing follow-up HDRS measurements. This resulted in a final sample of 93 participants.

Heteroscedasticity and normality. The current samples have 535 and 93 groups (individuals) with on average 37 and 45 observations, respectively, per individual. When checking our data, two main assumptions of the model did not hold for some of the analyses: homoscedasticity at level 1 (i.e. the variability of residuals within persons may differ from one person to the other) and normality (i.e. the distribution of scores within a person may not be normal). Violations of these assumptions were found through the inspection of residual plots. Estimates in the models may be slightly downwardly biased if the number of groups (level 2 units) is less than 50 and the normality assumption is violated. According to Hox (2010) at least 50 level 2 groups (in this case individuals) are needed with 20 or more observations within each group in order to accurately estimate standard errors in case of violation of the normality assumption. Thus, according to Hox (2010), the current sample sizes are adequate to yield accurate estimations of standard errors.

In order to test the potential influence of heteroscedasticity, all analyses were repeated with robust standard errors (using the so-called Huber–White or sandwich standard errors). These analyses yielded similar results and conclusions.

Estimating the potential function. We have considered the possibility to directly estimate the potential function. However, although the methodology is developed for a long time series (see e.g. Wagenmakers *et al.* (2005) and Brillinger (2007)), the extension to our case is far from trivial. The reason is that the data consist of a sample of quite short time series, which do not yield enough information for estimating a person-specific potential function that is flexible enough (i.e. not restricted to a specific parametric form). In principle, this would be possible by setting up the estimation problem in the aforementioned multilevel modeling framework. However, this is a completely new methodology that has not been developed, let alone been sufficiently tested. Therefore, we have refrained in this paper from estimating the potential function.

Appendix A8.3. Individual and group responses

All people differ in their response to changing conditions and in their underlying emotional vulnerability. For each individual the dynamic interplay between emotions may differ. For example, some individuals quickly become anxious if something happens that makes them sad, while others don't have a strong connection between these two emotions (Wigman *et al.* 2013). This may explain why some people slowly glide into a depression, while others shift much more suddenly and unexpectedly (Fig.

A8.8). The result of the complex interplay between the multiple different emotional states people experience may thus differ from individual to individual and may impact on moment and timing of transition. We can hypothesize that the critical moment and speed with which a system may shift to another level of depressive symptoms is different per individual. When data of many different individuals are grouped together we expect –*at group level*- early warning signals to be associated with a dimensional change in depressive symptoms (since every system has its own point to shift), which is a reason for not categorizing by diagnosis status. This also illustrates a second reason: we do not necessarily expect that transition moments coincide with man-made arbitrary DSM-IV criteria. For some individuals critical shifts may occur at subclinical levels while for other individuals shifts occur to clinical levels of depression. As explained above each individual likely has his/her own mood set points and thresholds for tipping points, and some may even have no thresholds at all, but simply a smooth response to changing conditions. The results of the study support this view on transitions since indicators of critical slowing down predicted dimensional transitions towards higher or lower levels of depressive symptoms.

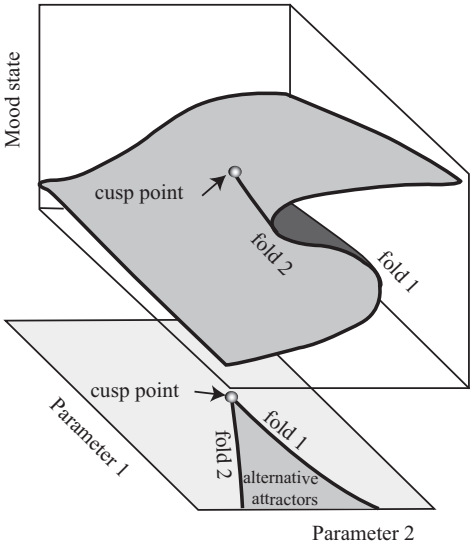

Fig. A8.8. The response of a dynamical system to a stressor (e.g. parameter 2) may be smooth or catastrophic depending on the strength of a positive feedback (e.g. parameter 1). The cusp point defines the parameter settings at which the system changes from smooth to catastrophic. The fold bifurcations define the parameter settings at which the system changes from two alternative stable states to one.

Table A8.1a. The socio-demographic and depression-related characteristics for the general population sample.

General population sample (n = 535)			
	Mean (SD) or percentage	n (individuals) N (observations)	
Age	27.6 (7.8)	n = 534	
Female gender	100%	n = 535	
No/only primary school education	1%	n = 4	
Secondary school education only	1%	n = 6	
Intermediate vocational education	34%	n = 184	
College/University	64%	n = 341	
Baseline SCL-90-R (item average)	1.44 (0.51)	n = 535	
Average follow-up SCL-90-R (item average)	1.47 (0.48)	n = 535	
Baseline average rating (1-7) of *cheerful*	4.63 (0.86)	n = 535	N = 19,752
Baseline average rating (1-7) of *content*	4.77 (0.86)	n = 535	N = 19,660
Baseline average rating (1-7) of *anxious*	1.22 (0.38)	n = 535	N = 19,673
Baseline average rating (1-7) of *sad*	1.35 (0.52)	n = 535	N = 19,732

Average follow-up SCL-90-R per tertile (low, medium or high follow-up score)	low: 1.08 (0.06) n = 182	medium: 1.33 (0.09) n = 177	high: 2.02 (0.48) n = 176
Baseline average rating (1-7) of *cheerful* per tertile of follow-up SCL-90-R score	4.90 (0.90)	4.54 (0.80)	4.43 (0.81)
Baseline average rating (1-7) of *content* per tertile of follow-up SCL-90-R score	5.07 (0.85)	4.73 (0.81)	4.51 (0.83)
Baseline average rating (1-7) of *anxious* per tertile of follow-up SCL-90-R score	1.13 (0.31)	1.16 (0.24)	1.38 (0.49)
Baseline average rating (1-7) of *sad* per tertile of follow-up SCL-90-R score	1.18 (0.43)	1.30 (0.41)	1.59 (0.62)

Table A8.1b. The socio-demographic and depression-related characteristics for the depressed patient sample.

Depressed patients (n = 93)		
	Mean (SD) or percentage	n (individuals) N (observations)
Age	41.7 (9.9)	n = 93
Female gender	40%	n = 93
No/only primary school education	19%	n = 18
Secondary school education only	27%	n = 25
Intermediate vocational education	39.8%	n = 37
College/University	10.8%	n = 10
Baseline HDRS-17 total score	24.0 (3.7)	n = 93
Follow-up HDRS-17 total score	12.5 (6.8)	n = 93
Baseline average rating (1-7) of *cheerful*	1.96 (0.92)	n = 93 N = 4.250
Baseline average rating (1-7) of *content*	2.19 (1.03)	n = 93 N = 4.270
Baseline average rating (1-7) of *anxious*	2.03 (1.40)	n = 93 N = 4.275
Baseline average rating (1-7) of *sad*	3.00 (1.32)	n = 93 N = 4.282
Intervention following baseline: -combination of pharmacotherapy and supportive psychotherapy -imipramine (as part of a trial) -placebo (as part of a trial)		 n = 43 n = 23 n = 27

Average follow-up HDRS-17 per tertile of change in follow-up HDRS-17 score (low, medium or high reduction in symptoms)	low: 19.1 (3.5) n = 33	medium: 12.2 (4.4) n = 32	high: 5.7 (3.4) n = 28
Baseline average rating of *cheerful* per tertile of change in follow-up HDRS-17 score	1.87 (0.77)	1.90 (0.82)	2.15 (1.15)
Baseline average rating of *content* per tertile of change in follow-up HDRS-17 score	2.09 (0.92)	2.17 (0.94)	2.32 (1.24)
Baseline average rating of *anxious* per tertile of change in follow-up HDRS-17 score	2.17 (1.50)	1.97 (1.31)	1.93 (1.43)
Baseline average rating of *sad* per tertile of change in follow-up HDRS-17 score	3.51 (1.34)	2.79 (1.14)	2.62 (1.35)

Table A8.2. Regression analysis in which the interaction effect represents the extent to which autoregression coefficients increase with increased follow-up change in depressive symptoms.

Autocorrelation				
	General population		Depressed patients	
	Beta-coefficient of interaction effect size[α]	p-value	Beta-coefficient of interaction effect size[β]	p-value
Cheerful	0.014	0.537	0.008	0.017
Content	-0.007	0.738	0.006	0.100
Anxious	0.060	0.029	-0.002	0.662
Sad	0.065	0.024	0.005	0.135

α: follow-up average SCL-90-R depression score X 'emotion' moment (t-1) on 'emotion' moment (t)
β: decrease in HDRS-17 score from baseline to follow-up X 'emotion' moment (t-1) on 'emotion' moment (t)

Table A8.3a. The overall significance tests for differences between variances across the three tertile groups for the general population and the depressed patients.

Variance									
	General population								
	Low FU symptoms		Medium FU symptoms		High FU symptoms		Overall Wald test		
	Coeff	SE	Coeff	SE	Coeff	SE	χ^2	df	p-value
Cheerful	1.02	0.009	1.13	0,01	1.20	0.010	165.52	2	< 0.001
Content	1.17	0.010	1.23	0,01	1.30	0.010	68.13	2	< 0.001
Anxious	0.50	0.004	0.58	0,005	0.87	0.008	1761.48	2	< 0.001
Sad	0.54	0.005	0.76	0,007	1.06	0.009	2623.37	2	< 0.001
	Depressed patients								
	Low decrease in FU symptoms		Medium decrease in FU symptoms		High decrease in FU symptoms		Overall Wald test		
	Coeff	SE	Coeff	SE	Coeff	SE	χ^2	df	p-value
Cheerful	0.90	0.016	0.88	0.016	1.04	0.021	41.41	2	< 0.001
Content	0.90	0.016	0.95	0.018	1.05	0.021	31.92	2	< 0.001
Anxious	1.01	0.018	0.90	0.017	0.90	0.018	23.56	2	< 0.001
Sad	1.20	0.022	1.08	0.020	1.11	0.022	17.16	2	< 0.001

Table A8.3b. P-values of the post-hoc Wald tests for differences between variances across the three tertile groups for the general population and the depressed patients.

Variance			
	General population		
	Low vs Medium FU symptoms	Low vs High FU symptoms	Medium vs High FU symptoms
Cheerful	< 0.001	< 0.001	< 0.001
Content	< 0.001	< 0.001	< 0.001
Anxious	< 0.001	< 0.001	< 0.001
Sad	< 0.001	< 0.001	< 0.001
	Depressed patients		
	Low vs Medium decrease in FU symptoms	Low vs High decrease in FU symptoms	Medium vs High decrease in FU symptoms
Cheerful	0.337	< 0.001	< 0.001
Content	0.049	< 0.001	< 0.001
Anxious	< 0.001	< 0.001	0.883
Sad	< 0.001	0.005	0.278

Table A8.4a. The overall significance tests for differences between correlations across the three tertile groups for the general population and the depressed patients.

Correlation									
	General population								
	Low FU symptoms		Medium FU symptoms		High FU symptoms		Overall Wald test		
	Coeff	SE	Coeff	SE	Coeff	SE	χ^2	df	p-value
Anxious-sad	0.25	0.012	0.26	0.011	0.34	0.012	34.13	2	< 0.002
Cheerful-content	0.50	0.009	0.54	0.009	0.56	0.009	22.19	2	< 0.001
Anxious-cheerful	-0.16	0.012	-0.19	0.012	-0.21	0.012	10.20	2	0.006
Anxious-content	-0.19	0.012	-0.24	0.012	-0.28	0.012	26.54	2	< 0.001
Sad-cheerful	-0.30	0.011	-0.35	0.011	-0.41	0.011	44.89	2	< 0.001
Sad-content	-0.28	0.011	-0.34	0.011	-0.39	0.011	51.52	2	< 0.001

	Depressed patients								
	Low decrease in FU symptoms		Medium decrease in FU symptoms		High decrease in FU symptoms		Overall Wald test		
	Coeff	SE	Coeff	SE	Coeff	SE	χ^2	df	p-value
Anxious-sad	0.30	0.024	0.32	0.024	0.37	0.024	5.09	2	0.078
Cheerful-content	0.47	0.020	0.52	0.019	0.61	0.018	25.79	2	< 0.001
Anxious-cheerful	-0.10	0.026	-0.12	0.026	-0.27	0.026	25.34	2	< 0.001
Anxious-content	-0.14	0.026	-0.12	0.026	-0.22	0.027	8.19	2	0.017
Sad-cheerful	-0.30	0.024	-0.35	0.023	-0.43	0.023	16.82	2	< 0.001
Sad-content	-0.31	0.023	-0.35	0.023	-0.36	0.025	2.20	2	0.332

Table A8.4b. P-values of the post-hoc Wald tests for differences between correlations across the three tertile groups for the general population and the depressed patients.

Correlation			
	General population		
	Low vs Medium FU symptoms	Low vs High FU symptoms	Medium vs High FU symptoms
Anxious-sad	0.294	< 0.001	< 0.001
Cheerful-content	0.001	< 0.001	0.225
Anxious-cheerful	0.107	0.001	0.112
Anxious-content	0.002	< 0.001	0.032
Sad-cheerful	0.002	< 0.001	< 0.001
Sad-content	< 0.001	< 0.001	< 0.001
	Depressed patients		
	Low vs Medium decrease in FU symptoms	Low vs High decrease in FU symptoms	Medium vs High decrease in FU symptoms
Anxious-sad	0.478	0.027	0.129
Cheerful-content	0.075	< 0.001	0.001
Anxious-cheerful	0.694	< 0.001	< 0.001
Anxious-content	0.659	0.024	0.007
Sad-cheerful	0.164	< 0.001	0.008
Sad-content	0.249	0.168	0.787

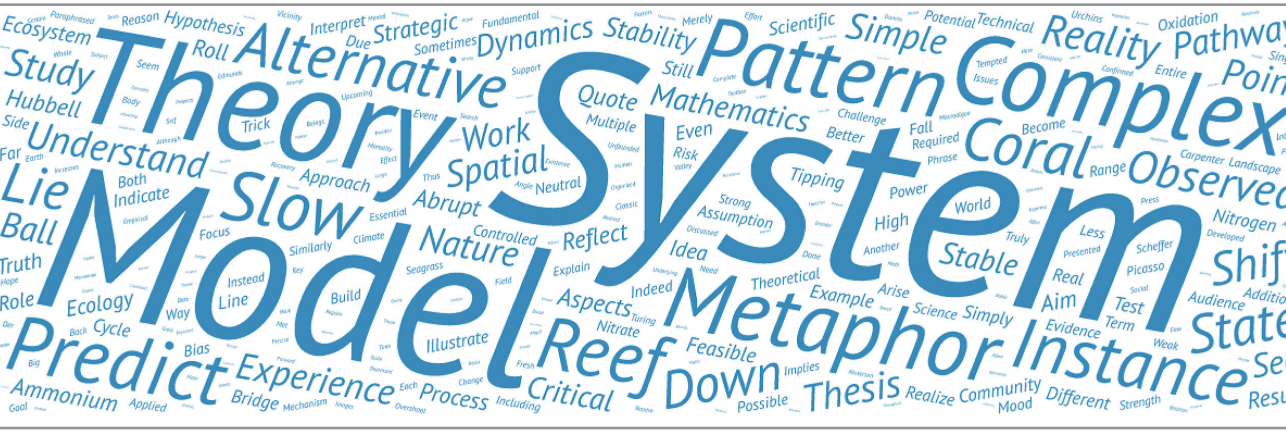

Chapter 9

Synthesis

Ingrid A. van de Leemput

Challenges of studying complexity

"*Art is a lie that makes us realize the truth.*" – Pablo Picasso

Throughout this thesis I used simple non-linear dynamical models (strategic models) to obtain insights into the stability of complex systems. I have presented some examples in which the abstract world of math can provide a fresh angle to the study of complex systems, mainly by providing search images for patterns in real systems. I have contributed to the theoretical toolbox for the anticipation of critical transitions (**chapters 5-7**), and elucidated multiple factors controlling dynamics of three real-world complex systems: the nitrogen cycle (**chapter 2**), the coral reef ecosystem (**chapter 3 and 4**), and the mental state of human beings (**chapter 8**). Each chapter reflects an attempt to isolate a key property of the complex behavior, in order to get a better understanding of the system as a whole. I used strong simplifications of reality including strategic models, metaphors, and analogies to point to patterns that mark certain aspects of the behavior of complex systems. I now take a step back and consider strengths and limitations of this approach. I also take a step forward reflecting on the prospects of gaining a better understanding of complex systems ranging from the earth to our body. The central theme I address is the tension between the complexity of the systems I studied and simplicity of the models and metaphors I have used as tools. The take home message I hope to confer can be summarized paraphrasing the above Picasso quote as "*Models are a lie that can help to make us realize the truth.*"

Simple models as theories

"*It can scarcely be denied that the supreme goal of all theory is to make the irreducible basic elements as simple and as few as possible without having to surrender the adequate representation of a single datum of experience*" – Albert Einstein 1934

Commonly paraphrased as: "*A scientific theory should be as simple as possible, but no simpler*".

While the above quote of Einstein might be fit for theories aimed for accurate prediction or simulation, here I address another important role of theories based on oversimplified models for the development of scientific understanding. Sometimes, the purpose of a theory is to investigate the simplest possible hypothesis one can think of, with the aim to identify discrepancies between the (over-)simplification and the real world. A classic example is the neutral theory of biodiversity of Stephen Hubbell (Hubbell 2001). Neutral theory assumes equivalence between members of an ecological community, implying that biodiversity arises at random (Hubbell

2001). Hubbell's theory has been highly criticized, and many articles showed its failure to capture the complexity of ecological communities in nature (Mcgill 2003). One can argue that the theory is just wrong. However, as a theory it functions as a working null-hypothesis, with testable predictions. As mentioned by Rosindell *et al.* (2012), the theory is about improving understanding by making simplifying assumptions and seeing what can be explained with the resulting models. In that context, neutral theory is useful as a foundation for other theories and models.

The theoretical models of spatially extended systems with local alternative stable states presented in this thesis (**chapters 6 and 7**) are over-simplifications of reality as well. Similar to Hubbell's neutral theory, the predicted dynamics function as a null-hypothesis for large-scale ecosystems with alternative stable states. However, the assumptions of spatial homogeneity and random dispersal are obviously rarely met in nature, still the notion of a Maxwell point is very important in practice, for instance for predicting the effect of restoration measures. Including more details in such simple models can sometimes produce fundamentally different dynamics. For instance, applied to seagrass dynamics, the theory for homogeneous conditions would predict abrupt shifts from complete seagrass cover to bare sea floor, but studies have shown that grazing of waterfowl tends to lead to spatial structuring of sea grass, and that this causes the shift from high to low seagrass cover to become gradual rather than abrupt (van der Heide *et al.* 2012).

Sometimes discrepancies between an oversimplification and reality reveal essential assumptions. An example is the nitrogen cycle pathway model in **chapter 2**. The *fundamental model* simply aimed at simulating thermo-dynamically and ecologically feasible nitrogen pathways. Interestingly, the fundamental model predicted high competitive strength for two ammonium oxidation pathways: anaerobic ammonium oxidation (anammox) using nitrate instead of nitrite, and ammonium oxidation to the level of dinitrogen gas (see **Appendix A2**). A closer look at these pathways revealed why they could be absent in nature. The activation energy of ammonium is high, so a pathway is only feasible if an ammonium molecule can react at a one-to-one ratio with a reactive chemical species (Strous *et al.* 1999; Dosta *et al.* 2008) (see **chapter 2**). After adding this new assumption to the fundamental model, it strikingly predicts all of the dominant pathways in the nitrogen cycle. In addition, two other unexpected pathways were predicted to be thermodynamically and ecologically feasible: 1) complete ammonium oxidation to nitrate (comammox), and 2) nitrite dismutation to nitrate and dinitrogen gas. No obvious reason could be found why these pathways have not been observed in nature. Strikingly, in December 2015, one of the two predicted pathways, complete ammonium oxidation to nitrate, was discovered as an abundant, but overlooked microbial pathway in nature (Daims *et al.* 2015; van Kessel *et al.* 2015).

This recent discovery illustrates the potential strength of extremely simple models for ecology. However, mostly the role of simple strategic models as presented in this thesis is more modest. Such models can serve to find potential explanations for observed patterns that would not easily arise from pure intuition. Their very nature implies that they capture only some aspects of reality. Starting from the incomplete representation of reality, we can detect deviations between their predictions and observations that put us on the track of additional aspects that may be important.

The use of metaphors

"*Every time I paint, I throw myself into the water in order to learn how to swim.*" -Édouard Manet

Another representation of reality that helps to understand a complex system is the metaphor. A metaphor is a figure of speech in which a word or phrase is applied to an object or action to which it is not literally applicable. The Manet quote is a metaphor for the challenging process of creating a work of art, which in my experience is not entirely unlike the scientific adventure of studying a new complex system such as the mood system or a coral reef. In this thesis, I have used multiple metaphors to communicate theoretical concepts. For instance, the illustrative ball-in-a-stability-landscape metaphor is used to explain alternative stable states and critical slowing down (see for instance **chapters 5 and 8**). On an even simpler level terms such as 'tipping point' and 'domino effect' are used as metaphors to aid an intuitive understanding of the essence of phenomena.

Metaphors are inherent to the human cognitive process and may greatly help to improve the scientific imagination (Lakoff and Johnson 1997), as well as the communication of complex ideas (Brown 2003). By using a metaphor, aspects of the system that do not fit the metaphorical approximation can be ignored, while the ones that do are highlighted (Lewontin 2002). However, this powerful subconscious process can also trick one's reasoning into unfounded conclusions (Ball 2011). For instance, one might be tempted to think that the rolling ball in stability landscapes could gain momentum on its way down and overshoot the valley to roll over the next hilltop. However, these potential landscapes only reflect the local derivatives without inertia, so when the ball is rolling down it slows down halfway and stops in the valley without any overshoot. Still the rolling ball is a useful aid to interpret stability, with the side effect of tricking us into the unfounded momentum interpretation. Indeed, the stability landscapes that have been so powerful in transmitting the central concepts of systems with alternative attractors to a broad audience are far-from-perfect analogs to reality.

Similarly, the choice to use a metaphor such as 'tipping point' instead of a technical mathematical term such as 'saddle-node bifurcation' has its strengths and weaknesses. Metaphors are easier to understand for a broad audience, but are less precise than mathematical terms. Hence, there is a trade-of between precise communication to a limited audience, or less accurate communication to a broader (interdisciplinary) group. The chapters in this thesis reflect different ends of this gradient. For instance, **chapter 4** on feedbacks in coral ecosystems aims to communicate essential aspects of non-linear systems to a non-mathematical audience of coral reef biologists in an intuitive way. By contrast, **chapter 6** on the stability of spatial systems is more technical. Still, the focus of my work is consistently on bridging between mathematics and applied fields rather than on the pure mathematics. Indeed, none of the models addresses truly novel mathematical issues. The very nature of this focus on bridging to a broader audience implies that the tension between mathematical precision and more metaphorical phrasing is omnipresent.

Resisting the confirmation bias

"*When men wish to construct or support a theory, how they torture facts into their service!"* – Mackay, 1852 (quoted in Nickerson (1998))

While metaphors are more evidently imperfect than simple models in their description of reality, both carry the risk of tempting one into embracing them too strongly. The tendency to see evidence for an idea everywhere is known as the confirmation bias. Considering that scientists are far from immune to this fallacy they should be alert to resist it (Nickerson 1998). As Chamberlin (1897) phrased it already in 1897, there is "*an unconscious selection and magnifying of the phenomena that fall into harmony with the theory and support it, and an unconscious neglect of those that fail of coincidence*". In the field of modeling a common pitfall is to interpret resemblance between model dynamics and observed dynamics as a proof of the validity of the model assumptions. Alternative mechanisms can often lead to the same or to similar dynamics. Let me briefly illustrate this with three examples from this thesis: *regular spatial patterns, abrupt shifts and slowing down.*

Regular spatial patterns in biota, such as the ones we observed on the Great Barrier Reef can arise by underlying heterogeneity in the landscape, or physical processes (**chapter 3**). In that case, Turing instability plays no role in the formation of the patterns. Even if the observed patterns are indeed self-organized, they can be explained by entirely different mechanisms, such as spatial resource accumulation comparable to what is found for patterned desert vegetation and spatial deflection of growth inhibitors (**chapter 3**).

Abrupt shifts in nature are often wrongly interpreted as evidence for the existence of alternative stable states (Scheffer and Carpenter 2003). Such shifts can however simply be a consequence of a strong environmental change or another abrupt event, rather than a critical transition to an alternative attracting regime. For instance, the shift from coral to macroalgae dominance on Caribbean reefs in 1983-1984 was preceded by a mass mortality event of sea urchins (Diadema antillarum) due to a disease (Hughes 1994). The resilience of these reefs was certainly low, because alternative grazers of macroalgae (herbivorous fish) were extremely overfished. However, after the return of the sea urchins, most reefs have shown signs of recovery (Edmunds and Carpenter 2001; Carpenter and Edmunds 2006). It could thus well be that the macroalgae-dominated state was not a true attractor and that the dramatic shift was simply a transient response to the rapid mortality of sea urchins (Dudgeon *et al.* 2010).

Slowing down may indicate the vicinity of a tipping point (e.g. **chapters 5 and 8**). However, there is a risk of over-interpreting indicators of slowing down. Although slowing down does appear in the vicinity of zero-eigenvalue bifurcations, it can also happen for other reasons. For instance, as temperature falls, most biological processes become slower. Similarly, changes in the environmental fluctuations can affect the indicators (Dakos *et al.* 2012b). Thus, observing slowing down of a system does not necessarily mean that the system approaches a catastrophic shift (Kéfi *et al.* 2012; Scheffer *et al.* 2015b).

These examples of alternative underlying mechanisms illustrate that, as mentioned in **chapter 1** and in the first paragraphs of this chapter, a strategic model should merely be seen as a qualitative hypothesis of a potential mechanism, that should be checked carefully against empirical observations.

Importantly, the hypothesis inspired by a strategic model becomes more plausible if it is confirmed by multiple lines of evidence (Scheffer and Carpenter 2003) or by predicting a pattern instead of single values (Grimm *et al.* 2005). For instance, the observation of the entire repertoire of Turing patterns, including bands, increases the likelihood that the observed regular patterns are indeed the result of spatial self-organization (**chapter 3**). Similarly, the idea that critical slowing down can indicate increased likelihood of a shift to an alternative state in the mood system is supported relatively strongly because it is consistent with evidence from multiple indicators of decreased resilience (variance, temporal autocorrelations, and cross-correlations), which are moreover observed for depressed patients in relation to upcoming recovery as well as for healthy subjects in relation to upcoming depression (**chapter 8**).

Controlled experiments are of course the classical approach to test hypotheses. However, such experiments are not always feasible in complex systems. For instance, experimentally testing the existence of alternative stable states in the climate system is simply impossible. Even testing stability of alternative states in an ecosystem such as a coral reef is hard as coral reefs are very slow systems, and isolating parts for replicated experiments without affecting essential ecosystem processes is hardly feasible. Clearly, even imperfect experiments can help probing a theory a bit further. For instance, a recent two-year double-blind experiment on a single subject obtained results in line with the proposed idea that critical slowing down of the mood can announce an upcoming tipping point into depression (Wichers *et al.* 2016). One may dismiss such non-replicated work as poor science. However, we may have to accept that complex systems such as humans, societies, coral reefs or the climate simply cannot be understood merely through the classical gold-standard approach of replicated controlled experiments also because of the complexity in causation (Scheffer and Beets 1994).

Prospect

The bottom line of this reflection on the challenges of using models to study complex systems is perhaps best summarized in the paraphrased quote from Picasso "*Models are a lie that can help to make us realize the truth"*. However, the bridge between strategic models and the reality of complex systems should be built with care. As the fierce discussion on Catastrophe Theory has illustrated (see **chapter 1**), the overenthusiasm of so-called catastrophists of that time, like Christopher Zeeman, gave rise to too many weak bridges between theory and reality, and finally resulted in a dismissal of the Catastrophe Theory. Currently, many of the theoretical concepts discussed in this thesis, such as alternative stable states, tipping points, and early warning signals, receive a lot of attention. The attractiveness is most likely due to the universality of these principles, and because they are relatively easy to understand. However, it is tempting to become overenthusiastic, and much work remains to be done to build convincing empirical foundations.

Although it may seem almost impossible to truly understand complex systems such as the ones discussed in this thesis, the time may be ripe for an effort to build a new science of complex systems. Definitely, to address a range of pressing societal issues we will need a better understanding of systems ranging from the brain to ecosystems and the climate. Simple mathematical models can merely help generating hypotheses and testing those through controlled experiments is rarely possible. However, additional power to resolve questions now comes from the

availability of big data from satellites, social media, wearable electronic sensors and numerous other sources. Clearly, a strong multidisciplinary effort is required to bring this all together. In addition to the technical insight in models and data analysis, one needs high system-specific expertise. Developing a new theory of the mood system (**chapter 8**) cannot be done without good psychologists and psychiatrists. An overarching theory of the global nitrogen cycle pathways (**chapter 2**) requires working with knowledgeable microbiologists. Similarly, a new theory on the functioning of coral reefs (**chapters 3 and 4**) can only be developed in close cooperation with ecologists with an expertise in the complex coral system.

In hindsight, results of such work may seem to make perfect sense. However, the interplay between me as a theoretician, and the different system-specialists was definitely not effortless. Rather there were frequent episodes of confusion that could only be resolved by perseverance from both sides, maintaining the dialogue in spite of the sometimes profound differences in scientific language. The combination of strategic mathematical models with big data and smart experiments seems a powerful approach to study a wide range of complex systems. However, the main challenge may lie in the social aspects of bridging disciplines rather than in technical aspects. Unravelling complex systems requires cooperation between diverse minds and personalities. It is slow science requiring not just technical skills, but also patience and perseverance. Participating in this science as a theoretician requires a delicate balance between modesty and boldness: "*Models are a lie that can help to make us realize the truth*".

Glossary

Alternative stable states	Multiple stable states of a system under the same external conditions (Fig. G1d).
Attractor	The dynamic regime to which a system converges after some time. Examples of attractors: point, cyclic (periodic), quasiperiodic, chaotic
Basin of attraction	Set of initial conditions that lead to a particular attractor (Fig. G1d).
Bifurcation point	A threshold in conditions at which the qualitative dynamics of a model change (e.g. from two stable states to one stable state).
Critical slowing down	The phenomenon that the return time of a disturbance back to equilibrium increases close to a local bifurcation where a stable equilibrium becomes unstable (Fig. G1e and f)
Critical transition	Abrupt shift in the behaviour of a system when certain parameters reach a threshold. A critical transition is often triggered by a disturbance or a small change in conditions (Fig. G1d).
Cusp-catastrophe fold	A diagram of a particular system in which two parameters are changed, illustrating both the fold bifurcation and the cusp bifurcation (Fig. G1c).
Eigenvalue (dominant)	One can approximate a nonlinear system close to an equilibrium point by a linear system. The eigenvalues of the linear system reflect the (possibly complex) exponents of the solution of the linear system. The maximum eigenvalue is called dominant as it determines largely the recovery rate after a small perturbation. (see also Jacobian matrix)
Equilibrium	The state of a system at which processes are balanced. A system returns to a stable equilibrium following a small perturbation. A system moves away from an unstable equilibrium upon a small perturbation.
Feedback	A closed loop process that feeds back to the inputs, influencing future changes.
Fold bifurcation	A bifurcation point at which a stable state collides with an unstable state. It marks the disappearance of both equilibria.
Hysteresis	The dependency of a systems' current state to the past. Following a critical transition to an alternative state due to an increase in driver level: if the driver level is lowered to pre-transition conditions the system stays in the new state ('is trapped') until a lower threshold is reached and the system flips back (Fig. G1b).
Jacobian matrix	One can approximate a nonlinear system close to an equilibrium point by a linear system. The Jacobian matrix contains the coefficients of this linear system, and comprises information about the stability of the equilibrium point. (See also Eigenvalue)
Negative feedback	A feedback that dampens an initial small change (e.g. increase A $\rightarrow$ increase B $\rightarrow$ decrease A).
Positive feedback	A feedback that amplifies an initial small change (e.g. increase A $\rightarrow$ increase B $\rightarrow$ increase A).
Resilience (ecological)	The magnitude of a disturbance a system can tolerate before it shifts to a different state (Fig. G1d).

System state	The size of the variables at a certain moment in time.
Tipping point	A threshold in time where once the threshold is passed, intrinsic processes in the system cause the accelerating change.
Threshold	A point at which the system is very sensitive to changing conditions or perturbations.
Zero-eigenvalue bifurcation	A bifurcation (in a continuous system) at which the real part of the dominant eigenvalue of the equilibrium crosses zero

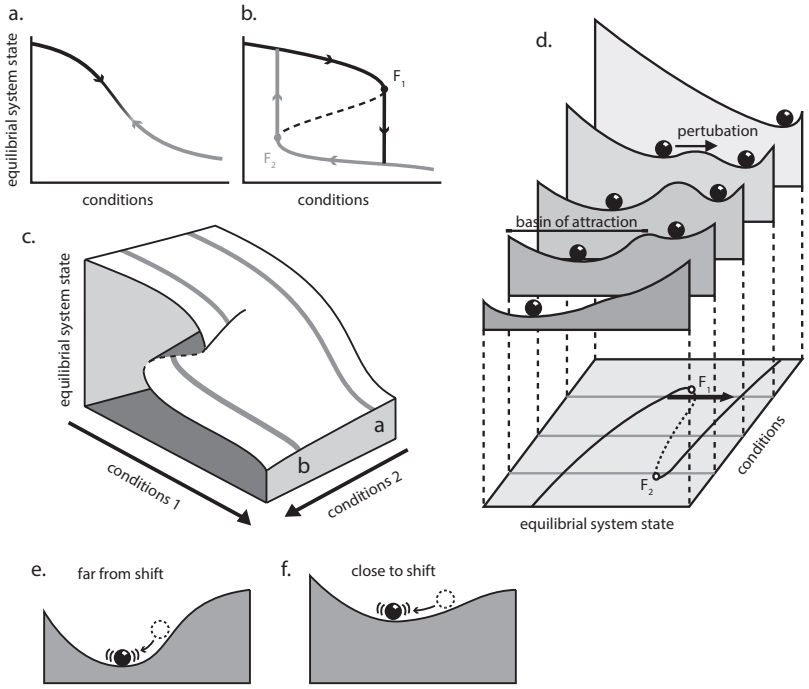

Fig. G1. a) Most systems respond smoothly to changing conditions, such that the same equilibrial trajectory is followed when conditions are changed slowly back and forth (grey vs. black). **b)** Some systems respond smoothly to changing conditions until a certain level is reached, F_1, at which the system abruptly shifts to an alternative state if conditions get close or beyond point F_1. Once the system is trapped in this new state, reversal of the conditions leads to a different backward trajectory with a backward shift around point F_2 (i.e. hysteresis). **c)** The cusp-catastrophe fold. The shape of the equilibrial response of a system to changing conditions depends on the interaction between variables in the system (see also chapter 4). In general, strong positive feedbacks (e.g. in shallow lakes: aquatic plants improve water clarity, water clarity increases growth of aquatic plants) increase the likelihood of critical transitions. **d)** A critical transition illustrated by a ball in a stability landscape: the one-dimensional landscape represents the stability of the system, and the position of a ball in that landscape represents the present state of the system. Far from the tipping point F_1, the size of the basin of attraction is large, and the resilience of the present state is high. However, when the system approaches the tipping point the landscape changes, and the resilience decreases. **e and f)** Critical slowing down illustrated by a ball in a stability landscape. If resilience is high (panel e), the ball will quickly return to equilibrium after a small disturbance. If resilience is low (panel f), the return rate is much lower.

References

Aderka IM, Nickerson A, Bøe HJ, and Hofmann SG. 2012. Sudden gains during psychological treatments of anxiety and depression: a meta-analysis. *J Consult Clin Psychol* **80**: 93–101.

Adger WN, Hallie E, and Winkels A. 2009. Nested and teleconnected vulnerabilities to environmental change. *Front Ecol Environ* **7**: 150–7.

Allesina S and Pascual M. 2009. Food web models: A plea for groups. *Ecol Lett* **12**: 652–62.

Altieri AH, Silliman BR, and Bertness MD. 2007. Hierarchical organization via a facilitation cascade in intertidal cordgrass bed communities. *Am Nat* **169**: 195–206.

An S and Gardner WS. 2002. Dissimilatory nitrate reduction to ammonium (DNRA) as a nitrogen link, versus denitrification as a sink in a shallow estuary (Laguna Madre/Baffin Bay, Texas). *Mar Ecol Prog Ser* **237**: 41–50.

Angeli D, Ferrell JE, and Sontag ED. 2004. Detection of multistability, bifurcations, and hysteresis in a large class of biological positive-feedback systems. Proc Natl Acad Sci U S A 101: 1822-1827.

Angelini C and Silliman BR. 2012. Patch size-dependent community recovery after massive disturbance. *Ecology* **93**: 101–10.

Aronson DG and Weinberger HF. 1975. Nonlinear diffusion in population genetics, combustion, and nerve pulse propagation. *Lect Notes Math* **446**: 5–49.

Ayre DJ and Hughes TP. 2004. Climate change, genotypic diversity and gene flow in reef-building corals. *Ecol Lett* **7**: 273–8.

Ball P. 2011. A metaphor too far. *Nature News*, 23 February 2011, doi:10.1038/news.2011.115 .

Barge-Schaapveld D, Nicolson NA, Gerritsen van der Hoop R, and DeVries MW. 1995. Changes in daily life experience associated with clinical improvement in depression. *J Affect Disord* **34**: 139–54.

Barnosky AD, Hadly EA, Bascompte J, *et al.* 2012. Approaching a state shift in Earth's biosphere. *Nature* **486**: 52–8.

Bascompte J, Jordano P, Melián CJ, and Olesen JM. 2003. The nested assembly of plant–animal mutualistic networks. *Proc Natl Acad Sci U S A* **100**: 9383–7.

Beaugrand G, Edwards M, Brander K, *et al.* 2008. Causes and projections of abrupt climate-driven ecosystem shifts in the North Atlantic. *Ecol Lett* **11**: 1157–68.

Bel G, Hagberg A, and Meron E. 2012. Gradual regime shifts in spatially extended ecosystems. *Theor Ecol* **5**: 591–604.

Bellwood DR. 1995. Carbonate transport and within-reef patterns of bioerosion and sediment release by parrotfishes (family Scaridae) on the Great Barrier Reef. *Mar Ecol Prog Ser* **117**: 127–36.

Bellwood DR, Hughes TP, Folke C, and Nyström M. 2004. Confronting the coral reef crisis. *Nature* **429**: 827–33.

Bertness MD, Trussell GC, Ewanchuk PJ, and Silliman BR. 2002. Do alternate stable community states exist in the gulf of maine rocky intertidal zone? *Ecology* **83**: 3434–48.

Bestelmeyer BT, Ellison AM, Fraser WR, *et al.* 2011. Analysis of abrupt transitions in ecological systems. *Ecosphere* **2**: art129.

Biggs R, Carpenter SR, and Brock WA. 2009. Turning back from the brink: Detecting an impending regime shift in time to avert it. *Proc Natl Acad Sci* **106**: 826–31.

Bijl R V, Ravelli A, and Zessen G van. 1998. Prevalence of psychiatric disorder in the general population: results of The Netherlands Mental Health Survey and Incidence Study (NEMESIS). *Soc Psychiatry Psychiatr Epidemiol* **33**: 587–95.

Blackwood JC, Hastings A, and Mumby PJ. 2010. The effect of fishing on hysteresis in Caribbean coral reefs. *Theor Ecol* **5**: 105–14.

Blackwood JC, Hastings A, and Mumby PJ. 2011. A model-based approach to determine the long-term effects of multiple interacting stressors on coral reefs. *Ecol Appl* **21**: 2722–33.

Borsboom D, and Cramer AOJ. 2013. Network analysis: an integrative approach to the structure of psychopathology. *Annu Rev Clin Psychol* **9**: 91–121.

Bowman AW and Azzalini A. 1997. Applied smoothing techniques for data analysis: the kernel approach with S-Plus illustrations (AW Bowman and A Azzalini, Eds). New York, USA: Oxford University Press.

Brandes JA, Devol AH, and Deutsch C. 2007. New developments in the marine nitrogen cycle. *Chem Rev* **107**: 577–89.

Brida JG and Punzo LF. 2003. Symbolic time series analysis and dynamic regimes. *Struct Chang Econ Dyn* **14**: 159–83.

Brillinger D. 2007. Learning a potential function from a trajectory. *IEEE Signal Process Lett* **14**: 1–4.

Bringmann LF, Vissers N, Wichers M, *et al.* 2013. A network approach to psychopathology: new insights into clinical longitudinal data. *PLoS One* **8**: e60188.

Brock WA and Carpenter SR. 2010. Interacting regime shifts in ecosystems: implication for early warnings. *Ecol Monogr* **80**: 353–67.

Broda E. 1977. Two kinds of lithotrophs missing in nature. *Z Allg Mikrobiol* **17**: 491–3.

Brown TL. 2003. Making truth: metaphor in science. Urbana: University of Illinois Press.

Brunet RC and Garcia-Gil LJ. 1996. Sulfide-induced dissimilatory nitrate reduction to ammonia in anaerobic freshwater sediments. *FEMS Microbiol Ecol* **21**: 131–8.

Bruno JF, Sweatman H, Precht WF, *et al.* 2009. Assessing evidence of phase shifts from coral to macroalgal dominance on coral reefs. *Ecology* **90**: 1478–84.

Buresh RJ and Patrick WH. 1981. Nitrate reduction to ammonium and organic nitrogen in an estuarine sediment. *Soil Biol Biochem* **13**: 279–83.

Burford JR and Bremner JM. 1975. Relationships between the denitrification capacities of soils and total, water-soluble and readily decomposable soil organic matter. *Soil Biol Biochem* **7**: 389–94.

Canavan RW, Laverman AM, and Slomp CP. 2007. Modeling nitrogen cycling in a coastal fresh water sediment. *Hydrobiologia* **584**: 27–36.

Carpenter SR. 2003. Regime shifts in lake ecosystems: pattern and variation. Oldendorf, Germany: International Ecology Institute.

Carpenter SR and Brock WA. 2006. Rising variance: a leading indicator of ecological transition. *Ecol Lett* **9**: 311–8.

Carpenter SR, Cole JJ, Pace ML, *et al.* 2011. Early warnings of regime shifts: a whole-ecosystem experiment. *Science* **332**: 1079–82.

Carpenter RC and Edmunds PJ. 2006. Local and regional scale recovery of Diadema promotes recruitment of scleractinian corals. *Ecol Lett* **9**: 271–80.

Carpenter SR, Ludwig D, and Brock WA. 1999. Management of eutrophication for lakes subject to potentially irreversible change. *Ecol Appl* **9**: 751–71.

Chamberlin TC. 1897. Method of multiple working hypotheses. *J Geol* **5**: 837–48.

Chen L, Liu R, Liu Z-P, *et al.* 2012. Detecting early-warning signals for sudden deterioration of complex diseases by dynamical network biomarkers. *Sci Rep* **2**: 1–8.

Chow S-N, Mallet-Paret J, and Vleck ES van. 1996. Dynamics of lattice differential equations. *Int J Bifurc Chaos* **6**: 1605–21.

Ciudad G, Rubilar O, Muñoz P, *et al.* 2005. Partial nitrification of high ammonia concentration wastewater as a part of a shortcut biological nitrogen removal process. *Process Biochem* **40**: 1715–9.

Cole LES, Bhagwat SA, and Willis KJ. 2014. Recovery and resilience of tropical forests after disturbance. *Nat Commun* **5**: 1–7.

Connell JH. 1997. Disturbance and recovery of coral assemblages. *Coral Reefs* **16**: S101–13.

Connell JH, Hughes TP, and Wallace CC. 1997. A 30-year study of coral abundance, recruitment, and disturbance at several scales in space and time. *Ecol Monogr* **67**: 461–88.

Costa E, Pérez J, and Kreft J-U. 2006. Why is metabolic labour divided in nitrification? *Trends Microbiol* **14**: 213–9.

Cottenie K and Meester L De. 2003. Connectivity and cladoceran species richness in a metacommunity of shallow lakes. *Freshw Biol* **48**: 823–32.

Couteron P and Lejeune O. 2001. Periodic spotted patterns in semi-arid vegetation explained by a propagation-inhibition model. *J Ecol* **89**: 616–28.

Cramer AOJ, Borsboom D, Aggen S, and Kendler K. 2012a. The pathoplasticity of dysphoric episodes: differential impact of stressful life events on the pattern of depressive symptom inter-correlations. *Psychol Med* **42**: 957–65.

Cramer AOJ, Sluis S van der, Noordhof A, *et al.* 2012b. Dimensions of normal personality as networks in search of equilibrium: you can't like parties if you don't like people. *Eur J Pers* **26**: 414–31.

Cramer AOJ, Waldorp LJ, Maas HLJ van der, and Borsboom D. 2010. Comorbidity: a network perspective. *Behav Brain Sci* **33**: 137–50; discussion 150–93.

Csikszentmihalyi M and Larson R. 1987. Validity and reliability of the Experience- Sampling Method. *J Nerv Ment Dis* **175**: 526–36.

Dai L, Korolev KS, and Gore J. 2013. Slower recovery in space before collapse of connected populations. *Nature* **496**: 355–8.

Dai L, Vorselen D, Korolev KS, and Gore J. 2012. Generic indicators for loss of resilience before a tipping point leading to population collapse. *Science* **336**: 1175–7.

Daims H, Lebedeva E V., Pjevac P, *et al.* 2015. Complete nitrification by *Nitrospira* bacteria. *Nature* **528**: 504–9.

Dakos V, Carpenter SR, Brock WA, *et al.* 2012a. Methods for detecting early warnings of critical transitions in time series illustrated using simulated ecological data. *PLoS One* **7**: e41010.

Dakos V, Carpenter SR, Nes EH van, and Scheffer M. 2015. Resilience indicators: prospects and limitations for early warnings of regime shifts. *Philos Trans R Soc B Biol Sci* **370**: 20130263.

Dakos V, Kéfi S, Rietkerk M, *et al.* 2011. Slowing down in spatially patterned systems at the brink of collapse. *Am Nat* **177**: E153–66.

Dakos V, Nes EH Van, D'Odorico P, and Scheffer M. 2012b. Robustness of variance and autocorrelation as indicators of critical slowing down. *Ecology* **93**: 264–71.

Dakos V, Nes EH Van, Donangelo R, *et al.* 2010. Spatial correlation as leading indicator of catastrophic shifts. *Theor Ecol* **3**: 163–74.

Dakos V, Scheffer M, Nes EH Van, *et al.* 2008. Slowing down as an early warning signal for abrupt climate change. *Proc Natl Acad Sci U S A* **105**: 14308–12.

Dalsgaard T, Thamdrup B, and Canfield DE. 2005. Anaerobic ammonium oxidation (anammox) in the marine environment. *Res Microbiol* **156**: 457–64.

Dayton P, Tegner M, Parnell P, and Edwards P. 1992. Temporal and spatial patterns of disturbance and recovery in a kelp forest community. *Ecol Monogr* **62**: 421–45.

DeAngelis DL, Post WM, and Travis CC. 1986. Positive feedback in natural systems. Berlin: Springer.

Delespaul PAEG. 1995. Assessing schizophrenia in daily life: the experience sampling method. Maastricht: University of Limburg.

deYoung B, Barange M, Beaugrand G, *et al.* 2008. Regime shifts in marine ecosystems: detection, prediction and management. *Trends Ecol Evol* **23**: 402–9.

Diaz-Pulido G and McCook LJ. 2003. Relative roles of herbivory and nutrients in the recruitment of coral-reef seaweeds. *Ecology* **84**: 2026–33.

Ditlevsen PD and Johnsen SJ. 2010. Tipping points: Early warning and wishful thinking. *Geophys Res Lett* **37**.

Donahue MJ, Desharnais RA, Robles CD, and Arriola P. 2011. Mussel bed boundaries as dynamic equilibria: thresholds, phase shifts, and alternative states. *Am Nat* **178**: 612–25.

Done TJ. 1992. Phase shifts in coral reef communities and their ecological significance. *Hydrobiologia* **247**: 121–32.

Dosta J, Fernández I, Vázquez-Padín JR, *et al.* 2008. Short- and long-term effects of temperature on the Anammox process. *J Hazard Mater* **154**: 688–93.

Drake JM and Griffen BD. 2010. Early warning signals of extinction in deteriorating environments. *Nature* **467**: 456–9.

Dudgeon SR, Aronson RB, Bruno JF, and Precht WF. 2010. Phase shifts and stable states on coral reefs. *Mar Ecol Prog Ser* **413**: 201–16.

Dunne JA, Williams RJ, and Martinez ND. 2002. Network structure and biodiversity loss in food webs: robustness increases with connectance. *Ecol Lett* **5**: 558–67.

Edmunds PJ and Carpenter RC. 2001. Recovery of Diadema antillarum reduces macroalgal cover and increases abundance of juvenile corals on a Caribbean reef. *Proc Natl Acad Sci U S A* **98**: 5067–71.

Elmhirst T, Connolly SR, and Hughes TP. 2009. Connectivity, regime shifts and the resilience of coral reefs. *Coral Reefs* **28**: 949-957.

Eppinga MB, Ruiter PC de, Wassen MJ, and Rietkerk M. 2009. Nutrients and hydrology indicate the driving mechanisms of peatland surface patterning. *Am Nat* **173**: 803–18.

Eriksson PG and Weisner SEB. 1999. An experimental study on effects of submersed macrophytes on nitrification and denitrification in ammonium-rich aquatic systems. *Limnol Oceanogr* **44**: 1993–9.

Ettwig KF, Butler MK, Paslier D Le, *et al.* 2010. Nitrite-driven anaerobic methane oxidation by oxygenic bacteria. *Nature* **464**: 543–8.

Fáth G. 1998. Propagation failure of traveling waves in a discrete bistable medium. *Phys D Nonlinear Phenom* **116**: 176–90.

Ferguson DJ, Richardson DJ, and Spanning RJ. van. 2007. Biochemistry and molecular biology of nitrification. In: Bothe S.J. Newton, W.E. HF (Ed). Biology of the nitrogen cycle. Amsterdam: Elsevier.

Fife P. 1979. Long time behavior of solutions of bistable nonlinear diffusion equations. *Arch Ration Mech Anal* **70**: 31–6.

Firestone MK, Firestone RB, and Tiedje JM. 1980. Nitrous oxide from soil denitrification: factors controlling its biological production. *Science* **208**: 749–51.

Folke C, Carpenter SR, Walker B, *et al.* 2004. Regime shifts, resilience, and biodiversity in ecosystem management. *Annu Rev Ecol Evol Syst* **35**: 557–81.

Frewen PA, Allen SL, Lanius RA, and Neufeld RWJ. 2012. Perceived causal relations: novel methodology for assessing client attributions about causal associations between variables including symptoms and functional impairment. *Assessment* **19**: 480–93.

Frewen PA, Schmittmann VD, Bringmann LF, and Borsboom D. 2013. Perceived causal relations between anxiety, posttraumatic stress and depression: extension to moderation, mediation, and network analysis. *Eur J Psychotraumatol* **4**: 20656.

Friedlander AM and Parrish JD. 1998. Habitat characteristics affecting fish assemblages on a Hawaiian coral reef. *J Exp Mar Bio Ecol* **224**: 1–30.

Fung T, Seymour R, and Johnson C. 2011. Alternative stable states and phase shifts in coral reefs under anthropogenic stress. *Ecology* **92**: 967–82.

Gagnon P, Himmelman JH, and Johnson LE. 2004. Temporal variation in community interfaces: kelp-bed boundary dynamics adjacent to persistent urchin barrens. *Mar Biol* **144**: 1191–203.

Gao H, Schreiber F, Collins G, *et al.* 2010. Aerobic denitrification in permeable Wadden Sea sediments. *ISME J* **4**: 417–26.

Geest G V van, Roozen F, Coops H, *et al.* 2003. Vegetation abundance in lowland flood plan lakes determined by surface area, age and connectivity. *Freshw Biol* **48**: 440–54.

Gell-Mann M. 1988. Simplicity and complexity in the description of nature. *Eng Sci* **Spring**: 2–9.

Gierer A and Meinhardt H. 1972. A theory of biological pattern formation. *Kybernetik* **12**: 30–9.

Goeij JM de, Oevelen D van, Vermeij MJA, *et al.* 2013. Surviving in a marine desert: the sponge loop retains resources within coral reefs. *Science* **342**: 108–10.

Gorban AN, Smirnova E V, and Tyukina TA. 2010. Correlations, risk and crisis: From physiology to finance. *Phys A Stat Mech its Appl* **389**: 3193–217.

Graham NAJ, Bellwood DR, Cinner JE, *et al.* 2013. Managing resilience to reverse phase shifts in coral reefs. *Front Ecol Environ* **11**: 541-548.

Graham NAJ, Nash KL, and Kool JT. 2011. Coral reef recovery dynamics in a changing world. *Coral Reefs* **30**: 283–94.

Graham NAJ, Wilson SK, Jennings S, *et al.* 2006. Dynamic fragility of oceanic coral reef ecosystems. *Proc Natl Acad Sci U S A* **103**: 8425–9.

Grimm V, Revilla E, Berger U, *et al.* 2005. Pattern-oriented modeling of agent-based complex systems: lessons from ecology. *Science* **310**: 987–91.

Guttal V and Jayaprakash C. 2008a. Changing skewness: an early warning signal of regime shifts in ecosystems. *Ecol Lett* **11**: 450–60.

Guttal V and Jayaprakash C. 2008b. Spatial variance and spatial skewness: leading indicators of regime shifts in spatial ecological systems. *Theor Ecol* **2**: 3–12.

Haldane AG and May RM. 2011. Systemic risk in banking ecosystems. *Nature* **469**: 351–5.

Halford AR and Caley MJ. 2009. Towards an understanding of resilience in isolated coral reefs. *Glob Chang Biol* **15**: 3031–45.

Halm H, Musat N, Lam P, *et al.* 2009. Co-occurrence of denitrification and nitrogen fixation in a meromictic lake, Lake Cadagno (Switzerland). *Environ Microbiol* **11**: 1945–58.

Handa IT, Harmsen R, and Jefferies RL. 2002. Patterns of vegetation change and the recovery potential of degraded areas in a coastal marsh system of the Hudson Bay lowlands. *J Ecol* **90**: 86–99.

Hankin BL, Fraley RC, Lahey BB, and Waldman ID. 2005. Is depression best viewed as a continuum or discrete category? A taxometric analysis of childhood and adolescent depression in a population-based sample. *J Abnorm Psychol* **114**: 96–110.

Hardenberg J von, Meron E, Shachak M, and Zarmi Y. 2001. Diversity of vegetation patterns and desertification. *Phys Rev Lett* **87**: 198101.

Harris MP, Williamson S, Fallon JF, *et al.* 2005. Molecular evidence for an activator-inhibitor mechanism in development of embryonic feather branching. *Proc Natl Acad Sci U S A* **102**: 11734–9.

Hayes AM and Strauss JL. 1998. Dynamic systems theory as a paradigm for the study of change in psychotherapy: an application to cognitive therapy for depression. *J Consult Clin Psychol* **66**: 939–47.

Heiby EM, Pagano IS, Blaine DD, *et al.* 2003. Modeling unipolar depression as a chaotic process. *Psychol Assess* **15**: 426–34.

Heide T van der, Eklöf JS, Nes EH van, *et al.* 2012. Ecosystem engineering by seagrasses interacts with grazing to shape an intertidal landscape. *PLoS One* **7**: e42060.

Heide T van der, Nes EH Van, Katwijk MM van, *et al.* 2011. Positive feedbacks in seagrass ecosystems - evidence from large-scale empirical data. *PLoS One* **6**: e16504.

Henderson PA. 2003. Practical Methods in Ecology.

Hewitt JE and Thrush SF. 2010. Empirical evidence of an approaching alternate state produced by intrinsic community dynamics, climatic variability and management actions. *Mar Ecol Prog Ser* **413**: 267–76.

Higgins SI and Scheiter S. 2012. Atmospheric CO2 forces abrupt vegetation shifts locally, but not globally. *Nature* **488**: 209–12.

Hilt S, Köhler J, Kozerski H-P, *et al.* 2011. Abrupt regime shifts in space and time along rivers and connected lake systems. *Oikos* **120**: 766–75.

Hines P, Cotilla-Sanchez E, and Blumsack S. 2011. Topological models and critical slowing down: Two approaches to power system blackout risk analysis. In: Proceedings of the Annual Hawaii International Conference on System Sciences. U. of Vermont, United States Pennsylvania State U., United States.

Hirota M, Holmgren M, Nes E Van, and Scheffer M. 2011. Global resilience of tropical forest and savanna to critical transitions. *Science*.

Hoey AS and Bellwood DR. 2011. Suppression of herbivory by macroalgal density: a critical feedback on coral reefs? *Ecol Lett* **14**: 267–73.

Holling CS. 1973. Resilience and stability of ecological systems. *Annu Rev Ecol Syst* **4**: 1–23.

Holling CS. 2001. Understanding the complexity of economic, ecological, and social systems. *Ecosystems* **4**: 390–405.

Holling CS and Meffe GK. 1996. Command and control and the pathology of natural resource management. *Conserv Biol* **10**: 328–37.

Holt RD, Keitt TH, Lewis MA, *et al.* 2005. Theoretical models of species' borders: single species approaches. *Oikos* **108**: 18–27.

Hooper AB, Arciero DM, Bergmann DJ, and Hendrich MP. 2004. The oxidation of ammonia as an energy source in Bacteria. In: Zannoni D (Ed). Respiration in Archaea and Bacteria: Diversity of Prakaryotic Respiratory Systems. Dordrecht, Netherlands: Springer.

Horgan J. 1997. The end of science, facing the limits of knowledge in the twilight of the scientific age. Broadway Books.

Houk P, Benavente D, Iguel J, *et al.* 2014. Coral reef disturbance and recovery dynamics differ across gradients of localized stressors in the Mariana Islands. *PLoS One* **9**: e105731.

Hox JJ. 2010. Multilevel analysis: techniques and applications (Quantitative Methodology Series). New York: Routledge.

Hsieh C-H, Reiss CS, Hunter JR, *et al.* 2006. Fishing elevates variability in the abundance of exploited species. *Nature* **443**: 859–62.

Hubbell SP. 2001. The unified neutral theory of biodiversity and biogeography. Princeton University Press.

Huber MT, Braun HA, and Krieg JC. 1999. Consequences of deterministic and random dynamics for the course of affective disorders. *Biol Psychiatry* **46**: 256–62.

Hughes TP. 1994. Catastrophes, phase shifts, and large-scale degradation of a Caribbean coral reef. *Science* **265**: 1547–51.

Hughes TP, Baird AH, Bellwood DR, *et al.* 2003. Climate change, human impacts, and the resilience of coral reefs. *Science* **301**: 929–33.

Hughes TP, Graham NAJ, Jackson JBC, *et al.* 2010. Rising to the challenge of sustaining coral reef resilience. *Trends Ecol Evol* **25**: 633–42.

Hughes TP and Tanner JE. 2000. Recruitment failure, life histories, and long-term decline of Caribbean corals. *Ecology* **81**: 2250–63.

Ives AR. 1995. Measuring resilience in stochastic systems. *Ecol Monogr* **65**: 217–33.

Jensen MM, Petersen J, Dalsgaard T, and Thamdrup B. 2009. Pathways, rates, and regulation of N2 production in the chemocline of an anoxic basin, Mariager Fjord, Denmark. *Mar Chem* **113**: 102–13.

Jetten MSM, Sliekers O, Kuypers MMM, *et al.* 2003. Anaerobic ammonium oxidation by marine and freshwater planctomycete-like bacteria. *Appl Microbiol Biotechnol* **63**: 107–14.

Jørgensen KS. 1989. Annual pattern of denitrification and nitrate ammonification in estuarine sediment. *Appl Environ Microbiol* **55**: 1841–7.

Katwijk MM van, Bos AR, Jonge VN de, *et al.* 2009. Guidelines for seagrass restoration: importance of habitat selection and donor population, spreading of risks, and ecosystem engineering effects. *Mar Pollut Bull* **58**: 179–88.

Kéfi S, Dakos V, Scheffer M, *et al.* 2012. Early warning signals also precede non-catastrophic transitions. *Oikos* **122**: 641–8.

Kéfi S, Rietkerk M, Alados CL, *et al.* 2007. Spatial vegetation patterns and imminent desertification in Mediterranean arid ecosystems. *Nature* **449**: 213–7.

Keitt TH, Lewis MA, and Holt RD. 2001. Allee effects, invasion pinning, and species' borders. *Am Nat* **157**: 203–16.

Keller MC, Neale MC, and Kendler KS. 2007. Association of different adverse life events with distinct patterns of depressive symptoms. *Am J Psychiatry* **164**: 1521–9.

Kelso JAS, Scholz JP, and Schöner G. 1986. Nonequilibrium phase transitions in coordinated biological motion: critical fluctuations. *Phys Lett A* **118**: 279–84.

Kelso B, Smith R V, Laughlin RJ, and Lennox SD. 1997. Dissimilatory nitrate reduction in anaerobic sediments leading to river nitrite accumulation. *Appl Environ Microbiol* **63**: 4679–85.

Kendler KS, Zachar P, and Craver C. 2011. What kinds of things are psychiatric disorders? *Psychol Med* **41**: 1143–50.

Kessel MAHJ van, Speth DR, Albertsen M, *et al.* 2015. Complete nitrification by a single microorganism. *Nature* **528**: 555–9.

Kessler R, McGonagle K, Zhao S, *et al.* 1994. Lifetime and 12-month prevalence of DSM-III-R psychiatric disorders in the United States: results from the National Comorbidity Survey. *Arch Gen Psychiatry* **51**: 8–19.

Kim NS and Ahn W. 2002. Clinical psychologists' theory-based representations of mental disorders predict their diagnostic reasoning and memory. *J Exp Psychol Gen* **131**: 451–76.

Klausmeier CA. 1999. Regular and irregular patterns in semiarid vegetation. *Science* **284**: 1826–8.

Kleinen T, Held H, and Petschel-Held G. 2003. The potential role of spectral properties in detecting thresholds in the Earth system: application to the thermohaline circulation. *Ocean Dyn* **53**: 53–63.

Klotz MG, Schmid MC, Strous M, *et al.* 2008. Evolution of an octahaem cytochrome c protein family that is key to aerobic and anaerobic ammonia oxidation by bacteria. *Environ Microbiol* **10**: 3150–63.

Klotz MG and Stein LY. 2008. Nitrifier genomics and evolution of the nitrogen cycle. *FEMS Microbiol Lett* **278**: 146–56.

Konar B and Estes JA. 2003. The stability of boundary regions between kelp beds and deforested areas. *Ecology* **84**: 174–85.

Kool JT. 2009. An object-oriented, individual-based approach for simulating the dynamics of genes in subdivided populations. *Ecol Inform* **4**: 136–46.

Koppel J van de and Crain CM. 2006. Scale-dependent inhibition drives regular tussock spacing in a freshwater marsh. *Am Nat* **168**: E136–47.

Koppel J van de, Gascoigne JC, Theraulaz G, *et al.* 2008. Experimental evidence for spatial self-organization and its emergent effects in mussel bed ecosystems. *Science* **322**: 739–42.

Koppel J van de, Herman PMJ, Thoolen P, and Heip CHR. 2001. Do alternate stable states occur in natural ecosystems? Evidence from a tidal flat. *Ecology* **82**: 3449–61.

Koppel J van de and Rietkerk M. 2004. Spatial interactions and resilience in arid ecosystems. *Am Nat* **163**: 113–21.

Koppel J van de, Rietkerk M, Dankers N, and Herman PMJ. 2005a. Scale-dependent feedback and regular spatial patterns in young mussel beds. *Am Nat* **165**: E66–77.

Koppel J van de, Rietkerk M, Langevelde F van, *et al.* 2002. Spatial heterogeneity and irreversible vegetation change in semiarid grazing systems. *Am Nat* **159**: 209–18.

Koppel J van de, Wal D van der, Bakker JP, and Herman PMJ. 2005b. Self-organization and vegetation collapse in salt marsh ecosystems. *Am Nat* **165**: E1–12.

Kramer J and Ross J. 1985. Stabilization of unstable states, relaxation, and critical slowing down in a bistable system. *J Chem Phys* **83**: 6234–41.

Kuehn C. 2011. A mathematical framework for critical transitions: Bifurcations, fastslow systems and stochastic dynamics. *Phys D Nonlinear Phenom* **240**: 1020–35.

Kuppens P, Allen NB, and Sheeber LB. 2010. Emotional inertia and psychological maladjustment. *Psychol Science* **21**: 984–91.

Kuppens P, Sheeber LB, Yap MBH, *et al.* 2012. Emotional inertia prospectively predicts the onset of depressive disorder in adolescence. *Emotion* **12**: 283–9.

Kuypers MMM, Sliekers O, Lavik G, *et al.* 2003. Anaerobic ammonium oxidation by anammox bacteria in the Black Sea. *Nature* **422**: 608–11.

Kuznetsov YA. 1995. Elements of applied bifurcation theory (JE Marsden and L Sirovich, Eds). New York: Springer.

Lakoff G and Johnson M. 2008. Metaphors we live by. Chicago: University of Chicago Press.

Lee SC. 2006. Habitat complexity and consumer-mediated positive feedbacks on a Caribbean coral reef. *Oikos* **112**: 442–7.

Leemput IA van de, Nes EH van, and Scheffer M. 2015. Resilience of alternative states in spatially extended ecosystems. *PLoS One* **10**: e0116859.

Lenton TM, Livina VN, Dakos V, *et al.* 2012. Early warning of climate tipping points from critical slowing down: comparing methods to improve robustness. *Philos Trans A Math Phys Eng Sci* **370**: 1185–204.

Levin SA. 2000. Fragile dominion: complexity and the commons. Cambridge, Massachusetts: Perseus Publishing.

Lewontin RC. 2002. The triple helix: gene, organism and environment. Cambridge: Harvard University Press.

Lim J and Epureanu BI. 2011. Forecasting a class of bifurcations: Theory and experiment. *Phys Rev E - Stat Nonlinear, Soft Matter Phys* **83:** 016203.

Lirman D. 2001. Competition between macroalgae and corals: effects of herbivore exclusion and increased algal biomass on coral survivorship and growth. *Coral Reefs* **19**: 392–9.

Litzow MA, Urban JD, and Laurel BJ. 2008. Increased spatial variance accompanies reorganization of two continental shelf ecosystems. *Ecol Appl* **18**: 1331–7.

Liu W, Dahab MF, and Surampalli RY. 2005. Nitrogen transformations modeling in subsurface-flow constructed wetlands. *Water Environ Res* **77**: 246–58.

Liu J-S, Vojinović V, Patiño R, *et al.* 2007. A comparison of various Gibbs energy dissipation correlations for predicting microbial growth yields. *Thermochim Acta* **458**: 38–46.

Livina VN, Kwasniok F, and Lenton TM. 2010. Potential analysis reveals changing number of climate states during the last 60 kyr. *Clim Past* **6**: 77–82.

Livina VN and Lenton TM. 2007. A modified method for detecting incipient bifurcations in a dynamical system. *Geophys Res Lett* **34**: L03712.

Lopez AD, Mathers CD, Ezzati M, *et al.* 2006. Global and regional burden of disease and risk factors, 2001: systematic analysis of population health data. *Lancet* **367**: 1747–57.

Lorenz EN. 1963. Deterministic nonperiodic flow. *J Atmos Sci* **20**: 130–41.

Lotka AJ. 1932. The growth of mixed populations: two species competing for a common food supply. *J Washingt Acad Sci* **22**: 461–9.

Lundberg J and Moberg F. 2003. Mobile link organisms and ecosystem functioning: implications for ecosystem resilience and management. *Ecosystems* **6**: 87–98.

Lux V and Kendler K. 2010. Deconstructing major depression: a validation study of the DSM-IV symptomatic criteria. *Psychol Med* **40**: 1679–90.

MacDonald GM, Kremenetski K V, and Beilman DW. 2008. Climate change and the northern Russian treeline zone. *Philos Trans R Soc Lond B Biol Sci* **363**: 2285–99.

Mackinson S, Sumaila UR, and Pitcher TJ. 1997. Bioeconomics and catchability: fish and fishers behaviour during stock collapse. *Fish Res* **31**: 11–7.

Madigan MT, Martinko JM, Dunlap PV, and Clark DP. 2003. Brock Biology of Microorganisms. Upper Saddle River, NJ, USA: Pearson Prentice Hall.

Mass T, Genin A, Shavit U, *et al.* 2010. Flow enhances photosynthesis in marine benthic autotrophs by increasing the efflux of oxygen from the organism to the water. *Proc Natl Acad Sci U S A* **107**: 2527–31.

Matsumoto G and Kunisawa T. 1978. Critical slowing-down near transition region from resting to time-ordered states in squid giant axons. *J Phys Soc Japan* **44**: 1047–8.

May RM. 1977. Thresholds and breakpoints in ecosystems with a multiplicity of stable states. *Nature* **269**: 471–7.

May RM, Levin SA, and Sugihara G. 2008. Complex systems - Ecology for bankers. *Nature* **451**: 893–5.

Mayer AL, Pawlowski C, Fath BD, *et al.* 2007. Applications of Fisher Information to the Management of Sustainable Environmental Systems Exploratory Data Analysis Using Fisher Information. In: Frieden BR, Gatenby RA (Eds). Exploratory Data Analysis Using Fisher Information. London: Springer London.

McClanahan TR, Uku JN, and Machano H. 2002. Effect of macroalgal reduction on coral-reef fish in the Watamu Marine National Park, Kenya. *Mar Freshw Res* **53**: 223–31.

McCook LJ and Price IR. 1997. Macroalgal distributions on the Great Barrier Reef: a review of patterns and causes. *Proc Gt Barrier Reef Sci Use Manag A Nat Conf* **2**: 37–46.

Mcgill BJ. 2003. A test of the unified neutral theory of biodiversity. *Nature* **422**: 881–5.

McManus JW and Polsenberg JF. 2004. Coral–algal phase shifts on coral reefs: Ecological and environmental aspects. *Prog Oceanogr* **60**: 263–79.

McSharry PE, Smith LA, and Tarassenko L. 2003. Prediction of epileptic seizures: are nonlinear methods relevant? *Nat Med* **9**: 241–2.

Meinhardt H. 1982. Models of biological pattern formation. London: Academic Press.
Meisel C and Kuehn C. 2012. Scaling effects and spatio-temporal multilevel dynamics in epileptic seizures. *PLoS One* **7**.
Melbourne-Thomas J, Johnson CR, Fung T, *et al.* 2011. Regional-scale scenario modeling for coral reefs: a decision support tool to inform management of a complex system. *Ecol Appl* **21**: 1380–98.
Meron E, Gilad E, Hardenberg J von, *et al.* 2004. Vegetation patterns along a rainfall gradient. *Chaos, Solitons and Fractals* **19**: 367–76.
Moberg F and Folke C. 1999. Ecological goods and services of coral reef ecosystems. *Ecol Econ* **29**: 215–33.
Mumby PJ. 2009. Phase shifts and the stability of macroalgal communities on Caribbean coral reefs. *Coral Reefs* **28**: 761–73.
Mumby PJ, Hastings A, and Edwards HJ. 2007. Thresholds and the resilience of Caribbean coral reefs. *Nature* **450**: 98–101.
Mumby PJ and Steneck RS. 2008. Coral reef management and conservation in light of rapidly evolving ecological paradigms. *Trends Ecol Evol* **23**: 555–63.
Mumby PJ, Steneck RS, and Hastings A. 2013. Evidence for and against the existence of alternate attractors on coral reefs. *Oikos* **122**: 481–91.
Murray JD. 2002. Mathematical Biology I: An Introduction (SS Antman, JE Marsden, L Sirovich, and S Wiggins, Eds). Berlin Heidelberg: Springer-Verlag.
Murray J. 2003. Mathematical biology II: spatial models and biomedical applications (S Antman, J Marsden, L Sirovich, and S Wiggins, Eds). Berlin Heidelberg: Springer-Verlag.
Myin-Germeys I, Oorschot M, Collip D, *et al.* 2009. Experience sampling research in psychopathology: opening the black box of daily life. *Psychol Med* **39**: 1533–47.
Nes EH van and Scheffer M. 2004. Large species shifts triggered by small forces. *Am Nat* **164**: 255–66.
Nes EH van and Scheffer M. 2005. Implications of spatial heterogeneity for catastrophic regime shifts in ecosystems. *Ecology* **86**: 1797–807.
Nes EH van and Scheffer M. 2007. Slow recovery from perturbations as a generic indicator of a nearby catastrophic shift. *Am Nat* **169**: 738–47.
Neuman Y, Nave O, and Dolev E. 2011. Buzzwords on their way to a tipping-point: A view from the blogosphere. *Complexity* **16**: 58–68.
Nickerson R. 1998. Confirmation bias: A ubiquitous phenomenon in many guises. *Rev Gen Psychol* **2**: 175–220.
Noy-Meir I. 1975. Stability of grazing systems: an application of predator-prey graphs. *J Ecol* **63**: 459.
Nyström M, Norström AV, Blenckner T, *et al.* 2012. Confronting feedbacks of degraded marine ecosystems. *Ecosystems* **15**: 695–710.
Oliva TA and Capdevielle CM. 1980. Sussman and Zahler: Throwing the baby out with the bath water. *Behav Sci* **25**: 229–30.
Oreskes N, Shrader-Frechette K, and Belitz K. 1994. Verification, validation, and confirmation of numerical models in the Earth sciences. *Science* **263**: 641–6.
Osinga R, Schutter M, Griffioen B, *et al.* 2011. The biology and economics of coral growth. *Mar Biotechnol (NY)* **13**: 658–71.
Otto SB, Rall BC, and Brose U. 2007. Allometric degree distributions facilitate food-web stability. *Nature* **450**: 1226–9.
Pascual M and Dunne JA. Ecological Networks: Linking Structure to Dynamics in Food Webs. New York: Oxford University Press.
Pascual M and Guichard F. 2005. Criticality and disturbance in spatial ecological systems. *Trends Ecol Evol* **20**: 88–95.
Patten SB. 2013. Major depression epidemiology from a diathesis-stress conceptualization. *BMC Psychiatry* **13**: 19.
Pe ML and Kuppens P. 2012. The dynamic interplay between emotions in daily life: augmentation, blunting, and the role of appraisal overlap. *Emotion* **12**: 1320–8.

Peeters F, Nicolson NA, Berkhof J, *et al.* 2003. Effects of daily events on mood states in major depressive disorder. *J Abnorm Psychol* **112**: 203–11.

Petraitis PS and Latham RE. 1999. The importance of scale in testing the origins of alternative community states. *Ecology* **80**: 429–42.

Pfeiffer T and Bonhoeffer S. 2004. Evolution of cross-feeding in microbial populations. *Am Nat* **163**: E126–35.

Pomeau Y. 1986. Front motion, metastability and subcritical bifurcations in hydrodynamics. *Phys D Nonlinear Phenom* **23**: 3–11.

Puglisi MP, Sneed JM, Sharp KH, *et al.* 2014. Marine chemical ecology in benthic environments. *Nat Prod Rep* **31**: 1510–53.

R Development Core Team. 2005. R: a language and environment for statistical computing.

Ramos O. 2010. Criticality in earthquakes. Good or bad for prediction? *Tectonophysics* **485**: 321–6.

Raspopovic J, Marcon L, Russo L, and Sharpe J. 2014. Digit patterning is controlled by a Bmp-Sox9-Wnt Turing network modulated by morphogen gradients. *Science* **566**: 10–5.

Renshaw E and Ford ED. 1983. The interpretation of process from pattern using two-dimensional spectral analysis. *Appl Stat* **32**: 51–63.

Rietkerk M, Boerlijst MC, Langevelde F van, *et al.* 2002. Self-organization of vegetation in arid ecosystems. *Am Nat* **160**: 524–30.

Rietkerk M, Dekker SC, Ruiter PC de, and van de Koppel J. 2004. Self-organized patchiness and catastrophic shifts in ecosystems. *Science* **305**: 1926–9.

Rietkerk M and van de Koppel J. 1997. Alternate stable states and threshold effects in semi-arid grazing systems. *Oikos* **79**: 69–76.

Rietkerk M and van de Koppel J. 2008. Regular pattern formation in real ecosystems. *Trends Ecol Evol* **23**: 169–75.

Risgaard-Petersen N, Rysgaard S, Nielsen LP, and Revsbech NP. 1994. Diurnal variation of denitrification and nitrification in sediments colonized by benthic microphytes. *Limnol Oceanogr* **39**: 573–9.

Roberts HH, Wilson PA, and Lugo-Fernández A. 1992. Biologic and geologic responses to physical processes: examples from modern reef systems of the Caribbean-Atlantic region. *Cont Shelf Res* **12**: 809–34.

Robles CD, Garza C, Desharnais RA, and Donahue MJ. 2010. Landscape patterns in boundary intensity: a case study of mussel beds. *Landsc Ecol* **25**: 745–59.

Rockström J, Steffen W, Noone K, *et al.* 2009. A safe operating space for humanity. *Nature* **461**: 472–5.

Rodríguez MR, Nuevo R, Chatterji S, and Ayuso-Mateos JL. 2012. Definitions and factors associated with subthreshold depressive conditions: a systematic review. *BMC Psychiatry* **12**: 181.

Rogers CS. 1990. Responses of coral reefs and reef organisms to sedimentation. *Mar Ecol Prog Ser* **62**: 185–202.

Rosindell J, Hubbell SP, He F, *et al.* 2012. The case for ecological neutral theory. *Trends Ecol Evol* **27**: 203–8.

Rosser JB. 2007. The rise and fall of catastrophe theory applications in economics: Was the baby thrown out with the bathwater? *J Econ Dyn Control* **31**: 3255–80.

Russell JA. 2003. Core affect and the psychological construction of emotion. *Psychol Rev* **110**: 145–72.

Saavedra S, Duch J, and Uzzi B. 2011. Tracking traders' understanding of the market using e-communication data. *PLoS One* **6**: e26705.

Scheffer M. 1998. Ecology of shallow lakes. London: Chapman and Hall.

Scheffer M. 2009. Critical transitions in nature and society. New Jersey: Princeton University Press.

Scheffer M, Barrett S, Carpenter SR, *et al.* 2015a. Creating a safe operating space for iconic ecosystems. *Science* **347**: 1317–9.

Scheffer M, Bascompte J, Brock WA, *et al.* 2009. Early-warning signals for critical transitions. *Nature* **461**: 53–9.

Scheffer M and Beets J. 1994. Ecological models and the pitfalls of causality. *Hydrobiologia* **275/276**: 115–24.

Scheffer M, Berg M van den, Breukelaar A, *et al.* 1994. Vegetated areas with clear water in turbid shallow lakes. *Aquat Bot* **49**: 193–6.

Scheffer M and Carpenter SR. 2003. Catastrophic regime shifts in ecosystems: linking theory to observation. *Trends Ecol Evol* **18**: 648–56.

Scheffer M, Carpenter SR, Dakos V, and Nes E van. 2015b. Generic indicators of ecological resilience: inferring the chance of a critical transition. *Annu Rev Ecol Evol Syst* **46**: 145–67.

Scheffer M, Carpenter SR, Lenton TM, *et al.* 2012a. Anticipating critical transitions. *Science* **338**: 344–8.

Scheffer M, Hirota M, Holmgren M, *et al.* 2012b. Thresholds for boreal biome transitions. *Proc Natl Acad Sci* **109**: 21384–9.

Scheffer M, Nes EH van, Holmgren M, and Hughes T. 2008. Pulse-driven loss of top-down control: the critical-rate hypothesis. *Ecosystems* **11**: 226–37.

Schmid MC, Risgaard-Petersen N, Vossenberg J van de, *et al.* 2007. Anaerobic ammonium-oxidizing bacteria in marine environments: widespread occurrence but low diversity. *Environ Microbiol* **9**: 1476–84.

Schmittmann VD, Cramer AOJ, Waldorp LJ, *et al.* 2013. Deconstructing the construct: A network perspective on psychological phenomena. *New Ideas Psychol* **31**: 43–53.

Scholz JP, Kelso JAS, and Schöner G. 1987. Nonequilibrium phase transitions in coordinated biological motion: Critical slowing down and switching time. *Phys Lett A* **123**: 390–4.

Schröder A, Persson L, and Roos DAM De. 2005. Direct experimental evidence for alternative stable states: a review. *Oikos* **110**: 3–19.

Schubert CJ, Durisch-Kaiser E, Wehrli B, *et al.* 2006. Anaerobic ammonium oxidation in a tropical freshwater system (Lake Tanganyika). *Environ Microbiol* **8**: 1857–63.

Schulz HN and Jørgensen BB. 2001. Big bacteria. *Annu Rev Microbiol* **55**: 105–37.

Scoffin TP. 1993. The geological effects of hurricanes on coral reefs and the interpretation of storm deposits. *Coral Reefs* **12**: 203–21.

Seitzinger S, Harrison JA, Böhlke JK, *et al.* 2006. Denitrification across landscapes and waterscapes: a synthesis. *Ecol Appl* **16**: 2064–90.

Shapiro OH, Fernandez VI, Garren M, *et al.* 2014. Vortical ciliary flows actively enhance mass transport in reef corals. *Proc Natl Acad Sci*: **111**: 13391–96.

Silliman BR, van de Koppel J, Bertness MD, *et al.* 2005. Drought, snails, and large-scale die-off of southern U.S. salt marshes. *Science* **310**: 1803–6.

Skeel RD and Berzins M. 1990. A method for the spatial discretization of parabolic equations in one space variable. *SIAM J Sci Stat Comput* **11**: 1–32.

Sliekers O, Derwort N, Gomez JLC, *et al.* 2002. Completely autotrophic nitrogen removal over nitrite in one single reactor. *Water Res* **36**: 2475–82.

Solé R V, Manrubia SC, Luque B, *et al.* 1996. Phase transitions and complex systems. *Complexity* **1**: 13–26.

Sornette D and Woodard R. 2010. Financial bubbles, real estate bubbles, derivative bubbles, and the financial and economic crisis. in: Takayasu M, Watanabe T, Takayasu H (Eds). Econophysics Approaches to Large-Scale Business Data and Financial Crisis. Tokyo: Springer Japan.

Spanning RJM van, Richardson DJ, and Ferguson SJ. 2007. Introduction to the biochemistry and molecular biology of denitrification. In: Bothe HF, Newton SJ (Eds). Biology of the Nitrogen Cycle. Amsterdam, The Netherlands: Elsevier.

Spérandio M and Queinnec I. 2004. Online estimation of wastewater nitrifiable nitrogen, nitrification and denitrification rates, using ORP and DO dynamics. *Water Sci Technol* **49**: 31–8.

Stafford-Smith MG. 1993. Sediment-rejection efficiency of 22 species of Australian scleractinian cor. *Mar Biol* **115**: 229–43.

StataCorp. 2009. Stata Statistical Software.

Staver AC, Archibald S, and Levin S. 2011a. Tree cover in sub-Saharan Africa: rainfall and fire constrain forest and savanna as alternative stable states. *Ecology* **92**: 1063–72.

Staver AC, Archibald S, and Levin SA. 2011b. The global extent and determinants of savanna and forest as alternative biome states. *Science* **334**: 230–2.

Steneck RS, Graham MH, Bourque BJ, *et al.* 2003. Kelp forest ecosystems: biodiversity, stability, resilience and future. *Environ Conserv* **29**: 436-459.

Steneck RS, Paris CB, Arnold SN, *et al.* 2009. Thinking and managing outside the box: coalescing connectivity networks to build region-wide resilience in coral reef ecosystems. *Coral Reefs* **28**: 367–78.

Sternberg LDSL. 2001. Savanna-forest hysteresis in the tropics. *Glob Ecol Biogeogr* **10**: 369–78.

Strogatz S. 1994. Nonlinear dynamics and chaos: with applications to physics, biology, chemistry and engineering. New York: Perseus.

Strohm TO, Griffin B, Zumft WG, and Schink B. 2007. Growth yields in bacterial denitrification and nitrate ammonification. *Appl Environ Microbiol* **73**: 1420–4.

Strous M, Fuerst JA, Kramer EHM, *et al.* 1999. Missing lithotroph identified as new planctomycete. *Nature* **400**: 446–9.

Strous M and Jetten MSM. 2004. Anaerobic oxidation of methane and ammonium. *Annu Rev Microbiol* **58**: 99–117.

Strous M, Pelletier E, Mangenot S, *et al.* 2006. Deciphering the evolution and metabolism of an anammox bacterium from a community genome. *Nature* **440**: 790–4.

Sussmann HJ and Zahler RS. 1978. Catastrophe theory as applied to the social and biological sciences: a critique. *Synthese* **37**: 117–216.

Taylor CM and Hastings A. 2005. Allee effects in biological invasions. *Ecol Lett* **8**: 895–908.

Thébault E and Fontaine C. 2010. Stability of ecological communities and the architecture of mutualistic and trophic networks. *Science* **329**: 853–6.

Thom R. 1972. Stabilité Structurelle et Morphogenèse: Essai d'une Théorie Générale des Modèles (English translation by Fowler, D.H., 1975. Structural Stability and Morphogenesis: An Outline of a Theory of Models. Benjamin, Reading). New York: Benjamin.

Thomas R. 1981. On the relation between the logical structure of systems and their ability to generate multiple steady states or sustained oscillations. In: Dora J Della, Demongeot J, Lacolle B (Eds). Numerical Methods in the Study of Critical Phenomena SE - 24. Springer Berlin Heidelberg.

Thompson JMT and Sieber J. 2011. Climate tipping as a noisy bifurcation: A predictive technique. *IMA J Appl Math (Institute Math Its Appl* **76**: 27–46.

Tiedje JM. 1988. Ecology of denitrification and dissimilatory nitrate reduction to ammonium. In: Zehnder AJB (Ed). Biology of anaerobic microorganisms. New York: Wiley.

Tijhuis L, Loosdrecht MCM Van, and Heijnen JJ. 1993. A thermodynamically based correlation for maintenance gibbs energy requirements in aerobic and anaerobic chemotrophic growth. *Biotechnol Bioeng* **42**: 509–19.

Tilman D and Downing JA. 1994. Biodiversity and stability in grasslands. *Nature* **367**: 363–5.

Tredicce JR, Lippi GL, Mandel P, *et al.* 2004. Critical slowing down at a bifurcation. *Am J Phys* **72**: 799–809.

Turing A. 1952. The chemical basis of morphogenesis. *Philos Trans R Soc Lond B Biol Sci* **237**: 37–72.

Tzur-Bitan D, Meiran N, Steinberg DM, and Shahar G. 2012. Is the looming maladaptive cognitive style a central mechanism in the (generalized) anxiety–(major) depression comorbidity: an intra-individual, time series study. *Int J Cogn Ther* **5**: 170–85.

Veraart AJ, Faassen EJ, Dakos V, *et al.* 2012. Recovery rates reflect distance to a tipping point in a living system. *Nature* **481**: 357–79.

Volterra V. 1926. Fluctuations in the abundance of a species considered mathematically. *Nature* **118**: 558–60.

Wagenmakers E-J, Molenaar PCM, Grasman RPPP, *et al.* 2005. Transformation invariant stochastic catastrophe theory. *Phys D* **211**: 263–76.

Warman L and Moles AT. 2009. Alternative stable states in Australia's Wet Tropics: a theoretical framework for the field data and a field-case for the theory. *Landsc Ecol* **24**: 1–13.

Watson D, Clark LA, and Tellegen A. 1988. Development and validation of brief measures of positive and negative affect: the PANAS scales. *J Pers Soc Psychol* **54**: 1063–70.

Watson J and Estes JA. 2011. Stability, resilience, and phase shifts in rocky subtidal communities along the west coast of Vancouver Island, Canada. *Ecol Monogr* **81**: 215–39.

Weber KA, Picardal FW, and Roden EE. 2001. Microbially catalyzed nitrate-dependent oxidation of biogenic solid-phase Fe(II) compounds. *Environ Sci Technol* **35**: 1644–50.

Weber KA, Urrutia MM, Churchill PF, *et al.* 2006. Anaerobic redox cycling of iron by freshwater sediment microorganisms. *Environ Microbiol* **8**: 100–13.

Weerman EJ, van de Koppel J, Eppinga MB, *et al.* 2010. Spatial self-organization on intertidal mudflats through biophysical stress divergence. *Am Nat* **176**: E15–32.

Weijerman M, Fulton EA, Janssen ABG, *et al.* 2015. How models can support ecosystem-based management of coral reefs. *Prog Oceanogr* **138**: 559–70.

Wesenbeeck BK van, van de Koppel J, Herman PMJ, *et al.* 2008. Potential for sudden shifts in transient systems: distinguishing between local and landscape-scale processes. *Ecosystems* **11**: 1133–41.

Wichers M. 2014. The dynamic nature of depression: a new micro-level perspective of mental disorder that meets current challenges. *Psychol Med* **44**: 1349–60.

Wichers M, Groot PC, Psychosystems, *et al.* 2016. Critical slowing down as a personalized early warning signal for depression. *Psychother Psychosom* **85**: 114–6.

Wichers M, Lothmann C, Simons CJP, *et al.* 2012. The dynamic interplay between negative and positive emotions in daily life predicts response to treatment in depression: a momentary assessment study. *Br J Clin Psychol* **51**: 206–22.

Wichers M, Myin-Germeys I, Jacobs N, *et al.* 2007. Genetic risk of depression and stress-induced negative affect in daily life. *Br J Psychiatry* **191**: 218–23.

Wigman JTW, Os J van, Thiery E, *et al.* 2013. Psychiatric diagnosis revisited: towards a system of staging and profiling combining nomothetic and idiographic parameters of momentary mental states. *PLoS One* **8**: e59559.

Wild C, Huettel M, Klueter A, *et al.* 2004. Coral mucus functions as an energy carrier and particle trap in the reef ecosystem. *Nature* **428**: 66–70.

Wild-Hartmann JA de, Wichers M, Bemmel AL van, *et al.* 2013. Day-to-day associations between subjective sleep and affect in regard to future depression in a female population-based sample. *Br J Psychiatry* **202**: 407–12.

Wilson WG and Nisbet RM. 1997. Cooperation and competition along smooth environmental gradients. *Ecology* **78**: 2004–17.

Wissel C. 1984. A universal law of the characteristic return time near thresholds. *Oecologia* **65**: 101–7.

Wolken JM, Hollingsworth TN, Rupp TS, *et al.* 2011. Evidence and implications of recent and projected climate change in Alaska's forest ecosystems. *Ecosphere* **2**: art124.

Zahler RS and Sussmann HJ. 1977. Claims and accomplishments of applied catastrophe theory. *Nature* **269**: 759–63.

Zeeman EC and Sussmann HJ. 1979. Catastrophe Theory, Selected Papers 1972-1977. *SIAM Rev* **21**: 268–76.

Summary

In this thesis I use mathematical models to explore the properties of complex systems ranging from microbial nitrogen pathways and coral reefs to the human state of mind. All are examples of complex systems, defined as systems composed of a number of interconnected parts, where the systemic behavior leads to the emergence of properties that would not be expected from behavior or properties of the individual parts of the system. Although the full behavior of the systems I address will probably never be fully understood, the strategic model analyses I present hint at mechanisms that may dominate the overall dynamics.

For instance, in chapter 2, I address the question whether all microbial nitrogen pathways that are realized in nature may be explained from basic physical-chemical principles. The approach is to compute conversion rates and energy yield of all potential pathways from stoichiometry and energy yield of the performed redox reaction. Surprisingly, much of the variation observed in nature could indeed be predicted from these basic principles. Interestingly, there were also deviations between the first round of predictions and observations. Those led us to the hypothesis that high ammonium activation energy may be an important biochemical factor creating barriers for the viability of ammonium oxidizing pathways. After inclusion of this additional assumption, the model predicted two pathways that had not been observed in nature so-far. A recent discovery of one of these pathways (complete nitrification of ammonium to nitrate) strengthens the idea that much of the emergent behavior of the complex global microbial nitrogen pathways may be explained from basic physical-chemical principles (chapter 9). Now, only one of the eleven predicted pathways remains to be confirmed: the dismutation of nitrite to the level of nitrate and dinitrogen gas.

Dynamical system theory can also provide new angles for thinking about the resilience of coral reefs, pointing to the role of local feedbacks and interactions that may determine systemic behavior (chapters 3 and 4). Chapter 3 reveals the widespread occurrence of previously unrecognized Turing patterns on coral reefs in Australia and New Caledonia. The famous mathematician Alan Turing was the first to show how patterns can spontaneously emerge in otherwise completely homogeneous systems. Turing used a reaction-diffusion system to describe how simple local interactions between an activator and an inhibitor, combined with diffusion of these substances, can lead to symmetry breaking. Since then, Turing patterns have been thoroughly analyzed in the literature, and the fundamental conditions for the formation of Turing patterns are well understood. Those mathematical insights imply that the observed Turing patterns on reefs point to a particular set of testable mechanisms that should govern reef growth at these scales. Moreover, the variation in Turing patterns across the reefs may hint at differences in resilience.

Chapter 4 is another example of how existing mathematical theory can help to guide our understanding of the complexity of coral reef ecosystems. A simple dynamical model is used to illustrate how multiple weak positive feedbacks can collectively lead to alternative stable states. Although these results do not reveal whether alternative stable states indeed occur on coral reefs, they imply that an ecosystem that responds gradually to changing conditions at one location may show an abrupt shift between alternative attractors on another location. This adds an important nuance to the polarized discussion about the question whether alternative stable states exist in coral reef systems. The results also reveal the need for a better understanding and quantification of feedbacks in coral reef ecosystems.

Chapter 5 provides a general perspective on the possibilities to anticipate shifts to alternative states in complex systems. We review two previously unconnected fields of research in relation to such critical transitions. First, we discuss how the architecture of complex networks can affect robustness, showing that for most kinds of networks, modularity and heterogeneity tend to decrease the likelihood of abrupt shifts. Second, we review the work showing how generic mathematical principles suggest ways to detect a decrease in resilience of the system as it approaches a tipping point. These generic indicators are related to the phenomenon of critical slowing down, or to the changing shape of the stability landscape. Together these two emerging fields open up novel generic ways of probing and managing the likelihood of critical transitions in complex systems. However, this overview also highlights important gaps in our understanding when it comes to various realistic situations.

One complicating aspect is the fact that many systems are large and heterogeneous. I address this issue in chapters 6 and 7. Here, the theory of alternative stable states and resilience of ecosystems is explored for spatially extended ecosystems. In chapter 6 we show that, in contrast to well-mixed systems, resilience against local disturbances does not decrease gradually as the system approaches a critical transition (a fold bifurcation in particular). Instead, the dominant state remains virtually indestructible, until at a critical point, known as a Maxwell point, resilience drops sharply in the sense that even a very local disturbance can cause a domino effect leading eventually to a systemic shift to the alternative state. Close to this Maxwell point both states have a comparable resilience, allowing long transient co-occurrence of alternative states side-by-side, and permanent co-existence if there are mild spatial barriers. For spatially extended biomes with alternative stable states, such as tundra, steppe and forest, these results imply that, as climatic change reduces the stability, the effect might be difficult to detect until a point where local disturbances inevitably induce a spatial cascade to the alternative state.

The most direct indicator of critical slowing down is the recovery rate after a small perturbation. However, if a system is not 'well-mixed', recovery depends critically on the way a perturbation is performed spatially. One may attempt to perform a weak, system-wide perturbation. However, in spatially extended ecosystems it may be typically more feasible to perform a local perturbation. In chapter 7, a simple, but spatially explicit, model with local alternative stable states is used to investigate the limitations of interpreting the recovery from local disturbances as an indicator of the resilience of the system as a whole. Although the recovery trajectory depends on the systemic resilience of the ecosystem, it is also strongly influenced by the rates of spatial exchange and by the spatial extent of the perturbation.

Both chapters 6 and 7 illustrate how local perturbations of sufficient size and amplitude may trigger a systemic collapse. Interestingly, while 'collapse' has a negative connotation, the same mathematical principles obviously apply to changes that are perceived as positive. For instance, local restoration efforts may create a domino effect invoking a large scale recovery of an ecosystem. In any case, the models for spatially extended systems predict that in a homogeneous landscape the entire system will tend to converge to the same state. From a restoration perspective this implies that local efforts may tend to either fail in the long run or alternatively trigger a landscape-wide transition. The dynamic response to natural or experimental local perturbations can hint at the likelihood for such systemic transitions between alternative states.

Chapter 8 applies the theory discussed in chapter 5 to the case of human depression, one of the main mental health hazards in the western world. Depression is hypothesized to be an alternative stable state of the 'normal' mental state under certain conditions. The view of depression as an alternative stable state implies that the shifts between depression and the normal healthy state should correspond to critical transitions that become more likely as the system is closer to a tipping point (a zero-eigenvalue bifurcation). We therefore hypothesized that the likelihood of transitions should be related to indicators of critical slowing down. Indeed, the data we have for a large group of healthy individuals and patients reveal that the probability of an upcoming shift is related to elevated cross-correlation as well as temporal autocorrelation and variance of fluctuations in four autorecorded aspects of mood. One problem in interpreting these results is that the recorded aspects of mood can hardly be considered real physical variables of a dynamical system. Instead, the mood system is often considered to have evolved as an indicator for the organism to reflect the overall conditions of an underlying complex somatic-mental-social system. We addressed this issue by analyzing the dynamics of principle components of a complex network with alternative attractors, demonstrating that

such indicators of the state of a complex system may faithfully reflect critical slowing down in the underlying system. Overall, these results support the hypothesis that mood may have alternative stable states separated by tipping points, and suggest an approach for assessing the likelihood of transitions into and out of depression.

In chapter 9 I take a step back to reflect on the strengths and weaknesses of the approach taken in this thesis, and on the challenges ahead. I argue that the attractiveness of simple models or theories almost inevitably implies the risk of becoming trapped into a tunnel vision. Simple models by themselves can never provide a proof of the role of a particular mechanism or process. Instead, profound cooperation with empirical scientists is necessary for theoreticians to contribute in useful ways to the understanding of any complex system. Such cooperation requires a subtle balance of modesty and perseverance. On the other hand, challenges of understanding truly complex systems can only be met through such transdisciplinary work. There is a large gap between the insights from controlled experiments and interpretation of the increasingly available 'big data'. Strategic mathematical models may help navigate this gap, carving corridors of clarity through the overwhelming complexity of nature and society. Any simple model necessarily neglects much of this complex reality. However, paraphrasing Pablo Picasso: '*models are a lie that can help to make us realize the truth*'.

Acknowledgements

My PhD journey in Wageningen started when my fellow student and friend Laura Salazar Jaramillo introduced me to Vasilis Dakos, in the period that I was orienting myself on research groups to do a MSc project for my master Theoretical Biology at Utrecht University. Vasilis, on his turn, introduced me to Annelies Veraart, Jeroen de Klein, and Marten Scheffer. That marked the start of a long-term relationship between AEW and me. Vasilis, I'm really happy that we have met; I have greatly enjoyed our time together in Wageningen, thank you for being such a good friend and colleague.

I am extremely grateful to Marten Scheffer and Egbert van Nes, who believed in me during the entire PhD journey. You were the most fantastic supervisors I could have ever imagined. Marten, you are a great inspiration for me. You are a master in thinking out-of-the-box, in crossing scientific borders, and in recognizing general patterns in complex system behavior. Thank you for all your efforts in making me a better scientist, and thank you for your mental support at all times. Egbert, you were always a great help with an endless amount of patience. You are a critical thinker, and always curious to new mathematical approaches and ideas. Thank you for all your help with mathematical and programming questions, and your nice sense of humor during breaks and parties. Egbert and Marten, I consider you both as good friends, and I'm very happy we will (hopefully) continue our journey together. I am looking forward to all scientific discussions, great trips and parties in the future!

Along this journey, I worked with various people from different scientific disciplines, which was sometimes difficult, but mostly fun and insightful. The seed for the microbial adventure was already planted during my BSc internship at the Microbiology department in Nijmegen, where Marc Strous was my supervisor. Marc, I am very grateful for your contribution to the microbial nitrogen cycle paper at a later stage. You helped us very much to frame the paper for the right community. The coral reef adventure started with prof. Terry Hughes. The first time I met Terry was in Townsville, Australia, where Egbert, Vasilis and I came to visit you after our trip to Heron Island. We bombarded you with all kind of wild ideas on coral reef dynamics. After this visit, you invited me to spend half a year in Townsville to work on these ideas. Since I was immediately intrigued by the complex nature of coral reefs, and Sjoerd and I like travelling, this was an easy decision for me to make. Terry, thank you for all the time you spend with me to discuss potential general patterns on coral reefs, and for introducing me to a life in the tropics. A lot of credits for the depression work go to Marieke Wichers, Angélique Cramer, Denny Borsboom, and Francis Tuerlinckx. It was inspiring to discuss the hypothesis, the data, and the implications with you. I really hope we can work more together in the

future. While not part of this thesis, I want to mention Johan Bollen from Indiana University, USA. Johan introduced me to the complex, 'nerdy', and exciting world of sentiment analysis of social media data. Johan, thank you for spending so much time with me, there are many unfinished projects lying on the shelf, that are all exciting to continue with. Besides a great scientist, you are a fun person to work and hang out with, thank you for the opportunity you gave me.

The last five years would not have been so much fun without everybody at AEW (Bart, Edwin, Frits, Jeroen, John, Marlies, Miquel, Paul, Rudi, Wendy, Wolf, Anita, Nancy, Annettem Ariadna, Arianna, Arie, Babak, Bastiaan, Bernardo, Bregje, Els, Goraw, Jacqui, Jan, Jing, Jelle, Jugk, Laura, Luuk, Maira, Paula, Pablo, Sanne Gijzel, Sanne van den Berg, Sebastian, Selvino, Trung, and Usman). This department feels like a warm bath, and I'm really happy I can be part of this. A special thanks should go to the theory team! I'm really enjoying our Thursday sessions, and I am looking forward to all the projects ahead.

I also would like to thank former AEW PhDs (Andrea, Andreu, Annelies, Darya, Gissell, Jacqui, Jochem, Jordie, Kristina, Marina, Nika, Noel, Sarian, and Vasilis) for the parties, the beers, jenevers, the laughs and the inspiration to really finish the book.

Dear Hanneke and Nils, chapter 4 of this thesis would not have been written without your hospitality on the Pélagie. Our joint trip with Sjoerd, Emmylou (5 months old by that time) on the Great Barrier Reef was unforgettable. Nils, you even used your diving experience, and your spare bottle of air to collect some water samples (everything for science!). Sjoerd and I were relieved that we had one day without wind, so we could fly the drone and make the beautiful pattern pictures. One of them is even shining on the cover of this thesis!

Ofcourse, a PhD journey is not only about science. I would like to thank all my friends for their distractions from science, great parties, dinners, holidays, and long weekends together. I especially would like to mention Mijke, Wiesje, Leonie, the 'Natuurwetenschappers', and the 'Gang-6 gang': you are all wonderful people, and I am happy I have you in my life!

My family has been a great support during my, still young, career in science. Jac, Mariette, Maurice, Ingrid, Roger and Wendy, thank you for listening to my stories, and for supporting Sjoerd and me while being abroad. Anita, next to being my sister, I consider you as one of my best friends. You are a fantastic listener, and always supportive. Papa and mama, you have always supported me and believed in me, thank you for everything. Lieve oma, bedankt dat je zo'n fijne oma, en superoma, voor ons allen bent. We houden allemaal heel veel van je!

Mijke and Marlies, I am looking forward to having you at my side during the defense. Mijke, thank you for being my friend, for your unconditional support, belief in my skills, and for always offering a 'soda' date. Marlies, our journeys at AEW walked parallel for quite some time already. You are always ready for a chat, and a great co-organizer of events and happenings. Hopefully we will be colleagues for a much longer time.

Last but not least, Sjoerd, our journey together has started 15 years ago, and I'm very happy and grateful that you are my partner in life. Without you, this thesis would not have been possible. You happily joined me on all my overseas scientific adventures (even quitting your job for that), and you have helped me with the development and writing of most chapters of this thesis. Two years ago we started a new adventure, the adventure of our own family. While it is sometimes hard to find quality time for us as a couple, every time we sing and dance through the living room with Emmylou, my eyes fill with tears, and I'm so grateful for having you both in my life. I'm looking forward to meet the new member of the family in August.

A few words about the author

Ingrid van de Leemput was born in Voorburg, the Netherlands, in 1983. In 2001, she started her scientific career at Radboud University Nijmegen, with 'Natuurwetenschappen', nowadays called Science, a BSc program aimed to work at the boundaries of biology, physics, and chemistry. After two years, she decided to specialize in Biology. During her BSc thesis, she studied ladderane phospholipids in anammox bacteria, which resulted in a publication in FEMS Microbiology in 2006. After graduating from her BSc Biology in 2004, she travelled around the world for a year. In 2006, she moved to Utrecht to pursue a MSc degree in Theoretical Biology, where she was introduced to the magic world of modelling biological processes. During her first Master's thesis with Paulien Hogeweg at Utrecht University, Ingrid studied the evolution of sulphur bacteria. During her second Master's thesis with Annelies Veraart, Jeroen de Klein, and Vasilis Dakos at Wageningen University, she explored multiple ways to model denitrification processes in ditches. After graduating in 2009, Ingrid started her PhD under the supervision of Marten Scheffer and Egbert van Nes at the Department of Aquatic Ecology and Water Quality Management in Wageningen University. During her PhD she spend six months at the ARC Centre of Excellence of Coral Reef Studies in Townsville, Australia, to collaborate with professor Terry Hughes on modeling feedback mechanisms and self-organized patterns in coral reefs. In 2015, she got the opportunity to work with Johan Bollen at Indiana University as a visiting research scholar, to explore the potential for early warning signals of social uprisings and depression, by analyzing social media data.

Ingrid is interested in the use of simple mathematical models to study complex dynamical systems. She studied a variety of topics under the supervision of Marten Scheffer and Egbert van Nes at Wageningen University in the Netherlands, ranging from microbial pathways to psychological disorders (this thesis). During her MSc and PhD, Ingrid has developed several technical skills to model biological processes. More importantly however, she learned to collaborate with scientists from completely different scientific disciplines, to recognize patterns in ecological and social systems, to translate observed dynamics to simple mathematical models, and to communicate and teach why simple mathematical models are relevant for the study of complex dynamical systems.

List of publications

van de Leemput IA, Hughes T, van Nes EH, and Scheffer M. (2016). Multiple feedbacks and the prevalence of alternate stable states in coral reefs. Coral Reefs, doi: 10.1007/s00338-016-1439-7

Bollen J, **van de Leemput IA,** Gonçalves B, and Ruan G. (2016). The happiness paradox: your friends are happier than you. ArXiv ID: 1602.02665. http://arxiv.org/abs/1602.02665

Olde Rikkert MGM, Dakos V, Buchman TG, de Boer R, Glass L, Cramer AOJ, Levin S, van Nes E, Sugihara G, Ferrari MD, Tolner EA, **van de Leemput IA**, *et al.* (2016). Slowing down of recovery as generic risk marker for acute severity transitions in chronic diseases. Crit Care Med 44(3), 601-6.

Scheffer M, Barrett S, Carpenter SR, Folke C. Green AJ, Holmgren M, Hughes TP, Kosten S, **van de Leemput IA**. *et al.* (2015). Creating a safe operating space for iconic ecosystems. Science 347, 1317–9.

van de Leemput IA, van Nes EH, and Scheffer M. (2015). Resilience of alternative states in spatially extended ecosystems. PLoS ONE 10(2), e0116859

Weijermans M, Fulton EA, Janssen ABG, Kuiper JJ, Leemans R, Robson BJ, **van de Leemput IA**, Mooij WM. (2015) How models can support ecosystem-based management of coral reefs. Prog in Oceanogr 138(B), 559–570

Wichers M, Groot PC, Psychosystems, ESM Group, and **EWS Group.** (2016). Critical slowing down as a personalized early warning signal for depression. Psychother Psychosom 85, 114-116

Wichers M, Borsboom D, Tuerlinckx F, Kuppens P, Viechtbauer W, **van de Leemput IA**, *et al.* (2014). Reply to Bos and De Jonge: Between-subject data do provide first empirical support for critical slowing down in depression. Proc Natl Acad Sci 111, E879–E879

van de Leemput IA, Wichers M, Cramer AOJ, Borsboom D, Tuerlinckx F, Kuppens P, *et al.* (2014). Critical slowing down as early warning for the onset and termination of depression. Proc Natl Acad Sci 111, 87–92. ScienceNOW: *"The holy grail of depression epidemiology is that we want to intervene early to prevent people from having depressive episodes," says social scientist Stephen Gilman of Harvard University, who was not involved in the study. "Where this work is headed is making an advance in that direction, toward early detection and therefore early intervention."*

Johansson CL, **van de Leemput IA**, Depczynski M, Hoey AS & Bellwood DR. (2013). Key herbivores reveal limited functional redundancy on inshore coral reefs. Coral Reefs 32, 963–972.

Scheffer M, Carpenter SR, Lenton TM, Bascompte J, Brock W, Dakos V, van de Koppel J, **van de Leemput IA**, *et al.* (2012). Anticipating critical transitions. Science 338, 344–348.

Hughes TP, Linares C, Dakos V, **van de Leemput IA**, and van Nes EH. (2013). Living dangerously on borrowed time during slow, unrecognized regime shifts. Trends Ecol Evol 28, 149–155.

van de Leemput IA, Veraart AJ, Dakos V, de Klein JJM, Strous M, and Scheffer M. (2011). Predicting microbial nitrogen pathways from basic principles. Environ Microbiol *13*(6), 1477–87 F1000 review by Robert Sterner: *I was fascinated by this paper because it correctly replicates the key structure of the nitrogen cycle in different environments by considering only stoichiometry, energy yield, and competition. There was no genetics, no evolution, in fact no organisms, and additionally a very limited periodic table, but nevertheless the nitrogen (N) cycle emerged.*

Boumann HA, Hopmans EC, **van de Leemput I**, Op den Camp HJM, van de Vossenberg J, Strous M, Jetten MSM, *et al.* (2006). Ladderane phospholipids in anammox bacteria comprise phosphocholine and phosphoethanolamine headgroups. FEMS Microbiol Lett 258(2), 297–304

Netherlands Research School for the
Socio-Economic and Natural Sciences of the Environment

D I P L O M A

For specialised PhD training

The Netherlands Research School for the
Socio-Economic and Natural Sciences of the Environment
(SENSE) declares that

Ingrid Antoinette van de Leemput

born on 11 July 1983 in Voorburg, The Netherlands

has successfully fulfilled all requirements of the
Educational Programme of SENSE.

Wageningen, 3 June 2016

the Chairman of the SENSE board	the SENSE Director of Education
Prof. dr. Huub Rijnaarts	Dr. Ad van Dommelen

The SENSE Research School has been accredited by the Royal Netherlands Academy of Arts and Sciences (KNAW)

KONINKLIJKE NEDERLANDSE
AKADEMIE VAN WETENSCHAPPEN

The SENSE Research School declares that **Ms. Ingrid van de Leemput** has successfully fulfilled all requirements of the Educational PhD Programme of SENSE with a work load of 55 ECTS, including the following activities:

SENSE PhD Courses
- Environmental Research in Context
- Research Context Activity: Organizing Workshop on "Mental Disorders in Terms of Dynamical Systems Theory" and coordinating output publication (Echteld, 27-29 June 2012)
- Spatial Ecology

Other PhD and Advanced MSc Courses
- Spatio-temporal models in Ecology
- Models of Biological Processes and Environmental Quality
- Ecological Models and Data in R
- Techniques for Writing and Presenting Scientific
- Forum Library course Adobe InDesign

Management and Didactic Skills Training
- Organizer Workshop on "Complex dynamics from simple mechanisms in coral reefs" in Wageningen, and coordinator output publication.
- Co-organizer Workshop on "Anticipating Critical Transitions" in Echteld
- Supervisor MSc Theses:
  "The resilience of coral reefs: the role of shelter limitation, connectivity, functional redundancy, and response diversity" (Andreas Dietzel) and "Scaling from node to network: increased recovery time as an early warning signal for systemic shifts" (Bas Buddendorf)
- Course assistant: Models of Biological Processes and Environmental Quality
- Guest Lecturer UvA course: "Quality of Life, Future Planet Studies"

Oral Presentations
- *Slow recovery from local disturbances: an early-warning signal for regime shifts?* Resilience 2011, 11-16 March 2011, Tempe, Arizona, USA
- *Dynamics of biotic and abiotic interactions: exploring the spatial dynamics of resilience.* PE&RC PhD Discussion Group: Ecological Theory and Application, 3 Aug 2011, Wageningen, Netherlands
- *Living on borrowed time: transgressing unrecognized tipping points.* 12th International Coral Reef Symposium, 9-13 July 2012, Cairns, Australia
- *'Tipping Points' Research.* Official opening Lorentz Centre@Snellius, 4 October 2012, Leiden, Netherlands
- *Early warning signals of critical transitions in mood.* Monthly meeting KNAW (The Royal Netherlands Academy of Sciences), department of Physics , 25 February 2013, Amsterdam, Netherlands
- *Critical slowing down as an early warning indicator of transitions in mood.* International Meeting of the Psychometric Society (IMPS), 22-26 July 2013, Arnhem, Netherlands
- *Spatial resilience: The role of local positive feedbacks for large-scale collapse and recovery.* ESA Annual Meeting, 4-8 August 2013, Minneapolis, Minnesota, USA

SENSE Coordinator PhD Education

Dr. ing. Monique Gulickx

The research described in this thesis was financially supported by the Ecoshape program 'Building with Nature' (NTW 2.1), and a European Research Council Advanced Grant (ERC Grant Agreement 268732) awarded to Marten Scheffer.

Financial support for printing this thesis, from the Aquatic Ecology and Water Quality Management Group (WUR) and the Synergy Program for analyzing Resilience and Critical transitionS (SPARCS) through a Spinoza award to Marten Scheffer, is gratefully acknowledged.

Cover: Ingrid A. van de Leemput
Layout: AgileColor Design Studio/Atelier || AgileColor.com
Printed by: Ridderprint, Ridderkerk (NL) || Ridderprint.nl